11-4403-cv

United States Court of Appeals

for the

Second Circuit

AEGIS INSURANCE SERVICES, INC., LIBERTY INSURANCE UNDERWRITERS, INC., NATIONAL UNION INSURANCE COMPANY OF PITTSBURGH, NUCLEAR ELECTRIC INSURANCE LIMITED, CERTAIN UNDERWRITERS AT LLOYDS, (Syndicates 1225 and 1511), as subrogor of Consolidated Edison Company of New York, Inc., and CONSOLIDATED EDISON COMPANY OF NEW YORK, INC.

Plaintiffs-Appellants,

(For Continuation of Caption See Inside Cover)

ON APPEAL FROM THE UNITED STATES DISTRICT COURT FOR THE SOUTHERN DISTRICT OF NEW YORK

JOINT APPENDIX
Volume 12 of 16 (Pages JA-3067 to JA-3320)

KATHERINE LINDSAY PRINGLE
FRIEDMAN KAPLAN SEILER & ADELMAN LLP
Seven Times Square, 28th Floor
New York, New York 10036
(212) 833-1100

Attorneys for Defendants-Cross-Defendants-Cross-Claimants-Third-Party-Plaintiffs-Appellees

THOMAS J. MOLONEY
CLEARY GOTTLIEB STEEN & HAMILTON LLP
One Liberty Plaza
New York, New York 10006
(212) 225-2000

Attorneys for Defendants-Cross-Defendants-Cross-Claimants-Appellees

FRANKLIN M. SACHS
GREENBAUM, ROWE, SMITH & DAVIS LLP
Metro Corporate Campus One
P.O. 5600
Woodbridge, New Jersey 07095
(732) 549-5600

– and –

MARK L. ANTIN
GENNET, KALLMANN, ANTIN & ROBINSON, P.C.
Six Campus Drive
Parsippany, New Jersey 07054
(973) 285-1919

Attorneys for Plaintiffs-Appellants

(For Continuation of Appearances See Inside Cover)

v.

7 WORLD TRADE COMPANY, L.P.,

Defendant-Cross-Defendant-Cross-Claimant-Third-Party Plaintiff-Appellee,

CITIGROUP INC., CITIGROUP GLOBAL MARKETS HOLDINGS INC., SALOMON SMITH BARNEY HOLDINGS, INC., SALOMON INC., SILVERSTEIN DEVELOPMENT CORP., SILVERSTEIN PROPERTIES, INC.,

Defendants-Cross-Defendants-Cross-Claimants-Appellees,

TISHMAN CONSTRUCTION CORPORATION,

Defendant-Cross-Defendant-Appellee,

OFFICE OF IRWIN G. CANTOR, P.C., FLACK & KURTZ, INC.,

Defendants-Cross-Defendants-Third-Party Defendants-Appellees,

SWANKE HAYDEN CONNELL ARCHITECTS, SYSKA & HENNESSY GROUP, INC., AKA SYSKA & HENNESSY ENGINEERS,

Defendants-Cross-Defendants-Cross-Claimants-Third-Party Plaintiffs,

H.O. PENN MACHINERY CO., INC., ALL FIRE SYSTEMS, INC.,

Defendants-Cross-Defendants-Cross-Claimants,

GRACE CONSTRUCTION PRODUCTS, EMERY ROTH & SON, P.C., SECURITAS AB, SECURITY SERVICES, INC., CENTIFUGAL ASSOCIATES, INC., SYSKA & HENNESSY, INC.,

Defendants-Cross-Defendants,

AMBASSADOR CONSTRUCTION CO., INC., COSENTINI ASSOCIATES INC., CANTOR SEINUK GROUP, P.C., SKIDMORE OWINGS AND MERRILL, L.L.P., AMBASSADOR CONSTRUCTION CO., INC., AMEC CONSTRUCTION MANAGEMENT, INC., FKA MORSE DIESEL INTERNATIONAL, INC.,

Defendants-Cross-Defendants-Third-Party Defendants,

DIC/UNDERHILL, a joint venture, KABACK ENTERPRISES, PREFERRED UTILITIES MANUFACTURING CORP., ELECTRIC POWER SYSTEMS, INC., G.C. ENGINEERING & ASSOCIATES, P.C., FIRECOM INC., FIBERLOCK TECHNOLOGIES, INC., ROSEBWACH TANK CO., INC., ABCO PEERLESS SPRINKLER CORPORATION, AMR CORPORATION, AMERICAN AIRLINES, INCORPORATED, UAL CORPORATION, UNITED AIRLINES INCORPORATED, COLGAN AIR, INCORPORATED, US AIRWAYS GROUP, INCORPORATED, US AIRWAYS, INCORPORATED, HUNTLEIGH USA CORPORATION, ICTS INTERNATIONAL NV, GLOBE

AVIATION SERVICES CORPORATION, BURNS INTERNATIONAL SECURITY SERVICES CORPORATION, PINKERTON'S INCORPORATED, BOEING COMPANY, AMEC, PLC, KABACK ENTERPRISES,

Defendants,

THE WTC PLAINTIFFS,

Plaintiff-Intervenor.

KENNETH G. SCHWARZ
COZEN O'CONNOR
45 Broadway Atrium, 16th Floor
New York, New York 10006
(212) 509-9400

Attorneys for Defendant-Cross-Defendant-Appellee

DAVID ABRAMOVITZ
ZETLIN & DE CHIARA LLP
801 Second Avenue
New York, New York 10017
(212) 682-6800

– and –

STEPHEN P. SCHRECKINGER
GOGICK, BYRNE & O'NEILL, LLP
11 Broadway, Suite 1560
New York, New York 10004
(212) 422-9424

Attorneys for Defendants-Cross-Defendants-Third-Party-Defendants-Appellees

---

TABLE OF CONTENTS

Franklin M. Sachs (FS6036)
GREENBAUM, ROWE, SMITH & DAVIS LLP
Metro Corporate Campus One
P.O. Box 5600
Woodbridge, New Jersey 07095
Telephone: (732) 549-5600

UNITED STATES DISTRICT COURT
SOUTHERN DISTRICT OF NEW YORK

IN RE: SEPTEMBER 11 PROPERTY DAMAGE AND BUSINESS LOSS LITIGATION	:	21 MC 101 (AKH)
AEGIS INSURANCE SERVICES, INC., et al., Plaintiffs, -against- 7 WORLD TRADE CENTER COMPANY, L.P., et al., Defendants.	:	04 CV 7272 (AKH) **SUPPLEMENTAL AND AMENDED SECOND DECLARATION OF COLIN G. BAILEY**

I, Colin G. Bailey, declare:

1. I have been a practicing structural engineer for 22 years and I am presently a Professor of Structural Engineering at Manchester University in Manchester, England.

2. Among my specialties are the fire safety engineering of structures and steel-concrete composite systems. I am a Fellow of the Institution of Civil Engineers (FICE), a member of the Institution of Structural Engineers (MIStructE), and a member of the Institution of Fire Engineers (MIFireE). My curriculum vita is attached hereto as Exhibit A.

3. In 2007, I was retained by counsel for Plaintiffs in this case to provide expert analysis with respect to the cause of the global collapse of World Trade Center 7 on September 11, 2001.

4. Since that time, I have reviewed thousands of documents, drawings, and photographs, and actively participated in and reviewed the computer fire modeling performed on behalf of the Plaintiffs in this case.

5. The opinions that follow are based on that review and activity, and are made to a reasonable degree of scientific probability. These opinions and the data and materials relied upon in forming these opinions are more fully set forth in my report dated February 15, 2010, attached hereto as Exhibit D and made a part hereof.

6. Based on my work to date, including computer modeling at the University of Edinburgh in which many columns were removed in the model to see the effect on the structure of the building, it is my opinion that any structural damage caused by debris from the collapse of WTC 1 or WTC2 played no part in the collapse of 7WTC.

7. Based on my work to date, including computer models by the University of Edinburgh, it is my opinion that if there had been a diesel fuel fire on September 11 involving between 7,350 and 9,300 gallons of diesel fuel on the fifth floor of 7WTC in the area of the transfer trusses, such a fire would have compromised the strength of the transfer trusses, and could have caused them to fail, resulting in the collapse of columns 79 and/or 80.

8. The computer modeling completed to date supports the conclusion that 7WTC would have collapsed as a result of typical office contents fires because of several design/construction failures, including the failure to adequately fireproof the flutes of the metal floor decking for 7WTC and the failure to ensure that a restrained floor system was constructed.

9. When a steel beam supports a composite deck, comprising a fluted (trapezoidal shaped) steel deck, concrete and mesh reinforcement, a cavity (or void) is formed between the top flange of the beam and the fluted deck. For fluted decks, such as those used on 7WTC, this cavity (or void) is large. Leaving the cavities between the fluted deck and top flange of the beam unfilled or inadequately filled with fire protection material results in:

    a. an increase in temperature of the top flange and web;
    b. an increase in temperature of the shear studs;
    c. reduction in load capacity of beams during a fire; and
    d. reduction in overall fire resistance.

In the UL Fire Resistance Directory for 1983 and 1985 the need to fill the voids is covered by the following statement: “Cavities, if any, between the upper beam flange and floor or roof units shall be filled with the fire protection material applied to the beam, unless stated otherwise on an individual design.”

10. The photographic evidence shows that the cavities were either not filled with fire protection at all, or were so inadequately filled as to have been unfilled for all practical purposes. See Exhibit A. An example of flutes in the process of being filled with fire protection on a different building is shown in Exhibit B. Exhibit C, which appears in the American Institute of Steel Construction Design Guide, shows another example where the flutes have been filled with fire protection.[1] Failure to construct the building with adequate fire protection by filling the voids reduced the fire resistance below building code requirements.

11. The structural fire protection was specified by the 7WTC architect based on a restrained system. However, the main girder from Column 79 to 44 was not designed and constructed as restrained. The girder did not have a sufficient number of shear studs[2] and the connections were not constructed to allow the adequate transfer of thermal thrusts to the supports as specified in the UL Fire Resistance Directory for 1983 and 1985. Specifying a level of fire protection based on restrained systems to a constructed unrestrained system resulted in a reduction of fire resistance for 7WTC.

12. The combination of very large floor bays, transfer trusses, cantilevered girders and unusual angles at which beams, girders and columns joined created a building that required careful examination and construction to ensure structural integrity. Such an examination and construction would include, but not necessarily be limited to:

i. Design and construction of connections to allow adequate tying;
ii. Design and construction of the building such that removal of one structural element, either a beam, column or truss, would not result in global collapse;
iii. Increasing the normal factor-of-safety against failure, through design and construction, of any structural member within a building which, if it failed, would lead to global collapse.

13. Inadequate consideration was given to the structural integrity of 7WTC, despite the structural issues listed above. Construction of 7WTC without regard for its structural integrity was the cause of the global collapse of WTC 7 on September 11, 2001.

---

[1] Steel Design Guide 19: *Fire Resistance of Structural Steel Framing.* American Institute of Steel Construction, December 2003

[2] Evidence discovered after June 15, 2009 revealed that, contrary to the information I had reviewed prior to that date, some shear studs were ultimately installed on each floor on the girder running between columns 79 and 44. This was done to increase the ability of this part of the structure to support an additional 10 psf load above the original design load. As a result, only 30 shear studs were installed, which, in my opinion, was not sufficient to transfer thermal thrusts. For a fully composite girder a total of 96 shear studs would be required, which would have transferred the thermal thrusts.

14. Because of the building's lack of structural integrity, an initial localized failure at column 79 precipitated a global collapse of the building.

15. Constructing the building with adequate structural integrity could have been achieved at a cost insignificant in relation to the total cost of construction of the building.

I declare under penalty of perjury that the foregoing statements made by me are true. I am aware that if any of the foregoing statements made by me are willfully false, I may be subject to punishment.

COLIN G. BAILEY

DATED: April 10, 2010

Franklin M. Sachs (FS6036)
GREENBAUM, ROWE, SMITH & DAVIS LLP
Metro Corporate Campus One
P.O. Box 5600
Woodbridge, New Jersey 07095
Telephone: (732) 549-5600

UNITED STATES DISTRICT COURT
SOUTHERN DISTRICT OF NEW YORK

IN RE: SEPTEMBER 11 PROPERTY DAMAGE AND BUSINESS LOSS LITIGATION	:	21 MC 101 (AKH)
AEGIS INSURANCE SERVICES, INC., et al., Plaintiffs, -against- 7 WORLD TRADE CENTER COMPANY, L.P., et al., Defendants.	:	04 CV 7272 (AKH) **SUPPLEMENTAL AND AMENDED SECOND DECLARATION OF COLIN G. BAILEY**

I, Colin G. Bailey, declare:

1. I have been a practicing structural engineer for 22 years and I am presently a Professor of Structural Engineering at Manchester University in Manchester, England.

2. Among my specialties are the fire safety engineering of structures and steel-concrete composite systems. I am a Fellow of the Institution of Civil Engineers (FICE), a member of the Institution of Structural Engineers (MIStructE), and a member of the Institution of Fire Engineers (MIFireE). My curriculum vita is attached hereto as Exhibit 1.

3. In 2007, I was retained by counsel for Plaintiffs in this case to provide expert analysis with respect to the cause of the global collapse of World Trade Center 7 on September 11, 2001.

4. Since that time, I have reviewed thousands of documents, drawings, and photographs, and actively participated in and reviewed the computer fire modeling performed on behalf of the Plaintiffs in this case.

5. The opinions that follow are based on that review and activity, and are made to a reasonable degree of scientific probability. These opinions and the data and materials relied upon in forming these opinions are more fully set forth in my report dated February 15, 2010, attached hereto as Exhibit D and made a part hereof.

6. Based on my work to date, including computer modeling at the University of Edinburgh in which many columns were removed in the model to see the effect on the structure of the building, it is my opinion that any structural damage caused by debris from the collapse of WTC 1 or WTC2 played no part in the collapse of 7WTC.

7. Based on my work to date, including computer models by the University of Edinburgh, it is my opinion that if there had been a diesel fuel fire on September 11 involving between 7,350 and 9,300 gallons of diesel fuel on the fifth floor of 7WTC in the area of the transfer trusses, such a fire would have compromised the strength of the transfer trusses, and could have caused them to fail, resulting in the collapse of columns 79 and/or 80.

8. The computer modeling completed to date supports the conclusion that 7WTC would have collapsed as a result of typical office contents fires because of several design/construction failures, including the failure to adequately fireproof the flutes of the metal floor decking for 7WTC and the failure to ensure that a restrained floor system was constructed.

9. When a steel beam supports a composite deck, comprising a fluted (trapezoidal shaped) steel deck, concrete and mesh reinforcement, a cavity (or void) is formed between the top flange of the beam and the fluted deck. For fluted decks, such as those used on 7WTC, this cavity (or void) is large. Leaving the cavities between the fluted deck and top flange of the beam unfilled or inadequately filled with fire protection material results in:

   a. an increase in temperature of the top flange and web;
   b. an increase in temperature of the shear studs;
   c. reduction in load capacity of beams during a fire; and
   d. reduction in overall fire resistance.

10. In the UL Fire Resistance Directory for 1983 and 1985 the need to fill the voids is covered by the following statement: "Cavities, if any, between the upper beam flange and floor or roof units shall be filled with the fire protection material applied to the beam, unless stated otherwise on an individual design."

11. The photographic evidence shows that the cavities were either not filled with fire protection at all, or were so inadequately filled as to have been unfilled for all practical purposes. See Exhibit A. An example of flutes in the process of being filled with fire protection on a different building is shown in Exhibit B. Exhibit C, which appears in the American Institute of Steel Construction Design Guide, shows another example where

the flutes have been filled with fire protection.[1] Failure to construct the building with adequate fire protection by filling the voids reduced the fire resistance below building code requirements.

12. The structural fire protection was specified by the 7WTC architect based on a restrained system. However, the main girder from Column 79 to 44 was not designed and constructed as restrained. The girder did not have a sufficient number of shear studs[2] and the connections were not constructed to allow the adequate transfer of thermal thrusts to the supports as specified in the UL Fire Resistance Directory for 1983 and 1985. Specifying a level of fire protection based on restrained systems to a constructed unrestrained system resulted in a reduction of fire resistance for 7WTC.

13. The combination of very large floor bays, transfer trusses, cantilevered girders and unusual angles at which beams, girders and columns joined created a building that required careful examination and construction to ensure structural integrity. Such an examination and construction would include, but not necessarily be limited to:

    i. Design and construction of connections to allow adequate tying;
    ii. Design and construction of the building such that removal of one structural element, either a beam, column or truss, would not result in global collapse;
    iii. Increasing the normal factor-of-safety against failure, through design and construction, of any structural member within a building which, if it failed, would lead to global collapse.

14. Inadequate consideration was given to the structural integrity of 7WTC, despite the structural issues listed above. Construction of 7WTC without regard for its structural integrity was the cause of the global collapse of WTC 7 on September 11, 2001.

15. Because of the building's lack of structural integrity, an initial localized failure at column 79 precipitated a global collapse of the building.

16. Constructing the building with adequate structural integrity could have been achieved at a cost insignificant in relation to the total cost of construction of the building.

---

[1] Steel Design Guide 19: *Fire Resistance of Structural Steel Framing.* American Institute of Steel Construction, December 2003

[2] Evidence discovered after June 15, 2009 revealed that, contrary to the information I had reviewed prior to that date, some shear studs were ultimately installed on each floor on the girder running between columns 79 and 44. This was done to increase the ability of this part of the structure to support an additional 10 psf load above the original design load. As a result, only 30 shear studs were installed, which, in my opinion, was not sufficient to transfer thermal thrusts. For a fully composite girder a total of 96 shear studs would be required, which would have transferred the thermal thrusts.

I declare under penalty of perjury that the foregoing statements made by me are true. I am aware that if any of the foregoing statements made by me are willfully false, I may be subject to punishment.

COLIN G. BAILEY

DATED: April 5, 2010

CURRICULUM VITAE.

Name: **PROFESSOR COLIN GARETH BAILEY** BEng, PhD, CEng, FICE, MIStructE, MIFireE

Address	18 Wellington Road	*Date of Birth*:	11/04/67
	Timperley	*Age:*	42
	Altrincham	*Tel. No.*	0161-306-5795
	Cheshire		
	WA15 7RE	E-mail	Colin.Bailey@manchester.ac.uk

Education.

1992 - 1995	University of Sheffield, Postgraduate studies (PhD), investigating the behaviour of steel-framed buildings subjected to fire.
1989 - 1992	University of Sheffield, Undergraduate studies in Civil and Structural Engineering.
1986 - 1988	Richmond Upon Thames College, Twickenham. (Part-time, day release studying Civil Engineering).
1984 - 1986	Slough College, Wellington Street, Slough. (Part-time, day release studying Civil Engineering).
1978 - 1984	Abbotsfield Comprehensive School.

Qualifications.

1995	Doctorate in Civil and Structural Engineering
1992	First Class Honours (BEng) in Civil and Structural Engineering (Position in year; 1st).
1988	Higher National Certificate (BTec) in Civil Engineering.
1986	National Certificate (BTec) in Civil Engineering.
1983	8 'O' levels in, Physics, Chemistry, Mathematics, Additional Mathematics, Statistics, Graphical Communication, English and History.

Professional Affiliation

- Fellow of the Institution of Civil Engineers; Chartered Civil Engineer.
- Member of the Institution of Structural Engineers; Chartered Structural Engineer.
- Member of the Institution of Fire Engineers; Chartered Fire Engineer.

Professional/academic prizes.

1. 2008: The Institution of Structural Engineers **Henry Adams Diploma Award,** for the research paper "Development of a new long span composite floor system", published in The Structural Engineer. Vol. 84, No. 21, Nov. 2006"
2. 2001: The Institution of Structural Engineers **Henry Adams Diploma Award,** for the research paper "*The structural behaviour of steel frames with composite floorslabs subject to fire: Part 1 and Part 2: Theory and Design*", published in The Structural Engineer, Vol. 78 No.11, 11th June 2000, pp 19-33.
3. 2000: The Institution of Structural Engineers **Henry Adams Diploma Award,** for the research paper "*The behaviour of full-scale steel-framed buildings subjected to compartment fires*", published in The Structural Engineer, Vol. 77 No. 8, 8th April 1999, pp 15-21.
4. 2000. **BRE Publication Award 2000:** Best Research Paper "*The structural behaviour of steel frames with composite floorslabs subject to fire: Part 1: Theory*" published in The Structural Engineer, Vol. 78 No. 11, June 2000, pp 19-33.
5. 1999. **BRE Publication Award 1999:** Best Research Paper "*The Structural behaviour of steel columns during a compartment fire in a multi-storey braced steel-frame*" published in the Journal of Constructional Steel Research, Vol. 52 No.2, 1999. pp 137-157
6. 1997: The Institution of Structural Engineers **Henry Adams Diploma Award,** for the research paper "*Computer simulation of a full-scale structural fire test*", published in The Structural Engineer, Vol.74 No. 6, 19th March 1996.
7. 1992: Institute of Civil Engineers prize and Mappin Medal (**Sheffield University faculty prize**), for first place in the final-year examinations at Sheffield University.

Publications.

95 journal papers, conference papers and design guides (books) have been published in the field of structural engineering and structural fire engineering (refer page 4).

Professional activities

- Elected Member of the Council of the Institution of Structural Engineers (2004-2007).
- Invited member of the Engineering Practice Committee and the Fire Engineering Task Group of the Institution of Structural Engineers (since 2004).
- Chairman of the Concrete Fire Forum, which is funded by Industry (since 2003).
- Member of the UK Steel Fire Strategy Group (since 2000).
- Member of the UK Steel Sector Committee on Codes and Standards (since 2002).
- UK National Technical Contact for BSEN1994-1-2 (European fire design of composite structures–since 1998).
- Member of the Joint Board of Moderators for accreditation of UG and PGT programmes (since 2006).
- Accreditation visits to various universities.
- Member of the Editorial Board for the Journal of Steel Constructional Research (since 2007).
- Co-Chair of the World Congress on Engineering (Mechanical Engineering) 2007
- Member of the EPSRC Review College (since 2004)
- Reviewer for research proposals from EPSRC, UK-India Education and Research Initiative, City University of Hong Kong, Singapore Ministry of Education, Levenhulme Trust and the Royal Society.
- Development of position papers (precast, prestressed structures and fire safety) for the concrete Industry.
- Invited Member of the European TC3 Technical Committee on fire design of steel structures.
- Member of the Working Group drafting the UK National Annex to Eurocodes EN1993-1-2 and EN1994-1-2.

Employment history. (1984 - to present day)

The University of Manchester
(August 2002-to-present day)
Head of School of Mechanical, Aerospace and Civil Engineering and Professor of Structural Engineering.
A summary of my main activities is listed below:

- September 2007 to present, Head of School responsible for a budget of £23.6M and line manager for 78 academic staff , 84 support staff and 63 research staff. The School has just over 1000 UG students, 400 PGT students and 200 PGR students. As well as the day-to-day running of the School I am responsible for developing the School's strategy to deliver the University's goal of to be one of the top 25 universities in the world by 2015.
- 2004-2007, Head of the Dynamics, Structures and Design Academic Interest Group and Head of the Fire and Structures Research Group within the School of Mechanical, Aerospace and Civil Engineering, which involved being line Manager for 30 academic staff, involving the management of staff's teaching, research, administration and personal development.
- 2002-2004, Head of the Structural Engineering Division.
- 2007- present: Member of the Faculty's Leadership Team.
- Since 2004 Member of the School's SLT, and UG, Research and Postgraduate Committees – now Chair of SLT.
- Teaching concept, concrete and steel design to Undergraduate and Postgraduate students.
- Monitoring and assessment of all design, materials and analysis courses.
- Obtaining 'personal' research income (current value £2.4M), and management of research projects (refer page 8).
- Project Manager for the Dti funded 'One-Stop-Shop for Structural Fire Engineering'.
- Conducting experimental and theoretical research in Fire and Structural Engineering.
- Supervision and management of 15 PhD students and 7 Research Associates.
- Director of the MSc course in Structural Engineering.
- 2004-2008 External Examiner for the University of Bradford undergraduate Civil Engineering programmes.
- 2003-2007 External Examiner for the University of Ulster undergraduate programme Civil Engineering with Industrial Studies.
- 2007-2010 External Examiner for City University London MSc programmes (MSc/PG Diploma Civil Engineering Structures and MSc/PG Diploma Design and Analysis of Structures for Hazards).

- 2007-2010 External Examiner for Newcastle University for MEng/BEng degrees in Civil Engineering and Civil and Structural Engineering.
- External PhD examiner for University of Edinburgh, University of Sheffield, University of Central Lancashire [2], Aston University, Swansea University [2], Ulster University, Heriot Watt University and Nanyang Technological University Singapore [2].
- Internal examiner for numerous PhD students.
- Expert Witness in Fire Engineering.
- Third Party Reviewer for London City and Southwark.
- Keynote presentations at 5 International Conferences.
- Numerous International and National presentations and workshops to practitioners.
- Development of design guides in Structural Fire Engineering and Wind Loading.
- Collaboration with Industry including Chiltern Fire, The London Fire Brigade, Steel Construction Institute, Corus, The Concrete Centre, Building Research Establishment, Westok, Pilkington, British Constructional Steelwork Association, Tegral, Offshield, Arup, City of London, British Precast, Brick Development Association, Concrete Block Association, Tarmac, HSL, Buro Happold, WSP, Halcrow, and British Cement Association.

The Building Research Establishment:
(January 1998 – August 2002)
My main duties at the Building Research Establishment comprised;

- Conducting experimental and theoretical research into all aspects of structural fire design (comprising steel, concrete, timber and masonry structures).
- Carrying out experimental and theoretical research into steel connections.
- Writing design guides (BRE digests and SCI Publications) in structural fire design and wind loading.
- Writing proposals for research and consultancy work.
- Managing projects/contracts to ensure they stay within budget.
- Securing an annual income exceeding £250K.
- Calibration of the Eurocodes dealing with the design of steel and composite structures.
- Acting as National Technical Contact for Eurocode 4 Part 1.2.
- Chairman of the Working Group to draft the amendment to BS5950-8 (Fire Design of Structural Steelwork).
- Presentations to practising designers.

The Steel Construction Institute (SCI).
(January 1996 – January 1998)
Whilst employed by the Steel Construction Institute, my main duties comprised;

- Writing SCI published guides for the design of steel-framed buildings in fire.
- Manning an advisory desk, which involved answering questions from practising engineers on all aspects of steel design.
- Presenting on CPD courses run by the Institution of Structural Engineers and SCI.
- Providing background research and comments on the structural fire parts of the Eurocodes to allow development of the UK. National Application Documents.
- Non-linear modelling of steel structures at ambient and elevated temperatures.
- Development of fire design rules for the UK slim floor systems, marketed by Corus.

University of Sheffield.
(April 1994 - January 1996)
Research Assistant.
I completed a research contract which involved developing a computer program to investigate the behaviour of steel-framed buildings subjected to fire spread. The work required to fulfil this contract was completed in parallel

to my Doctorate studies. I also gained valuable experience of supervising undergraduates and teaching IT skills during this period.

(From September 1989 to April 1994, I was in full-time education at the University of Sheffield)

Clarke Nicholls and Marcel, Consulting Civil and Structural Engineers.
(November 1988 - September 1989).
Design Engineer.
During this period I was employed as Chief Designer for a seven-storey concrete framed office block, erected at Camomile Court, London (Value £15.5 Million). This involved producing full design calculations and supervising a team of draughtsmen in the production of general arrangement and reinforcement drawings. I also carried out feasibility studies for a £38 Million building project at Elephant and Castle, London and once the contract was awarded, load path calculations and foundation designs, comprising raft and piled foundations were produced.

Cameron Taylor Partners, Consulting Civil and Structural Engineers.
(September 1986 - November 1988)
Technician / draughtsman.
My main duties consisted of producing full working drawings for new-build and refurbishment works. These drawings comprised general layouts, steel connection details and reinforcement layouts. Numerous site visits were carried out, mainly to check reinforcement fixing before pouring of concrete. Design calculations for both steel and concrete projects were also undertaken.

Lovell Construction Services Limited, Design Department.
(September 1984 - September 1986)
Technician / draughtsman.
My main duties comprised production of working drawings including general arrangement and reinforcement layouts, together with reinforcing schedules. I also checked site work and provided design advice when required.

Journal and Conference Publications

1. **Bailey C.G.**, Burgess I.W. and Plank R.J. The Behaviour of Steel-Framed Structures Subjected to Local Fire Conditions. *Proceedings of the Nordic Steel Construction Conference '95 Melmo, Sweden.* June 1995, pp 693-700 Swedish Institute of Steel Construction. Publication 150, Vol. II.

2. **Bailey C.G**, Burgess I.W. and Plank R.J. The Lateral-torsional Buckling of Unrestrained Beams in Fire. *Journal of Constructional Steel Research* Vol. 36 No.2 1996. pp 101-119.

3. **Bailey C.G**, Burgess I.W. and Plank R.J. Computer simulation of a full-scale structural fire test. *The Structural Engineer.* Vol. 74 No.6 1996. pp 93-100.

4. **Bailey C.G.**, Burgess I.W. and Plank R.J. Analyses of the Effects of Cooling and Fire Spread on Steel-Framed Buildings. *Fire Safety Journal.* No.26 1996 pp 273-293.

5. Plank R.J., Burgess I.W. and **Bailey C.G**. Modelling the behaviour of steel-framed building structures by computer. *Proceedings of the Second Cardington Conference.* March 1996.

6. **Bailey C.G.**, Burgess I.W. and Plank R.J. 'Structural Simulation of Fire Tests on a Full-Scale Composite Building Frame' , SSRC IC/Brasil '96 - 5th Colloquium on Structural Stability, Rio de Janeiro, August 1996.

7. **Bailey C.G.**, Burgess I.W. and Plank R.J. Bridging and Restraint Effects of Localised Fires in Composite Frame Structures. *Composite Construction - Conventional and Innovative International Conference Innsbruck, Austria.* September 16-18 1997, pp 379-384 IABSE.

8. Rose P.S., Burgess I.W., Plank R.J. and **Bailey C.G.** The influence of floor slabs on the structural behaviour of composite frames in fire. *The Fourth International Kerensky Conference, Hong Kong.* September 3-5 1997, pp 511-518.

9. **Bailey C.G.** and Newman G.M. The design of steel framed buildings without applied fire protection. *The Structural Engineer.* Vol. 76 No.5 1998. pp 77-81.

10. **Bailey C.G.** Development of computer software to simulate the structural behaviour of steel-framed buildings in fire. *Computers and Structures* **67** 1998 pp 421-438.

11. **Bailey C.G.** Computer modelling of the corner compartment fire test on the large-scale Cardington test frame. *Journal of Constructional Steel Research* Vol. 48 No.1 1998. pp 27-45.

12. Rose, P.S., **Bailey, C.G.**, Burgess, I.W. and Plank, R.J.'The Influence of Floor Slabs on the Structural Performance of the Cardington Frame in Fire', Second World Conference on Constructional Steel Design, San Sebastian, *Journal of Constructional Steel Research*, 46:1-3, Paper No. 181 (1998).

13. **Bailey C.G.** The behaviour of asymmetric slim floor steel beams in fire. *Journal of Constructional Steel Research* Vol. 50 No.3 1999. pp 235-257.

14. **Bailey C.G.**, Lennon T., and Moore D.B. The behaviour of full-scale steel-framed buildings subjected to compartment fires. *The Structural Engineer* Vol. 77 No. 8 April 1999 pp. 15 - 21.

15. **Bailey C.G.**, Moore D.B and Lennon T. The structural behaviour of steel columns during a compartment fire in a multi-storey braced steel-frame. *Journal of Constructional Steel Research* Vol. 52 No.2 1999. pp 137-157.

16. **Bailey C.G.**, Lennon T., and Moore D.B. Full scale fire test on the new UK slim floor system. *Advances in Steel Structures. Proceedings of the Second International Conference on Advances in Steel Structures.* 15-17 Dec 1999, Hong Kong China. pp 1055- 1062.

17. **Bailey C.G.** The influence of the thermal expansion of beams on the structural behaviour of columns in steel-framed structures during a fire. *Engineering Structures* Vol. 22 No. 7 2000. pp 755-768.

18. **Bailey C.G.** Effective lengths of concrete-filled steel square hollow sections in fire. *Proceedings of the Institution of Civil Engineers, Structures and Buildings.* May 2000. pp 169-178.

19. **Bailey C.G**, White D.S. and Moore D.B. The tensile membrane action of unrestrained composite slabs simulated under fire conditions. *Engineering Structures* Vol. 22 No. 12 2000. pp 1583-1595.

20. **Bailey C.G.** and Moore D.B. The structural behaviour of steel frames with composite floorslabs subject to fire: Part 1: Theory. *The Structural Engineer* Vol. 78 No. 11 June 2000 pp. 19 – 27.

21. **Bailey C.G.** and Moore D.B. The structural behaviour of steel frames with composite floorslabs subject to fire: Part 2: Design. *The Structural Engineer* Vol. 78 No. 11 June 2000 pp. 28 – 33.

22. **Bailey C.G.** The experimental and theoretical behaviour of composite floor slabs during a fire. *Proceedings of the Seventh International Symposium on Structural Failure and Plasticity (IMPLAST 2000).* 4-6th October 2000 Melbourne, Australia. pp. 635-640.

23. **Bailey C.G.** Membrane action of unrestrained lightly reinforced concrete slabs at large displacements. *Engineering Structures* Vol. 23 No. 5 2001. pp 470-483.

24. **Bailey C.G.** A Simple new fire design method to predict the structural response of steel frames with composite floors. *NSCC 2001 9th Nordic Steel Construction Conference, Helsinki, Finland 18-20 June 2001.* pp 557-564.

25. HuangZ., Burgess, I.W., Plank, R.J., and **Bailey C.G.** Strategies for Fire Protection of Large Composite Buildings. *Proceedings Interflam 2001.* Edinburgh (2001) pp 395-406.

26. **Bailey C.G.** Simplified wind net pressures coefficients for the design of portal frames. *The Structural Engineer.* Vol. 80. No.4. 14 February 2002. pp 21-27.

27. HuangZ., Burgess, I.W., Plank, R.J., and **Bailey C.G.** Comparison of BRE Simple Design Method for Composite Floor Slabs in Fire with Non-Linear FE Modelling. *Proceedings of the Second International Workshop on Structures in Fire.* Christchurch, New Zealand (2002) pp 83-94.

28. Lennon T., **Bailey C.G.** and Clayton N. The Performance of High Grade Concrete Columns in Fire. *6th International Symposium on Utilization of High Strength / High Performance Concrete.* Leipzig. June 2002. pp 341- 353.

29. **Bailey C.** Holistic behaviour of concrete buildings in fire. *Proceedings of the Institution of Civil Engineers: Structures & Buildings 152.* Aug 2002, Issue 3. pp 199-212.

30. **Bailey C.G.** Structural Fire Design of Unprotected Steel Beams Supporting Composite Floor Slabs. Keynote: *II CICOM, II International Conference on Steel Construction.* São Paulo, Brazil. Nov.2002.

31. **Bailey C.G.** Efficient arrangement of reinforcement for membrane behaviour of composite floor slabs in fire conditions. *Journal of Constructional Steel Research* Vol. 59 No. 7 July 2003, pp.931-949.

32. **Bailey** C.G. Large scale fire test on a composite slim-floor system. *Steel and Composite Structures.* Volume 3, Number 3, June 2003 pp.153-168.

33. **Bailey C.** Holistic behaviour of concrete buildings in fire. Journal of the Structural Engineering Society New Zealand. Vol. 16 No. 1 April 2003. pp 35 51.

34. Foster S.J, **Bailey C.G**, Burgess I.W and Plank R.J. Experimental Behaviour of Concrete Floor Slabs at Large Displacements. *Engineering Structures.* 26 (2004) pp 1231-1247.

35. **Bailey C.G.** Structural fire design: core or specialist subject? *The Structural Engineer.* Vol.82. No. 9, May 2004, pp 32-38.

36. Huang Z., Burgess I., Plank R. and **Bailey** C. Comparison of BRE simple design method for composite floor slabs in fire with non-linear FE modelling. *Fire and Materials.* Vol. 28, No. 2-4. March-August 2004, pp. 127-138.

37. **Bailey C.G.** Membrane action of composite floor systems in fire. *Third International Workshop, Structures in Fire. Ottawa* May 2004 Paper S7-1, pp 335-352.

38. **Bailey C.G.** Membrane Action of Slab/Beam Composite Floor Systems in Fire. *Engineering Structures.* 26, 2004. pp 1691-1703.

39. **Bailey C.G.** Indicative Fire Tests to Investigate the Behaviour of Cellular Beams Protected with Intumescent Coatings. *Fire Safety Journal.* 39 2004 pp 689-709.

40. **Bailey C.G.** Recent advances in the fire engineering design of steel structures. Keynote: Innovation and Advances in Steel Structures. International Symposium 30-31 August 2004, Singapore pp. 155-175.

41. **Bailey C.G.** A Simplistic or Holistic Approach to Structural Fire Engineering? Keynote: Tall Buildings in Historical Cities – Culture & Technology for Sustainable Cities. *Proceedings of the CTBUH 2004 Seoul Conference October 10-13 2004.* pp 1- 11.

42. Pope, N., and **Bailey C. G.**, *Modelling of Compartment Fires: Analysis of the Importance of Grid Resolution and Sub-grid-scale Constants in the Validation of FDS.* International Technical Congress in Computational Simulation Models in Fire Engineering and Research, GIDAI, Spain, October 2004, pp29-45.

43. **Bailey C.G.** Fire Engineering Design of Steel Structures. *Advances in Structural Engineering.* (Invited paper) Vol.8 N0. 3. 2005.

44. Wu, Z.J. and **Bailey C.G.**, Fracture resistance of a cracked concrete beam post-strengthened with FRP sheets *International Journal of Fracture.* **135,** 2005: pp 35-49

45. Pope, N., and **Bailey C. G.**, Sub-Grid-Scale Parameters in Computational Fluid Dynamics Modelling of Compartment Fires. *Proceedings of the Tenth International Conference on Civil, Structural and Environmental Engineering Computing.* Paper 113. Italy, 30 Aug–2 Sep 2005.

46. **Bailey C.G.** Recent Advances in the Fire Engineering Design of Steel Structures. *Proceedings of the Institution of Civil Engineers: Structures & Buildings.* Paper 13998. SB1. Feb 2006. pp 21-35..

47. Pope, N., and **Bailey C. G.**, Quantitative Comparison of FDS and Parametric Fire Curves with Post-Flashover Compartment Fire Test Data. *Fire Safety Journal.* 41 (2006) pp 99-110.

48. **Bailey C.G.**, Currie P.M and Miller F.R. Development of a new long span composite floor system. *The Structural Engineer.* Vol. 84, No. 21, Nov. 2006.

49. Winter S.L, **Bailey C.G.**, Apsley D.D., Computational Fluid Dynamics Modelling of Compartment Fires. *5th International Symposium on Turbulence, Heat and Mass Transfer* pp 613-616, 2006.

50. **Bailey C.G.** and Toh, W.S. Experimental behaviour of concrete floor slabs at ambient and elevated temperatures. Proceedings of the Fourth International Workshop Structures in Fire pp 709-720, 2006.

51. Lee D.Y.C. and **Bailey C.G.** The Behaviour of Post-Tensioned Floor Slabs under Fire Conditions. *International Congress on Fire Safety in Tall Buildings,* pp 183-201. 2006

52. **Bailey C.G.** Recent Developments in Structural Fire Safety. *International Congress on Fire Safety in Tall Buildings*, pp 59-78. 2006.

53. Nadjai, A. **Bailey C.G**, Siamak B.M, Ali, F, Talamona D, Allam, A. Behaviour of Composite Floor Cellular Steel Beams at Elevated Temperatures. *International Congress on Fire Safety in Tall Buildings*, pp 359-371. 2006.

54. . Tafreshi A, **Bailey C G**. 2007. "Instability of Imperfect Composite Cylindrical Shells under Combined Loading". Composite Structures. Vol. 80. Issue 1. pp 49-64.

55. Pope N, **Bailey C G**. 2007. "Development of a Gaussian glass breakage model within a fire field model". Fire Safety Journal. Vol. 42. Issue 5. pp 366-376. July.

56. **Bailey C G**, Toh W.S. 2007. "Small-scale concrete slab tests at ambient and elevated temperatures". Engineering Structures. Issue 29. pp 2775-2791.

57. **Bailey C G**, Johnson K.A., Alonso-Rasgado T A, Orzechowski M.A.. 2007. "The quality of design within the built environment". The Structural Engineer. Vol. 23/24. Issue 85. pp 49-55. December

58. Miller F.R, **Bailey C G**. 2007. "Design concept for a novel long span composite floor system". The Structural Engineer. Vol. 85. No. 21. pp 38-47. November.

59. **Bailey C G**, Toh W.S. 2007. "Behaviour of concrete floor slabs at ambient and elevated temperatures". Fire Safety Journal. Vol. 42. Issue 6-7. pp 425-436. September.

60. **Bailey C G**. "Structural fire engineering of steel framed buildings - Keynote". Proceedings of the 3rd International Conference on Steel and Composite Structures (ICSCS07), Manchester, UK. pp 57-65. 30 July 2007.

61. Lee D.Y., **Bailey C G**. "The Behaviour of Post-Tensioned Floor Slabs under Fire Conditions.". SEMC 2007 The Third International Conference on Structural Engineering, Mechanics and Computation, University of Cape Town, South Africa. pp 1253-1257. September 2007.

62. Gweli S S, Nedwell P J, **Bailey C G**. "The use of high performance non metallic fibre in Ferrocement". SEMC 2007, The Third International Conference on Structural Engineering, Mechanics and Computation, University of Cape Town, South Africa. pp 1417-1422. September 2007.

63. Bake S, **Bailey C G**. "Performance of cellular steel beams at ambient and elevated temperatures". SEMC 2007 The Third International Conference on Structural Engineering, Mechanics and Computation, University of Cape Town, South Africa. pp 1268-1273. September 2007.

64. Ellobody E, **Bailey C G**. "Experimental and Numerical Investigation of Post-Tensioned Unbonded Concrete Slabs in Fire". Interflam 2007 11th International Fire Science & Engineering Conference, UK. pp 617-628. 3 September 2007.

65. Dai X, Wang Y C, **Bailey C G**. "Temperature distributions in unprotected steel connections in fire". Proceedings of the 3rd International Conference on Steel and Composite Structures (ICSCS07), Manchester, UK. Editor Wang, Y.C. & Choi, C.K.. pp 535-540. 30 July 2007.

66. Bake S, **Bailey C G**. "Numerical studies of cellular beams at elevated temperatures". ICASS 2007, The Fifth International Conference on Advances in Steel Structures, Singapore.. pp 750-756. December 2007.

67. Nadjai A, Goodfellow N, Talamona D, Ali F, **Bailey C G**, Siamak B.M. "Experimental and numerical investigation on composite floor cellular steel beams in fire". Proceedings of the 3rd International Conference on Steel and Composite Structures (ICSCS07), Manchester, UK. pp 673-679. 30 July 2007.

68. Giroldo F, **Bailey C G**. "Bond behaviour of welded mesh reinforcement at elevated temperatures". SEMC 2007 The Third International Conference on Structural Engineering, Mechanics and Computation, University of Cape Town, South Africa. pp 1236-1241. September 2007.

69. Toh W.S, **Bailey C G**. "Comparison of Simple and Advanced Models for Predicting Membrane Action on Long Span Slab Panels in Fire". Interflam 2007 11th International Fire Science & Engineering Conference, UK. pp 791-796. 3 September 2007.

70. Giroldo F, **Bailey C G**. 2008. "Experimental bond behaviour of welded mesh reinforcement at elevated temperatures". Magazine of Concrete Research. Vol. 60. No. 1. pp 23-31. February.

71. **Bailey C G**, Toh W.S, Chan B.M. 2008. "Simplified and Advanced Analysis of Membrane Action of Concrete Slabs". ACI Structural Journal. Vol. 105. No. 1. pp 30-40. January.

72. Ellobody E, **Bailey C G**. 2008. "Behaviour of Unbonded Post-tensioning One-Way Concrete Slabs". Advances in Structural Engineering. Vol. 11. No. 1. pp 107-120.

73. **Bailey C G**, Lennon T. "Full-scale fire tests on hollowcore floors". The Structural Engineer. pp 33-39. March 2008.

74. Ellobody E, **Bailey C G**. "Testing and modelling of bonded and unbonded post-tensioned concrete slabs in fire". Proceedings of the Fifth International Conference in Structures in Fire. Singapore. pp 392-405. 28-30 May 2008

75. Dai X, Wang Y C, **Bailey C G**. "Temperature developments in partially protected steel-concrete composite joints using intumescent coating". Proceedings of the Fifth International Conference in Structures in Fire. Singapore. pp 172-183. 28-30 May 2008

76. **Bailey C G**, Ellobody E. "Fire Tests on Unbonded Post-Tensioned One-Way Concrete Slabs" Magazine of Concrete Research. Vol. 61 No. 1 2009 pp 67-76

77. Ellobody E, **Bailey C G**. "Modelling of Unbonded Post-Tensioned Concrete Slabs Under Fire Conditions". Fire Safety Journal. Vol. 44 Issue 2. 2009 pp 159-167

78. Dai X H, Wang Y C, **Bailey C G**. In Press. "Effects of partial fire protection on temperature developments in steel joints protected by intumescent coating". Journal of Constructional Steel Research.

79. Ellobody E, **Bailey C G**. "Modelling of bonded post-tensioned concrete slabs". Proceedings of ICE, Structures and Buildings. Vol. 161. Issue 6. 2008 pp 311-323

80. **Bailey C G**, Ellobody E,. 'Fire Tests on Bonded Post-Tensioned Concrete Slabs. Engineering Structures Vol. 31 Number 3, 2009 pp 686-696

81. **Bailey C G**, In Press 'Developments in Structural Fire Engineering' Structural Engineering International.

82. Dai X H, Wang Y C, **Bailey C G**. "A Simple Method to Predict Temperatures in Steel Joints with Partial Intumescent Coating Fire Protection" Fire Technology. In Press

83. **Bailey C.G**, Ellobdy E. 'Whole-building behaviour of bonded post-tensioned concrete floor plates exposed to fire'. Engineering Structures. In Press.

84. Ellobody, E. and **Bailey, C.G**. Holistic behaviour of post-tensioned concrete floors under fire conditions. Proceedings of the 11th International conference on Fire and Materials, Fire and Materials-09, San Francisco, USA, pp. 511-524, 26-28 January, 2009

Books/Design Guides:

1. **Bailey C.G.**, Newman G.M and Simms W.I., *Design of Steel Framed Buildings without Applied Fire Protection.* SCI Publication 186. The Steel Construction Institute, Ascot. 1999. ISBN 1 85942 062 1
2. Newman G.M., Robinson J,T. and **Bailey C.G.**, *Fire Safe design: A New Approach to Multi-Storey Steel-Framed Buildings.* SCI Publication P288. The Steel Construction Institute, Ascot. 2000. ISBN 1 85942 120 2.
3. **Bailey C.G.** Steel Structures supporting composite floor slabs: design for fire. BRE Digest 462. December 2001. ISBN 1 86081 527 8.
4. **Bailey C.** New fire design method for steel frames with composite floor slabs. Foundation for the Built Environment, FB5, 2003, BRE Bookshop, London. ISBN 1 86081 608 8.
5. **Bailey C.G.** *Guide to evaluating design wind loads to BS6399-2:1997.* SCI Publication P286. The Steel Construction Institute. 2003. ISBN 1 85942 134 2.
6. Introduction to the fire safety engineering of structures. The Institution of Structural Engineers. 2003. ISBN 0901297291. Member of the Task Group and contributor to drafting of text.

7. **Bailey C.G.** Structural fire engineering design: materials behaviour – Steel. BRE Digest 462. June 2004. ISBN 1 86081 699 1.
8. Advanced Structural Fire Engineering, The Institution of Structural Engineers. August 2007 (main author).
9. Newman G.M., Robinson J,T. and **Bailey C.G.**, *Fire Safe design: A New Approach to Multi-Storey Steel-Framed Buildings (Second Edition).* SCI Publication P288. The Steel Construction Institute, Ascot. 2006. ISBN 1 85942 169 5.
10. Lennon T, Moore D B, Wang Y C, **Bailey C G.** "Designers guide to EN 1991-1-2, EN 1993-1-2, EN 1994-1-2: Fire engineering (actions on steel and composite structures)". Thomas Telford, London. ISBN 978-0-7277-3157-9. 2007.
11. **Bailey C.G**, and Khoury G.A. Guide to the Fire Engineering of Concrete Structures. To be published 2009

Research Grants secured since joining Manchester in August 2002

As sole and Principal Investigator
1. Fire Performance of Concrete Structures. *The Concrete Centre*. 2003-2006. £45,000.
2. Removing Barriers to Innovative Design of Concrete Structures Imposed by antiquated Fire Design Procedures *BRE*. 2003-2006. £10,250.
3. Development of BRE Digest. 2003. *BRE*. £8,000.
4. Technical Assistance to Background Study on Concrete Fire Design. *BRE*. 2003. £5,000.
5. CFD Modelling of Compartment Fires. *EPSRC and Corus Industrial Case*. 2002-2005. £54,175
6. Development of Standard Reference Document for Steel Construction. *SCI*. 2002-2004. £19,000
7. Technical Advice *BCSA*. 2003. £3,000
8. Research and development of Cellular beams. *Westok* 2003-2005.£29,400.
9. One Stop Shop for Structural Fire Engineering *DTI* 2003-2006. £198,000
10. Pilkington Contribution to the One Stop Shop, *Pilkington*, 2005-2006 £13,333.
11. Membrane Behaviour of Composite Floor Slabs. *EPSRC Industrial Case* 2003-2006. £44,700
12. One-Day Conference on Fire Safety 2003. £18,353
13. Guide to the Fire Engineering Eurocodes. *SCI*. 2004-2006. £15,000
14. Assessment of Fire Walls using Zeta Systems. *Tegral*. 2005. £5,200
15. Research & Development into new floor system (TEKDEK) 2004-2005. £40,500
16. Advanced Fire Safety Engineering. *Institution of Structural Engineers*. 2005-2005. £9,500
17. Fire Resistance of Post-Tensioned Floor Slabs. *The Concrete Centre*. 2005. £7,500
18. Extension of the Bailey Fire Design Method. *Corus*. 2004-2005. £15,000
19. Post-tension slabs in fire *EPSRC and Arup Industrial CASE*. 2004- 2007. £64,757
20. Holistic Robustness of Post-tensioned Floor Slabs under Fire Attack *EPSRC* 2004-2007. £227,447
21. Holistic Risk Analysis for Structural Fire Engineering *Buro Happold* 2005-2008. £24,900
22. Development of Design Modules *CITB* 2006-2009. £90,000
23. Development of EBL design modules UOM 2006-2009. £60,000.
24. Behaviour of Composite Floor Plates during the Cooling Phase of a Fire. EPSRC 2007-2010. £366,000
25. Design and modelling of precast floor systems. British Precast. 2007. £25,000
26. Third Party Review – Herron Tower. City of London. 2007, £8,800
27. Third Party Review – Pinnacle. City of London. 2008, £9,600
28. Third Party Review – Trinity. City of London. 2008, £9,600
29. Third Party Review – Leadenhall. City of London. 2008, £8,800
30. Third Party Review – The Shard. Southwark. 2008, £10,600
31. Development of the Bailey Design Method with cellular beams, 2008-2010. Steel Construction Institute. £32,000

As Principal Investigator with Co-Investigators

32. CFD Modelling of Carpark Fires (with David Apsley) *EPSRC and Corus Industrial CASE*. 2004-2007. £69,257
33. Engineering Design Systems Thinking (with Anna Hiley) *Institution of Civil Engineers*. 2005. £25,000
34. Research into Engineering Design (with Teresa Alonso) *CITB and Arup*. 2005-2006. £40,000
35. Testing of blind bolts (with Paul Nedwell) Steel Construction Institute. £14,900.

As Co-Investigator

36. Robustness of Steel joints in steel framed structures in fire (with Yong Wang) *EPSRC*. 2005-2008. £240,000.

37. Characterising fundamental fire protection performance of intumescent coating under realistic conditions (with Yong Wang) EPSRC. 2008-2011. £425,000.

As Head of School

39 Support for Nuclear Fuels Technology. *Westinghouse*. 2008-2012 £500,000.

40 Securing funding from EDF to support a Chair and Research Fellow in Computational Mechanics 2009-2014. £800,000.

41 Funding from HSE to support a Chair, Lectureship and Research Fellow in Nuclear Graphite 2009-2014 (contract to be finalised) £1,100,000

Invited Lectures (since 2001)

1. Presentation to the Fire Brigade, designers and contractors for Heathrow Thermal 5, 11th Jan 2001.
2. Presentation/Workshop with SCI and Corus on the new 'Bailey' fire design method. Institution of Structural Engineers Midland Counties Branch, 23rd Jan 2001, Institution of Structural Engineers Yorkshire Branch, 24th Jan 2001 and Institution of Structural Engineers Northern Counties Branch, 20th Feb 2001.
3. Presentation at CPD course on the fire behaviour of steel framed buildings. Sheffield University 16 April 2002.
4. Presentation at the Institution of Structural Engineers on the behaviour of concrete buildings in fire. 13th June 2002.
5. Presentation to Sheffield University's research groups on the behaviour of buildings subjected to fire Sep. 2002.
6. Chairman and presenter at a one-day conference on 'Fire Safety in Buildings-What is New' Aston University 10 Sep 2002.
7. Presentation at the Institution of Structural Engineers on the behaviour of steel framed buildings in fire. 13th Feb 2003.
8. Presentation at CPD course on the fire behaviour of steel framed buildings. Sheffield University 12 May 2003.
9. Technical presentation on 'Wind Loading' to the Lancashire and Cheshire Branch of the Institution of Structural Engineers. 12th Nov. 2003. Salford University.
10. Keynote presentation on structural fire behaviour at The Steel Construction Institute's conference for academics. 12-13 Dec 2003.
11. Institution of Structural Engineers CPD Course on BS6399-2 (7 hour course presented to 60 practitioners – sole presenter June 2004).
12. Presentation of a 3-day CPD course on the design and behaviour of concrete buildings in fire at a Fire Engineering seminar organised by DICTUC and the Catholic University of Chile. Santiago, Chile. Sep 2004.
13. Presentation at one-day conference on 'Fire Safety in Buildings-What is New' Aston University 16 Sep 2004.
14. Institution of Structural Engineers CPD Course on BS6399-2 (7 hour course presented to 65 practitioners – sole presenter, April 2005).
15. Presentation at ICE Conference 'Designing for Fires in the UK – can we learn from the NIST report? 27th March 2006.
16. The Institution of Fire Engineers Graduate Lecture. Keynote Presentation 'The Art of Structural Fire Engineering' April 2007.
17. Presentation at the International Prestressed Hollowcore Association Technical Seminar Gotenburg Sweden, 6-7th November 2007.
18. Presentation at the International Prestressed Hollowcore Association – 13th Annual Conference – Stockholm Sweden, May 31st-June 2nd 2008.
19. Presentation to Building Control, Fire Brigade and design consultants on the fire parts of Eurocode 3 and 4 and the use of the Bailey Design Method – Scotland. 11th November 2008.
20. Presentation to Foster Wheeler on the fire parts of Eurocode 3 and 4 and the use of the Bailey Design Method – Reading. 3rd December 2008

Supervision of Research Associates (Since joining the university in August 2002)

1) Dr Paul Currie, January 2004-December 2005, funded by various Research Funds.
2) Dr Adam Wee Siang Toh, October 2003 – September, 2006, funded by Dti.
3) Dr Wei Hu, October 2003- September 2006, funded by Dti.
4) Dr Maciej Orzechowski, January 2005 – October 2006. funded by ICE and CITB.
5) Dr Dia Xianghe October 2005-October 2008, funded by EPSRC (with Yong Wang).
6) Dr Ehab Ellobody July 2006-June 2009, funded by EPSRC.
7) Dr Guo March 2007-Feb 2010, funded by EPSRC.

PhD Supervision (Since joining the university in August 2002)

1) Mr N. Pope, Graduated 2005, funded by EPSRC Industrial Case Studentship.
2) Mr A Melandinos, Graduated 2007, funded by The Concrete Centre,
3) Mr Salah Gweli – Graduated 2007, funded by Libyan Government (with Paul Nedwell)
4) Mr Ziyad Amer (MPhil) – Graduated 2007 funded by the Libyan Government
5) Mr D B M Chan, Graduated 2008, funded by EPSRC Industrial Case Studentship
6) Miss X Hao, 2004 – 2007, Self funded (writing up).
7) Miss F Giroldo, 2004 – 2007, funded by the Brazilian Government (writing up)
8) Mr S. Winter, 2004 – 2007, funded by EPSRC Industrial Case Studentship (with David Apsley)
9) Miss D. Lee, 2004 – 2007, funded by EPSRC Industrial Case Studentship.(writing up)
10) Mr Siamak Bake Mohamadi – 2004 – 2007, Self funded and funded by Westok. (writing up)
11) Mr Ahmad Abdullah – 2006-2009, funded by Egyptian Government (with Jack Wu)
12) Mr Fabian Ruvalcaba – 2006-2009, funded by Mexican Government (with Adrian Bell).
13) .Miss Tumadhir Borhan – 2008-2011, Funded by Iran Government.
14) Mr Muhammad Yaqub – 2006-2009, Self funded.
15) My Renga Rao Krishnamoorthy – 2007-2010, Self funded.

EXHIBIT A

10.0 APPENDIX A
Photographs showing fire protection during tenant fit-out stage

The construction of WTC7 was completed in 1987. These photographs were taken during 'fit-out' of the floors in 1989. They show that the flutes were not filled with fire protection as required. They also show in a number of cases wires being passed through the open flutes.

Figure A1: Photograph showing wire placed through flutes (46^{th} Floor).

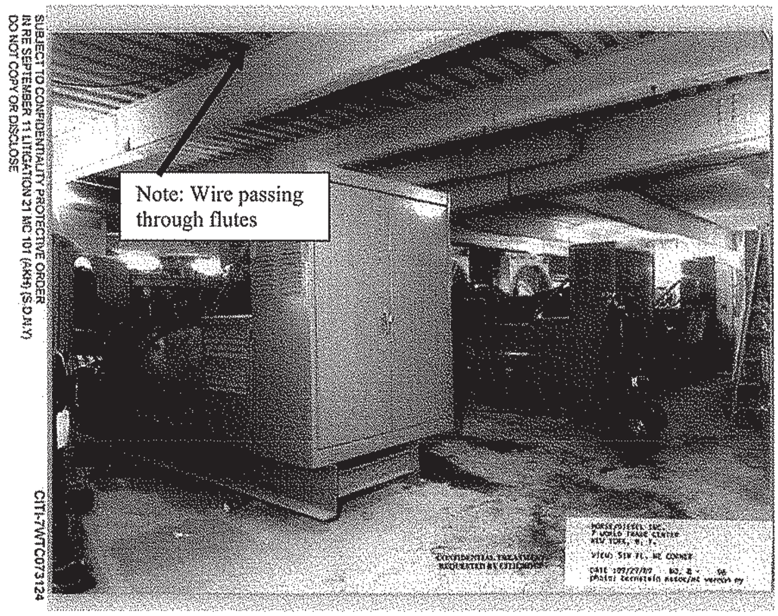

Figure A2: Photograph showing wire placed through flutes (5th Floor).

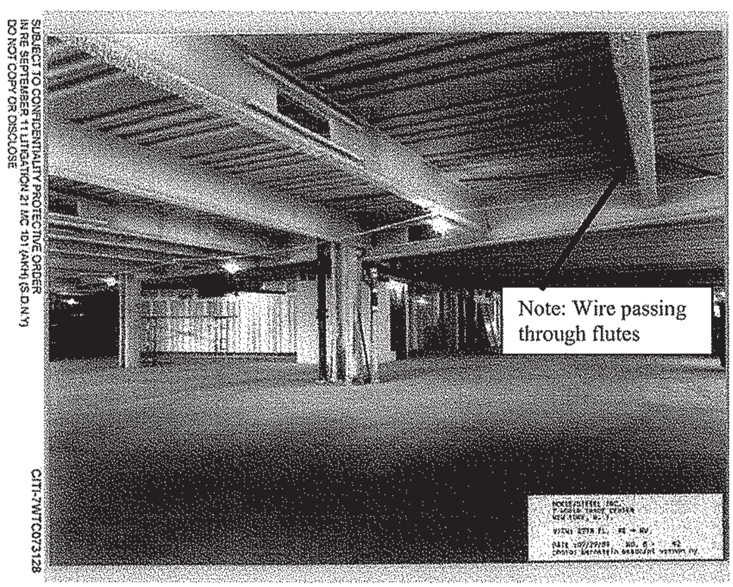

Figure A3: Photograph showing wire placed through flutes (29th Floor).

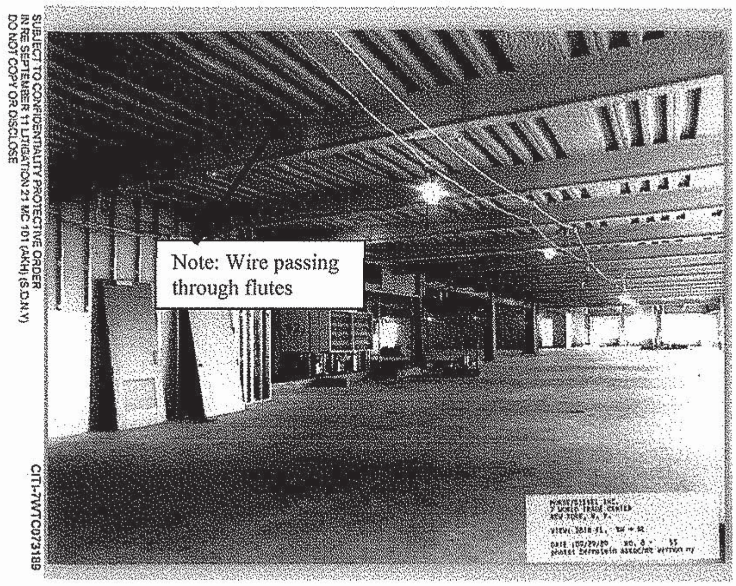

Figure A4: Photograph showing wire placed through flutes (38th Floor).

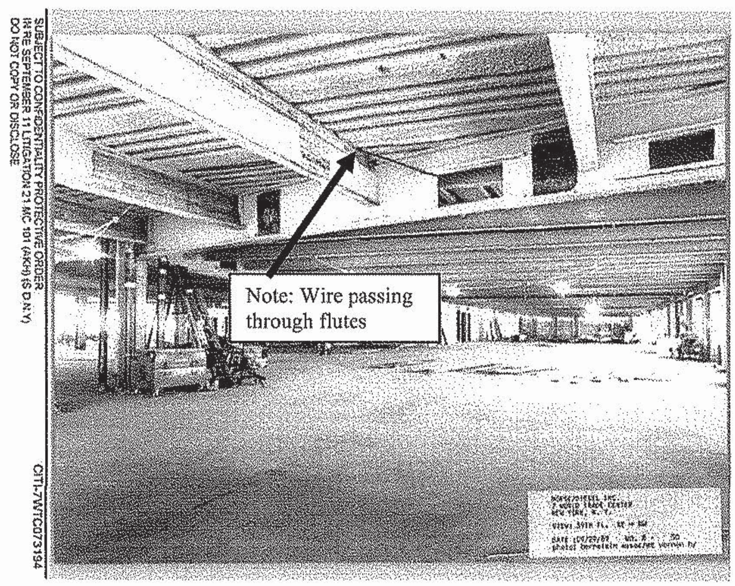

Figure A5: Photograph showing wire placed through flutes (39th Floor).

Figure A6: Photograph showing wire placed through flutes (46th Floor).

Figure A7: Photograph showing wire placed through flutes (39th Floor)

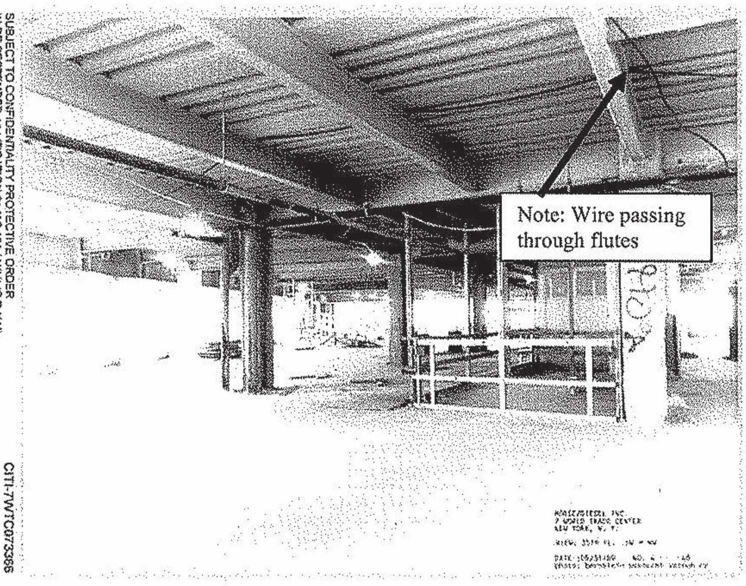

Figure A8: Photograph showing wire placed through flutes (35th Floor)

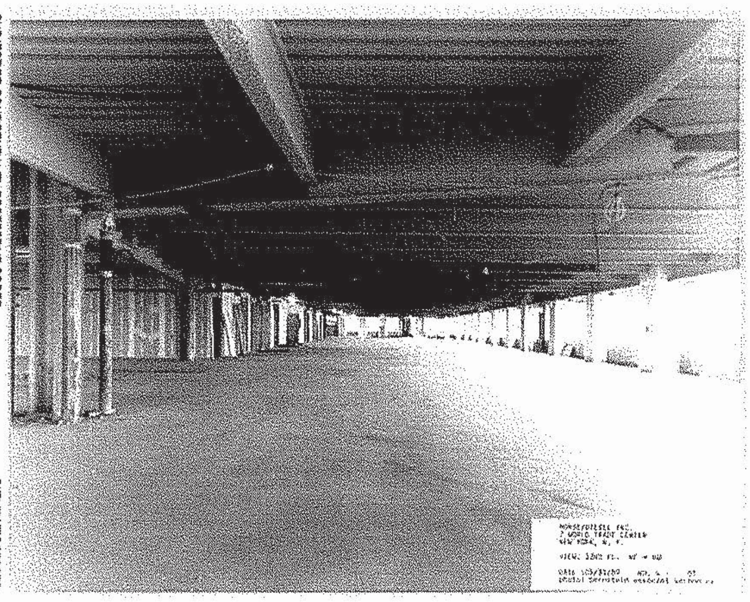

Figure A9: Photograph showing wire placed through flutes (32nd Floor)

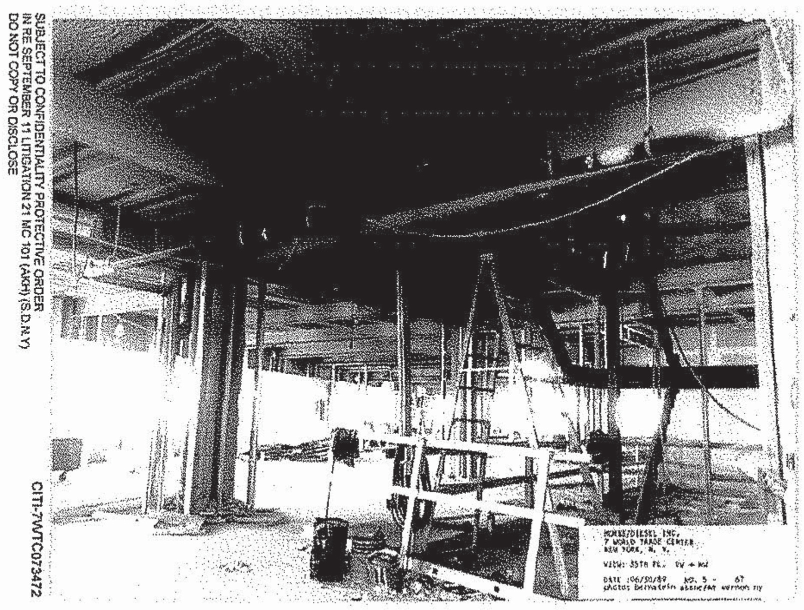

Figure A10: Photograph showing wire placed through flutes (35nd Floor)

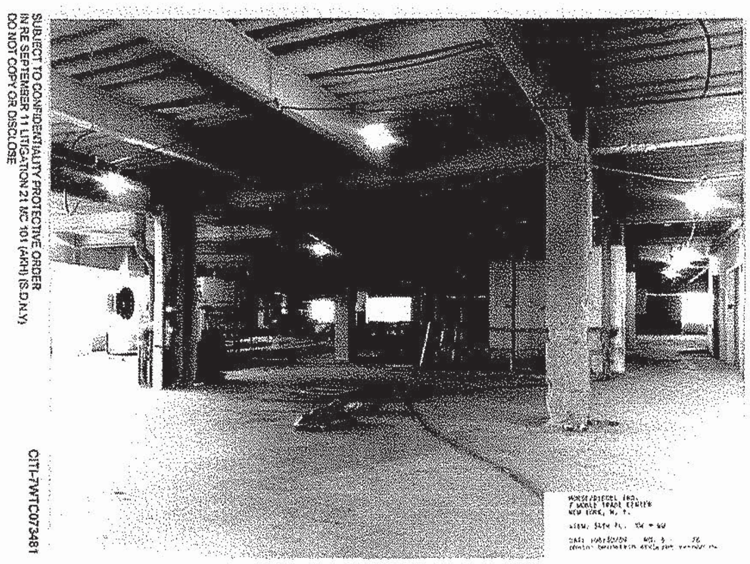

Figure A11: Photograph showing wire placed through flutes (34th Floor)

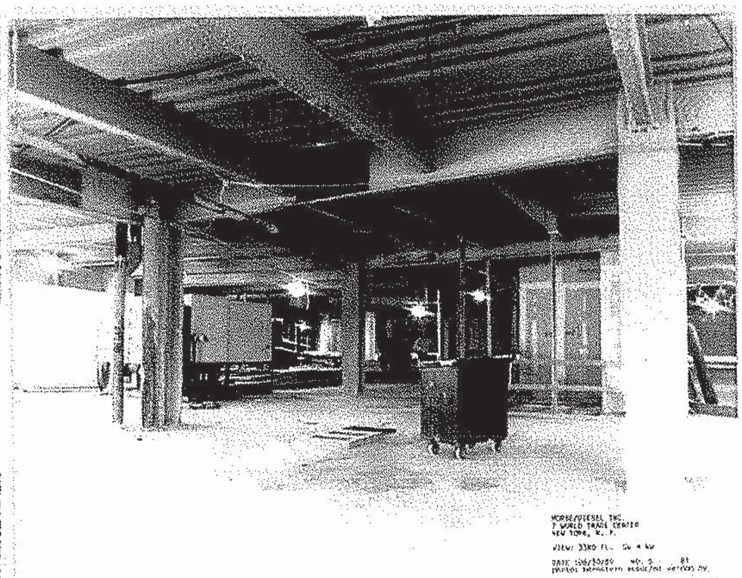

Figure A12: Photograph showing wire placed through flutes (33rd Floor)

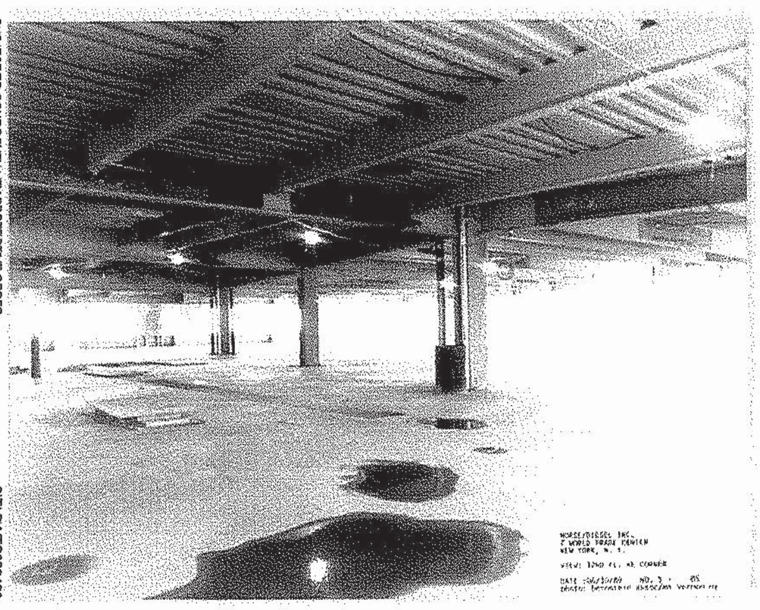

Figure A13: Photograph showing wire placed through flutes (32nd Floor)

CITI-7WTC073528

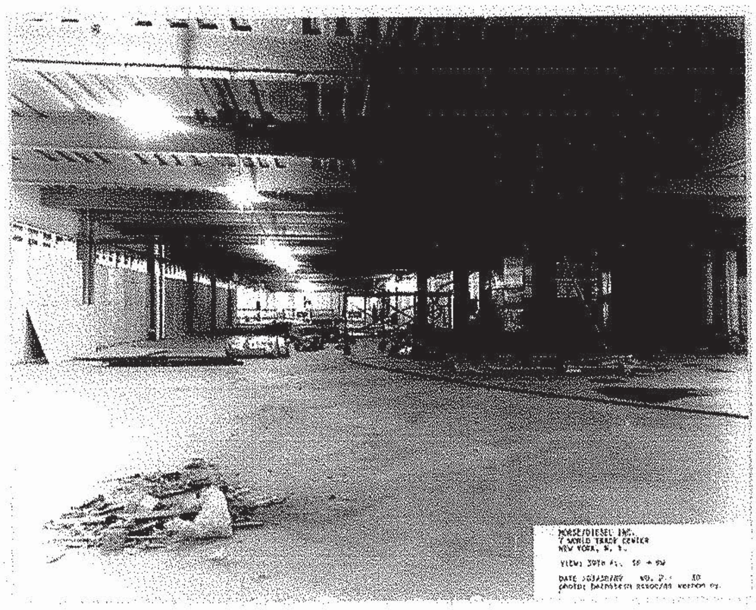

Figure A14: Photograph showing light through flutes (39th Floor)

CITI-7WTC073549

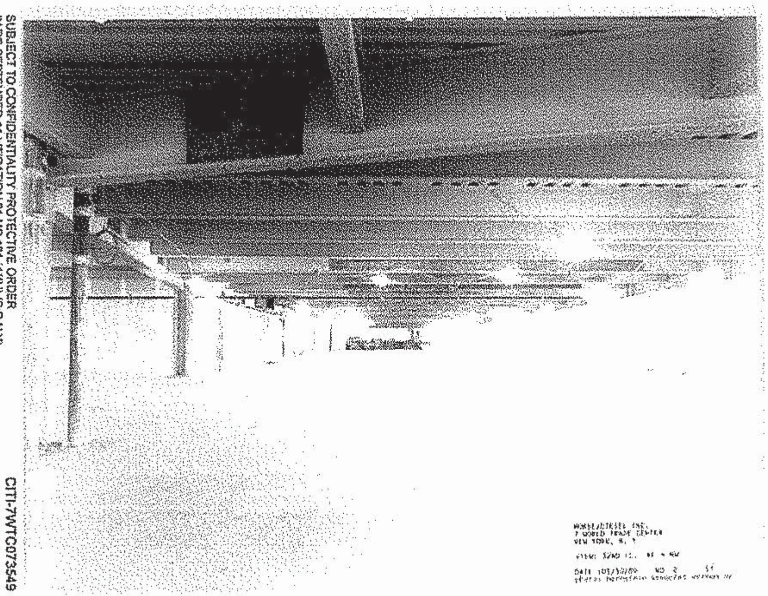

Figure A15: Photograph on 32rd floor showing unfilled flutes above girder

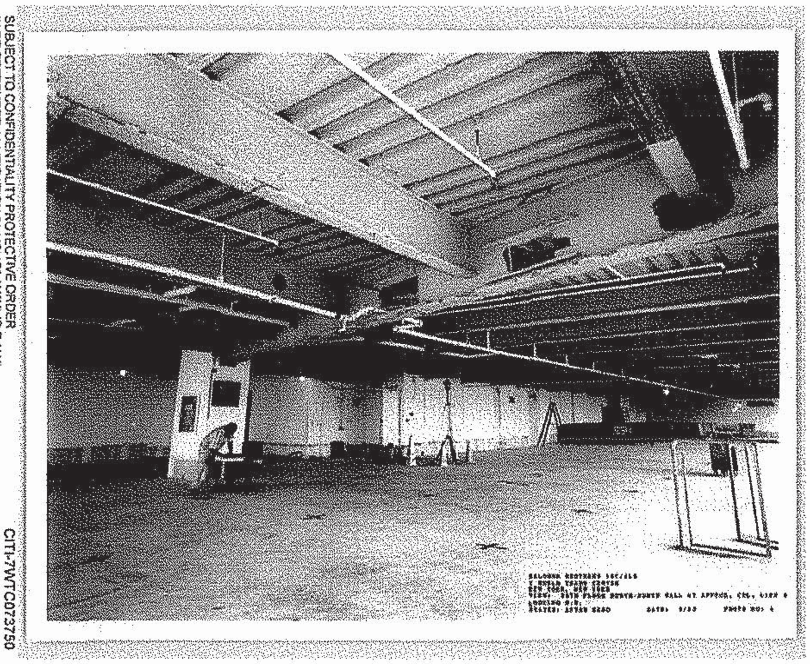

Figure A16 Photograph on 24th floor showing unfilled flutes above girder

EXHIBIT B

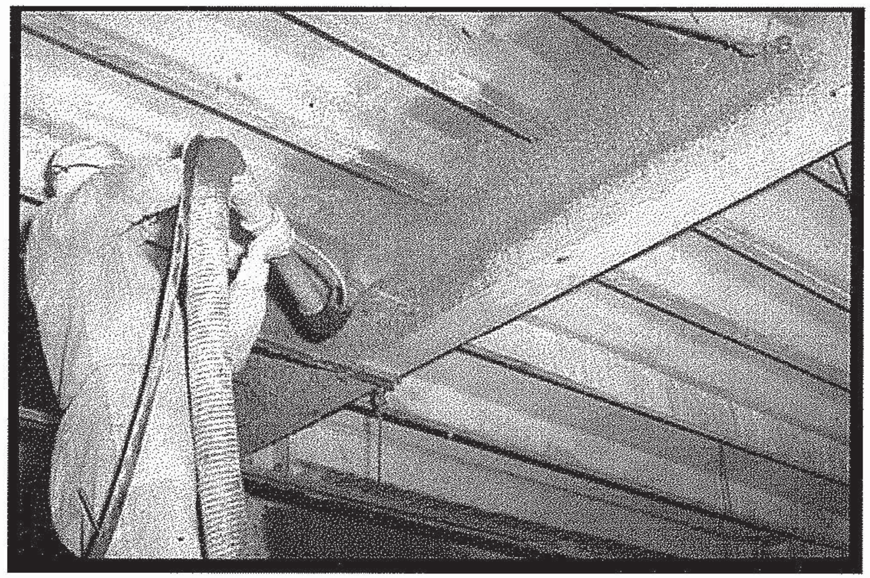

Figure 6 *Application of SPRM where the voids between the beam and floor are filled with material.*

EXHIBIT C

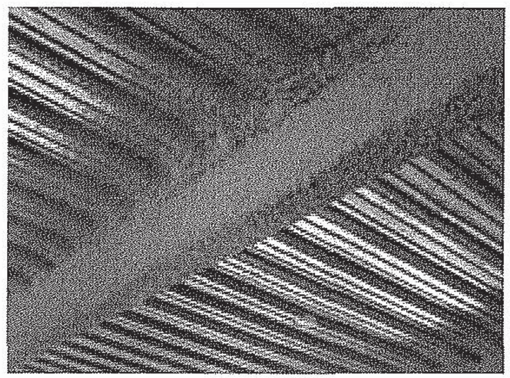

Figure 7 *Flutes filled with SFRM*[4]

EXHIBIT D

Due to its size, Exhibit D has not been e-filed. If you wish to receive a copy, please email Marilyn Francisquini at mfrancisquini@greenbaumlaw.com. A hardcopy of Exhibit D has been filed with the Court, and has been served upon the following counsel:

Katherine L. Pringle, Esq.
Friedman, Kaplan, Seiler & Adelman LLP
1633 Broadway, 46th Floor
New York, NY 10019

Christopher P. Moore, Esq.
Cleary, Gottlieb, Steen & Hamilton LLP
One Liberty Plaza
New York, NY 10006

Response of WTC7 to Standard Office Fires and Collapse Initiation

Professor Colin Bailey
BEng, PhD, CEng, FICE, MIStructE, MIFireE

15th February 2010

Summary

The collapse of WTC7 is the only known case where a multi-story steel framed building has collapsed due to standard office fires. It was found that the collapse was due to design errors which significantly weakened the resistance of the structure to standard office fires and overall progressive collapse [1]. This opinion, and all opinions stated in this report are expressed to a reasonable degree of scientific probability.

This report presents the mechanism leading to the initial structural failure due to standard office fires. It was found that the initial failure was due to the instability of girder 79-44 either during peak heating of a fire or during the cooling stage of a fire. The mode of failure of girder 79-44 was dependent on the severity of the standard office fire. The structural design faults leading to overall progressive collapse, following instability of girder 79-44, is discussed in the report by Guy Nordenson and Associates.

The main design fault precipitating the initial failure was due to the flutes between the top of the beams/girders and underside of the slab not being filled with spray fire-resistance fire material. Failure to fill the flutes resulted in increased temperatures in the top flange, web and shear studs of the girders/beams, with the consequence that the fire resistance of the structure was significantly reduced. Detailed finite-element modeling presented in this report shows that if the flutes were filled, as required, the WTC7 building would not have collapsed and the fire damage could have been repaired.

The fire protection was specified assuming a restrained structure to allow specification of the minimum fire protection thickness and to keep costs to a minimum. This required the use of 'engineering judgment' and the design of connections to adequately transfer thermal thrusts to supports. The connections to girder 79-44 were not designed to transfer thermal thrusts, with the 4 bolts in each connection fracturing very early in the fire. If the seated connections were designed to transfer thrusts, or the system classed as unrestrained and thus the protection thickness increased, it is almost certain that localized failure leading to overall collapse would not have occurred.

Contents

1.0 Introduction

Apart from the collapse of WTC7 there has been no known overall structural collapse of multi-story steel-framed buildings in fire, with buildings surviving standard office fire burnout.

In the 1980's, at the time of design and construction of WTC7, the typical method of providing fire resistance to steel-framed buildings was to encase the exposed steel in a fire protection material, which at the time was generally a spray fire-resistive material (SFRM). This report highlights the fact that the fire protection did not conform to the design specification which led to initial structural failure.

Other structural design faults which covered the robustness and redundancy of the structure, particularly relating to tying between girders and columns, resulted in the localized failure developing into overall collapse of the building. These structural design faults are covered in the report by Guy Nordenson and Associates[2] and Dr. Joseph Colaco.[13]

This report explains how localized failure occurred in WTC7 and highlights the design specification faults leading to this failure. In addition, this report also highlights that if these design specification faults where not present, and the building was protected to the specified requirements, then localized failure would not have occurred and the building would have remained standing and the fire damage could have been repaired The reports by Guy Nordenson and Associates[2] and Dr. Joseph Colaco[13] explain how the initial failure propagates into overall collapse due to further design faults. Their reports highlight that if the building was designed correctly overall collapse would not have occurred.

2.0 Collapse of WTC7

On September 11th 2001, the 47-story office building WTC7 collapsed due to standard office fires. The building was not struck by an airplane and was subjected to exterior structural damage on its south face and south-west corner due to the collapse of WTC1. This exterior damage was inconsequential to the structural integrity of WTC7. The debris from the collapse of WTC1 at 10.28am ignited fires within WTC7. Standard office fires occurred which traveled throughout the building for the next 7 hours. The traveling fires allowed the design faults within the building to be found resulting in overall collapse at 5.20pm. This is the only known case of a high-story building collapsing due to fire. This was due to simple design faults within WTC7.

Photographic evidence (Figure 1) shows that the east roof penthouse collapsed first into the building. Figure 2 shows the location of the east penthouse highlighting that failure of column 79, or possibly column 80, occurred allowing the penthouse to sink into the building. Overall progressive collapse occurred following the collapse of the east penthouse.

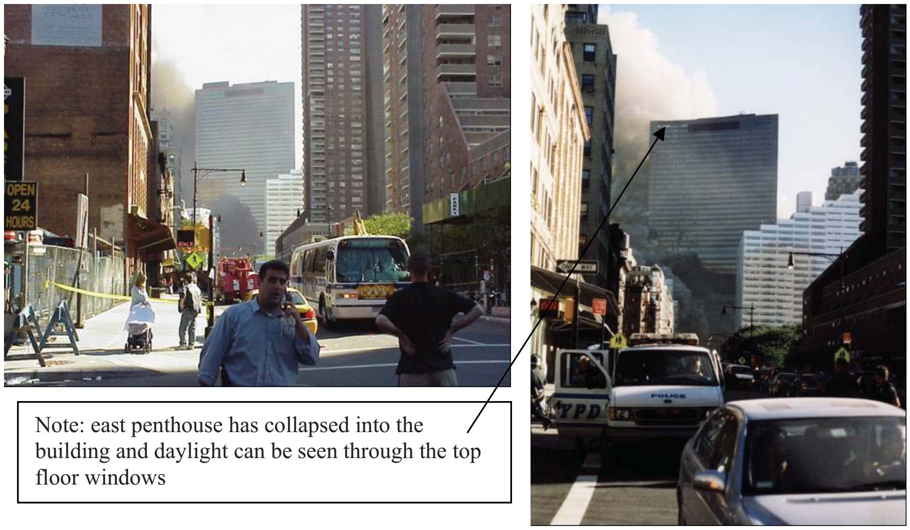

Figure 1 *WTC7 before collapse (left) and during collapse (right)*

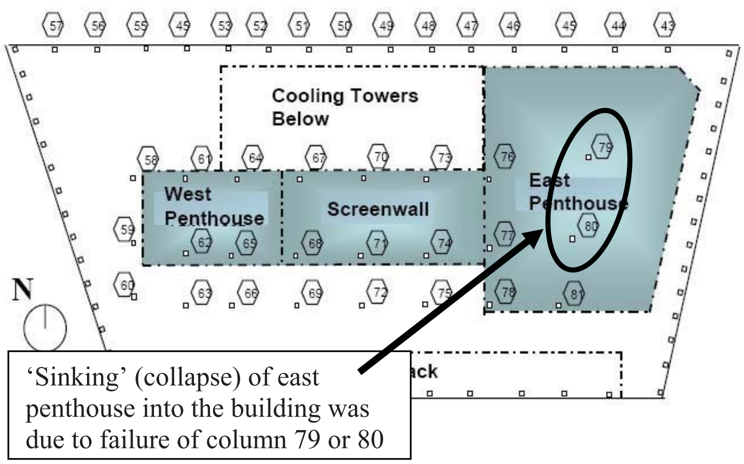

Figure 2 *Location of east penthouse*

Investigation shows that during a fire in the immediate vicinity of columns 79 and 80, the girder spanning from column 79 to 44 (denoted girder 79-44) and the connections to column 79 are weak points in the structure (Figure 3). This is due to:

1. The large span of girder 79-44 (45ft).
2. Column 79 supporting the largest tributary area of 1891 ft^2.
3. 52ft secondary beams framing into the girder on one side only.
4. Girder 79-44 supported on seating cleats, with top cleats, and four 7/8 in bolts at each end.

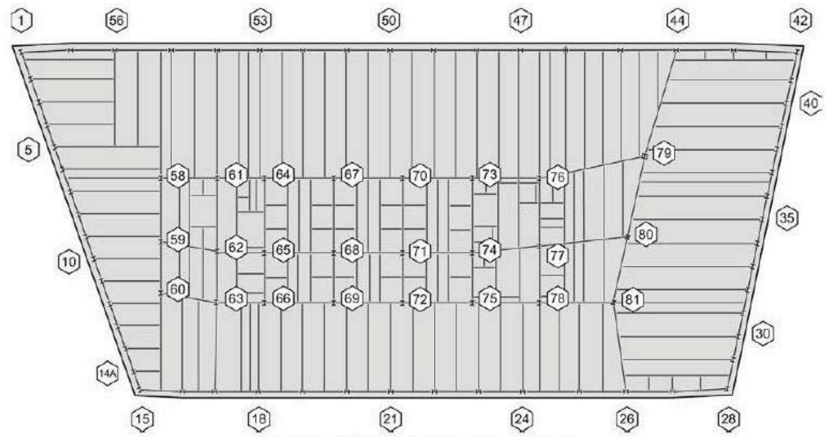

Figure 3 *Typical structural layout for WTC7*

Closer investigation of the collapse of the penthouse also indicates that it was column 79 which failed first. Figure 4 shows a clear 'kink' in the north face of the penthouse, with the east and west walls being pulled inwards as it collapses into the building. This suggests that the girder 79-44 which is supporting the steel post to the penthouse on the roof at the location of the kink (Figure 4), is failing. Since the external column 44 remains stable as the penthouse sinks into the building (Figure 1) then Column 79 must have collapsed first.

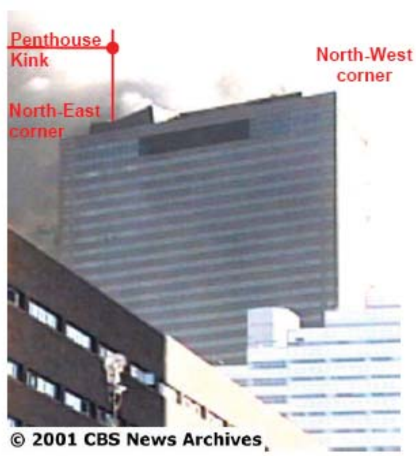

Figure 4 *Collapse of the penthouse.*

Due to the lack of significant glass breakage (Figure 4), as the penthouse sinks into the building, it can be concluded that the collapse of column 79 initiated lower down in the building at the location of the office fires below Floor 13. Visual evidence shows that there were two primary ways in which the standard office floor fires moved within WTC7: clockwise and counterclockwise, as outlined in expert report by Dr Fred Mower(9). The office fires on Floors 11, 12, and 13 were first observed on the eastern side of the building and travelled in a counterclockwise direction. Conversely, the office fires located on Floors 7, 8, and 9 were first observed on the western side of the building and proceeded clockwise. In relation to the building's collapse, at 5:20pm, a heating failure in the north east corner would have had to occur on either Floor 7, 8, or 9, or a failure late in the cooling stage of a fire to Floors 11, 12, or 13. From the available visual evidence it is likely that a fire was present in the north east corner on the 9th Floor at the time of collapse, with the height of the fires on Floors 7 and 8 having already moved past the north east corner at the time of collapse (refer to details in Dr Fred Mower's Expert Report[(9)]).

3.0 Fire Protection to the Steel Structure on WTC7

The WTC7 was specified as a Class 1B building with the columns having 3 hours fire resistance and the floor construction having 2 hours fire resistance. To achieve this level of resistance, passive fire protection in the form of a sprayed applied material was specified. The spray fire-resistive material (SFRM) used on WTC7 was a Monokote MK-5; a gypsum-based material containing vermiculite aggregate. The product was manufactured by W.R. Grace and Co., who ceased production of the MK-5 product in the 1980s.

According to the Underwriters Laboratories (UL) Fire Resistance Directory[3] (1983) the specified fire resistance ratings required a thickness of 7/8in to be applied to heavy columns, 1/2in to be applied to the beams/girders and 3/8in to be applied to the bottom of the metal deck. The thicknesses applied to the beams/girders and to the bottom of the metal deck assumed that the structural system was classed as restrained.

The issue of whether the system should have been classed as restrained or unrestrained is discussed in Section 6.

4.0 Basic Design Faults

There were a number of basic design faults relating to the collapse of WTC7 which resulted in the initial localized failure followed closely by overall progressive collapse. This report is focused on the basic design fault relating to the fire protection system, which resulted in the initiating event causing localized failure. The design faults relating to the robustness and redundancy of the structure to arrest progressive collapse are presented in the reports by Guy Nordenson and Associates[(1)] and Dr. Joseph Colaco[13]

4.1 Unfilled Flutes on WTC7

When a steel beam supports a composite deck comprising a steel deck, concrete and mesh reinforcement, a void is formed between the top flange of the beam and deck within the flutes. For trapezoidal shaped decks, such as that used on WTC7, this void can be large. Leaving the flutes between the deck and top flange of the beam unfilled with fire protection results in:

- An increase in temperature of the top flange and web.
- An increase in temperature of the shear studs.
- A reduction in overall fire resistance.

In the UL Fire Resistance Directory for 1983[(2)] it is stated '*Cavities, if any, between the upper beam flange and floor or roof units shall be filled with the fire protection material applied to the beam, unless stated otherwise on an individual design.'* The identical statement was repeated in the UL Fire Resistance Directory for 1985[4]. The issue of filling the flutes between the top flange of the supporting beam and underside of the floor continues to be specified in the Underwriters Laboratories (UL) documentation with the June 2006 version of BXUV.D739 stating that '*when steel deck is used, the area between the steel deck and the beams top flange shall be filled*'.

Therefore the flutes should have been filled with fire protection on WTC7. Figure 5 shows the flutes (voids) above the top flange of the beam for the protected beams in WTC7, where it can be seen that the flutes are not filled with fire protection as required. Further pictures of the applied fire protection on WTC7 are presented in Appendix A, where it can be seen that throughout the building the flutes were not filled. In many cases the photographs in Appendix A show wires being simply passed through the flutes during the tenant fit-out work in 1989, which was 2 years after completion of the building and application of the fire protection in 1987.

Figure 5 *Picture of the WTC7 showing unfilled flutes*.

It is also worth noting that the Testwell Craig Laboratories reports dated 6/30/86 to 3/26/87, which summaries the firestopping inspection, states that the fluted decks over rated walls are to be filled with firestopping material. In some cases steel beams would have coincided with the position of fire rated walls, for example around stair and lift shafts. Therefore this also suggests that the flutes between the steel beam and underside of the deck were unfilled throughout the building, since if they were filled with SFRM there would have not been the requirement to fill these with firestopping material.

As an example, Appendix B shows 2 plans, sketched by Testwell Craig Laboratories, covering the 11th, 12th floor and 14th floor where the flutes over fire-rated walls were unfilled. Around the stair and lift shafts this would have coincided with steel beams which should have been filled with SFRM.

4.2 Examples of Filled Flutes on other Buildings

An example, on a different building, where the voids are being filled with SFRM during application is shown in Figure 6. Figure 7 shows a further example where the flutes are filled by SFRM which is presented in the American Institute of Steel Construction Design Guide[5] on the Fire Resistance of Structural Steel Framing. Comparison between Figure 7, and the pictures in Appendix A, shows clearly that the flutes on WTC7 were not filled, resulting in a lower fire resistance compared to that specified.

Figure 6 *Application of SFRM where the voids between the beam and floor are filled with material.*

Figure 7 *Flutes filled with SFRM* (5)

Figures 8 and 9 show how the SFRM should have been applied to fill the flute when the beams run perpendicular and parallel to the flutes respectively. It should be noted that the SFRM should be 'proud' of the edge of the flange as shown in Figures 6 and 7 and thus the line defining the top flange of the beam/girder should not seen if the voids are filled. Comparison with Figure 5, and the pictures shown in Appendix A, shows that the flutes were not filled on WTC7.

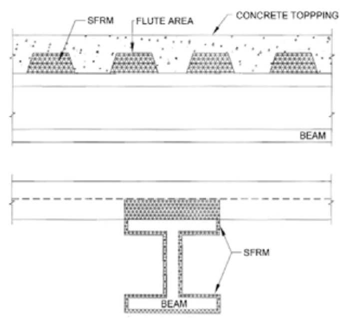

Figure 8 *Flutes filled with SFRM when deck is perpendicular to beams*[10]

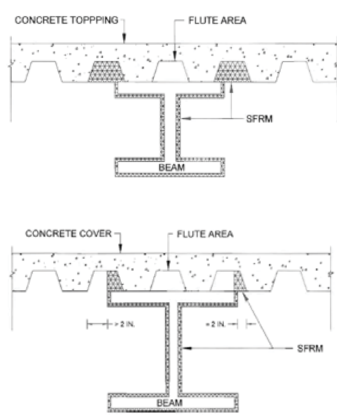

Figure 9 *Flutes filled with SFRM when deck is parallel to beams*[(10)]

4.3 Test Data showing the Effect of Unfilled Flutes (Voids)

In the UK a series of tests[(6-8)] were conducted in the late 1980s and early 1990s. The results from these tests are discussed in detail in the report present in Appendix C. As an example, Figure 10 shows the results from a test where the temperatures of the top flange were measured at locations where the flute was filled and the flute was left unfilled. It can be seen that leaving the flutes unfilled increases the top flange temperature by 55%, significantly reducing the fire resistance to the beam.

Additional test data relating to filled and unfilled flutes is presented in the report in Appendix C together with shear stud temperatures.

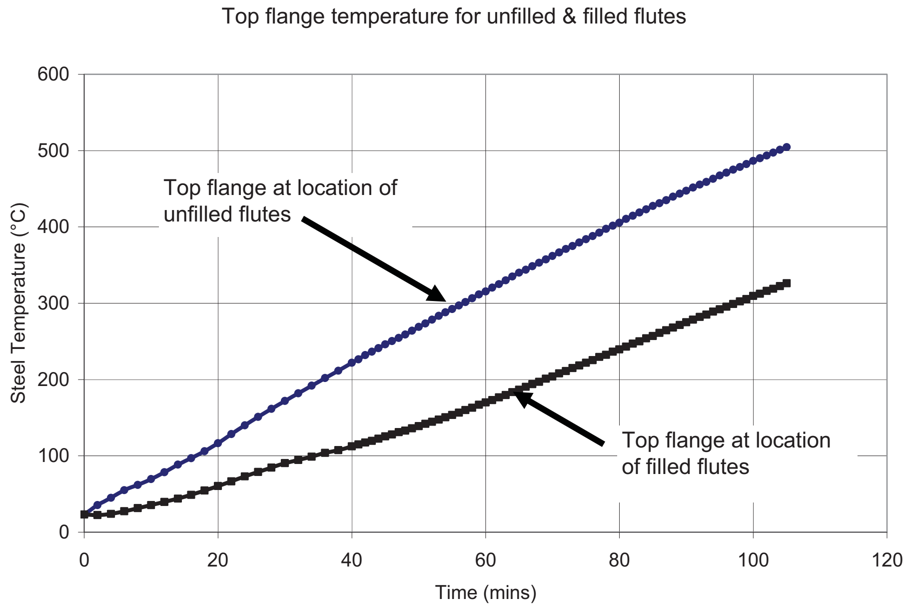

Figure 10 *Top flange temperatures at location of filled and unfilled flutes for trapezoidal deck (PMF CF60) with normal weight concrete.*

5.0 Structural Response of WTC7 During a Fire

Before more detailed finite-element models are presented it is worth discussing the structural behavior using simple mechanics, together with the known behavior of steel structures in fire, to highlight the cause of the initial collapse.

The initial failure, leading to overall collapse, occurred in the connection between column 79 and girder 79-44. During the initial stages of the fire the girder expanded longitudinally as it increased in temperature. This expansion placed a thrust onto the seated connections at columns 79 and 44 as shown in Figure 11.

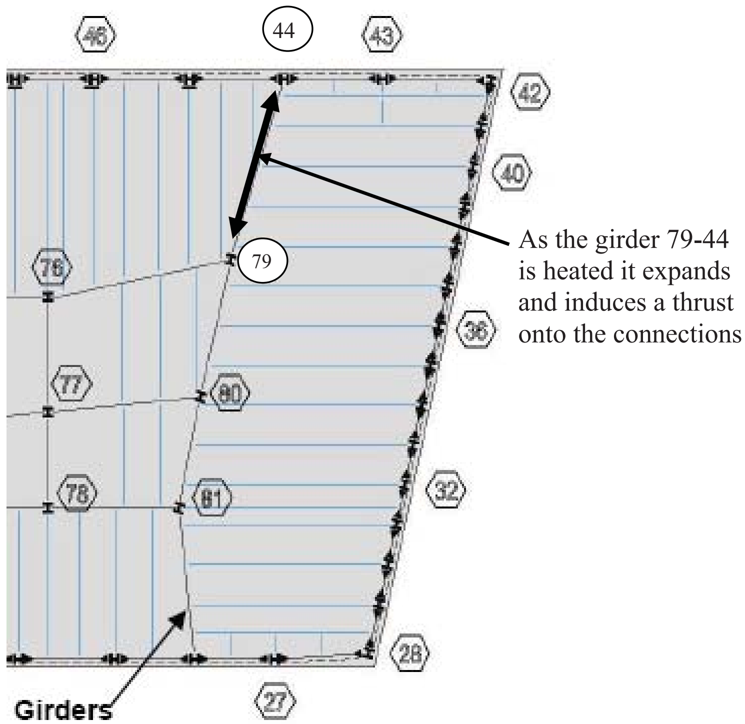

Figure 11 *Expansion of girder 79-44 in the early stages of the fire*

The details of the seated connections at columns 79 and 44, between the 8th to 15th floors, are shown in Figure 12, which are taken from Frankel Steel Shop Drawing Numbers 9102 and 9114.

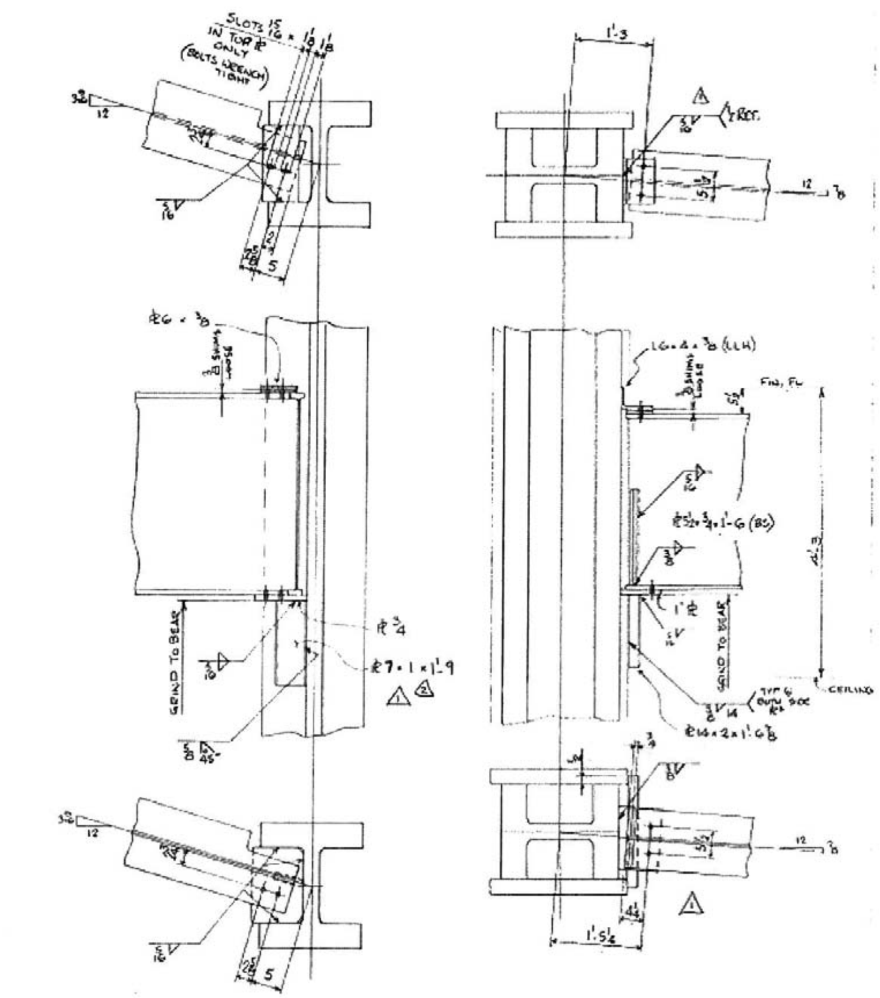

Column 44 Column 79

Figure 12 *Details of seated connections at columns 44 and 79*

The connections have four bolts (7/8in A325) at each end, 2 fixing the girder to the bottom seat and 2 fixing the girder to the top cleat, with an overall shear capacity of 180kip. From the fabrication drawings it can be calculated that the gap between the end of girder and the columns is a total of 3.5in, with the length of the girder being 537in. (Frankel Steel Shop Drawing Numbers 1352, 1090, 9102 and 9114).

If we assume that the girder (W33×130) is uniformly heated to 100°C, which will occur early in the fire, the load required to resist the axial thermal expansion is given by:

$Q = AE(T)\alpha\Delta T$

A = area of girder = 38.3in^2
E(T) = modulus of elasticity at temperature T = 30,000 ksi at 100°C
α = coefficient of thermal expansion = 1.4E-5
ΔT = increase in temperature

Therefore
Q = 38.3 × 30000 × 1.4E-5 × (100-20) = 1286.9 kip

This force far exceeds the strength of the bolts indicating that the bolts will fail below 100°C (i.e. very early in the fire).

Although a simple calculation, this gives an indication of the compression force on the connections as the girder expands which is only resisted by four 7/8in bolts, which will fail very quickly in a fire.

Once the bolts fail the seating cleat still provides vertical support and the girder is then free to expand longitudinally until it hits the columns at each end. However, the girder has no fixity to the connections; it simply slides about on the seating cleat with its movement dependent on the movement of the structure around it. At column 44 the girder is restrained from lateral movement when it hits the inside flanges of the column since the girder spans onto the column's web. However, at column 79 the girder is supported off the column's flange and there is no resistance to lateral movement. Therefore any lateral movement of the girder at column 79 will either push or pull the girder off the seat connection laterally.

As the girder continues to expand during heating it will hit the columns 79 and 44. The gap between the end of girder and the columns is a total of 3.5in and the length of the girder is 537in. Therefore the temperature of the girder (assuming uniform temperature distribution) when it hits the columns is given by:

1.4E-5 × 537 × (T-20) = 3.5

Therefore, T = 485°C.

The girder must reach 485°C before it hits the columns. Once the girder hits the columns its thermal expansion is restrained. Compression forces are induced into the girder and it effectively becomes wedged between the columns.

As the temperature of the fire increases the secondary beams framing into one side of the girder will push the girder laterally (Figure 13) as they expand. Until the girder has expanded sufficiently longitudinally to hit columns 79 and 44 the lateral restraint to expansion of the secondary beams provided by the girder 79-44 is significantly less than the restraint provided by the external columns. This is mainly due to the fact that there are no secondary beams framing west to east on the west side of girder 79-44. Therefore greater lateral movement of the girder 79-44 will occur compared to lateral movement of the external columns due to the lower restraint from the girder to the expansion of the secondary beams.

As well as thermal expansion of the secondary beams causing lateral movement of the girder 79-44, the vertical deflection of the secondary beams, as they lose strength and stiffness with increase in temperature, will cause the girder 79-44 to twist.

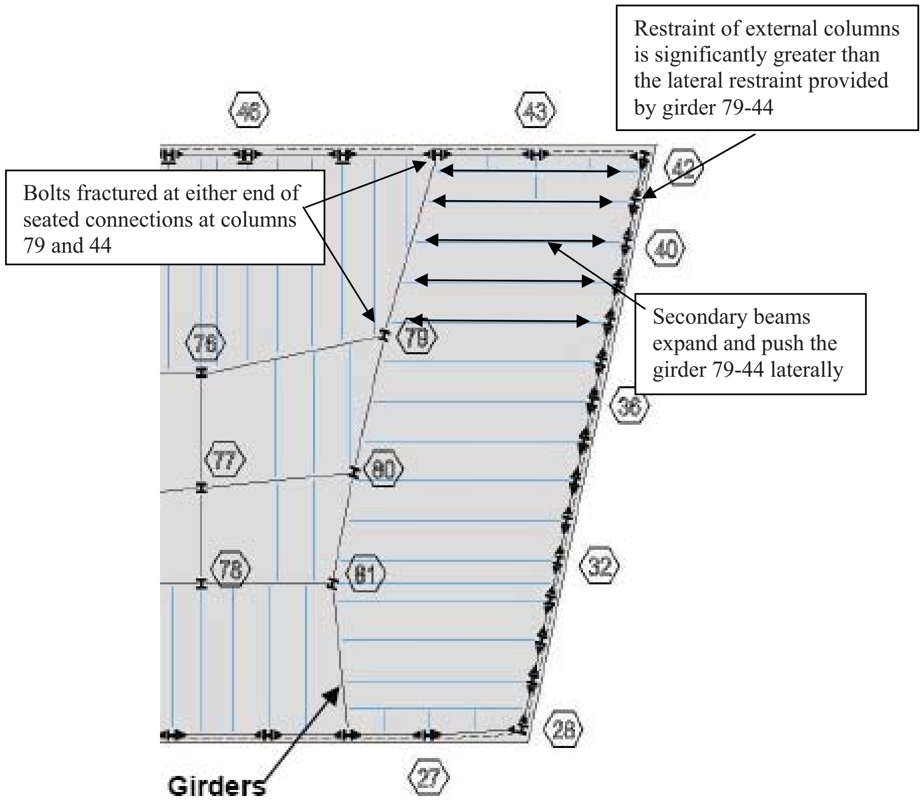

Figure 13 *Showing thermal expansion of secondary beams*

To push the girder off the seat it will need to move laterally 5.5in during the heating phase. To reach 5.5in the secondary beams will need to be heated to 650°C (assuming all the movement is pushing the girder and the secondary beams do not deflect). At this temperature the girder is compressed between columns 79 and 44 and vertical support will continue to be provided, to some extent, by the 2in plate fixed across column 79. It is therefore unlikely that the girder was pushed off the seat laterally at column 79 during heating. If failure did occur during the heating stage of the fire it would be due to flexural (strength) failure of the secondary beams and girder 79-44 and not by pushing the girder 79-44 off its seated connection. However, once the girder starts to cool, and contract, the girder is no longer wedged between the columns and plate will not offer any vertical support.

As the structure begins to cool the girder 79-44 will contract from a plastic state and will be simply 'skating about' on the seated connections. The secondary beams will also contract from a plastic state which, together with twisting, will cause the girder to be pulled off the seat at column 79 (Figure 14) during cooling and thus initiate collapse.

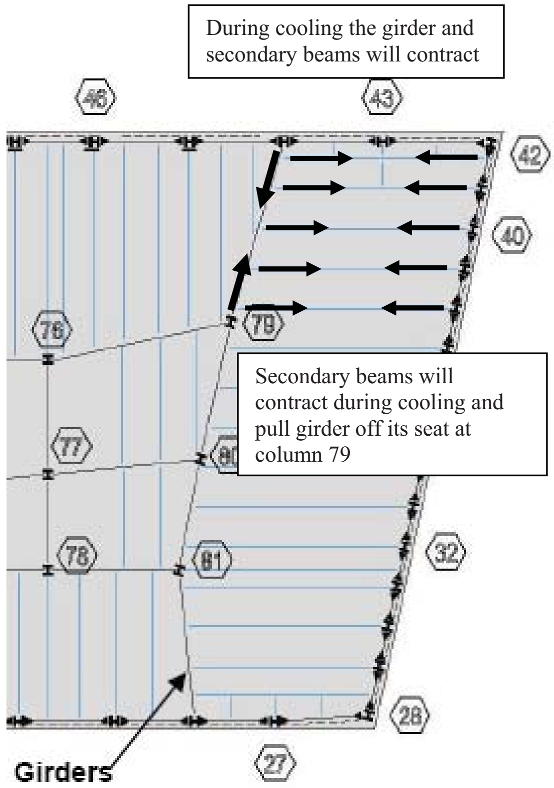

Figure 14 *Behavior during cooling*

Both the secondary beams and girder have shear studs, which to some extent provide restraint to longitudinal thermal expansion to beams/girders. The girder is designed for partial interaction and has minimal studs (30 total, as per Cantor Drawing S-8 Revision I) which will have a maximum slip before fracture (assumed 6mm). The temperature of the studs and thus strength and ductility of the studs (together with the surrounding concrete) will be dependent on the filling of the flutes with SFRM. In WTC7 the flutes were not filled with SFRM, as required, resulting in high temperatures in the studs which will cause them to fracture earlier in the fire.

6.0 Fire Resistance Based on a Restrained System

The WTC7 Architect, Emery Roth & Sons, specified application of a sprayed on fireproofing stating that '*All steel framing shall be considered as being of the restrained type*'. The specification also stated:

"The 'Design Information Section' including 'Floor-Ceiling Assemblies,' 'Roof-Ceiling Assemblies,' 'Beams,' 'Columns,' 'Wall and Partitions,' of the Underwriters' Laboratories 'Fire Resistance Index' dated January, 1975, and any later revisions and the 'Guide for Determining Conditions of Restraint.....' including Appendix 'C' from standard U.L. 263 shall form the basis of all required work and shall be referred to for guidance by the Sub-Contractor." (Refer document 'Section 9K, Instructions to Bidders, Sprayed-on Fireproofing, 7 World Trade Centre, New York – Document reference PANYNJ0037124 to PANYNJ0037132).

Following the Architects specification, the fire protection to the beams and underside of the slab was specified assuming a restrained system, resulting in 1/2in thickness to the beams/girders and 3/8in to the bottom of the metal deck. If the structure was assumed to be unrestrained then the thickness of the fire protection would have been higher and the overall resistance of the structure to fire would have been higher. However, there are significant savings to be made in terms of fire protection if the system can be classified as restrained.

As stated in the Architects specification, guidance for determining conditions of restraint was given in Appendix C of the 1983[3] Underwriters Laboratories Fire Resistance Directory.

Appendix C states:

GUIDE FOR DETERMINING CONDITIONS OF RESTRAINT FOR FLOOR AND ROOF ASSEMBLIES AND FOR INDIVIDUAL BEAMS

One of the major changes in the new rating criteria was the establishment of restrained and unrestrained ratings. To help determine the appropriate rating to use in a particular building situation, the following Guide is presented. It is Appendix C from the Standard for Fire Tests of Building Construction and Materials, UL263.

"C1. The revisions adopted in 1970 have introduced, for the first time in the history of the Standard, the concept of fire endurance classifications based on two conditions of support: restrained and unrestrained. As a result, most specimens will be fire tested in such manner as to derive these two classifications."

"C2. A restrained condition in fire tests, as used in this Standard, is one in which expansion at the supports of a load-carrying element resulting from the effects of the fire is resisted by forces external to the element. An unrestrained condition is one in which the load-carrying element is free to expand and rotate at its supports."

"C3. Some difficulty is recognized in determining the condition of restraint that may be anticipated at elevated temperatures in actual structures. Until a more satisfactory method is developed, this Guide recommends that all constructions be temporarily classified as either restrained or unrestrained. The classification will enable the architect, engineer, or building official to correlate the fire endurance classification, based on conditions of restraint, with the construction type under consideration."

"C4. For the purpose of this Guide, restraint in buildings is defined as follows:
Floor and roof assemblies and individual beams in buildings shall be considered restrained when the surrounding or supporting structure is capable of resisting substantial thermal expansion throughout the range of anticipated elevated temperatures. Constructions not complying with this definition are assumed to be free to rotate and expand and shall therefore be considered as unrestrained."

"C5. This definition requires the exercise of engineering judgement to determine what constitutes restraint to "substantial thermal expansion." Restraint may be provided by the lateral stiffness of supports for floor and roof assemblies and intermediate beams forming part of the assembly. In order to develop restraint, connections must adequately transfer thermal thrusts to such supports. The rigidity of adjoining panels or structures should be considered in assessing the capability of a structure to resist thermal expansion. Continuity, such as that occurring in beams acting continuously over more than two supports, will induce rotational restraint which will usually add to the fire resistance of structural members. In the following table, only the common types of constructions are listed. Having these examples in mind, as well as the philosophy expressed in the preamble, the user should be able to rationalize the less common types of construction."

There are 2 points to consider relating to Appendix C above. The first is that the definition of restraint given in C4 states '*shall be considered restrained when the surrounding or supporting structure is capable of resisting substantial thermal expansion throughout the range of anticipated elevated temperatures.'* The second point is in C5 where it states '*This definition requires the exercise of engineering* *judgment to determine what constitutes restraint to substantial thermal expansion……….connections must adequately transfer thermal thrust to such supports.'*

Considering the guidance given in Appendix C, of the 1983(2) Underwriters Laboratories Fire Resistance Directory, it is difficult to see how 'exercising engineering judgment' the girder 79-44 can be classed as restrained since the transfer of the thermal thrust from the girder to the column is only through four 7/8in bolts which fail very early in a fire. Due to the large gap between the ends of the girder and columns, the girder is unrestrained and thus should have had greater thickness of fire protection or designed to be restrained. The simple calculation presented in Section 5, together with simple 'engineering judgment' shows that the seated connections to girder 79-44 does not provide the required restraint.

To ensure that the connections at the ends of girder 76-44 were adequate for transferring thermal thrust an alternative connection should have been specified (double shear tab) or the gap for the specified seat connections filled with a shim to allow the thrust to be transferred to the column. If a shim was provided, or an alternative connection specified, the bolts would probably not have fractured and the initial failure would not have occurred.

Table C1 gives some guidance for <u>common</u> construction. Due to its scale, long spans and asymmetrical framing details, WTC7 is not common construction. The details of Table C1 are shown below:

TABLE C1
CONSIDERATIONS OF RESTRAINT FOR COMMON CONSTRUCTION

I. Wall Bearing:
  A. Single span and simply supported end spans of multiple bays.[1]
    (1) Open-web steel joists or steel beams supporting concrete slab, precast units, or metal decking .... Unrestrained
    (2) Concrete slabs, precast units, or metal decking .... Unrestrained
  B. Interior spans of multiple bays.
    (1) Open-web steel joists or steel beams, or metal decking supporting continuous concrete slab .... Restrained
    (2) Open-web steel joists or steel beams, supporting precast units or metal decking .... Unrestrained
    (3) Cast-in-place concrete slab systems .... Restrained
    (4) Precast concrete, where the potential thermal expansion is resisted by adjacent construction[2] .... Restrained

II. Steel Framing:
  (1) Steel beams welded, riveted, or bolted to the framing members .... Restrained
  (2) All types of cast-in-place floor and roof systems (such as beam-and-slabs) where the floor or roof system is secured to the framing members .... Restrained
  (3) All types of prefabricated floor or roof systems where the structural members are secured to the framing members and the potential thermal expansion of the floor or roof system is resisted by the framing system or the adjoining floor or roof construction[2] .... Restrained

III. Concrete Framing:
  (1) Beams securely fastened to the framing members .... Restrained
  (2) All types of cast-in-place floor or roof systems (such as beam-and-slabs, flat slabs, pan joists and waffle slabs) where the floor system is cast with the framing members .... Restrained
  (3) Interior and exterior spans of precast systems with cast-in-place joints resulting in restraint equivalent to that which would exist in Condition III(1) ... Restrained
  (4) All types of prefabricated floor or roof systems where the structural members are secured to such systems and the potential thermal expansion of the floor or roof system is resisted by the framing system or the adjoining floor or roof construction[2] .... Restrained

IV. Wood Construction:
  All types .... Unrestrained

[1]Floor and roof systems can be considered restrained if they are tied into walls with or without tie beams, which are designed and detailed to resist thermal thrust from the floor or roof system.

[2]For example, resistance to potential thermal expansion is considered to be achieved if:
  (1) Continuous structural concrete topping is used.
  (2) The space between the ends of precast units or between the ends of units and the vertical face of supports is filled with concrete or mortar.
  (3) The space between the ends of precast units and the vertical faces of supports, or between the ends of solid or hollow core slab units does not exceed 0.25 percent of the length for normal-weight concrete members or 0.1 percent of the length for structural lightweight concrete members.

Table C1 above deals with the secondary beams supported by the framing members. It could be argued that the shear studs to the girder, added during construction, could provide some restraint. However, as the purpose for installing the shear studs was to support additional 10psf vertical load, only 30 studs were added creating partial interaction between the girder and slab. More studs would have been required to provide the restraint required. If the girder was fully tied and designed as fully composite a total of 96 shear studs would have been required (over 3 times more than the number used).

Although there continues to be debate about restrained and unrestrained systems in the USA, it is difficult, as previously stated, to argue 'exercising engineering judgment' that girder 79-44 (even with 30 shear studs) is restrained with the specified seated connections. If the engineer would have considered the thermal thrust on the connection, as outlined in Appendix C of Underwriters Laboratories Fire Resistance Directory, the conclusion would have been reached of specifying a different connection, adding shims or classing the structure as unrestrained, which would have almost certainly stopped the initial failure occurring and therefore the overall collapse of the building would not have been initiated..

7.0 The Influence of Unfilled Flutes Initiating the Collapse of WTC7

As explained in Section 4 the major design fault from a fire protection standpoint was not filling the flutes with SFRM as specified in the Underwriters Laboratories Fire Resistance Directory.

To highlight the effect of unfilled flutes, initiating the collapse of the WTC7, detailed structural modeling at elevated temperature was conducted using the finite element program ABAQUS. The 13th floor was modeled structurally, with the fire being on the 12th floor. The 'as-built' condition of the structure was modeled using drawings prepared by The Office of Irwin G. Cantor, the structural engineer and Frankel Steel, the fabricator, and any documented construction change orders. The main project documents used to develop the structural model are shown in Table 1

Drawing by	Dwg Description	Dwg No / Ref	Rev	Date	Comment
Cantor	Typ. Floor Framing Plan 8th to 20th & 24th to 45th	S-8	I	10-14-85	Floor plan and beam layout and shear stud numbers
Frankel	Col 79 7th 8th & 9th Tier	1091	2	May 23rd 985	Column 79 plan view and elevations
Frankel	Beams (12th & 13th floor)	2015		May 21 1985	Elevations and sections of girder 76-79
Frankel	Beams (81 to 79) (22nd Fl to 29th Fl)	2157		May 21 1985	Elevations and sections of girder 80-79
Frankel	Beams (79 to 44) (8th & 21st floor)	2001		May 1, 1985	Elevations and sections of girder 44-79
Frankel	Beam to Colm. Connections – Core	9114	E	July 8th 1985	Column 79 details
Frankel	Beam to column connections (North & south walls)	9102	I	March 23, 1985	Column 44 details
Cantor	Column schedule No.1	S17	E	August 5th 1985	Column Schedule
Cantor	Column schedule No.2	S17A	D	May 10th 1985	Column Schedule

Table 1: Main Cantor and Frankel documents used to develop structural model.

The photographic evidence shows that the fire on the 12th floor had progressed passed the north-east corner suggesting that collapse occurred late in the cooling phase of the fire (refer to Dr Fred Mower's Expert Report).

Alternatively, if the fire was hotter and collapse occurred during the heating phase of the fire the photographic evidence suggests that this occurred on the 9th floor (with the 10th floor being heated). The 10th and 13th floor had the same structural arrangement therefore since the initial failure was governed by horizontal structural members the model represents both the 13th and 10th structural floor arrangement.

Details of the structural model and results are presented in detail in Appendix D.

7.1 Description of the Model.

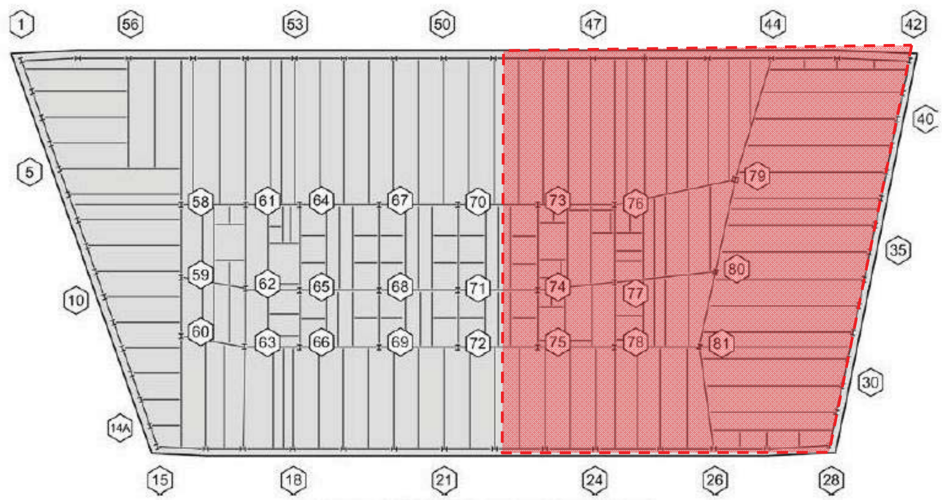

Figure 15 *Extent of floor area of structural fire model on the 13th floor.*

From the video evidence it can be concluded that collapse initiated in the north-east area of the building around column 79. The extent of the structural model is shown in Figure 15, which covers a significant proportion of the east side of the building.

Figure 16 shows the detail of the model. The girders spanning between columns 79-44, columns 80-79 and columns 76-79 were modeled using detailed shell elements, since these girders cover the observed area of the initial collapse, as discussed in Section 2. By using shell elements, detailed localized buckling and plasticity can be identified as well as the overall behavior. The other beams and girders were also modeled in detail using beam elements to investigate the potential for alternative initiating collapse mechanisms. Each shear stud connected to the beams in the north-east bay were modeled individually as well as the shear studs connected to the girders 79-44, 80-79, and 76-79. Columns 44 and 79 were modeled using detailed shell elements, with the rest of the columns modeled using beam-column elements. In total 138 beams and girders and were modeled. The girders and columns modeled using shell elements were focused around column 79 where the initiating collapse occurred, as shown in Figure 17.

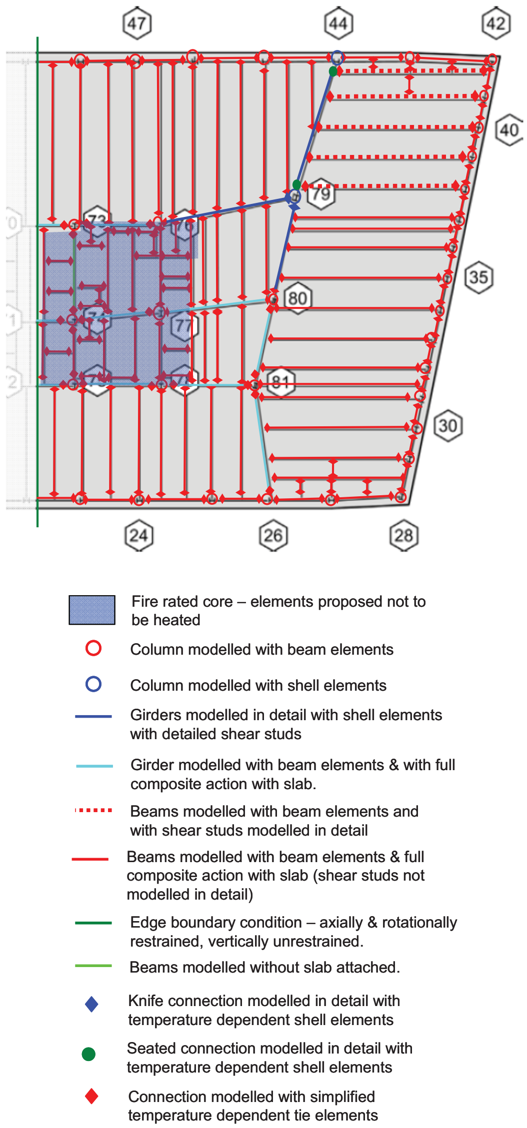

Figure 16 *Figure highlighting the types of elements adopted within the model*.

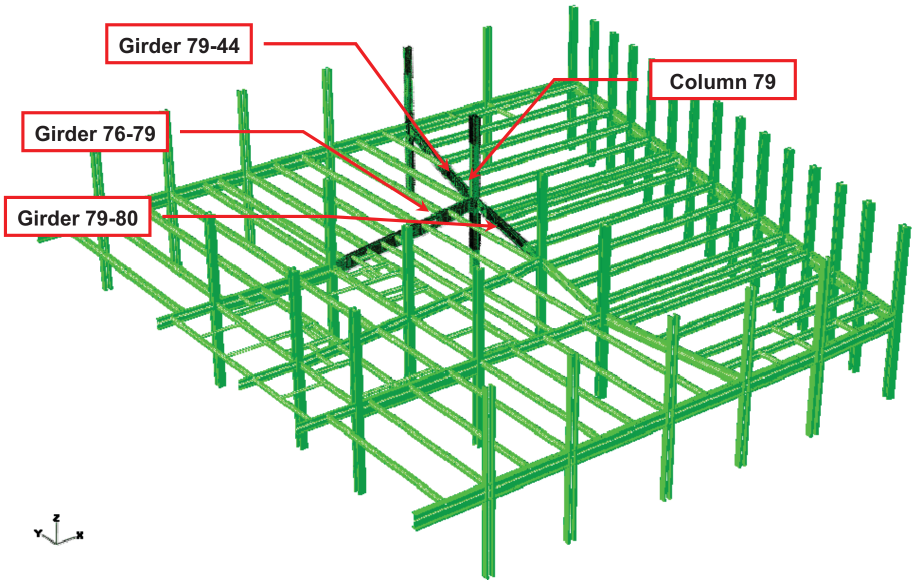

Figure 17 *Figure showing steel elements modeled using shell elements*

The trench headers, which were generally 3' wide, were included within the model since these provided a discontinuity in the slab. The location of the trench headers is shown in Figure 18 (refer Cantor Drawing No. E-14 - PANYNJ0102202 and MacFab T13 - CANTOR2005509)..

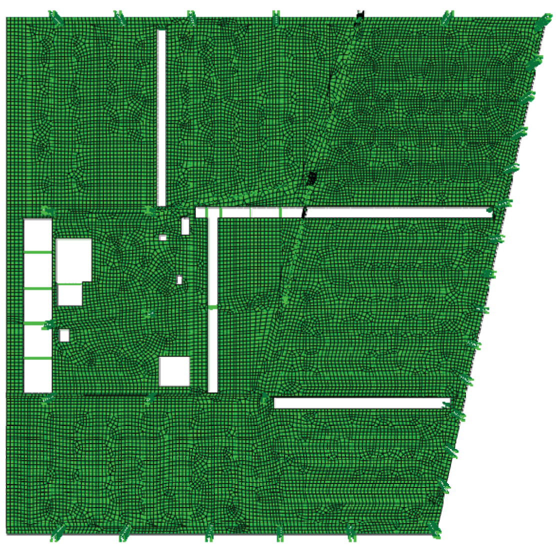

Figure 18 *Location of trench headers.*

Modeling of the connections is extremely important. In total 258 connections were modeled, with defined breakage limits based on the tensile capacity of the connection.

Four connections were modeled in detail (including the detailed behavior of the bolts) comprising 2 knife connections at column 79, 1 seated connection at column 79, and 1 seated connection at column 44.

Considering the girder connections to column 79, Figures 19 and 20 show the location of the 2 knife connections (K5) and (K8) and the seated connection for the girder spanning between columns 44 and 79.

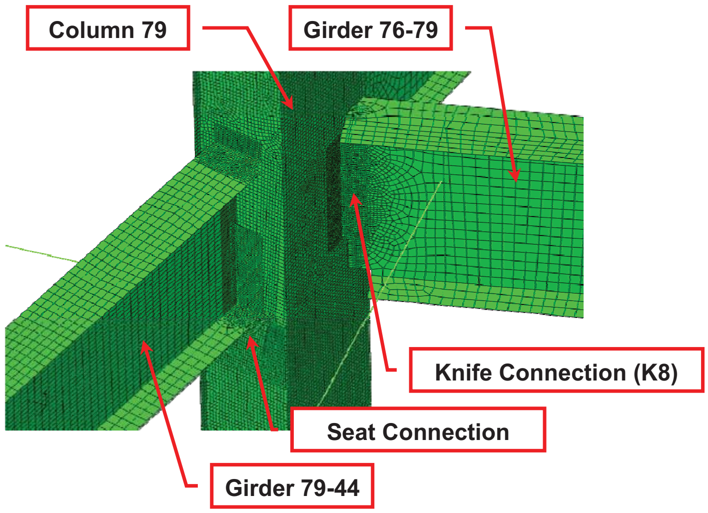

Figure 19 *Figure showing connection K8 and set connection at column 79*

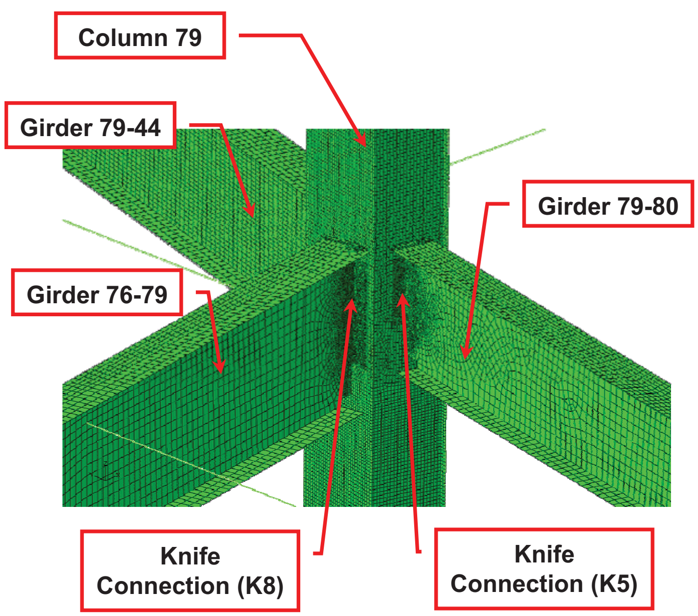

Figure 20 *Figure showing connection K8 and K5*

The detailed modeling of the K5 and K8 connections is shown in Figures 21 and 22 respectively.

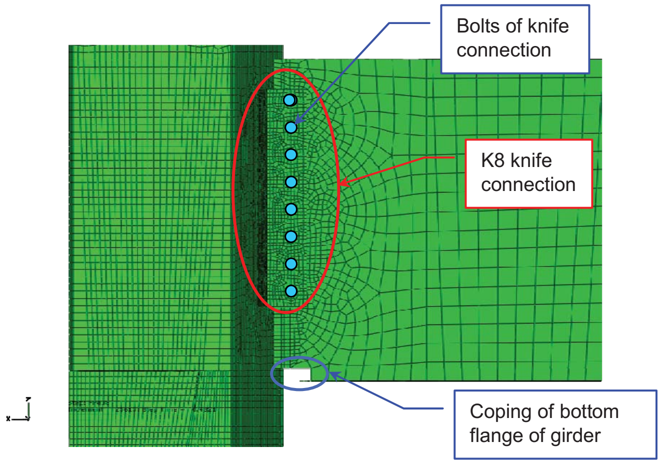

Figure 21 *Detail of connection K8*

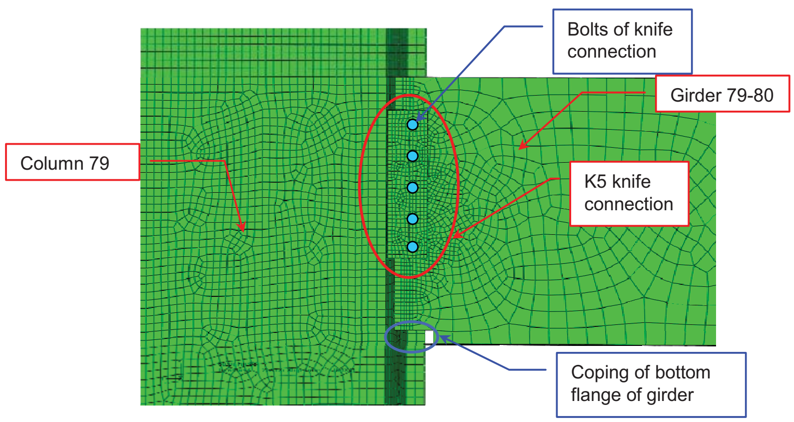

Figure 22 Detail of connection K5

The seated connection at column 44 for the girder spanning between columns 79 and 44 is shown in Figure 23. A plan view showing the girders spanning into column 79 is shown in Figure 24.

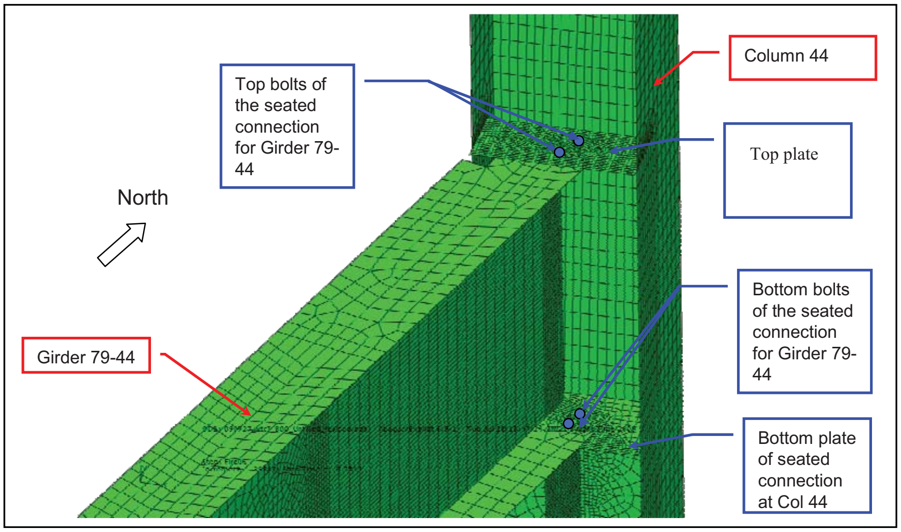

Figure 23 *Figure showing seated connection at column 44*

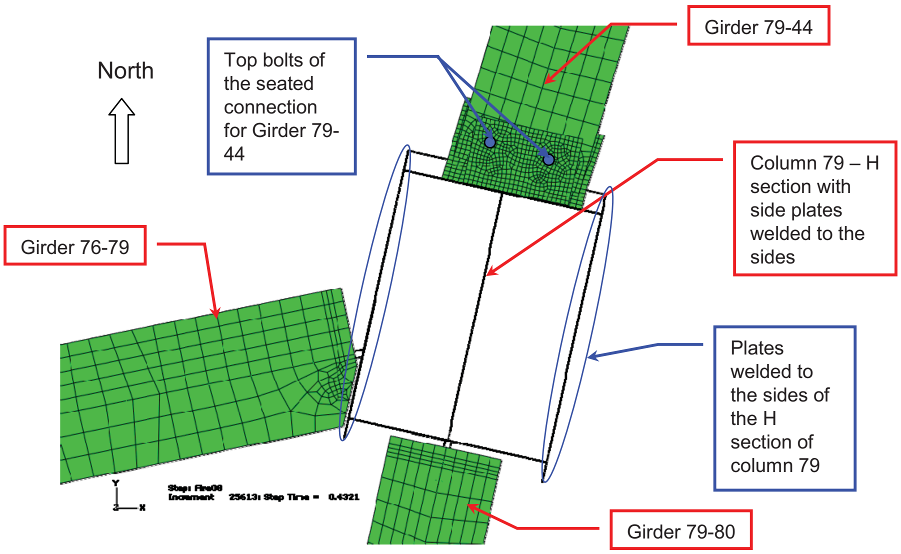

Figure 24 *Plan view at column 79*

7.2 Representation of the Fire

To investigate the effect of fire on the structure of the WTC7, two simple fire curves (representing the heat from a fire) were adopted (refer Fred Mower's Expert Report[9]). The two fire curves were chosen to represent the bounds of the likely structural behavior from standard office fires to highlight the mechanism leading to the initial structural failure. The bounds represented initial structural failure occurring during the heating and cooling stages of the fire.

The duration of the assumed fire was for 2 hours using the temperature-time relationships (fire curves) shown in Figure 25. For the first hour of the fire a constant gas temperature exposure was assumed over the entire modeled floor area of Level 12, which heats the underside of the floor slab of Level 13 and the columns of Level 12. For the first fire curve the temperature reached 700°C and for the second fire curve the temperature reached 800°C. For the second hour, of both assumed fire curves, the structure was subjected to ambient temperature (20°C). The fire curves are not intended to represent the actual fire within WTC7, but were derived to allow the structure to be investigated to highlight the weak points in the design of the building. The report by Fred Mower[9], provides more detail on the adopted fire curves (and thermal analysis) and also highlights that the fire curves adopted fit within the envelop of the likely fire behavior in WTC7.

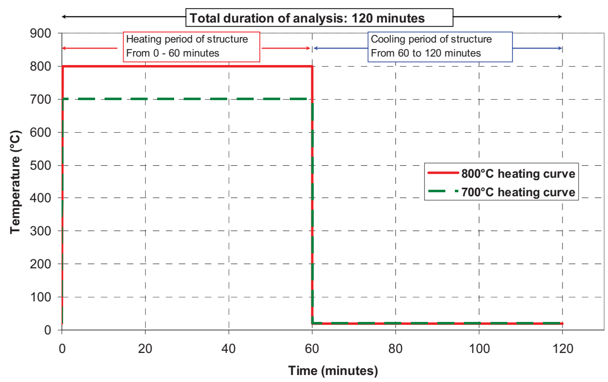

Figure 25 *Temperature-time curves assumed.*

7.3 Effect of Unfilled and Filled Flutes

A total of 4 cases were considered based on the 2 different fire curves, and the assumption that the flutes were filled or unfilled. The 4 cases are summarized in Table 1. Direct comparison between case 1 and 2 and case 3 and 4 will allow the effect of leaving the flutes unfilled, on the structural behavior, to be investigated.

Case	Fire Curve	Flutes filled or unfilled?
1	700°C for the first hour followed by 20°C for the second hour.	Unfilled
2	700°C for the first hour followed by 20°C for the second hour	Filled
3	800°C for the first hour followed by 20°C for the second hour	Unfilled
4	800°C for the first hour followed by 20°C for the second hour	Filled

Table 1 *Summary of the different models considered*

The temperature of the top flange of steel beams and girders will be different depending on whether the flutes are filled or unfilled, as shown from the test data discussed in Section 4 and in Appendix C.

An example of the different temperature distribution in the girder between columns 79-44 for 800°C one hour heating followed by a further hour at 20°C is shown in Figure 26. It can be seen that for the filled case the temperature is assumed uniform, whereas for the unfilled case the temperature of the top flange and web is higher. The temperature distribution for the 700°C fire curve for the secondary composite beams is shown in Figure 27, which highlights a similar heating response.

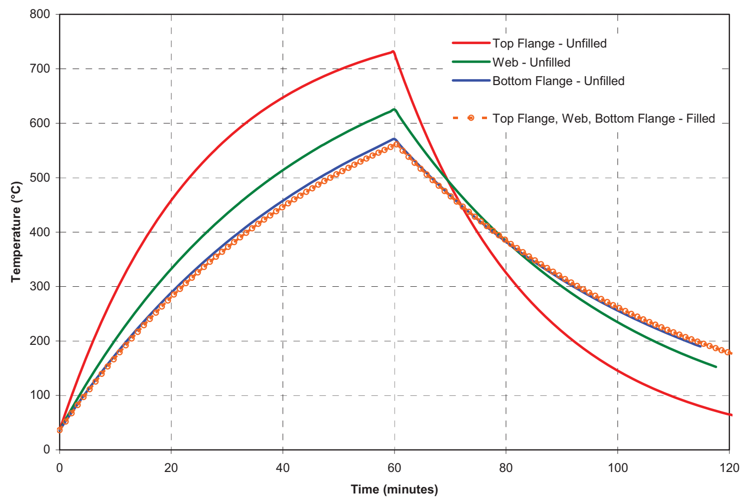

Figure 26 *Heating distribution through girder 79-44 for unfilled and filled flutes (800°C heating).*

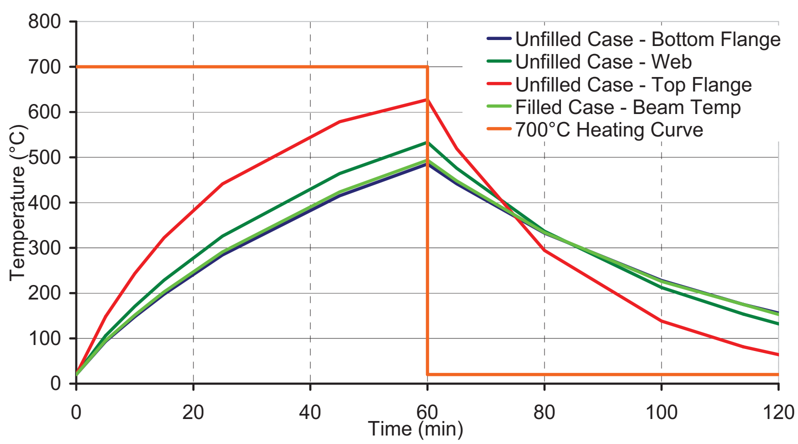

Figure 27 *Heating distribution through secondary beams for unfilled and filled flutes (700°C heating).*

7.4 Case 1 (700°C Unfilled Flutes Model) and Case 2 (700°C Filled Flutes Model)

A detailed description of structural behavior is presented in Appendix D. For case 1, with the flutes unfilled, failure occurred by girder 79-44 being pulled off its seated

. 15/02/2010 12:45:00

connection at column 79. Failure occurred late in the cooling stage of the fire, which corresponds to the observed fire behavior on Floor 12. For case 2 where the flutes were filled no failure occurred.

The behavior of the girder 79-44, at the connection with column 79, is shown in Figure 28 for case 1 (unfilled flutes) and case 2 (filled flutes). The important observation is the significant difference in structural behavior due to the filling of the flutes.

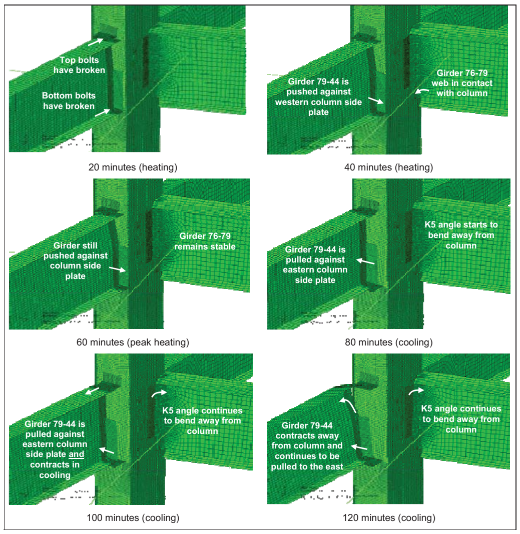

Behavior with unfilled flutes

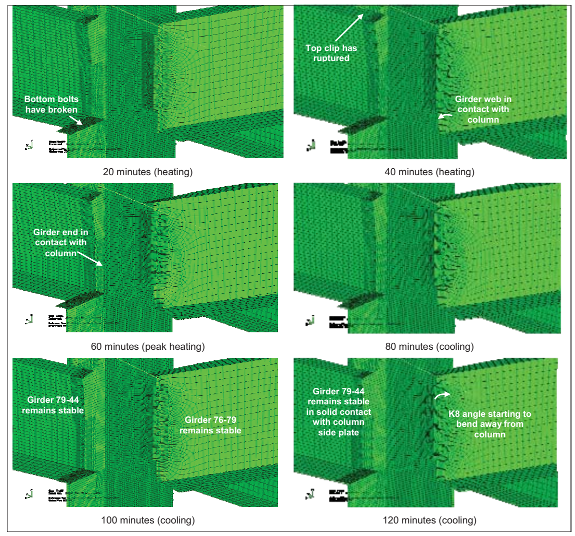

Behavior with filled flutes

Figure 28 *Behavior of girder 79-44 at column 79 for unfilled flutes (left-hand figure) and filled flutes (right-hand figure)*

The behavior of the girder 79-44 for unfilled and filled flutes is summarized in Table 2.

Time (mins)	Case 1: 700°C maximum temperature & unfilled flutes		Case 2: 700°C maximum temperature & filled flutes	
	Observation	**Temperature of top flange of girder 79-44 (°C)**	**Observation**	**Temperature of top flange of girder 79-44 (°C)**
0 to 60	Secondary beams in the north-east bay push the girder 79-44 laterally from east to west.	20 to 627	Secondary beams in the north-east bay push the girder 79-44 laterally from east to west.	20 to 494
4 to 8			The bottom bolts of girder 79-44 break at both column 79 and column 44.	85 to 137
8 to 9	All 4 Bolts in the seated connection at column 79 fracture due to thermal expansion of the girder. This leaves the end of the girder free at column 79 to slide on the seating plate	212 to 230		
21 to 23			The top clip of girder 79-44 ruptures at column 79. This allows the girder to be able to move laterally and longitudinally at the seated connection at the column 79 end.	247
34 to 35	At column 44 all 4 bolts break. This allows the bottom flange to be pushed across the seat until it contacts the column flange. The top flange is largely restrained by the shear studs.	503 to 510		
41			The bolts of the top clip of girder 79-44 break at column 44 break. The girder is also free to move laterally and longitudinally at the seated connection at column 44.	397
60 to 120	Structural begins to cool and secondary beams in the north-east bay pull the girder 79-44 laterally from west to east	627-81	Structural begins to cool and secondary beams in the north-east bay pull the girder 79-44 laterally from west to east	494-153
120	**Localized structural collapse:** Girder 79-44 is falling from the seated connection at column 79 due to end rotation and lateral pulling from the secondary beams in the north-east corner	81	Analysis completed. **No structural collapse**	153

Table 2: *Observed structural behavior for case 1 (unfilled flutes) and case 2 (filled flutes) for 700°C fire curve.*

The failure of the shear studs for both case 1 and case 2 is summarized in Figure 29, where the red dots denote failure of the studs. It can be seen that most studs fail during the cooling stage of the fire, with greater stud failure occurring in case 1, where the flutes were unfilled.

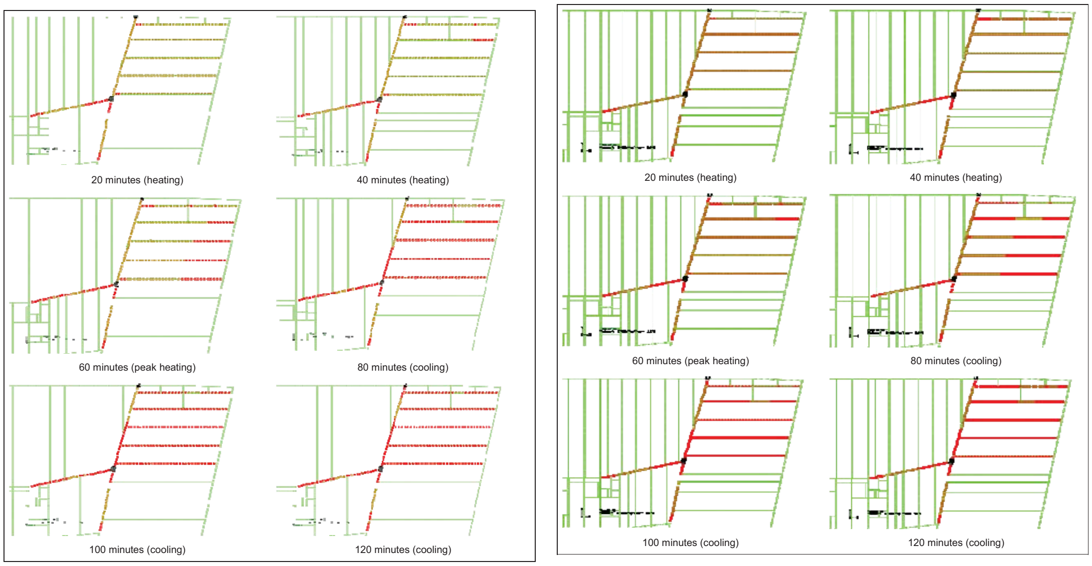

Case 1: Flutes unfilled 700°C fire Case 2: Flutes filled 700°C fire

Figure 29 *Breakage of shear studs at 20 min intervals for Case 1 (unfilled flutes) and Case 2 (filled flutes)*

For the 700°C fire case 1, with the flutes unfilled, the analysis showed that failure occurred late into the cooling stage of the fire, which corresponds to the observed fire behavior on the 12th Floor. This case represents the 'lower' bound of the structural behavior with the modeled, as built condition, failing late in the cooling stage. Direct comparison with the case 2, where the flutes were assumed to be filled as required, showed that no structural failure occurred.

7.5 Case 3 (800°C Unfilled Flutes Model) and Case 4 (800°C Filled Flutes Model)

A detailed description of structural behavior is presented in Appendix D. For case 3 with the flutes unfilled, failure of girder 79-44 occurred during the heating stage at 57 minutes, as shown in Figure 30. For the identical case 4, but with the flutes filled, no failure occurred. Failure during the heating stage corresponds to the visual evidence of fire on the 9th Floor heating the 10th Floor.

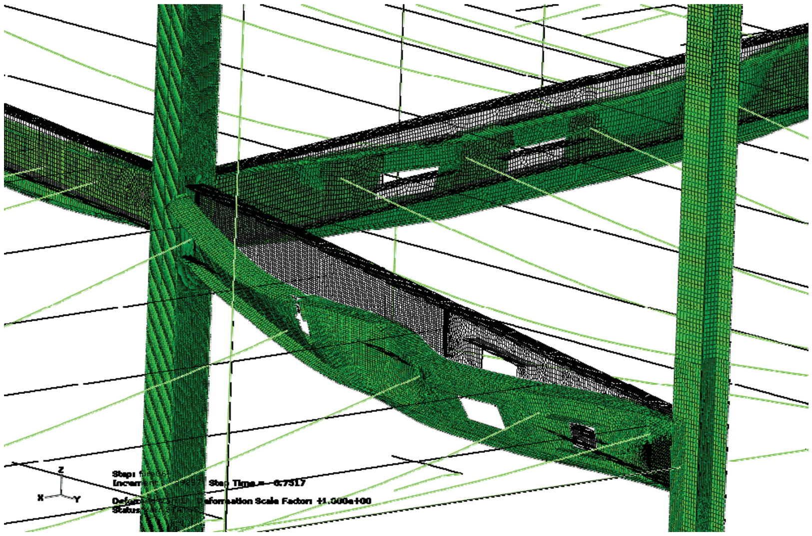

Figure 30 *Failure of girder 79-44 for Case 3 (unfilled flutes)*

The behavior of the girder 79-44, at the connection with column 79, is shown in Figure 31 for case 3 (unfilled flutes) and case 4 (filled flutes).

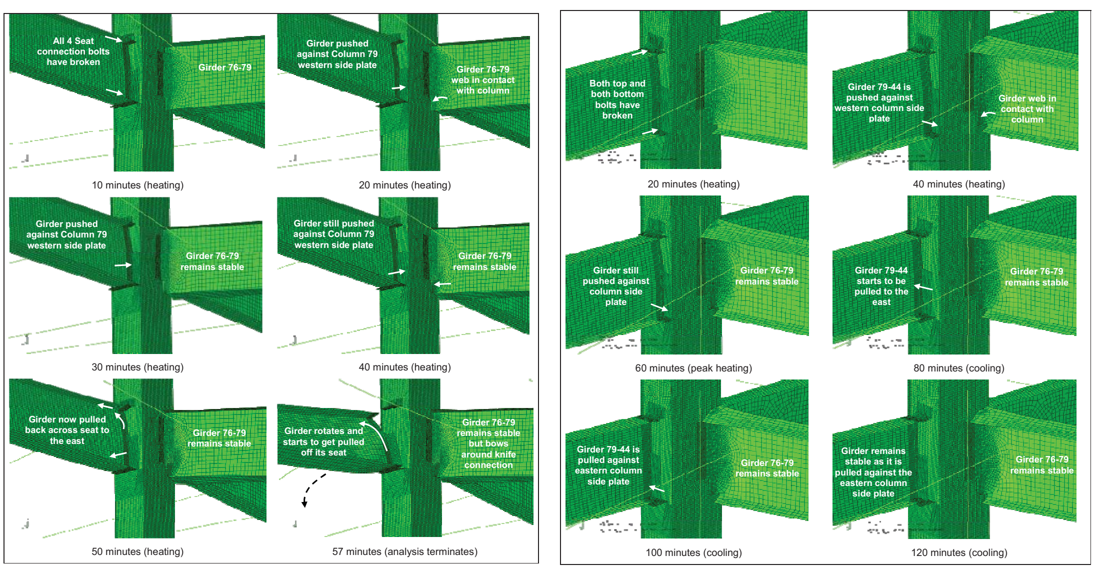

Behavior with unfilled flutes *Behavior with filled flutes*

Figure 31 *Behavior of girder 79-44 at column 79 for unfilled flutes (left-hand figure) and filled flutes (right-hand figure)*

The behavior of the girder between columns 79-44 for unfilled and filled flutes is summarized in Table 3.

Time (mins)	Case 3: 800°C maximum temperature & unfilled flutes		Case 4: 800°C maximum temperature & filled flutes	
	Observation	**Temperature of top flange of girder 79-44 (°C)**	**Observation**	**Temperature of top flange of girder 79-44 (°C)**
0 to 57	Secondary beams in the north-east bay push the girder 79-44 laterally from east to west.	20 to 717		
0-60			Secondary beams in the north-east bay push the girder 79-44 laterally from east to west.	20 to 559
3	Both bolts on the seat plate connection to lower flange of Girder 79-44 at Column 79 break	100	Both bolts on the seat plate connection to lower flange of Girder 79-44 at Column 79 break	72
8	Both bolts at the top clip plate to top flange of Girder 79-44 at Column 79 break	244		
10			Both bolts on the seat plate connection to lower flange of Girder 79-44 at Column 44 break	80
15			Both bolts at the top clip plate to top flange of Girder 79-44 at Column 79 break	170
29	Both bolts on the seat plate connection to lower flange of Girder 79-44 at Column 44 break	548		
35			Both bolts at the top plate to top flange of Girder 79-44 at Column 44 break	228
57	One bolt at the top plate to top flange of Girder 79-44 at Column 44 breaks	717		
57	**Localized structural failure** of girder 79-44	717		
60-120			Structural begins to cool and secondary beams in the north-east bay pull the girder 79-44 laterally from west to east	559 to 178
120			Analysis completed. **No structural collapse**	178

Table 3: *Observed structural behavior for case 3 (unfilled flutes) and case 4 (filled flutes) for 800°C fire curve.*

The failure of the shear studs for both case 3 and case 4 is summarized in Figure 32, where the red dots denote failure of the studs.

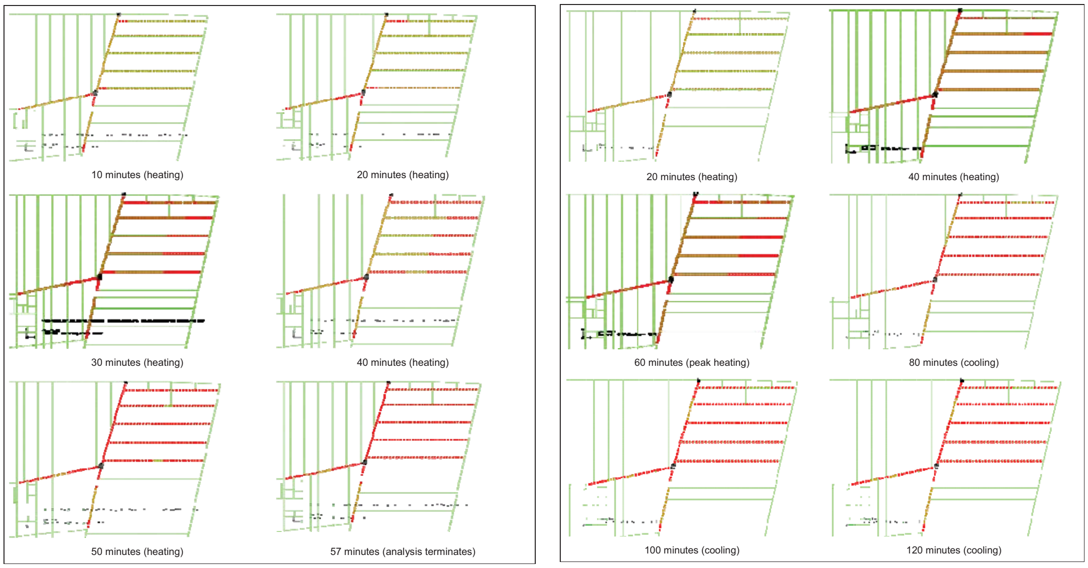

Case 3: Flutes unfilled 800°C fire   Case 4: Flutes filled 800°C fire

Figure 32 *Breakage of shear studs for case 3 (unfilled flutes) and case 4 (filled flutes)*

With case 3 (800°C fire scenario with the flutes unfilled) the analysis showed that localized failure occurred in the heating stage of the fire, which corresponds to the visual evidence of the fire on the 9th Floor. This case represents the 'upper' bound of the structural behavior, with the modeled as built condition failing in the heating stage of the fire. Direct comparison with case 4, where the flutes were assumed to be filled as required, showed that no localized structural failure occurred.

7.4 Summary of the Modeled Cases

Two fire scenarios were chosen to represent fire scenarios where the as-built structure of WTC7 failed during the cooling stage of the fire or the heating stage of the fire. These fire scenarios represent the lower and upper bounds of localized structural failure for the cases where the flutes were unfilled.

The 700°C fire curve showed failure late during cooling (case 1) whereas the 800°C hotter fire scenario showed failure during the heating stage (case 3). In both cases girder 79-44 failed. As a direct comparison identical analyses were conducted except the flutes were assumed to be filled as specified in the 1983 Underwriters Laboratories Fire Resistance Directory[3]. In both cases (case 2 and 4) the structure did not fail, highlighting that if the flutes where filled, as required, collapse of WTC7 would not have occurred.

8.0 Conclusions

1. The flutes (cavities) between the top of the girders and beams on WTC7 were not filled with sprayed fire-resistive material (SFRM), as specified by 1983 Underwriters Laboratories Fire Resistance Directory. This construction fault significantly reduced the resistance of the structure to withstand standard office fires and resulted in localized structural behavior which, coupled with other design faults, propagated into overall progressive collapse.

2. By not filling the flutes the fire resistance of the girders and beams was reduced due to an increase in temperature of the top flange, web and shear studs.

3. Depending on the severity of the standard office fire, failure was shown to occur due to the instability of girder 79-44, either late during the cooling stage of the fire or for a hotter fire at the peak of the heating stage of the fire. Visual evidence suggests that failure late during the cooling stage occurred due to the fire on the 12^{th} Floor, whereas failure at the peak of the heating stage occurred due to fire on the 9^{th} Floor.

4. Detailed finite-element modeling was conducted to highlight the failure modes leading to localized failure which would initiate global collapse as outlined in the report by Guy Nordenson and Associates. For a fire where the maximum temperature was limited to 700°C failure was due to the girder 79-44 being pulled off its seated connection at column 79 during the late cooling stage. For a hotter fire, where the maximum temperature was limited to 800°C, failure was due to flexural instability of the secondary beams and girder 79-44 occurring late in the heating stage. Identical models were run where the flutes were assumed to be filled as required to ensure adequate fire resistance. In the models where the flutes were filled no structural failure was identified leading to the collapse of girder 79-44. This proves that if the flutes were filled then WTC7 would not have collapsed and the damage could have been repaired.

5. The fire protection thickness to the beams and girders was specified assuming a restrained system. However, the structural system was not designed as being restrained, especially the seated connections supporting girder 79-44. The 1983 Underwriters Laboratories Fire Resistance Directory states that the definition of restraint requires the exercise of engineering judgment. It is difficult to see how 'exercising engineering judgment' that the seated connections on girder 79-44, with four 7/8in bolts, provided restraint to adequately transfer thermal thrusts as required. Had the structural system been properly classed as unrestrained and received additional fireproofing required for such a system, the initiating failure of girder 79-44 and the subsequent global collapse of WTC7 would not have occurred.

COLIN G. BAILEY, BEng, PhD, CEng, FICE, MIStructE, MIFireE

9.0 References

1. The term "progressive collapse" is sometimes referred to in the United States codes and regulations as "disproportionate collapse."
2. Guy Nordenson and Associates. Report and Summary of Findings: Global Collapse Analysis, World Trade Center 7 Collapse Investigation. 2009.
3. Fire Resistance Directory, January 1983, Underwriters Laboratories Inc. Testing For Public Safety. 1983.
4. Fire Resistance Directory, January 1985, Underwriters Laboratories Inc. Testing For Public Safety. 1985.
5. Steel Design Guide 19: *Fire Resistance of Structural Steel Framing.* American Institute of Steel Construction, December 2003
6. Indicative Fire Test on Composite Concrete/Steel Deck Floor System. British Steel (RS/RSC/S10244/1/87/D) 1987
7. Joint Industry Sponsored Research: The Fire Resistance of Composite Beams with Unfilled Voids. The Steel Construction Institute. Document SCI/RT/135 July 1990.
8. Fire Resistance of Composite Beams. The Steel Construction Institute. Technical Report SCI Publication 109. 1991.
9. Fred Mower. Assessment of WTC7 Fire Protection and Fire Conditions on 9/11.
10. National Fireproofing Contractors Association. Guidance Information -Bulletin No. 1003: 2008.
11. If the initiating event were a diesel fuel fire, as detailed in the report of Dr. Jose Torero, there would still have been a global collapse., as detailed in the report of Guy Nordenson and Associates.
12. Guy Nordenson and Associates. Report and Summary of Findings: Global Collapse Analysis, World Trade Center 7 Collapse Investigation. 2009.
13. Joseph Colaco. World Trade Center 7: Expert Report

10.0 Documents Reviewed

The list below highlights the main documents reviewed in this study.
This list is only limited to the main documents relevant to this report and does not included the full list of documents reviewed by the author.

Document	Description
PANYNJ0089051	Fire Protection Plan
CANTOR0020570	Bracing connection at 5th floor
CANTOR0008845	Additional load
CANTOR0007743	Additional studs/load
CANTOR0006189	Stud layout
CANTOR0014739	Testwell Craig Laboratories Reports
PANYNJ0037451	Tenant Construction Review Manual
CANTOR0025255 to CANTOR0025276	Testwell Craig Laboratories Reports
CANTOR0020989 to CANTOR0020994	Testwell Craig Laboratories Reports
CANTOR0021000	Testwell Craig Laboratories Reports
CANTOR0023713 to CANTOR0023720	Testwell Craig Laboratories Reports
CANTOR0026207 to CANTOR0026216	Testwell Craig Laboratories Reports
SPI022876	Standby Generator Ventilation
CANTOR0014741 to CANTOR0014741	Testwell Craig Laboratories Reports
CANTOR0025272	Testwell Craig Laboratories Reports
PANYNJ0037124 to PANYNJ0037132	Instruction to Bidders Sprayed-on Fire Protection.
Structural Drawings S1-S8,S12-25	Irwin Cantor and Associates Structural Drawings
CANTOR0004195-CANTOR0002082	Typical Floor Calculations (Vol. 1)
Architectural Drawings	Emery Roth and Sons PC Architects & S.O.M. Drawings
Pictures & videos of collapse	Various Pictures
Pictures prior to collapse	Various Pictures
Pictures following collapse	Various Pictures
Structural Shop Drawings 1-2000,3001-3141,4001 4501,9100-9202	Frankel Steel Limited Drawings
CITI-7WTC072468 to CITI-7WTC073673	Photographs at fit-out
Structural Drawing S-8-10 Rev I	Irwin Cantor and Associates Structural Drawing
Structural Drawing S-8-19 Rev I	Irwin Cantor and Associates Structural Drawing

11.0 List of Papers Published by C.G. Bailey

1. **Bailey C.G**, Burgess I.W. and Plank R.J. The Lateral-torsional Buckling of Unrestrained Beams in Fire. *Journal of Constructional Steel Research* Vol. 36 No.2 1996. pp 101-119. (Cited: Web of Science = 11; Harzing's Publish or Perish = 21)
2. **Bailey C.G**, Burgess I.W. and Plank R.J. Computer simulation of a full-scale structural fire test. *The Structural Engineer.* Vol. 74 No.6 1996. pp 93-100. (Cited: Harzing's Publish or Perish = 45)
3. **Bailey C.G.**, Burgess I.W. and Plank R.J. Analyses of the Effects of Cooling and Fire Spread on Steel-Framed Buildings. *Fire Safety Journal*. No.26 1996 pp 273-293. (Cited: Web of Science = 20; Harzing's Publish or Perish = 27)
4. **Bailey C.G**. and Newman G.M. The design of steel framed buildings without applied fire protection. *The Structural Engineer.* Vol. 76 No.5 1998. pp 77-81. (Cited: Harzing's Publish or Perish = 15)
5. **Bailey C.G**. Development of computer software to simulate the structural behaviour of steel-framed buildings in fire. *Computers and Structures* **67** 1998 pp 421-438. (Cited: Web of Science = 14; Harzing's Publish or Perish = 18)
6. **Bailey C**. Computer modelling of the corner compartment fire test on the large-scale Cardington test frame. *Journal of Constructional Steel Research* Vol. 48 No.1 1998. pp 27-45. (Cited: Web of Science = 6; Harzing's Publish or Perish = 10)
7. **Bailey C.G**. The behaviour of asymmetric slim floor steel beams in fire. *Journal of Constructional Steel Research* Vol. 50 No.3 1999. pp 235-257. (Cited: Web of Science = 6; Harzing's Publish or Perish = 5)
8. **Bailey C.G.**, Lennon T., and Moore D.B. The behaviour of full-scale steel-framed buildings subjected to compartment fires. *The Structural Engineer* Vol. 77 No. 8 April 1999 pp. 15 - 21. (Cited: Harzing's Publish or Perish = 74).
9. **Bailey C.G.**, Moore D.B and Lennon T. The structural behaviour of steel columns during a compartment fire in a multi-storey braced steel-frame. *Journal of Constructional Steel Research* Vol. 52 No.2 1999. pp 137-157. (Cited: Web of Science = 4; Harzing's Publish or Perish = 8)
10. **Bailey C.G**. The influence of the thermal expansion of beams on the structural behaviour of columns in steel-framed structures during a fire. *Engineering Structures* Vol. 22 No. 7 2000. pp 755-768. (Cited: Web of Science = 9; Harzing's Publish or Perish = 16)
11. **Bailey C.G**. Effective lengths of concrete-filled steel square hollow sections in fire. *Proceedings of the Institution of Civil Engineers, Structures and Buildings.* May 2000. pp 169-178. (Cited: Harzing's Publish or Perish = 2)
12. **Bailey C.G**, White D.S. and Moore D.B. The tensile membrane action of unrestrained composite slabs simulated under fire conditions. *Engineering Structures* Vol. 22 No. 12 2000. pp 1583-1595. (Cited: Web of Science = 12; Harzing's Publish or Perish = 18)
13. **Bailey C.G**. and Moore D.B. The structural behaviour of steel frames with composite floorslabs subject to fire: Part 1: Theory. *The Structural Engineer* Vol. 78 No. 11 June 2000 pp. 19 – 27. (Cited: Harzing's Publish or Perish = 48)
14. **Bailey C.G**. and Moore D.B. The structural behaviour of steel frames with composite floorslabs subject to fire: Part 2: Design. *The Structural Engineer* Vol. 78 No. 11 June 2000 pp. 28 – 33. (Cited: Harzing's Publish or Perish = 32)
15. **Bailey C.G**. Membrane action of unrestrained lightly reinforced concrete slabs at large displacements. *Engineering Structures* Vol. 23 No. 5 2001. pp 470-483. (Cited: Web of Science = 13; Harzing's Publish or Perish = 25)
16. **Bailey C**.G. Simplified wind net pressures coefficients for the design of portal frames. *The Structural Engineer.* Vol. 80. No.4. 14 February 2002. pp 21-27.
17. **Bailey C.** Holistic behaviour of concrete buildings in fire. *Proceedings of the Institution of Civil Engineers: Structures & Buildings 152***.** Aug 2002, Issue 3. pp 199-212. (Cited: Harzing's Publish or Perish = 18)
18. **Bailey C.G**. Efficient arrangement of reinforcement for membrane behaviour of composite floor slabs in fire conditions. *Journal of Constructional Steel Research* Vol. 59 No. 7 July 2003, pp.931-949. (Cited: Web of Science = 9; Harzing's Publish or Perish = 12)
19. **Bailey C**.G. Large scale fire test on a composite slim-floor system. *Steel and Composite Structures.* Volume 3, Number 3, June 2003 pp.153-168. (Cited: Web of Science = 4; Harzing's Publish or Perish = 6)
20. **Bailey C**. Holistic behaviour of concrete buildings in fire. Journal of the Structural Engineering Society New Zealand. Vol. 16 No. 1 April 2003. pp 35 51. Invited paper.
21. Foster S.J, **Bailey C.G**, Burgess I.W and Plank R.J. Experimental Behaviour of Concrete Floor Slabs at Large Displacements. *Engineering Structures.* 26, 2004 pp 1231-1247. (Cited: Web of Science = 5; Harzing's Publish or Perish = 8)
22. **Bailey C.G.** Structural fire design: core or specialist subject? *The Structural Engineer*. Vol.82. No. 9, May 2004, pp 32-38. (Cited: Harzing's Publish or Perish = 14)
23. Huang Z., Burgess I., Plank R. and **Bailey C**. Comparison of BRE simple design method for composite floor slabs in fire with non-linear FE modelling. *Fire and Materials.* Vol. 28, No. 2-4. March-August 2004, pp. 127-138. (Cited: Web of Science = 2; Harzing's Publish or Perish = 7)
24. **Bailey C.G.** Membrane Action of Slab/Beam Composite Floor Systems in Fire. *Engineering Structures.* 26, 2004. pp 1691-1703. (Cited: Web of Science = 11; Harzing's Publish or Perish = 18)

25. **Bailey C.** Indicative Fire Tests to Investigate the Behaviour of Cellular Beams Protected with Intumescent Coatings. *Fire Safety Journal*. 39 2004 pp 689-709. (Cited: Web of Science = 7; Harzing's Publish or Perish = 11)
26. **Bailey C.G**. Fire Engineering Design of Steel Structures. *Advances in Structural Engineering.* (Invited paper) Vol.8 N0. 3. 2005. (Harzing's Publish or Perish = 1)
27. Wu, Z.J. and **Bailey C.G.**, Fracture resistance of a cracked concrete beam post-strengthened with FRP sheets *International Journal of Fracture*. **135,** 2005: pp 35-49. (Cited: Web of Science = 1; Harzing's Publish or Perish = 2)
28. **Bailey C.G**. Advances in the Fire Engineering Design of Steel Structures. *Proceedings of the Institution of Civil Engineers: Structures & Buildings.* Paper 13998. SB1. Feb 2006. pp 21-35. (Cited: Harzing's Publish or Perish = 3)
29. Pope, N., and **Bailey C. G.**, Quantitative Comparison of FDS and Parametric Fire Curves with Post-Flashover Compartment Fire Test Data. *Fire Safety Journal.* 41, 2006 pp 99-110. (Cited: Web of Science = 5; Harzing's Publish or Perish = 9)
30. **Bailey C.G.**, Currie P.M and Miller F.R. Development of a new long span composite floor system. *The Structural Engineer*. Vol. 84, No. 21, Nov. 2006.
31. Tafreshi A, **Bailey C G**. "Instability of Imperfect Composite Cylindrical Shells under Combined Loading". Composite Structures. Vol. 80. Issue 1. 2007 pp 49-64. (Cited: Web of Science = 1; Harzing's Publish or Perish = 5)
32. Pope N, **Bailey C G**. "Development of a Gaussian glass breakage model within a fire field model". Fire Safety Journal. Vol. 42. Issue 5. 2007, pp 366-376. (Cited: Harzing's Publish or Perish = 1)
33. **Bailey C G**, Toh W.S. "Small-scale concrete slab tests at ambient and elevated temperatures". Engineering Structures. Issue 29. 2007, pp 2775-2791. (Cited: Web of Science = 1; Harzing's Publish or Perish = 3)
34. **Bailey C G**, Johnson K.A., Alonso-Rasgado T A, Orzechowski M.A.. "The quality of design within the built environment". The Structural Engineer. Vol. 85. 2007, pp 49-55.
35. Miller F.R, **Bailey C G**. "Design concept for a novel long span composite floor system". The Structural Engineer. Vol. 85. No. 21. 2007 pp 38-47.
36. **Bailey C G**, Toh W.S. "Behaviour of concrete floor slabs at ambient and elevated temperatures". Fire Safety Journal. Vol. 42. Issue 6-7. 2007 pp 425-436. (Cited: Web of Science = 1; Harzing's Publish or Perish = 4)
37. Giroldo F, **Bailey C G**. "Experimental bond behaviour of welded mesh reinforcement at elevated temperatures". Magazine of Concrete Research. Vol. 60. No. 1. 2008 pp 23-31.
38. **Bailey C G**, Toh W.S, Chan B.M. "Simplified and Advanced Analysis of Membrane Action of Concrete Slabs". ACI Structural Journal. Vol. 105. No. 1. 2008 pp 30-40. (Cited: Web of Science = 1)
39. Ellobody E, **Bailey C G**. "Behaviour of Unbonded Post-tensioning One-Way Concrete Slabs". Advances in Structural Engineering. Vol. 11. No. 1. 2008 pp 107-120. (Cited: Web of Science = 4; Harzing's Publish or Perish = 5)
40. **Bailey C G**, Lennon T. "Full-scale fire tests on hollowcore floors". The Structural Engineer. Vol. 86 pp 33-39. March 2008.
41. Ellobody E, **Bailey C G**. "Modelling of bonded post-tensioned concrete slabs". Proceedings of ICE, Structures and Buildings. Vol. 161. Issue 6. 2008 pp 311-323. (Cited: Harzing's Publish or Perish = 1)
42. **Bailey C G**, Ellobody E. "Fire Tests on Unbonded Post-Tensioned One-Way Concrete Slabs". Magazine of Concrete Research. Vol. 61 No. 1 2009 pp 67-76. (Cited: Web of Science = 2)
43. Ellobody E, **Bailey C G**. "Modelling of Unbonded Post-Tensioned Concrete Slabs Under Fire Conditions". Fire Safety Journal. Vol. 44 Issue 2. 2009 pp 159-167. (Cited: Web of Science = 1; Harzing's Publish or Perish = 3)
44. **Bailey C G,** Ellobody E. 'Fire Tests on Bonded Post-Tensioned Concrete Slabs. Engineering Structures Vol. 31 Number 3, 2009 pp 686-696. (Cited: Web of Science = 1; Harzing's Publish or Perish = 2)
45. Dai X H, Wang Y C, **Bailey C G**. "Effects of partial fire protection on temperature developments in steel joints protected by intumescent coating". Fire Safety Journal. Vol. 44. 2009. pp 376-386.
46. **Bailey C G,** "Science and Technology Developments in Structural Fire Engineering". Structural Engineering International. Vol. 19. No. 2. pp 155-164. May 2009 (Invited paper).
47. **Bailey C.G,** Ellobdy E. 'Whole-building behaviour of bonded post-tensioned concrete floor plates exposed to fire'. Engineering Structures. Vol. 31. Issue 8. August 2009. pp 1800-1810.
48. Dai X H, Wang Y C, **Bailey C G**. "A Simple Method to Predict Temperatures in Steel Joints with Partial Intumescent Coating Fire Protection" Fire Technology. In Press.
49. **Bailey C.G**. Ellobody E. 'Comparison of unbonded and bonded post-tensioned concrete slabs under fire conditions' The Structural Engineer. In Press.

Books/Design Guides.

1. **Bailey C.G**., Newman G.M and Simms W.I., Design of Steel Framed Buildings without Applied Fire Protection. SCI Publication 186. The Steel Construction Institute, Ascot. 1999. ISBN 1 85942 062 1
2. Newman G.M., Robinson J,T. and **Bailey C.G.**, Fire Safe design: A New Approach to Multi-Storey Steel-Framed Buildings. SCI Publication P288. The Steel Construction Institute, Ascot. 2000. ISBN 1 85942 120 2. (Cited: Harzing's Publish or Perish = 58)
3. **Bailey C.G**. Steel Structures supporting composite floor slabs: design for fire. BRE Digest 462. December 2001. ISBN 1 86081 527 8.

4. **Bailey C**. New fire design method for steel frames with composite floor slabs. Foundation for the Built Environment, FB5, 2003, BRE Bookshop, London. ISBN 1 86081 608 8.
5. **Bailey C.G**. Guide to evaluating design wind loads to BS6399-2:1997. SCI Publication P286. The Steel Construction Institute. 2003. ISBN 1 85942 134 2.
6. Introduction to the fire safety engineering of structures. The Institution of Structural Engineers. 2003. ISBN 0901297291. Member of the Task Group and contributor to drafting of text.
7. **Bailey C.G**. Structural fire engineering design: materials behaviour – Steel. BRE Digest 462. June 2004. ISBN 1 86081 699 1.
8. Newman G.M., Robinson J,T. and **Bailey C.G**., Fire Safe design: A New Approach to Multi-Storey Steel-Framed Buildings (Second Edition). SCI Publication P288. The Steel Construction Institute, Ascot. 2006. ISBN 1 85942 169 5.
9. Lennon T., Moore D.B., Wang Y.C. and **Bailey C.G**., Designers' guide to EN1991-1-2, EN1992-1-2, EN1993-1-2, and EN1994-1-2. Thomas Telford Publishing, London. 2007. ISBN 978-0-7277-3157-9
10. Advanced Structural Fire Engineering, The Institution of Structural Engineers. August 2007. (main author, working with a Task Group). ISBN 978-0-901297-46-4.
11. **Bailey C.G**, and Khoury G.A. Guide to the Fire Engineering of Concrete Structures. To be published 2009.

Refereed Conference Papers.

1. **Bailey C.G**., Burgess I.W. and Plank R.J. The Behaviour of Steel-Framed Structures Subjected to Local Fire Conditions. *Proceedings of the Nordic Steel Construction Conference '95 Melmo, Sweden.* June 1995, pp 693-700 Swedish Institute of Steel Construction. Publication 150, Vol. II.
2. Plank R.J., Burgess I.W. and **Bailey C.G**. Modelling the behaviour of steel-framed building structures by computer. *Proceedings of the Second Cardington Conference.* March 1996.
3. **Bailey C.G**., Burgess I.W. and Plank R.J. 'Structural Simulation of Fire Tests on a Full-Scale Composite Building Frame' , SSRC IC/Brasil '96 - 5th Colloquium on Structural Stability, Rio de Janeiro, August 1996.
4. **Bailey C.G**., Burgess I.W. and Plank R.J. Bridging and Restraint Effects of Localised Fires in Composite Frame Structures. *Composite Construction - Conventional and Innovative International Conference Innsbruck, Austria.* September 16-18 1997, pp 379-384 IABSE.
5. Rose P.S., Burgess I.W., Plank R.J. and **Bailey C.G**. The influence of floor slabs on the structural behaviour of composite frames in fire. *The Fourth International Kerensky Conference, Hong Kong.* September 3-5 1997, pp 511-518.
6. Rose, P.S., **Bailey, C.G.**, Burgess, I.W. and Plank, R.J.'The Influence of Floor Slabs on the Structural Performance of the Cardington Frame in Fire', Second World Conference on Constructional Steel Design, San Sebastian, *Journal of Constructional Steel Research*, 46:1-3, Paper No. 181 (1998).
7. **Bailey C.G**., Lennon T., and Moore D.B. Full scale fire test on the new UK slim floor system. *Advances in Steel Structures. Proceedings of the Second International Conference on Advances in Steel Structures.* 15-17 Dec 1999, Hong Kong China. pp 1055- 1062.
8. **Bailey C.G**. The experimental and theoretical behaviour of composite floor slabs during a fire. *Proceedings of the Seventh International Symposium on Structural Failure and Plasticity (IMPLAST 2000).* 4-6th October 2000 Melbourne, Australia. pp. 635-640.
9. HuangZ., Burgess, I.W., Plank, R.J., and **Bailey C.G**. Strategies for Fire Protection of Large Composite Buildings. *Proceedings Interflam 2001.* Edinburgh (2001) pp 395-406.
10. **Bailey C.G**. Simplified wind net pressures coefficients for the design of portal frames. *The Structural Engineer.* Vol. 80. No.4. 14 February 2002. pp 21-27.
11. HuangZ., Burgess, I.W., Plank, R.J., and **Bailey C.G.** Comparison of BRE Simple Design Method for Composite Floor Slabs in Fire with Non-Linear FE Modelling. *Proceedings of the Second International Workshop on Structures in Fire.* Christchurch, New Zealand (2002) pp 83-94.
12. Lennon T., **Bailey C.G**. and Clayton N. The Performance of High Grade Concrete Columns in Fire. *6th International Symposium on Utilization of High Strength / High Performance Concrete.* Leipzig. June 2002. pp 341- 353.
13. **Bailey C.G**. Structural Fire Design of Unprotected Steel Beams Supporting Composite Floor Slabs. **Keynote**: *II CICOM, II International Conference on Steel Construction.* São Paulo, Brazil. Nov.2002.
14. **Bailey C.G.** Membrane action of composite floor systems in fire. *Third International Workshop, Structures in Fire. Ottawa* May 2004 Paper S7-1, pp 335-352.
15. **Bailey C.G**. Recent advances in the fire engineering design of steel structures. **Keynote**: Innovation and Advances in Steel Structures. International Symposium 30-31 August 2004, Singapore pp. 155-175.
16. **Bailey C.G**. A Simplistic or Holistic Approach to Structural Fire Engineering? **Keynote**: Tall Buildings in Historical Cities – Culture & Technology for Sustainable Cities. *Proceedings of the CTBUH 2004 Seoul Conference October 10-13 2004.* pp 1- 11.
17. Pope, N., and **Bailey C. G.**, Sub-Grid-Scale Parameters in Computational Fluid Dynamics Modelling of Compartment Fires. *Proceedings of the Tenth International Conference on Civil, Structural and Environmental Engineering Computing.* Paper 113. Italy, 30 Aug–2 Sep 2005.
18. Winter S.L, **Bailey C.G**., Apsley D.D., Computational Fluid Dynamics Modelling of Compartment Fires. *5th International Symposium on Turbulence, Heat and Mass Transfer* pp 613-616, 2006.
19. Lee D.Y.C. and **Bailey C.G**. The Behaviour of Post-Tensioned Floor Slabs under Fire Conditions. *International Congress on Fire Safety in Tall Buildings,* pp 183-201. 2006

20. **Bailey C.G**. Recent Developments in Structural Fire Safety. *International Congress on Fire Safety in Tall Buildings,* pp 59-78. 2006.
21. Nadjai, **A**. **Bailey C.G,** Siamak B.M, Ali, F, Talamona D, Allam, A. Behaviour of Composite Floor Cellular Steel Beams at Elevated Temperatures. *International Congress on Fire Safety in Tall Buildings,* pp 359-371. 2006.
22. **Bailey C G**. "Structural fire engineering of steel framed buildings - **Keynote**". Proceedings of the 3rd International Conference on Steel and Composite Structures (ICSCS07), Manchester, UK. pp 57-65. 30 July 2007.
23. Lee D.Y., **Bailey C G**. "The Behaviour of Post-Tensioned Floor Slabs under Fire Conditions.". SEMC 2007 The Third International Conference on Structural Engineering, Mechanics and Computation, University of Cape Town, South Africa. pp 1253-1257. September 2007.
24. Gweli S S, Nedwell P J, **Bailey C G**. "The use of high performance non metallic fibre in Ferrocement". SEMC 2007, The Third International Conference on Structural Engineering, Mechanics and Computation, University of Cape Town, South Africa. pp 1417-1422. September 2007.
25. Bake S, **Bailey C G**. "Performance of cellular steel beams at ambient and elevated temperatures". SEMC 2007 The Third International Conference on Structural Engineering, Mechanics and Computation, University of Cape Town, South Africa. pp 1268-1273. September 2007.
26. Ellobody E, **Bailey C G**. "Experimental and Numerical Investigation of Post-Tensioned Unbonded Concrete Slabs in Fire". Interflam 2007 11th International Fire Science & Engineering Conference, UK. pp 617-628. 3 September 2007.
27. Dai X, Wang Y C, **Bailey C G**. "Temperature distributions in unprotected steel connections in fire". Proceedings of the 3rd International Conference on Steel and Composite Structures (ICSCS07), Manchester, UK. Editor Wang, Y.C. & Choi, C.K.. pp 535-540. 30 July 2007.
28. Bake S, **Bailey C G**. "Numerical studies of cellular beams at elevated temperatures". ICASS 2007, The Fifth International Conference on Advances in Steel Structures, Singapore.. pp 750-756. December 2007.
29. Nadjai A, Goodfellow N, Talamona D, Ali F, **Bailey C G**, Siamak B.M. "Experimental and numerical investigation on composite floor cellular steel beams in fire". Proceedings of the 3rd International Conference on Steel and Composite Structures (ICSCS07), Manchester, UK. pp 673-679. 30 July 2007.
30. Giroldo F, **Bailey C G**. "Bond behaviour of welded mesh reinforcement at elevated temperatures". SEMC 2007 The Third International Conference on Structural Engineering, Mechanics and Computation, University of Cape Town, South Africa. pp 1236-1241. September 2007.
31. Toh W.S, **Bailey C G**. "Comparison of Simple and Advanced Models for Predicting Membrane Action on Long Span Slab Panels in Fire". Interflam 2007 11th International Fire Science & Engineering Conference, UK. pp 791-796. 3 September 2007.
32. Ellobody E, **Bailey C G**. "Testing and modelling of bonded and unbonded post-tensioned concrete slabs in fire". Proceedings of the Fifth International Conference in Structures in Fire. Singapore. pp 392-405. 28-30 May 2008
33. Dai X, Wang Y C, **Bailey C G**. "Temperature developments in partially protected steel-concrete composite joints using intumescent coating". Proceedings of the Fifth International Conference in Structures in Fire. Singapore. pp 172-183. 28-30 May 2008.
34. Ellobody, E. and **Bailey, C.G**. Holistic behaviour of post-tensioned concrete floors under fire conditions. Proceedings of the 11th International conference on Fire and Materials, Fire and Materials-09, San Francisco, USA, pp. 511-524, 26-28 January, 2009
35. Abdullah, A., **C. Bailey**, and J. Wu. Behaviour Of Concrete Column-Slab Connections Strengthened With Pre-stressed Carbon Fibre Plates. Proceeding of The 9th International Symposium on Fibre-Reinforced Polymer Reinforcement for Concrete Structures. Sydney-Australia. Vol. 19: p. 11-15. July 2009.
36. Guo, S. and **Bailey C**. Experiment and numerical research on multi-span composite slab, Proceeding of the 9th International Conference on Steel Concrete Composite and Hybrid Structures(ASCCS 2009), Leeds, UK, 8-9 July, 2009. pp. 339-344.
37. Krishnamoorthy,R.R., **Bailey,C.G**. Temperature distribution of intumescent coated steel framed connection at elevated temperature. Proc.Nordic Steel Construction Conference'09,Malmo,Sweden,2-4 Sept 2009, pp 572-579, Swedish Institute of Steel Construction, Publication 181,Vol.I
38. **Bailey C.G**. Structural Fire Engineering – Research to Practice. **Keynote** 5th Chinese Conference on Structures in Fire Jinan, China, To be presented Oct. 29 and 30, 2009.

12.0 Rate Schedule

I am being compensated at the rate of £1000.00 (UK Pounds) per day (7.5 hours) for time spent working on this project. Reimbursable expenses are being charged at actual cost with supporting receipts.

13.0 APPENDIX A
Photographs showing fire protection during tenant fit-out stage

The construction of WTC7 was completed in 1987. These photographs were taken during 'fit-out' of the floors in 1989. They show that the flutes were not filled with fire protection as required. They also show in a number of cases wires being passed through the open flutes.

Figure A1: Photograph showing wire placed through flutes (46th Floor).

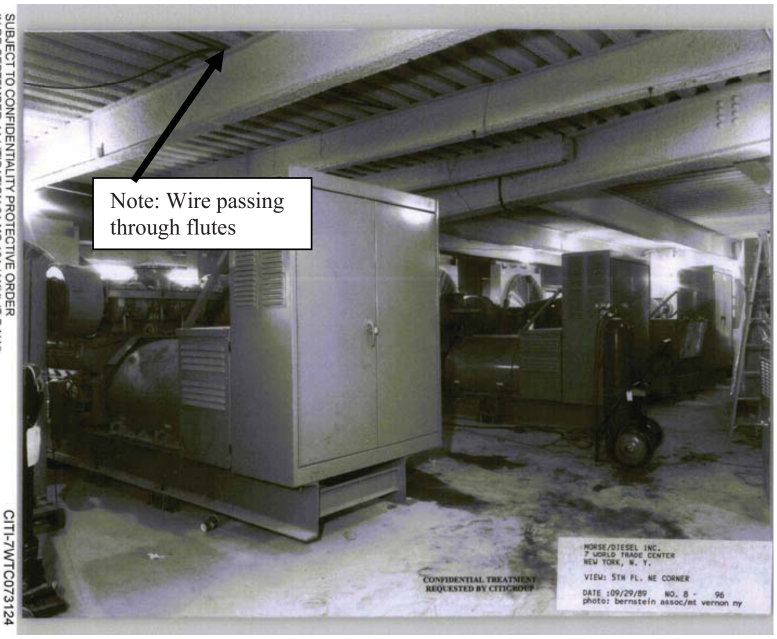

Figure A2: Photograph showing wire placed through flutes (5th Floor).

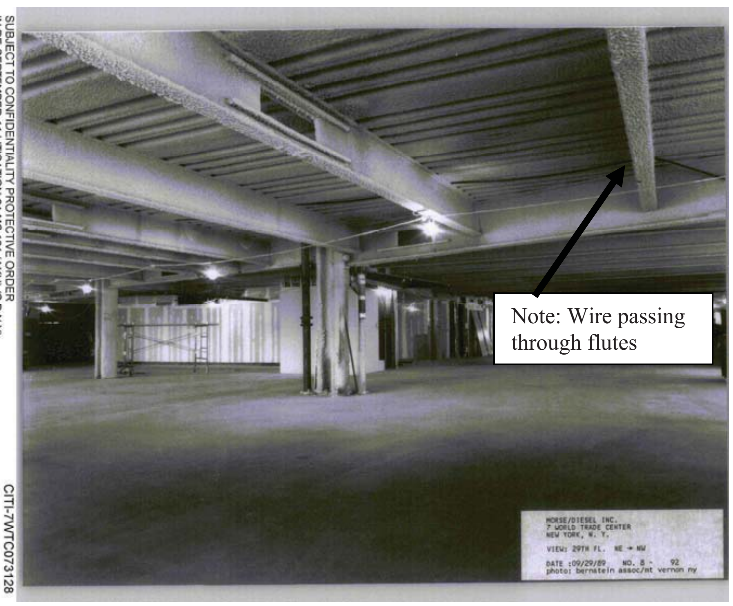

Figure A3: Photograph showing wire placed through flutes (29th Floor).

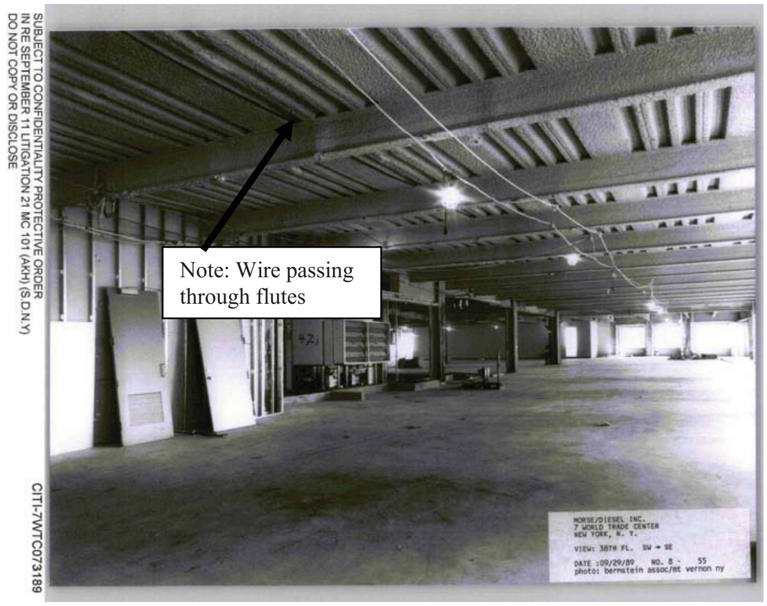

Figure A4: Photograph showing wire placed through flutes (38th Floor).

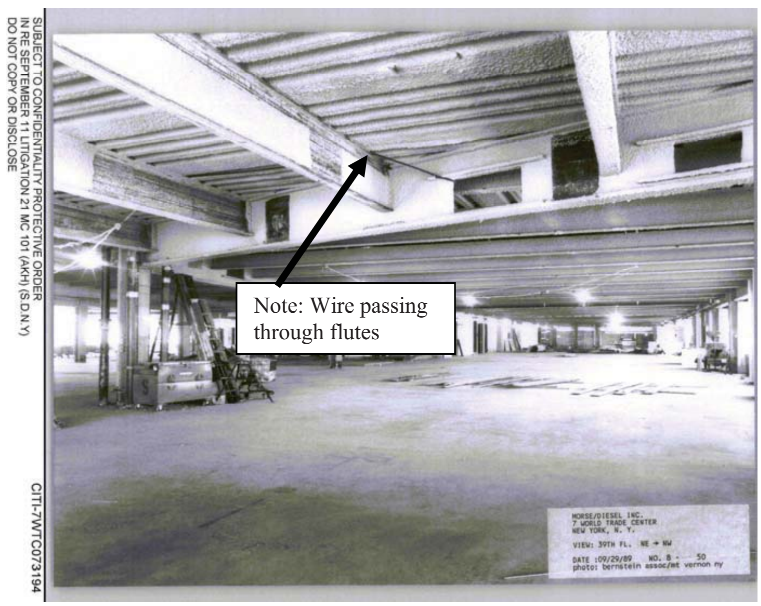

Figure A5: Photograph showing wire placed through flutes (39th Floor).

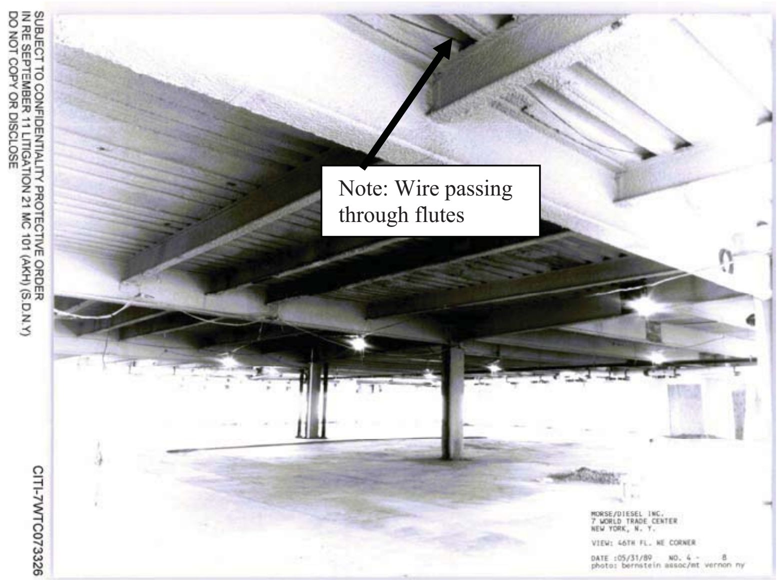

Figure A6: Photograph showing wire placed through flutes (46th Floor).

Figure A7: Photograph showing wire placed through flutes (39th Floor)

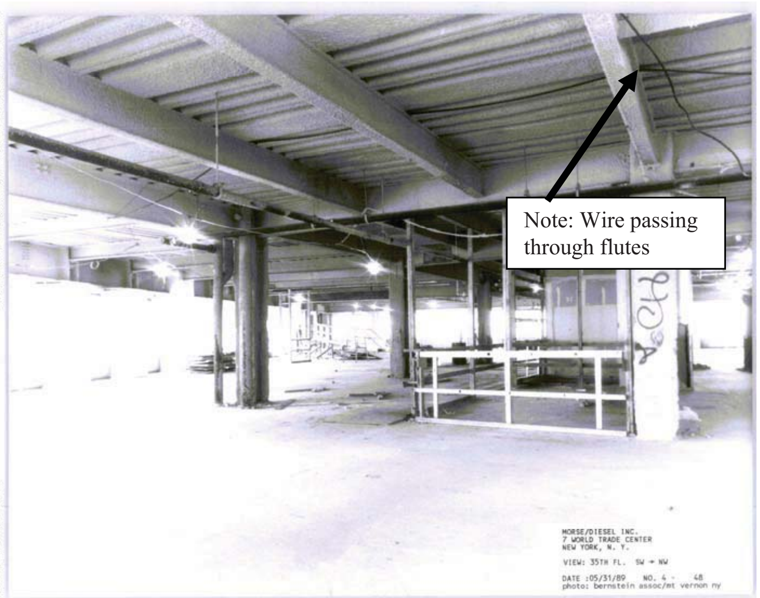

Figure A8: Photograph showing wire placed through flutes (35th Floor)

Figure A9: Photograph showing wire placed through flutes (32nd Floor)

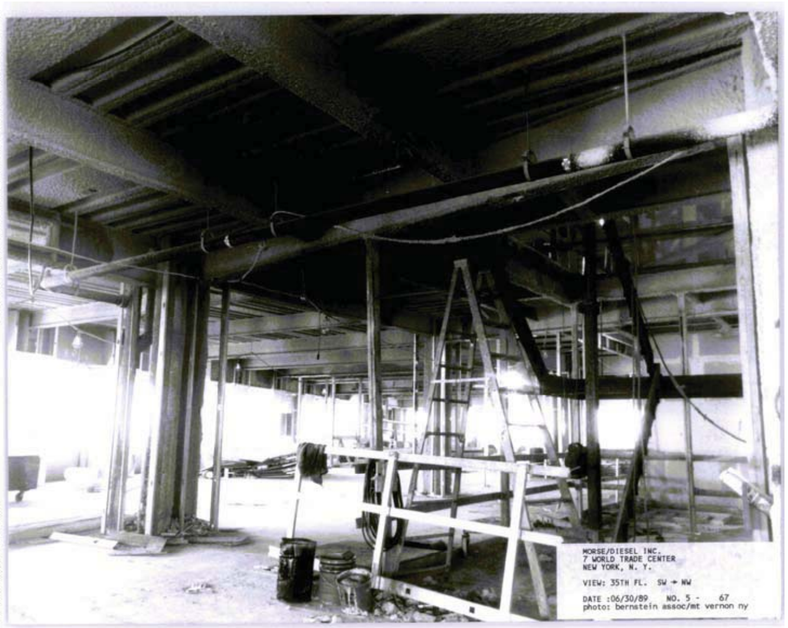

Figure A10: Photograph showing wire placed through flutes (35nd Floor)

Figure A11: Photograph showing wire placed through flutes (34th Floor)

Figure A12: Photograph showing wire placed through flutes (33rd Floor)

Figure A13: Photograph showing wire placed through flutes (32nd Floor)

Figure A14: Photograph showing light through flutes (39th Floor)

Figure A15: Photograph on 32rd floor showing unfilled flutes above girder

Figure A16 Photograph on 24th floor showing unfilled flutes above girder

14.0 APPENDIX B
Testwell Craig Laboratories reports

Details from Testwell Craig Laboratories reports showing unfilled flutes over fire rated walls.

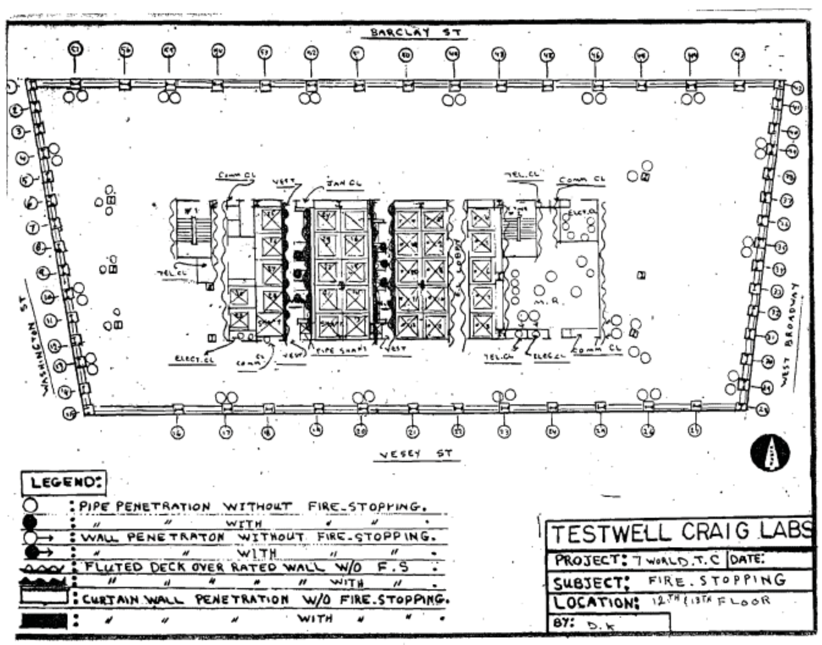

Figure B1 Sketch showing unfilled flutes above fire walls which had firestopping missing (12th and 13th floors).

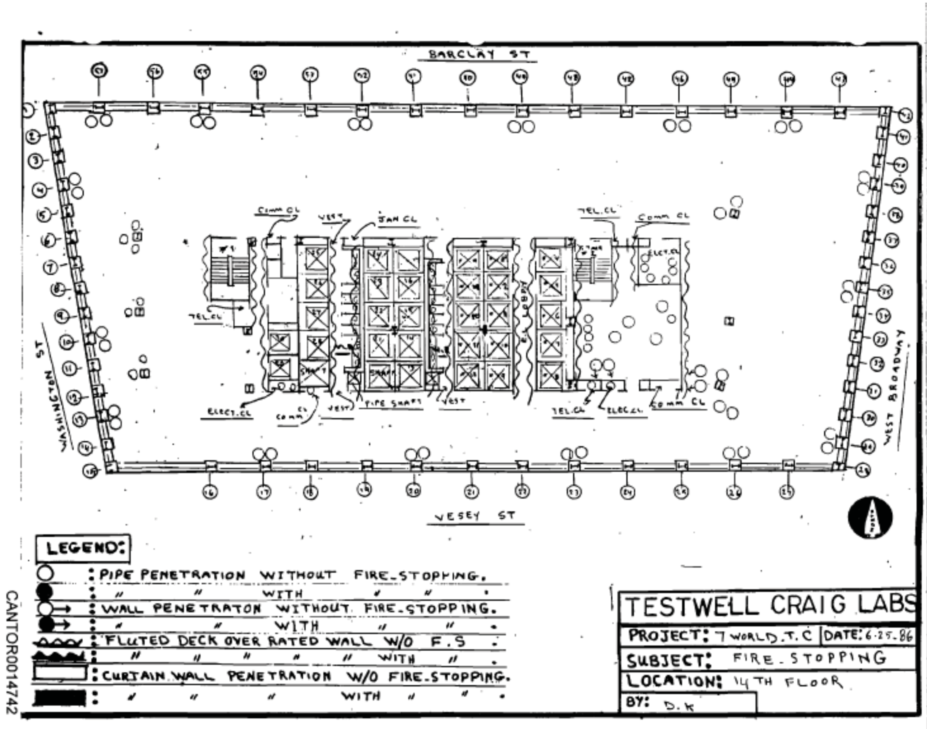

Figure B2 Sketch showing unfilled flutes above fire walls which had firestopping missing (14th floor).

15.0 APPENDIX C
Report on the Background Testing into Unfilled/Filled Voids (Flutes)

Summary

This report presents the background testing carried out relating to unfilled voids (flutes). The test data shows that the top-flange temperature is greater than the bottom flange when the voids are unfilled, whereas when the voids are filled the bottom flange temperature is greater. The non-filling of voids also results in higher temperatures of the shear studs in composite beams, which could lead to failure of these studs compared to beams were the voids are filled.

C1.0 Introduction

When a steel beam supports a composite deck, comprising a steel deck, concrete and mesh reinforcement, a void is formed between the top flange of the beam and deck. For trapezoidal shaped decks, such as that used on WTC7, this void can be large. Figure C1 shows the voids above the top flange of the beam for the protected beams in WTC7. Leaving the voids between the deck and top flange of the beam unfilled with fire protection results in:

- An increase in temperature of the top flange and web.
- An increase in temperature of the shear studs.
- A reduction in overall fire resistance.

Figure C1 *Picture of the WTC7 showing unfilled voids.*

The spray fire-resistive material (SFRM) used on WTC7 was a Monokote MK-5; a gypsum-based material containing vermiculite aggregate. The product was manufactured by W.R. Grace and Co., who ceased production of the MK-5 product in the 1980s. The Underwriters Laboratories (UL) document BXUV.D739 covered the specification of Monokote MK-5. The June 2006 version of BXUV.D739 states that '*when steel deck is used, the area between the steel deck and the beams top flange shall be filled*'. In the UL Fire Resistance Directory for 1983 it is stated '*Cavities, if any, between the upper beam flange and floor or roof units shall be filled with the fire protection material applied to the beam, unless stated otherwise on an individual design.'* The identical statement was repeated in the UL Fire Resistance Directory for 1985.

It can therefore be concluded that the voids (cavities) should have been filled with fire protection on WTC7. Figure C2 shows an example where the voids have been filled with SFRM. Comparison with Figure 1 shows clearly that the voids on WTC7 were not filled, resulting in a lower fire resistance compared to that specified.

Figure C2 *Voids filled with SFRM*

C2.0 UK design rules for filled/unfilled voids

In the UK, it is possible to have unfilled voids, which saves cost and application time. To allow unfilled voids the fire protection thickness needs to be increased as shown in Table C1(1).

Beam Type	Fire Protection on beam	Fire Resistance (minutes)		
		Up to 60	90	Over 90
Composite	Materials assessed at 550°C	No increase in thickness	Increase thickness by 10% or assess thickness using A/V increased by 15%*	Fill Voids
	Materials assessed at 620°C	Increase in thickness or assess thickness using A/V increased by 30%*	Increase thickness by 30% or assess thickness using A/V increased by 50%*	Fill Voids
Non-composite	All types	Fill Voids		

* The least onerous option may be used

Table C1: *UK design rules*

In the UK, materials are typically assessed at 550°C or 620°C, which means that the steel section will not exceed these temperatures for the fire resistance period specified. For columns with 4-sided heating the 550°C value is typically used and for beams with 3-sided heating the 620°C value is typically used.

According to the generally accepted test standard ASTM E-119 one of the criteria for establishing the fire resistance rating for a steel column or floor beam is derived from the time at which, during a standard fire exposure, the average column temperature exceeds 538°C (1000°F) or the average floor beam temperature exceeds 593°C (1100°F).

It can been seen that it is possible in the UK to design for unfilled voids for up to 90 mins provided the thickness of the protection is increased or the section factor, which can be used to specify the protection, is increased. The section factor defines how quickly the section heats up and can be used to design the actual thickness of the protection.

For fire resistance periods above 90 mins the voids need to be filled.

The WTC7 building was specified as Class 1B with the columns having 3 hours fire resistance and the floor construction having 2 hours fire resistance. Therefore the UK rules state that the voids would need to be filled. With the voids being unfilled on the WTC7 the fire resistance was lower than that specified.

C3.0 Background research and testing

To develop the UK design rules relating to unfilled voids a program of testing work was carried out in the late 1980s and early 1990s.

Indicative fire tests

In 1987 a series of unloaded indicative fire tests[(2)] were conducted to investigate the effect of unfilled voids. Two steel beams (406×178×60UB) supported a trapezoidal deck (PMF CF60). In one case the concrete composite floor was lightweight whereas in the other case the concrete was normal weight. The steel beams were protected using the SFRM Mandolite. A dovetail deck was also tested but this is not relevant to this study. Prior to spraying the voids were packed with mineral fibre. Before testing two of the voids had their fibre protection removed (Figure C3) to allow a comparison with the area where the protection remained. The instrumentation was limited and it is only possible to compare the top flange temperatures of the beam at the location of unfilled voids, the top flange temperatures at the location of filled voids and the bottom flange temperature. The bottom flange temperature was only measured at the part of the beam that had filled voids but it is expected that the bottom flange temperatures are similar along the length of the beam irrespective of whether the voids are filled or not.

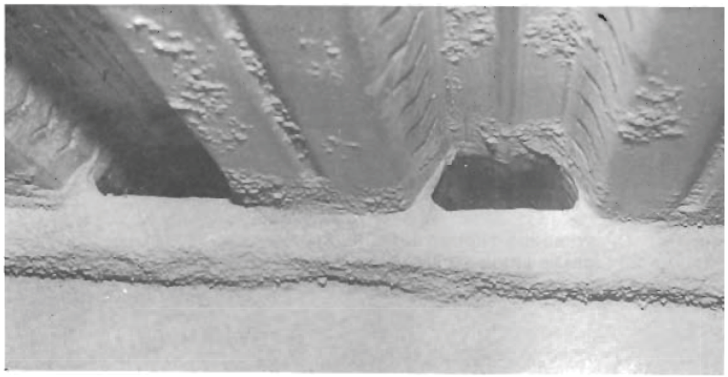

Figure C3 *Location of unfilled voids*

The test results showing the temperatures of the top and bottom flange are shown in Figure C4, for the case where normal weight concrete was used. It can be seen that the top flange temperatures at the location of the unfilled voids are significantly higher than the temperatures at the location where the voids were filled. At 105 mins, when the test was terminated the top flange temperature at the unfilled location was 505°C compared to the top flange temperature of 326°C at the filled location. This represents an increase in temperature of 55%.

The case with lightweight concrete was similar with the top flange temperature being 389°C at the location of filled voids, 551°C at the location of unfilled voids with the temperature of the bottom flange being 563°C at 105mins. In this case the temperature increase of the top flange between filled and unfilled voids was 42%

8.3.2 Cooling phase

During the early stages of the cooling phase the vast majority of the remaining shear studs on the north-east secondary beams are broken due to differential cooling between the slab and the beams. Runaway failure is not observed in the north-east corner of Case 4 as the beams are able to cool below the critical temperature of the secondary beams is reached and before total shear connection is lost.

Figure 76 shows the vertical deflection contours of the slab at the end of cooling. The large deflection in the NE bay is linked to the fact that significant shear stud breakage is observed during cooling. The reduction in restraint to the beams by the slab that results from the stud breakage also allows the secondary beams in the north-east bay to topple during the analysis as they attempt to contract into the slab. This combination of strength reducing effects leads to a larger deflection than observed in the other Cases.

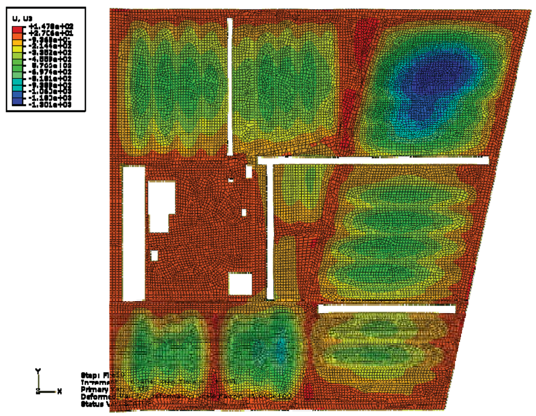

Figure 76: 800°C Filled Flutes Case 4 - Vertical Deflection Contours at End of Cooling

As the secondary beams cool they try to return to their original position. In order for them to be able to do this they must attempt to lift the slab up somewhat and this leads to increasing tension in the beam connections. As indicated in Figure 27 the loss of composite connection between the slab and beams can lead to the secondary beams rotating around their long axis, reducing their bending strength. It is considered that this rotation is caused by the beams attempting to contract into the slab. Compatibility between the slab and the beams means that it is easier for the beams to deform, compared to the force required to lift the concrete slab.

Figure 77 also indicates that the large tensile forces developed as the secondary beams contract against the slab are sufficient to rupture their connections leading to local failure.

Over the course of the cooling phase there is little appreciable reduction in deflection in the north-east bay. This is due to the combination of secondary beam connection failure and a general build up of local distortion of the secondary beams. The beams are not strong enough lift the slab up as they contract and therefore undergo local deformations.

The key responses in the floor structure during the cooling phase are:

- Large displacements in north-east corner are not recovered during cooling
- Secondary beam connection failure reduces robustness of north-east corner floor
- Contraction of secondary beams act to pull Girder 79-44 eastward on seated connection
- Analysis ends at 2 hours with the end of girder 79-44 well seated and restrained by column side plates

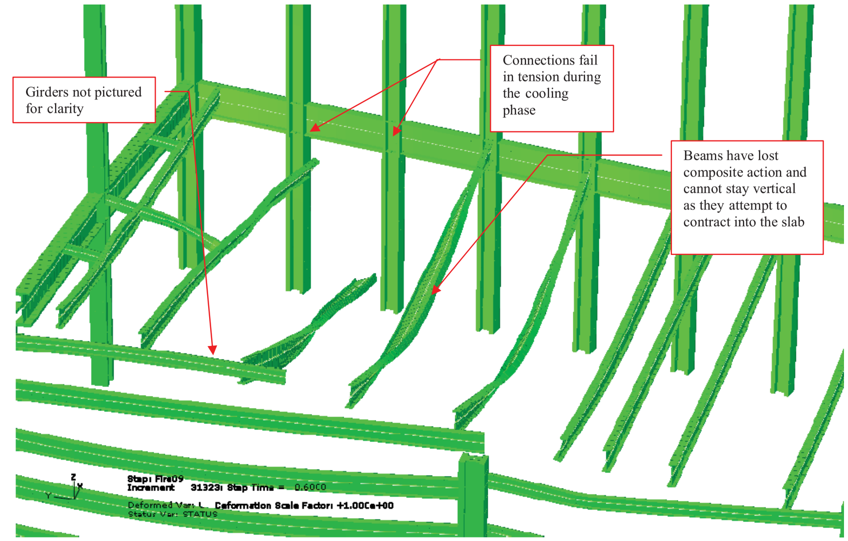

Figure 77: 800°C Filled Flutes Case 4 - Beam Orientation During Cooling Phase (90 minutes, Girders removed for clarity)

8.4 Details of Connection Behaviour

8.4.1 Detailed Connections

The movement of the 3 connections around Column 79 are imaged in Figure 78, Figure 79 and Figure 80. These images are taken at ambient, peak heating and the end of cooling.

8.4.1.1 Column 79 Seat

The most relevant connection response is that of the seated connection at Column 79. It is this connection that has been highlighted as the most likely potential failure mechanism. The following key responses are observed at this connection:

- Seating bolts break early in the fire due to longitudinal expansion of Girder 79-44. The bolts in the top clip break shortly thereafter.
- End of girder is then free to be moved about on the seating plate. This movement is consistent with the response seen in the other three cases analysed.
- Toward the middle of the heating phase the girder end is jammed into the corner between the column flange and the extension of the column side plate beyond the flange.
- As the structure begins to cool the contraction of the structure pulls the end of Girder 79-44 eastward across the seating plate at Column 79.
- At the end of cooling the girder end is solidly seated and in good contact with the column side plate.

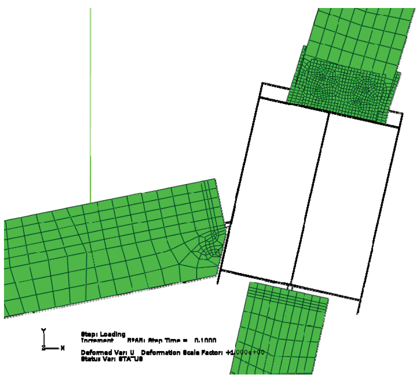

Figure 78: 800°C Filled Flutes Case 4 - Column 79 Seat Connection at Ambient

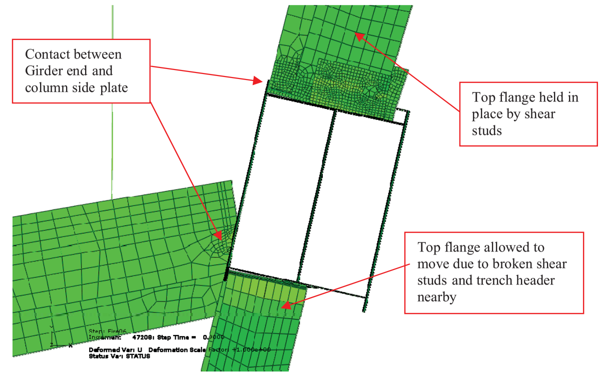

Figure 79: 800°C Filled Flutes Case 4 - Column 79 Seat Connection at Peak Heating

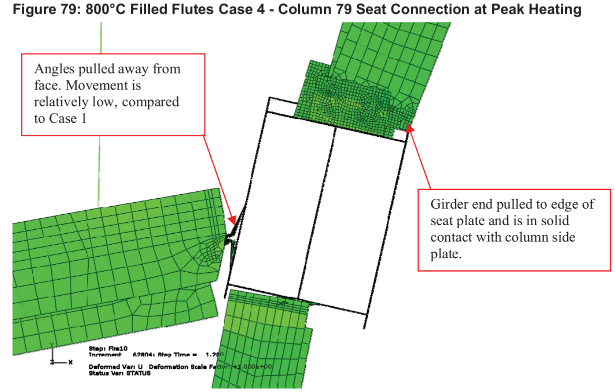

Figure 80: 800°C Filled Flutes Case 4 - Column 79 Seat Connection at End of Cooling

8.4.1.2 Column 79 Knife Connections

The other 2 connections at Column 79 (K8 and K5 knife connections) are also affected during the fire, although to a lesser extent than the seated connection.

- During the heating phase of the fire compression forces in the attached girders cause some plate bending, however no substantial damage is observed either in the plates or in the bolts of either knife connection.
- As the girders contract during the cooling phase the angle plates of the connection are pulled away from the face of the column (this is observed in Cases 1, 2 and 4 where the analyses continue through the cooling phase).

It is considered that neither of the knife connections at Column 79 exhibit definite signs of failure in Case 4.

JA-3199

8.4.2 Simplified Connections

During the cooling phase of the Case 4 analysis 19 of the 247 simplified connector elements are observed to break. As with the Case 1 and 2 analyses, the majority of these broken connections are clustered in the central bay as indicated in Figure 81. Except for the 2 connections in the NE corner, all the broken connections are variations on the SWC type connection. Failure of these connections is due to the high tension forces formed in the connections caused by contraction of the sagging secondary beams during the cooling phase.

The breakage of the central connections does not significantly affect the response of the building as the beams they connect remain in full composite action with the concrete slab.

The failure of the 2 connectors in the NE corner of the building after 80 minutes of analysis time is related to the tensile forces induced during cooling. This breakage leads to the falling away of the secondary beams as they have also lost composite connection to the slab above. This response leads to larger residual deflection in the north-east bay compared to the rest of the structure.

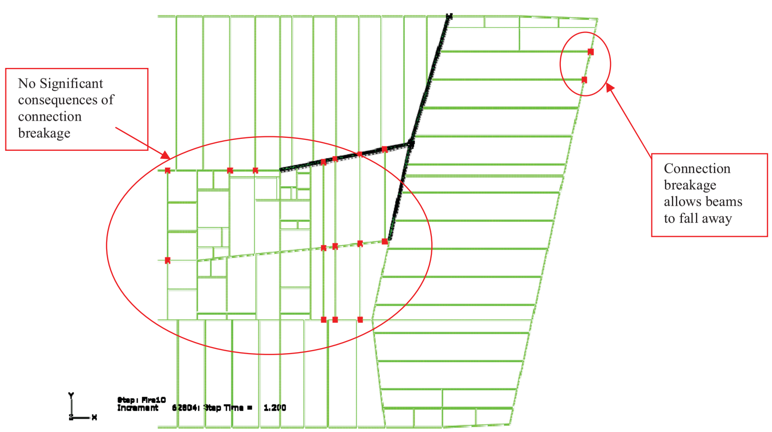

Figure 81: 800°C Filled Flutes Case 4 - Breakage of Simplified Connections

8.5 Timeline of Key Behaviour

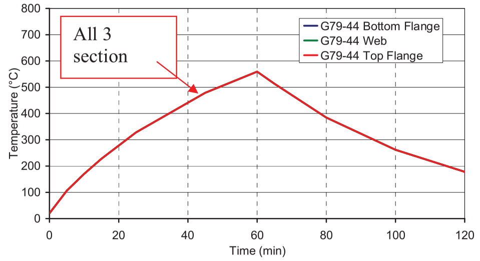

Figure 82: 800°C Filled Flutes Case 4 - G79-44 Temperatures

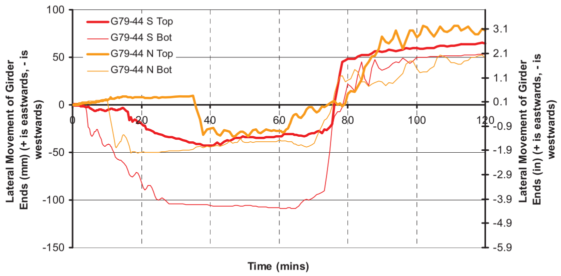

Figure 83: 800°C Filled Flutes Case 4 - G79-44 End Displacements (East-West)

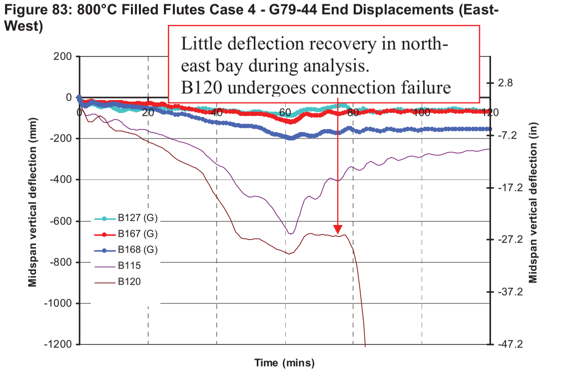

Figure 84: 800°C Filled Flutes Case 4 - Selected Beam and Girder Vertical Deflections

Event	Time Mins	Location and failure comments	Girder 79-44 Top Flange Temp °C
1	3.0 to 3.4	Bottom Bolts in seated connection at Column 79 break. This allows the end of the girder to slide on the seating plate. Restraint from the top clip is minimal.	72 to 80
2	10.0	At column 44 the bottom bolts break. The bottom flange on this connection is then pushed across the seat to contact the column flange	170
3	15.0	Top bolts in seated connection at Column 79 break. Lateral restraint to the girder comes only from shear studs to slab.	228
4	18.5	Bottom flange of G79-44 at Column 44 contacts the column flange.	263
5	29.0	Bottom flange of G79-44 contacts column 79 side plate.	358
6	30.0	Mid-span deflection of central beam in the north east corner bay has now reached 315mm (12.4”)	366
7	35.1	Top bolts in seated connection at column 44 break. Girder end is now restrained only by shear connection to slab.	404
8	60.0	Mid-span deflection of central beam in the north east corner bay has now reached 760mm (30”)	559
9	65.7	Bottom flange of G79-44 at Column 79 seat is pulled eastward	507
10	80.0	End of G79-44 pulled against eastern side plate of Column 79. The girder end stays in solid contact with this plate for the remaining analysis time.	
11	90	Mid-span deflection of north east corner bay has now reached 1270mm (50”). Other, similar bays have returned to a deflection of 550 to 600mm (21.7 to 23.6”)	323
12	120	Mid-span deflection of north east corner bay has now reached 1300mm (51.1”). Other, similar bays have returned to a deflection of 450 to 600mm (17.7 to 23.6”)	178

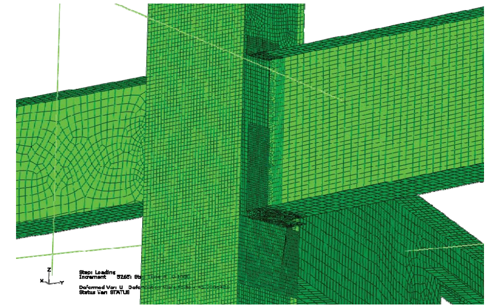

Figure 85: 800°C Filled Flutes Case 4 - Column 79 Seat Connection @ Ambient

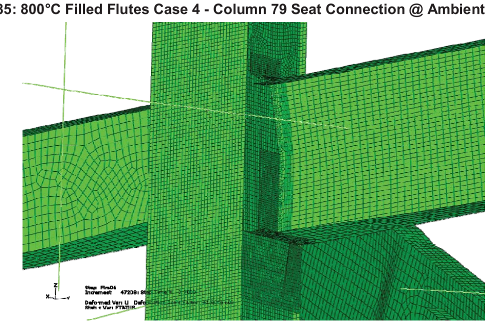

Figure 86: 800°C Filled Flutes Case 4 - Column 79 Seat Connection @ Peak Heating

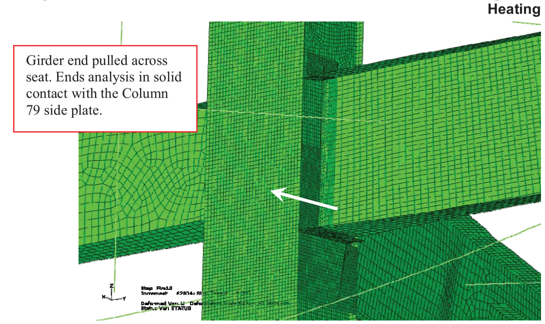

Figure 87: 800°C Filled Flutes Case 4 - Column 79 Seat Connection @ End of cooling

9 Comparison of Output

This section of the report provides a comparison of the key output variables relating the structural performance of Girder 79-44 and the north-east bay for Cases 1 (700°C unfilled), 2 (700°C filled), 3 (800°C unfilled)and 4 (800°C filled),. Specifically these are: -

- Lateral movement of the end of Girder 79-44 and Column 79 (top and bottom)
- Lateral movement of Girder 79-44 at mid-span
- Vertical deflection of Girder 79-44 at mid-span
- Vertical deflections of beams in the north-east bay

9.1 Lateral movement of the end of Girder 79-44 at Column 79 (top and bottom)

Figure 88 shows the comparison of lateral movement of the top flange of Girder 79-44 at Column 79 for all four cases. It is seen that in all cases, the initial movement is to the west as a result of the secondary beams expanding and pushing on the girder. In all cases the top flange of the beam is then pulled back (eastwards). In the 800°C flutes unfilled (Case 3) the sudden eastward movement observed after approximately 40 minutes of the fire is due to the failure of the girder during the heating phase as described in Section 7. The sudden eastward movements observed in the other 3 Cases occur at the times when significant shear stud failure begins to take place in each model. In each case the contraction of the cooling secondary beams is able to pull the girder end eastward as it is no longer rigidly attached to the slab.

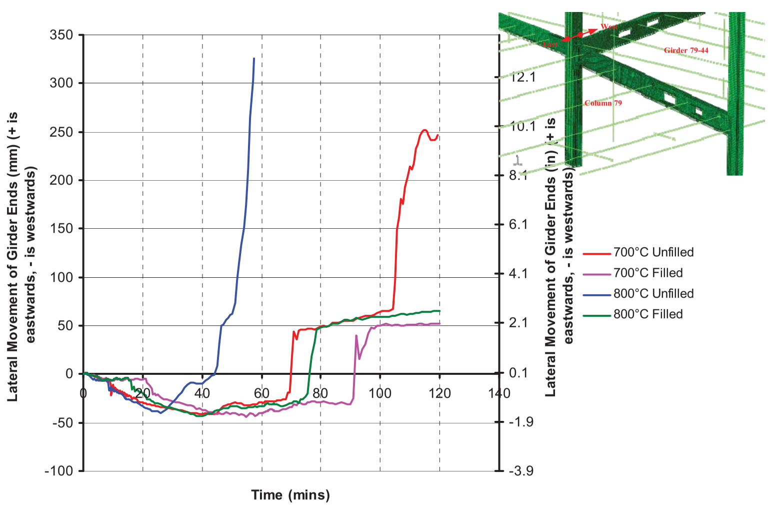

Figure 88: Comparison of east-west movement of top of Girder 79-44 at Column 79 for all four Cases

In cases 1, 2 and 4, the eastward movement of the top flange is then restrained as the flange contacts the inside face of the column side plate. In Case 3 Girder 79-44 collapses before this stage is reached. In Case 1 (700°C Unfilled Flutes) the flange-plate contact is lost due to movement of the girder on the seat and as described in Section 5 the top flange of the girder rotates significantly during the later stages of cooling. Cases 2 and 4 remain largely stable in contact with the column side plate.

Figure 89 shows the comparison of lateral movement of the bottom flange of Girder 79-44 at Column 79 for all four cases. A similar response to that shown in Figure 88 is observed due to the expansion and contraction of the secondary beams during heating and cooling respectively. The key difference is the amount of lateral restraint available to the bottom flange of the connection. Unlike the top flange, which is rigidly connected to the slab, the bottom flange has only 2 bolts available to provide lateral restraint. Once these bolts have broken (after approximately 5-10 minutes of heating in each case) the bottom flange of the girder can be pushed westward until It contacts the inside surface of the column side plate as described in Sections 5 to 8.

Similar to the top flange, the bottom flange in Cases 1, 2 and 4 is pulled eastward in the cooling phase until it contacts the inside face of the column side plate. Girder 79-44 in Case 3 collapses before this stage is reached. For Case 1 there is a sudden spike in westward movement after approximately 110 minutes. This movement is related to the loss of contact at the top flange which leads to a sudden rotation of the girder end. The location of the bottom flange again moves eastward after this spike indicating further movement toward the edge of the seating plate as described in Section 5.

In Cases 2 and 4 the girder location is maintained by contact with the column side plate until the end of the analysis.

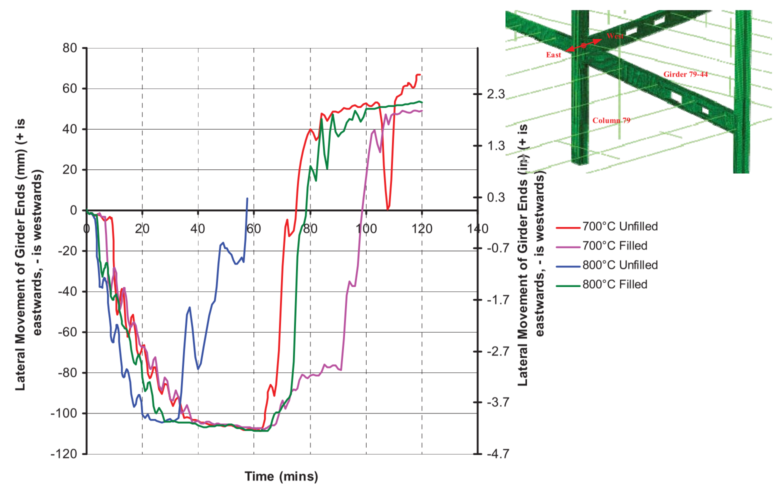

Figure 89: Comparison of east-west movement of bottom of Girder 79-44 at Column 79 for all four cases

For all cases the general behaviours of the end of the girder on the seat connection at Column 79 are similar. This is due to the similarity in heating and cooling exposure between the cases.

The key indicators are:

- Bottom of girder is pushed to the west
- Bottom of girder is pushed against the western side plate of Column 79
- Girder is pulled to the east as the attached secondary beams sag

- Girder is pulled against eastern side plate of Column 79
- Top of girder rotates to the east and downwards

9.2 Lateral movement of Girder 79-44 at mid-span

Figure 90 shows the comparison of lateral movement at the mid-span of Girder 79-44 for all four cases. This shows that the girder is pushed to the west by the expanding secondary beams in the NE bay for the duration of the fire for Cases 1, 2 and 4. The response of Case 3 (800°C flutes unfilled) differs due to the collapse mechanism observed during the heating phase when it undergoes mid-span buckling of its top flange.

The rapid westward movement in Cases 1 and 4 after approximately 80 minutes is related to the failure of secondary beam connections in the NE bay. As the secondary beams fall away from the underside of the slab they are still connected to Girder 79-44, inducing some rotation at mid-span. As noted in Sections 5 and 8 this local failure does not lead to a global collapse mechanism, however they do have some effect on the lateral displacement of Girder 79-44.

This rapid westward movement is not observed in the response of Case 2 (700°C filled flutes) as connection failure is not observed in the secondary beams of the NE bay.

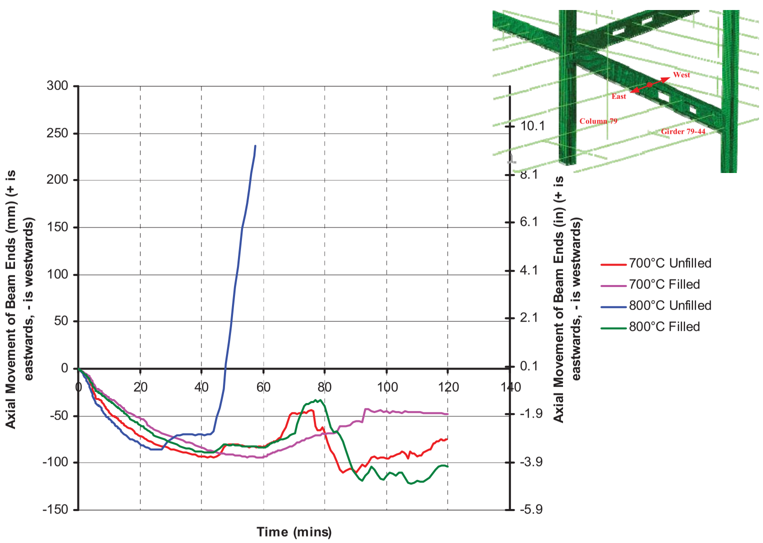

Figure 90: Comparison of east-west movement of mid-span of Girder 79-44 for all four Cases

9.3 Vertical deflection of Girder 79-44 at mid-span

Figure 91 shows the comparison of vertical deflection at the mid-span of Girder 79-44 for all four cases. This plot shows that throughout the duration of the fire the girder remains stable with minor deflections for cases 1, 2 and 4. Case 3 (800°C flutes unfilled) shows runaway failure of the girder at the end of the heating phase of the fire because of a combination of shear stud breakage and thermal degradation of the steel strength and stiffness (Section 7).

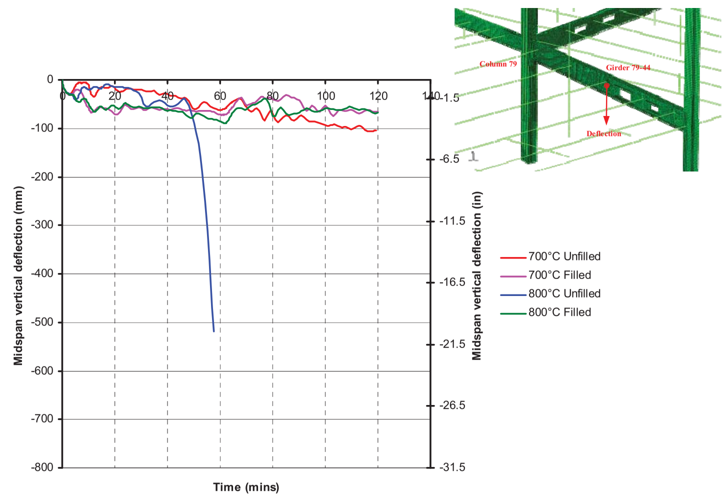

Figure 91: Comparison of vertical deflection at mid-span of Girder 79-44 for all four Cases

9.4 Vertical deflections of beams in the north-east bay

Figure 92 shows the comparison of vertical deflection at the mid-span of Beam 120 in the north-east bay for all four fire cases. This shows that runaway failure of this beam and resulting large deflections occur for all cases with the exception of Case 2 (700°C filled flutes). For Case 3 (800°C flutes unfilled), this runaway occurs late in heating and is linked to the general failure of Girder 79-44. For Case 1 (700°C flutes unfilled) and Case 4 (800°C flutes filled) runaway deflections are observed during cooling.

The reason for the observed runaway failure of the beam in the cooling phase for cases 1 and 4 is attributed to tension failure of its connection of the secondary beam at the eastern façade. Tension forces form in the secondary beams when the secondary beams (which have formed large vertical deflections) cool and contract.

The 700°C flutes filled case (Case 2) does not show runaway failure due to relatively small deflections in the north-east bay and therefore lower tension forces in the connections at the eastern façade.

The 800°C flutes unfilled case (Case 3) shows runaway failure towards the end of heating as significant numbers of shear studs break as the secondary beams deflect due to the high temperatures of the top flanges of the steel sections. These large deflections continue and induce tension failure of the secondary beam's connection at the eastern façade.

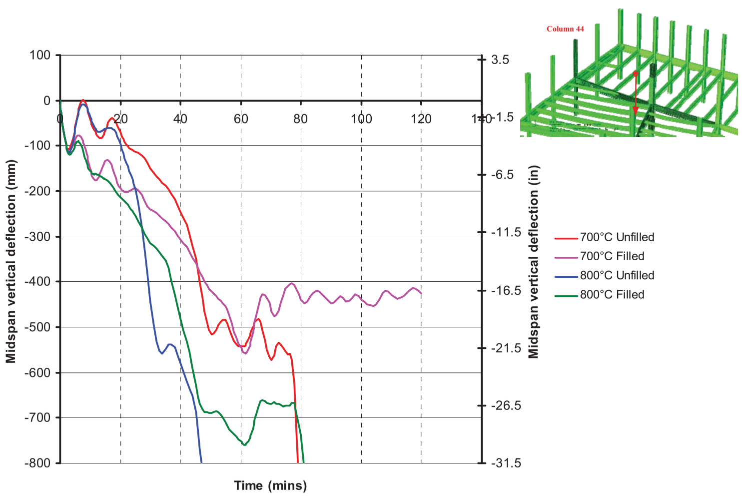

Figure 92: Comparison of vertical deflection of mid-span of Beam 120 in the north-east bay for all four Cases

10 Conclusions

The output from the numerical models (Case 1, 2, 3 and 4) are presented here.

A collapse initiation mechanism is clearly shown in Case 3 (800°C unfilled) in the form of girder 79-44 being pulled off its seat at column 79 by the secondary beams in the North-East corner, during the advanced stages of heating period of the fire.

Case 1 (700°C flutes unfilled) shows that an initiation mechanism is also observed in the form of girder 79-44 being pulled off its seat at column 79 by the secondary beams in the North-East corner, during the cooling period of the fire.

A collapse initiation mechanism was not observed in Cases 2 and 4 when the flutes of the girder and beams were filled for 700°C and 800°C heating, respectively. The filling of the flutes resulted in lower beam temperatures compared with unfilled flutes and hence, lower strength and stiffness degradation and also lower amount of thermal expansion.

References

[1] Master Assumption List – Refer Appendix B of this report.

A1 Appendix Overview

The following appendices present detailed output for each of the four scenarios reported as part of this study. These appendices are provided as additional reference material to complement the findings within the main report.

For each of the four scenarios, data is presented for: -

- Brief overview of observed behaviours
- Detailed sequence of events and associate timings
- Failed connection locations
- Column lateral movements
- Vertical contours of deflections on the concrete slab
- Selected beam and girder mid-span vertical deflections
- Lateral end movement of girders around Column 79
- Shear stud failures
- Bolt deformations in the knife connections
- Axial forces in the connections at the end of a beam in the north-east bay
- Images of detailed connections
- Images of the global structural response

Where appropriate, comments have been added to explain certain behaviours, however, reference should be made to the corresponding section within the main report for a general description of the observed behaviour.

JA-3206

A2 CASE 1: 700°C Fire – Unfilled Flutes

A2.1 Overview

This section presents detailed output for the 700°C unfilled flutes assessment to complement the data presented as an overview in Section 5.

This analysis shows that following exposure to the prescribed 1-hour of heating and 1-hour of cooling the Girder 79-44 at Column 79 is left resting precariously at the eastern side of its seating plate.

A limited number of connection failures of secondary beams framing into girders are observed during the cooling phase.

A2.2 Detailed Sequence of Events

The sequence of events for the 700°C fire with unfilled flutes is shown in Table 6. Identified connection failures are referenced using a beam numbering notation that is shown in Figure 93.

Table 5: Sequence of events for the 700°C fire with unfilled flutes. Red numbers indicate heating, blue numbers indicate cooling. Temperatures are taken as the top flange of Girder 79-44.

Event	Time (mins)	Observation	Temp (°C)
1	9	All bolts (top and bottom flange) of the connection of Girder 79-44 at Column 79 break	224
-	30	Mid-span deflection of central beam in the north east corner bay: 150mm (6")	476
2	34	All bolts (top and bottom flange) of the connection of Girder 79-44 at Column 44 break	503
-	60	Mid-span deflection of central beam in the north east corner bay: 555mm (21.8")	627
3	65	Connection B301 to B257 fails in tension	519
4	67	Connection B301 to B165 fails in tension	489
5	68	Connection B302 to B165 fails in tension	474
6	68	Connection B246 to B165 fails in tension	474
7	68	Connection B302 to B257 fails in tension	474
8	72	Connection B248 to B168 fails in tension	414
9	72	Connection B247 to B168 fails in tension	414
10	75	Connection B250 to B257 fails in tension	369
11	75	Connection B300 to B257 fails in tension	369
12	76	Connection B120 to C40 fails in tension	354
13	78	Connection B137 to B169 fails in tension	324
14	78	Connection B250 to B168 fails in tension	324
15	80	Connection B136 to B169 fails in tension	294
16	80	Connection B121 to C41 fails in tension	294
17	85	Connection B215 to B170 fails in tension	255
-	90	Mid-span deflection of central beam in the north east corner bay: 1080mm (42.5")	216
18	116	Connection B246 to B168 fails in tension	75
19	120	Analysis completes. Girder 79-44 at Column 79 is left resting precariously at the eastern side of its seating plate	64

A2.3 Connection Failures

Figure 93 shows the location and sequence of connection failures observed during the analysis. Refer to Table 5 for times of failures.

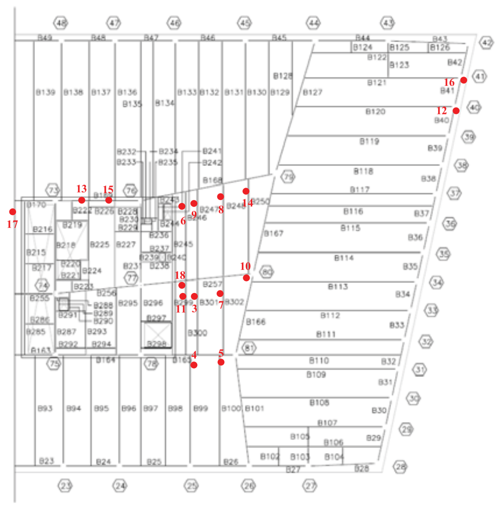

Figure 93: Locations and sequence of connection failures (sequence numbers correspond to Table 5)

A2.4 Column Lateral Movements

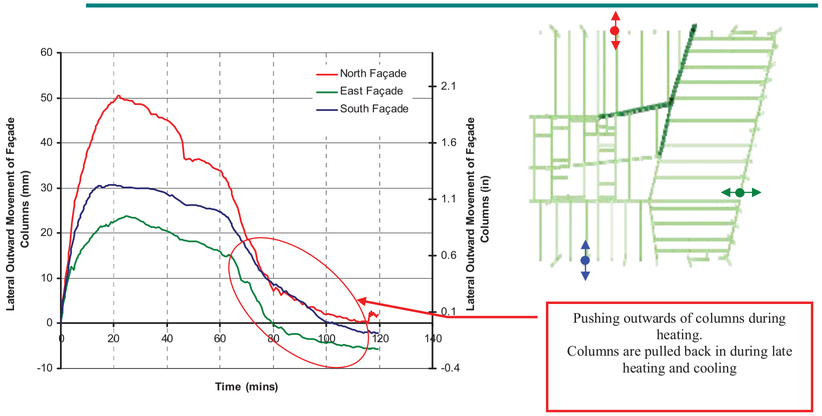

Figure 94: Lateral outward column movements at the façade of the building. Column locations see are shown to the right of the plot.

A2.5 Vertical Deflection Contours

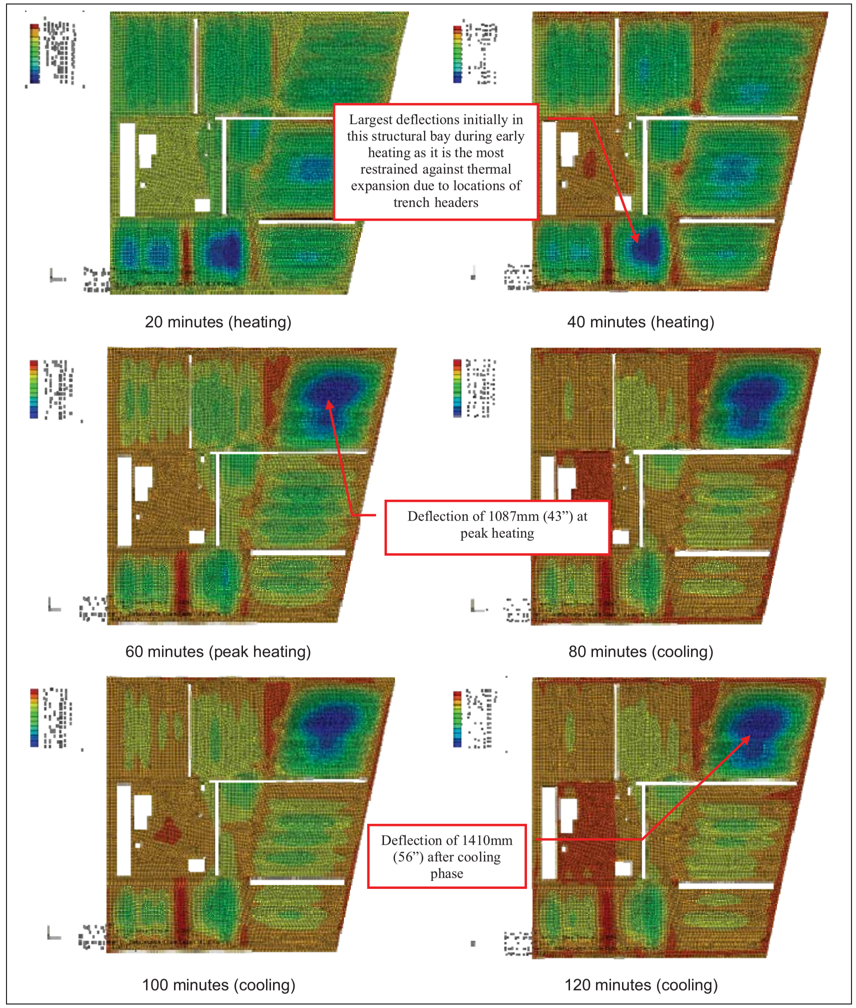

Figure 95: Vertical deflection contours on the slab for 20 minute intervals throughout the duration of the analysis. Key denotes the magnitude of vertical deflection (mm)

A2.6 Mid-span Vertical Deflections

Maximum girder deflection is approximately 200mm (7.9") at peak heating. Deflections are not recovered during cooling.

B120 in the north-east bay shows runaway failure as its connection to the perimeter column fails in cooling

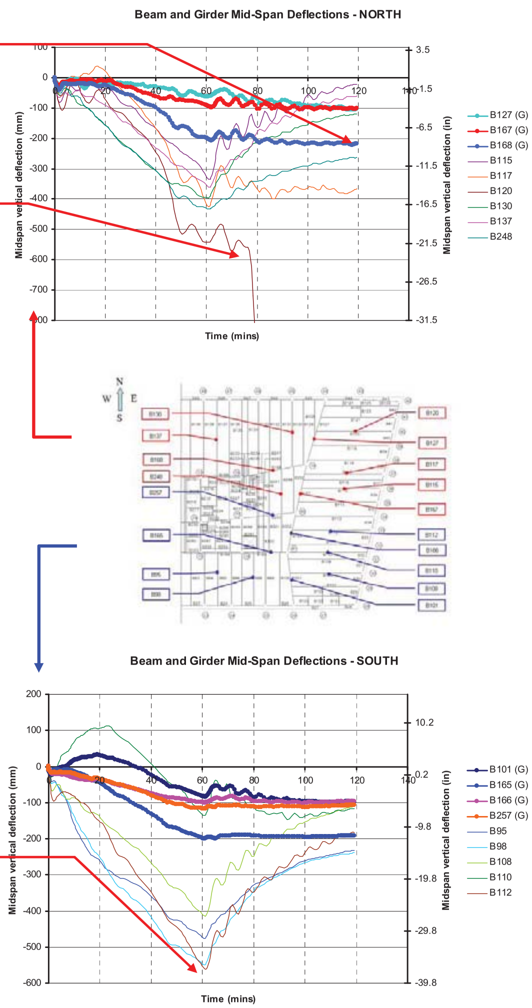

General Behaviour

All girders (in the north and south structural floor areas) exhibit low deflections.

Largest deflections are observed in secondary beams

Beams, but not girders, exhibit partial recovery of deflections. Some residual deflection occurs following cooling, i.e. they do not recover to their ambient position.

Greatest deflections in the southern region of the structure observed (B112)

Figure 96: Vertical mid-span deflection of selected beams and girders (G) with evolution of the analysis. Key for beam and girder locations shown in the centre of the figure.

JA-3208

A2.7 Lateral Displacements at the End of the Girders Around Column 79

The plots on the right side of this page show the lateral movement of the top and bottom of the end of each girder framing into Column 79 as shown in the diagram image below.

Main Observations

- **Girder 79-44**
  The girder is pushed and pulled laterally by the secondary beams to the extent that late in cooling it is sitting precariously on the eastern edge of its seat at Column 79.
- **Girder 76-79**
  As the girder expands and contracts with heating and cooling its movements are accommodated by ductility in the knife angle plates. Angle plates remain intact and do not tear.
- **Girder 79-80**
  As the girder expands and contracts with heating and cooling its movements are accommodated by ductility in the knife angle plates. Angle plates remain intact and do not tear.

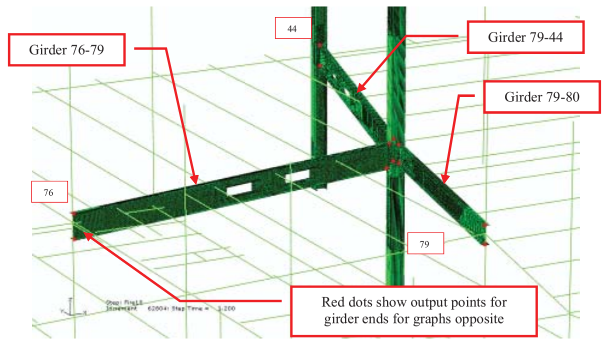

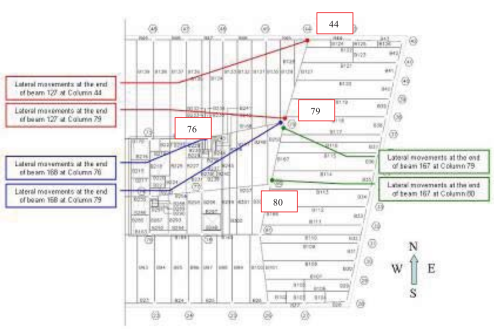

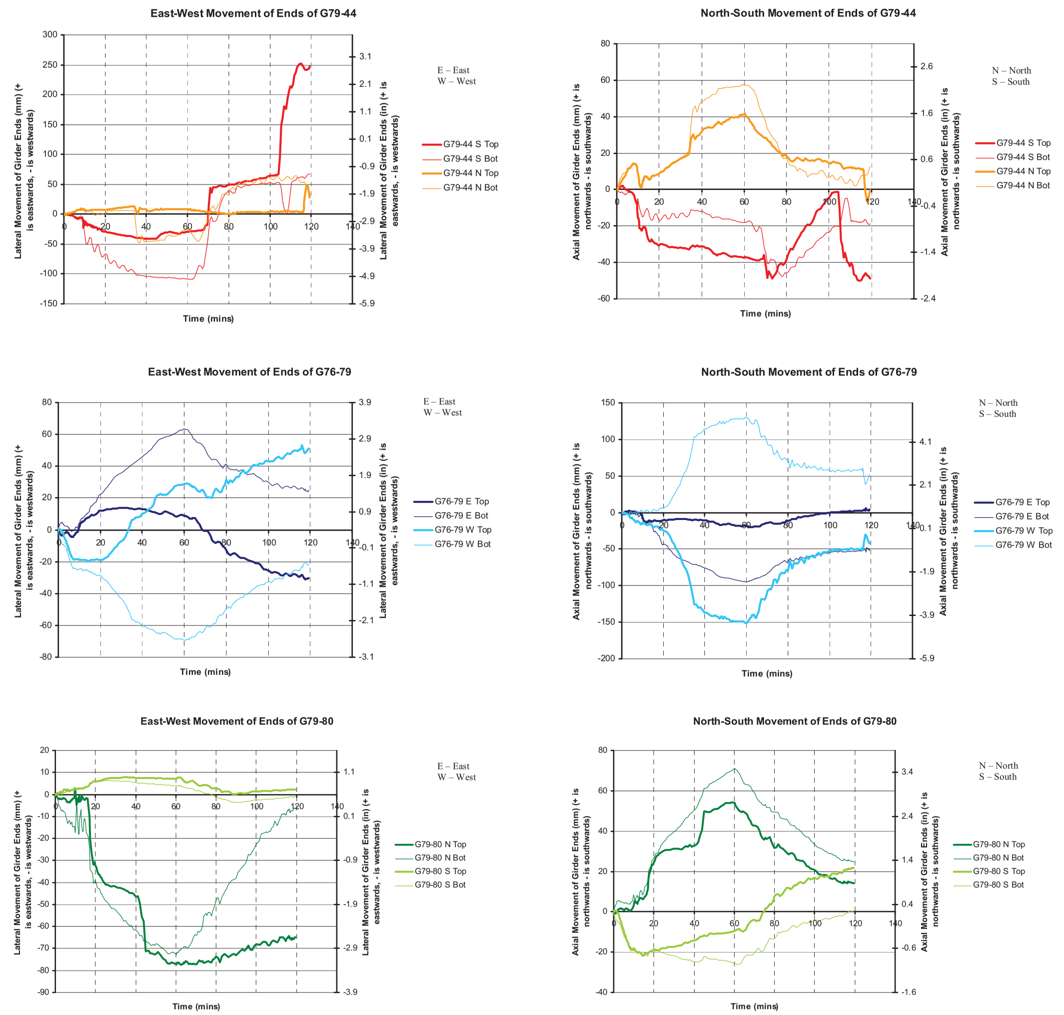

Figure 97: Lateral movements (top and bottom) at each end of the girders framing into Column 79. Images on the left show the locations of the output points on each girder.

JA-3209

A2.8 Lateral Movement at the Ends of the Beams in the North-East Bays

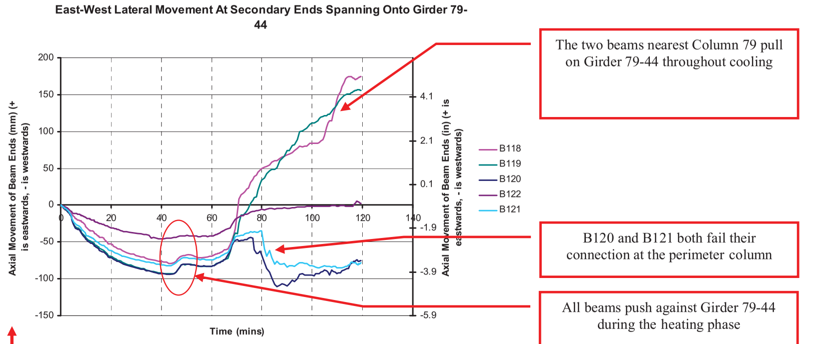

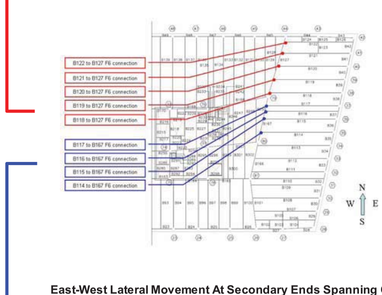

General Behaviour

Beams spanning onto Girder 79-44

Beams push on the girder throughout heating as they expand and pull on the girder during cooling as they contract. Movement generally to the West during heating and to the East during cooling.

Beams spanning onto Girder 79-80

Beams nearer to Column 79 exhibit largest push/pull movements due to the presence of a trench header in this area running over the girder.

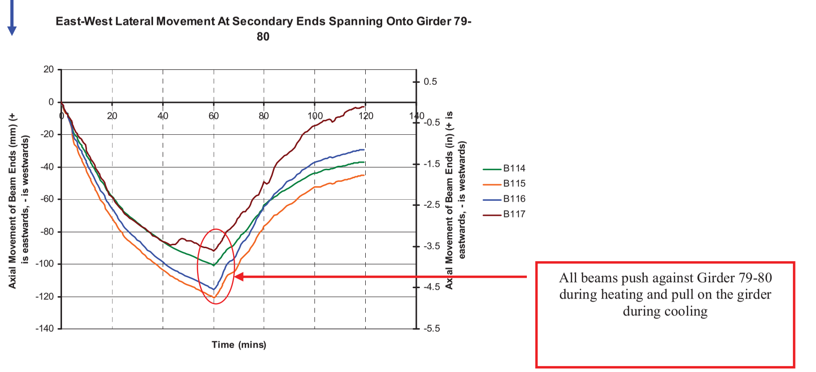

Figure 98: Lateral movements (east-west) of the western end of the beams framing into Girder 79-44 and Girder 79-80

A2.9 Shear Stud Failures

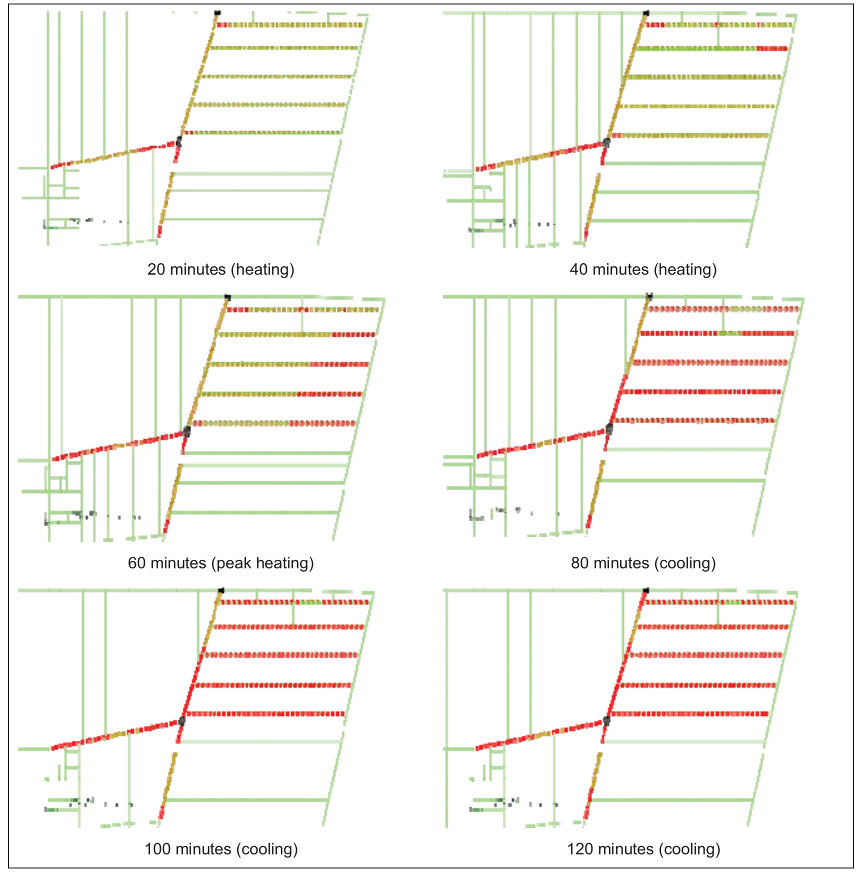

Figure 99: Shear stud failures within the north-east bay at 20 minute intervals throughout the duration of the analysis. Brown markers indicate unbroken shear studs while red markers indicate broken shear studs

During the heating phase of the fire, shear stud breakages are observed at either end of Girders 76-79 and 79-80 and also on the eastern third of beams in the north-east bay.

During the initial cooling phase, a significant number of shear studs break due to differential cooling between the concrete slab and the steel beams. These include almost all shear studs on the secondary beams and the majority on each of the three girders into Column 79.

A2.10 Knife Connection Bolt Deformations and North-East Secondary Beam Connector Forces

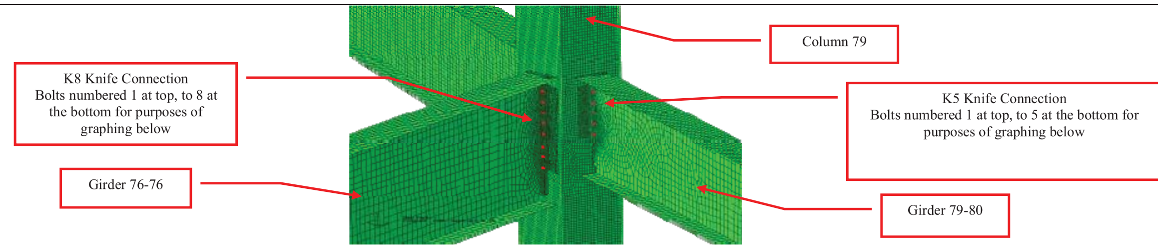

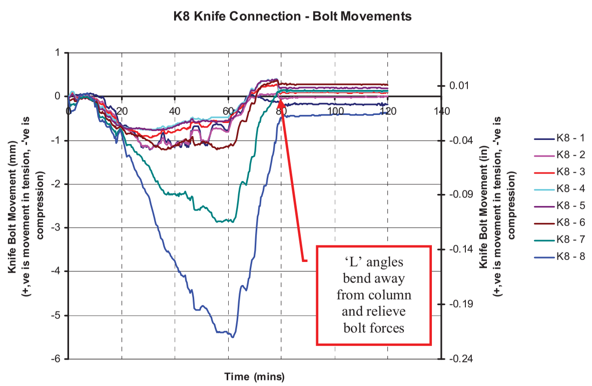

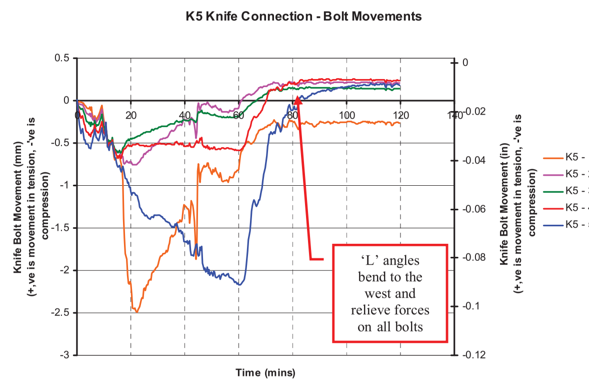

General behaviour of knife connections

During the early stages of the fire (up to 20 minutes), the knife connections rotate with the applied load as the girder expands and the coped bottom flanges move towards the column.

As the fire continues to heat the structure, the girders expand and push the bolts into compression and the bolts and plate start to deform.

As the structure starts to cool, the compression forces and bolt deformations are relieved.

As cooling continues, the girder contracts and starts to pull on the connection in tension.

As the tension forces develop, the 'L' angles forming the connection start to bend away from the column – only being connected to the column by their weld.

At this point, connection deformation is governed by the 'L' angle bending and no further change in bolt deformation is observed

K8 Knife Connection Bolts (Girder 76-79)

Maximum bolt deformation is in bottom bolt and occurs at peak heating of 5.5mm (0.22")

K5 Knife Connection Bolts (Girder 79-80)

Maximum bolt deformation is in top bolt during early heating of approximately 2.5mm (0.1")

The bolt deformation observed in the analysis is a representation of combined deformation of bolts, bolt holes and plates incorporated in the connection.

Note: simplified connectors have an associated movement prior to breakage that relates to bolt and plate ductility.

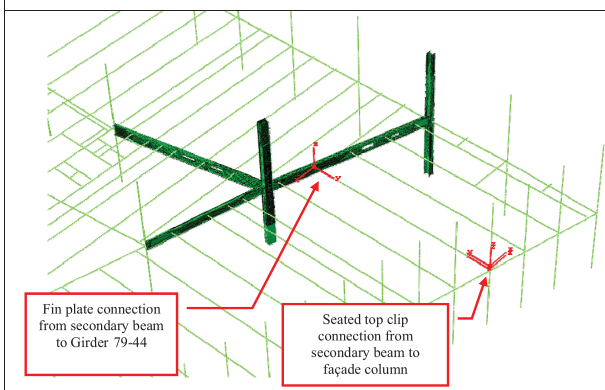

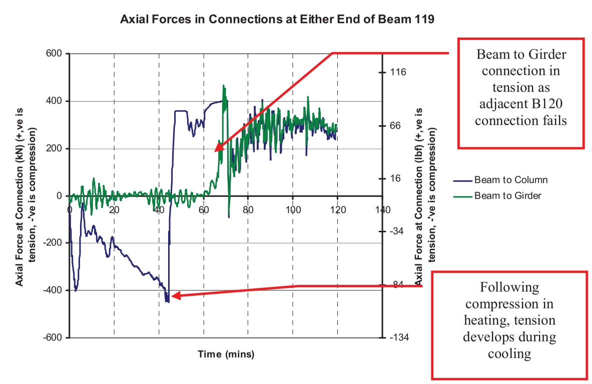

Push/Pull Forces At Either End of a Selected Secondary Beam in the North-East Bay

The fin plate connection of the secondary beam into the girder exhibits low axial force as the girder is relatively free to be pushed and pulled following early breakage of the bolts connecting it to the columns. It exhibits tension as it shares the load that was previously taken by the two adjacent beams that have failed at their connections.

For the STP connection where the beam connects to the column, compressive forces are transferred to column during heating. During cooling, the beam pulls on the column as tension forces develop.

Figure 100: Lateral movement of knife connection bolts for the K8 and K5 knife connections. Also shown are the axial forces in the connections at the end of one beam in the north-east corner

A2.11 Seat Connection and K8 Knife Connection at Column 79 Deformations

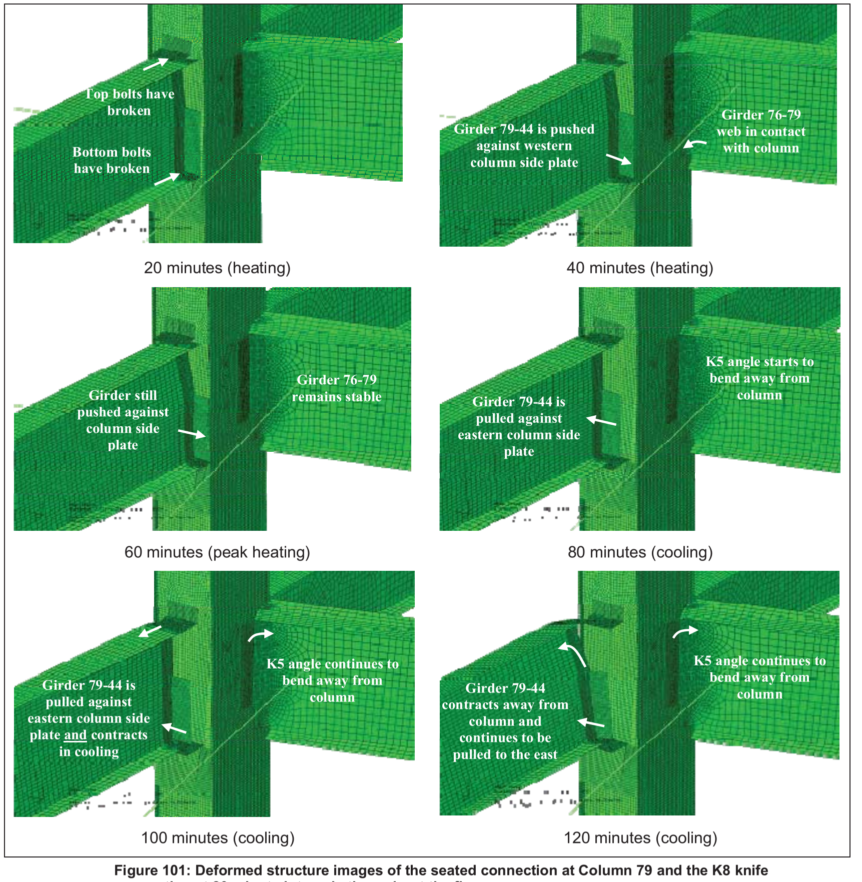

Figure 101: Deformed structure images of the seated connection at Column 79 and the K8 knife connection at 20 minute intervals throughout the fire

A2.12 Structural Deformations

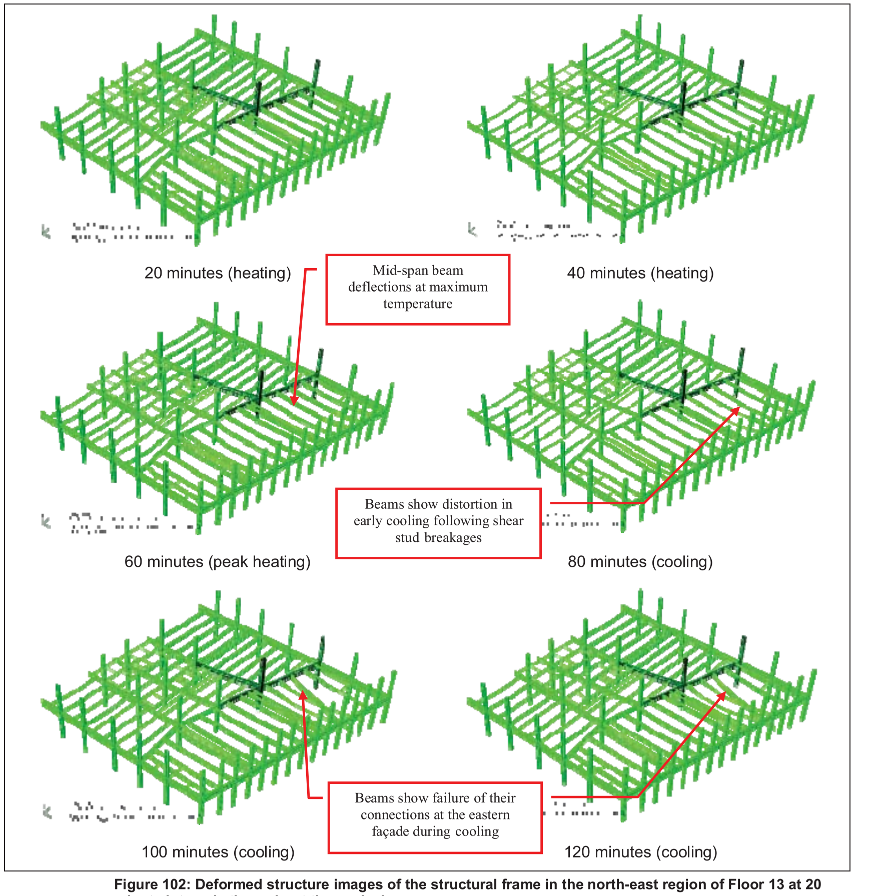

Figure 102: Deformed structure images of the structural frame in the north-east region of Floor 13 at 20 minute intervals throughout the analysis

Two secondary beams in the north-east bay fail at their connections to the eastern façade columns as the beams contract due to cooling and create large tension forces.

Girder 79-44 is pulled across its seat plate during cooling by the secondary beams and is left resting precariously at the eastern side of this plate

A3 CASE 2: 700°C Fire – Filled Flutes

A3.1 Overview

This section presents detailed output for the 700°C filled flutes assessment to complement the data presented as an overview in Section 6.

This analysis shows that no significant deformation or structural collapse is observed following exposure to the prescribed 1-hour of heating and 1-hour of cooling.

A limited number of connection failures of secondary beams framing into girders are observed during the cooling phase.

A3.2 Detailed Sequence of Events

The sequence of events for the 700°C fire with filled flutes is shown in Table 6. Identified connection failures are referenced using a beam numbering notation that is shown in Figure 103.

Table 6: Sequence of events for the 700°C fire with filled flutes. Red numbers indicate heating, blue numbers indicate cooling. Temperatures are taken as the top flange of Girder 79-44.

Event	Time (mins)	Observation	Temp (°C)
1	4.2 to 6.3	Both bolts on the seat plate connection to lower flange of Girder 79-44 at Column 79 break	85 to 137
2	8.8	Both bolts on the seat plate connection to lower flange of Girder 79-44 at Column 44 break	137
3	21 to 23	The top clip plate to top flange of Girder 79-44 at Column 79 ruptures	247
-	30	Largest midspan deflections are observed in the south at beam 98, reaching 350mm (13.7")	324
4	41	Both bolts at the top plate to top flange of Girder 79-44 at Column 44 break	397
-	60	Largest mid-span deflections are in the south at B98: 650mm (25.5") Mid-span deflections of the secondary beams in the north-east corner: 560mm (22")	494
5	69	Connection B301 to B257 fails in tension	418
6	70	Connection B302 to B165 fails in tension	413
7	70	Connection B302 to B257 fails in tension	413
8	70	Connection B300 to B165 fails in tension	407
9	73	Connection B300 to B257 fails in tension	390
10	77	Connection B247 to B168 fails in tension	356
11	79	Connection B137 to B169 fails in tension	339
12	80	Connection B250 to B257 fails in tension	339
13	80	Connection B136 to B169 fails in tension	333
14	85	Connection B248 to B168 fails in tension	311
15	86	Connection B215 to B170 fails in tension	301
16	90	Connection B250 to B168 fails in tension	279
-	90	Vertical mid-span deflections decrease because structure is cooling and starts to contract Largest mid-span deflections are in the south at B98: 424mm (16.7") Mid-span deflections of the secondary beams in the north–east corner: 440mm (17.3")	280
17	120	Vertical mid-span deflections continue to decrease because structure is cooling. Largest mid-span deflections in the floor plate are observed in the north–east corner i.e. 425mm (16.7") at the end of cooling. Greater recovery of deflections is observed in Beam 98 in the south, i.e.: 352mm (13.9"). Analysis completes. No structural collapse	153

A3.3 Connection Failures

Figure 103 shows the location and sequence of connection failures observed during the analysis. Refer to Table 6 for times of failures.

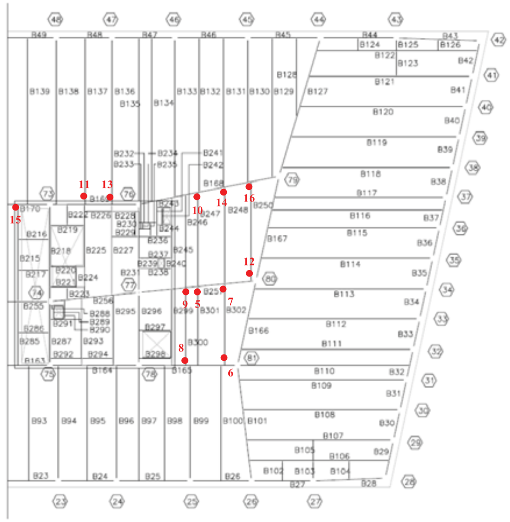

Figure 103: Locations and sequence of connection failures (sequence numbers correspond to Table 6)

A3.4 Column Lateral Movements

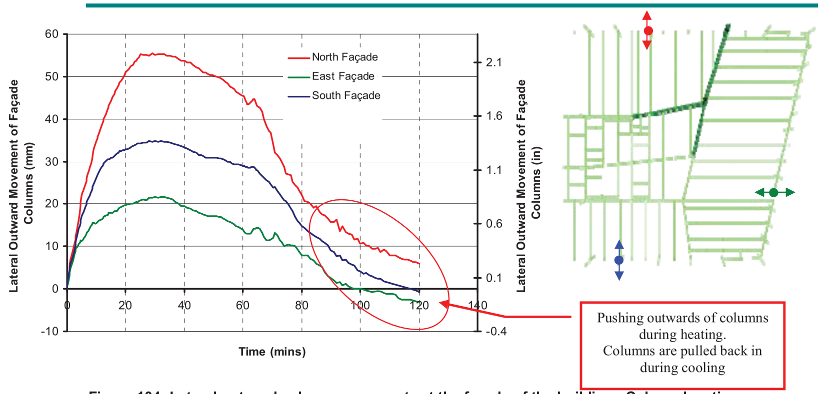

Figure 104: Lateral outward column movements at the façade of the building. Column locations see are shown to the right of the plot.

A3.5 Vertical Deflection Contours

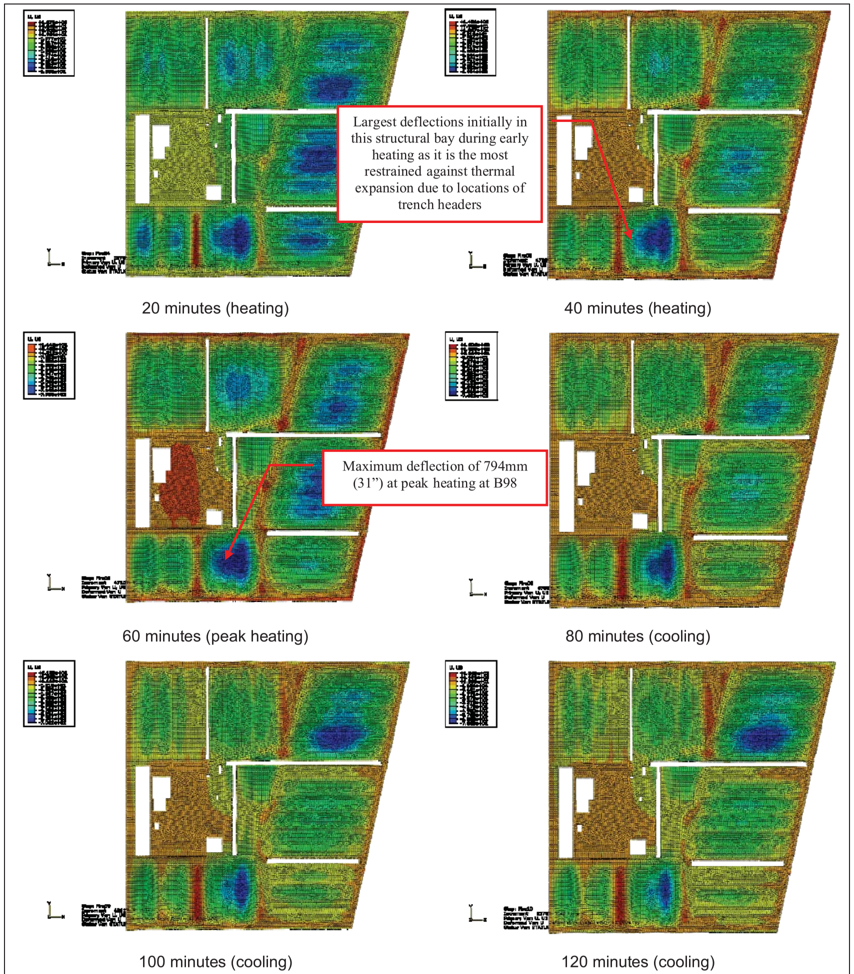

Figure 105: Vertical deflection contours on the slab for 20 minute intervals throughout the duration of the analysis. Key denotes the magnitude of vertical deflection (mm)

A3.6 Mid-span Vertical Deflections

Girders deflect less than 160mm (6.3") with peak deflections occurring at maximum temperature

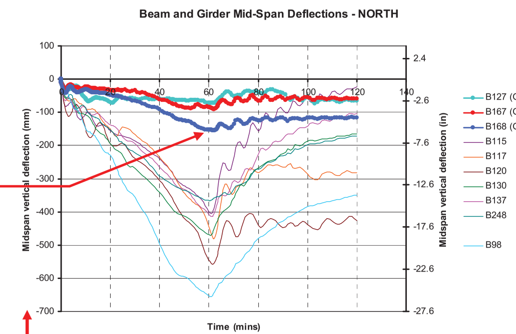

General Behaviour

All girders (in the north and south structural floor areas) exhibit low deflections.

Largest deflections are observed in secondary beams

All beams and girders exhibit partial recovery of deflections. Some residual deflection occurs following cooling, i.e. they do not recover to their ambient position.

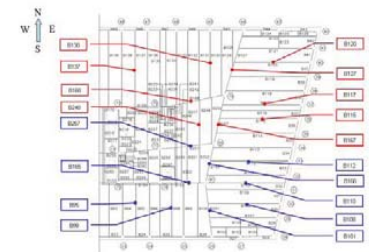

Greatest deflections observed in beams in the southern region of the structure coinciding with the largest deflections on the concrete slab

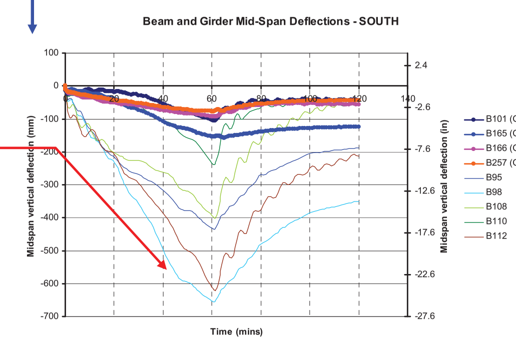

Figure 106: Vertical mid-span deflection of selected beams and girders (G) with evolution of the analysis. Key for beam and girder locations shown in the centre of the figure.

. 15/02/2010 12:45:00

JA-3215

A3.7 Lateral Displacements at the End of the Girders Around Column 79

The plots on the right side of this page show the lateral movement of the top and bottom of the end of each girder framing into Column 79 as shown in the diagram image below.

Main Observations

- **Girder 79-44**

  The girder remains stable on its seats at Column 79 and Column 44 throughout the entire analysis despite all its connection bolts breaking early in the fire. It is pushed and pulled laterally by the secondary beams but does not fall off its seats.

- **Girder 76-79**

  As the girder expands and contracts with heating and cooling, its movements are accommodated by ductility in the knife angle plates. Angle plates remain intact and do not tear.

- **Girder 79-80**

  As the girder expands and contracts with heating and cooling its movements are accommodated by ductility in the knife angle plates. Angle plates remain intact and do not tear.

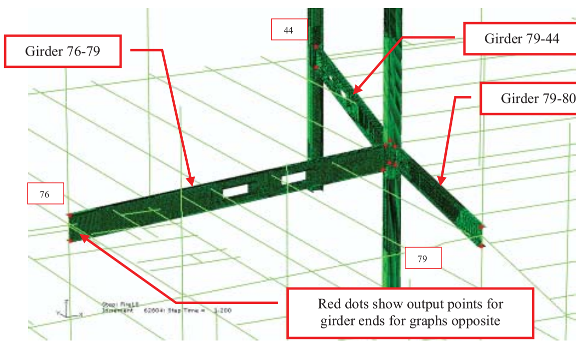

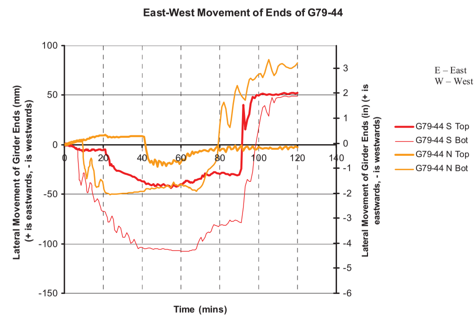

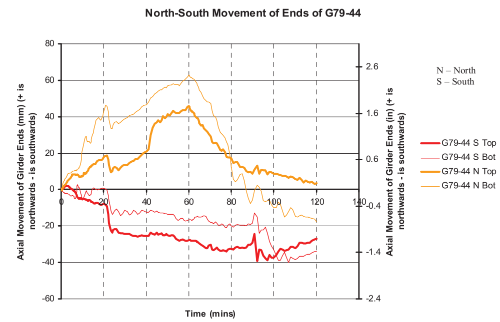

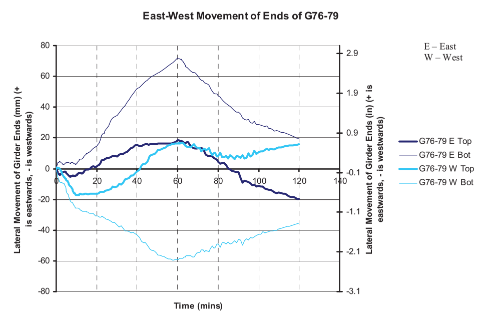

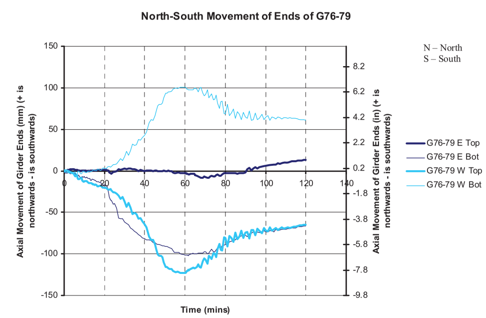

JA-3216

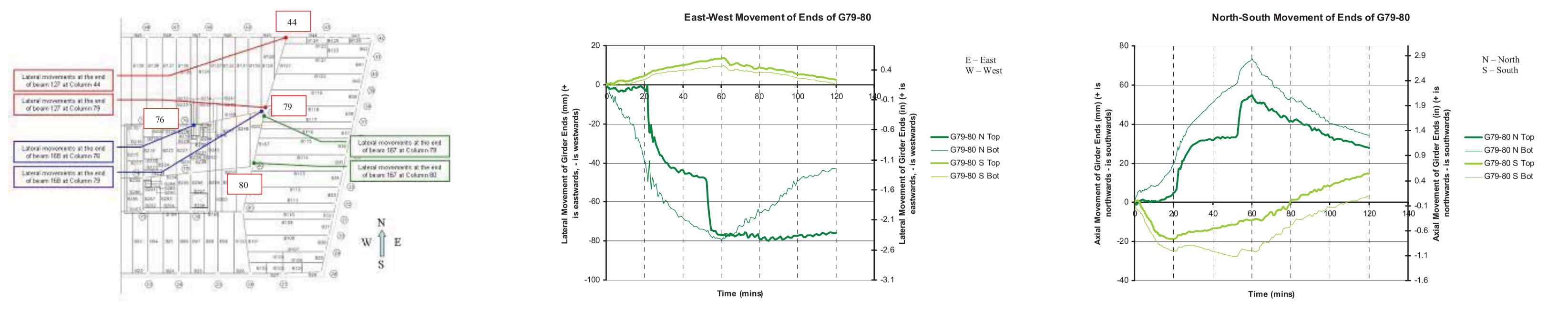

Figure 107: Lateral movements (top and bottom) at each end of the girders framing into Column 79. Images on the left show the locations of the output points on each girder.

. 15/02/2010 12:45:00

A3.8 Lateral Movement at the Ends of the Beams in the North-East Bays

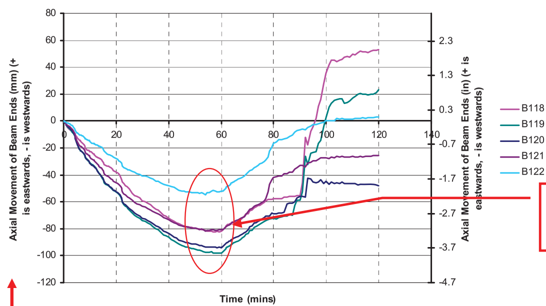

Beams push against Girder 79-44 during the heating phase and pull on girder during the cooling phase.

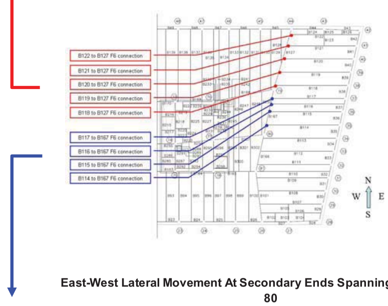

General Behaviour

Beams spanning onto Girder 79-44

Beams push on the girder throughout heating as they expand and pull on the girder during cooling as they contract. Movement generally to the West.

Beams spanning onto Girder 79-80

Beams nearer to Column 79 exhibit largest push/pull movements due to the presence of a trench header in this area running over the girder.

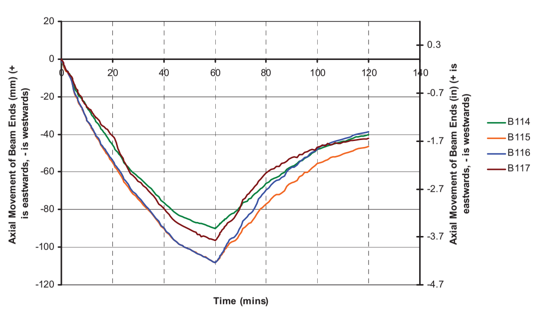

The lateral movements of the beams spanning onto Girder 79-44 and Girder 79-80 are strongly influenced by the position of the trench headers in their vicinity.

Figure 108: Lateral movements (east-west) of the western end of the beams framing into Girder 79-44 and Girder 79-80

A3.9 Shear Stud Failures

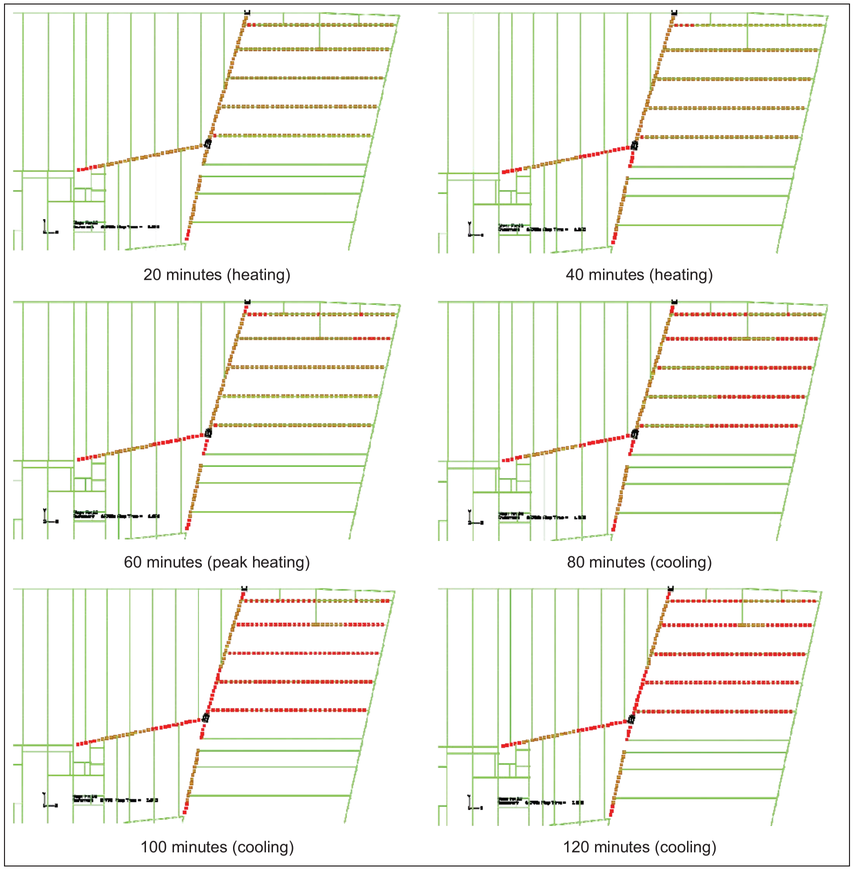

Figure 109: Shear stud failures within the north-east bay at 20 minute intervals throughout the duration of the analysis. Brown markers indicate unbroken shear studs while red markers indicate broken shear studs

During the heating phase of the fire, shear stud breakages are observed at both ends of Girders 76-79 and 79-80 and on Girder 79-44 near to Column 44.

Throughout the cooling phase, significant numbers of shear studs break due to differential cooling between the concrete slab and the steel beams. The majority of shear studs breakages occur after 75 minutes of the analysis (15 minutes into heating). By this time the secondary beams have cooled below approximately 400°C they have recovered significant strength. Therefore the loss of shear connection to the slab in Case 2 is less significant compared to Case 1 where significant loss of shear connection occurs when the beams are hotter than 500°C.

A3.10 Knife Connection Bolt Deformations and North-East Secondary Beam Connector Forces

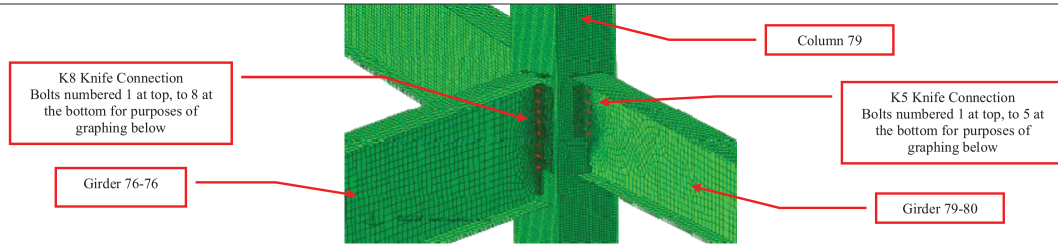

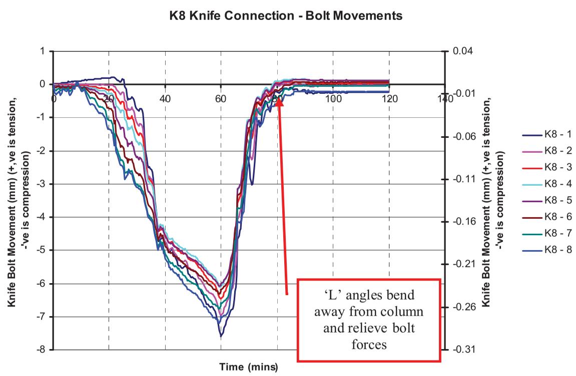

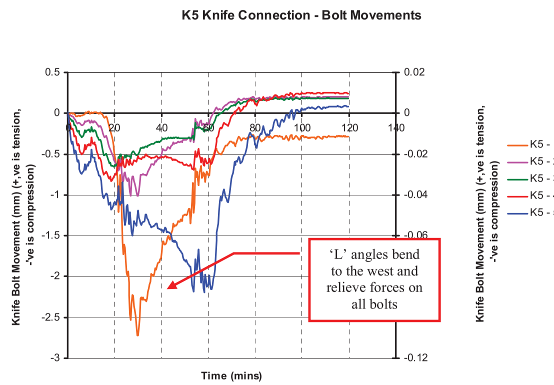

General behaviour of knife connections

During the early stages of the fire (up to 20 minutes), the knife connections rotate with the applied load as the girder expands and the coped bottom flanges move towards the column.

As the fire continues to heat the structure, the girders expand and push the bolts into compression and the bolts and plate start to deform.

As the structure starts to cool, the compression forces and bolt deformations are relieved.

As cooling continues, the girder contracts and starts to pull on the connection in tension.

As the tension forces develop, the 'L' angles forming the connection start to bend away from the column – only being connected to the column by their weld.

At this point, connection deformation is governed by the 'L' angle bending and no further change in bolt deformation is observed

K8 Knife Connection Bolts (Girder 76-79)

Maximum bolt deformation in all bolts occurs at peak heating of 6mm – 7.5mm (0.24"-0.3")

K5 Knife Connection Bolts (Girder 79-80)

Maximum bolt deformation in top bolt during heating of approximately 2.5mm (0.1")

The bolt deformation observed in the analysis is a representation of combined deformation of bolts, bolt holes and plates incorporated in the connection.

Note: simplified connectors have an associated movement prior to breakage that relates to bolt and plate ductility.

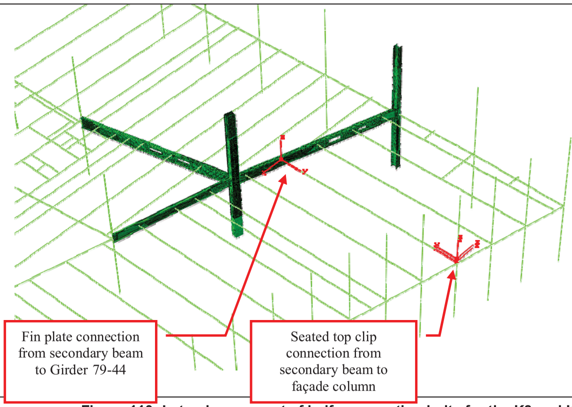

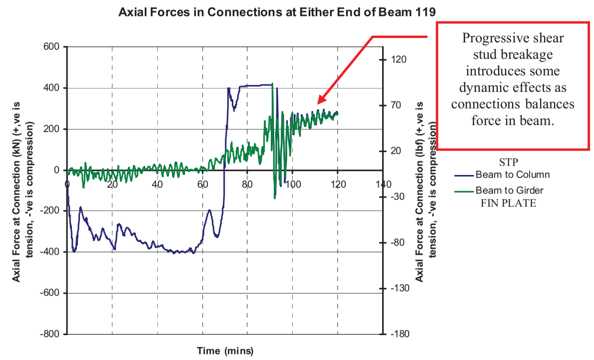

Push/Pull Forces At Either End of a Selected Secondary Beam in the North-East Bay

The fin plate connection of the secondary beam into the girder exhibits low axial force as the girder is relatively free to be pushed and pulled following early breakage of the bolts connecting it to the columns.

For the STP connection where the beam connects to the column, compressive forces are transferred to column during heating. During cooling, the beam pulls on the column as tension forces develop. Towards the end of heating, the connection starts to yield in tension, but failure does not occur.

Figure 110: Lateral movement of knife connection bolts for the K8 and K5 knife connections. Also shown are the axial forces in the connections at the end of one beam in the north-east corner.

A3.11 Seat Connection and K8 Knife Connection at Column 79 Deformations

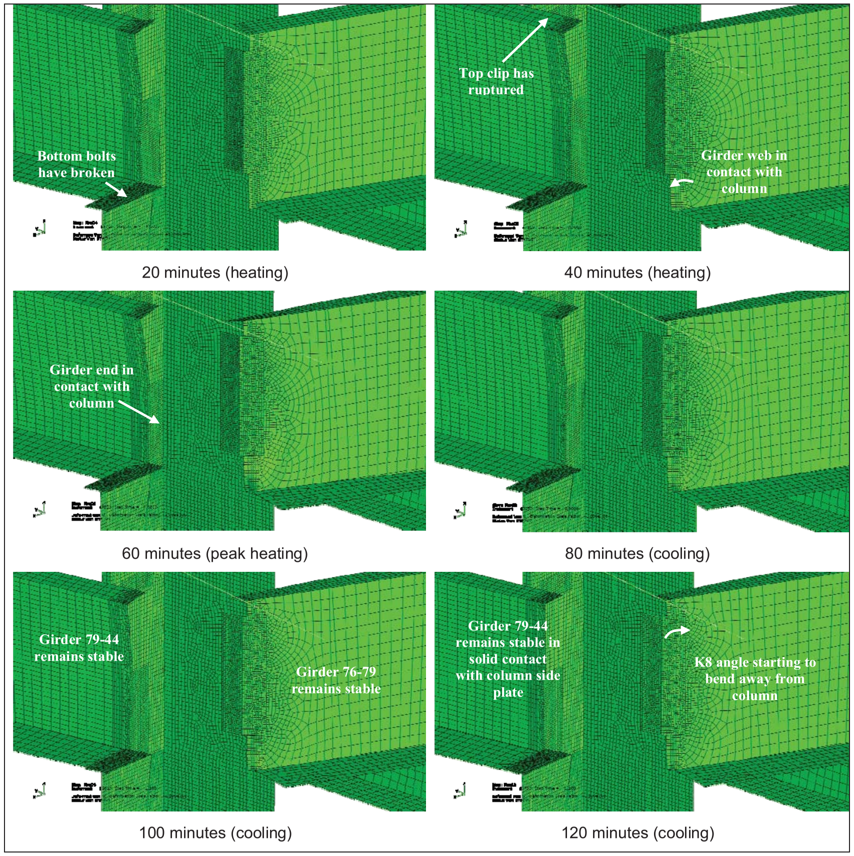

Figure 111: Deformed structure images of the seated connection at Column 79 and the K8 knife connection at 20 minute intervals throughout the fire

A3.12 North-East Structural Bay Deformations

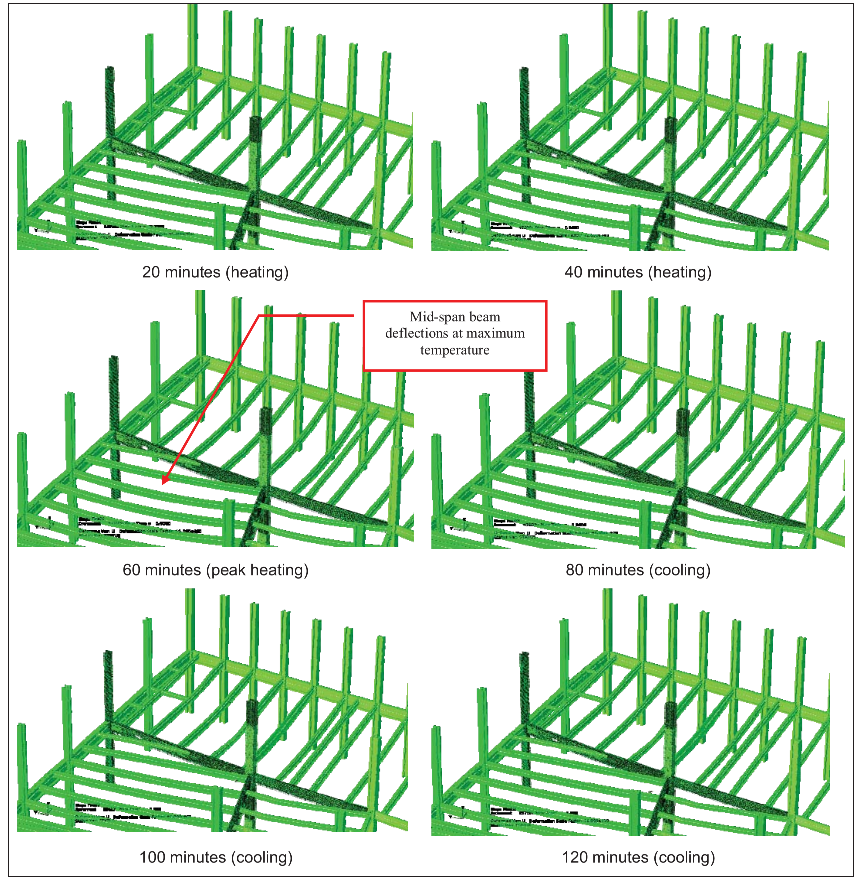

Figure 112: Deformed structure images of the structural frame in the north-east region of Floor 13 at 20 minute intervals throughout the analysis

The structural frame of Floor 13 remains stable throughout both the heating and cooling phases.

The secondary beams and girders exhibit vertical deformations, some of which are partially recovered during the cooling phase.

No initiating collapse mechanism is observed.

A4 CASE 3: 800°C Fire – Unfilled Flutes

A4.1 Overview

This section presents detailed output for the 800°C unfilled flutes assessment to complement the data presented as an overview in Section 7.

This analysis shows a potential initiating collapse mechanism towards the end of the heating phase. Girder 79-44 at Column 79 is pulled to the east across its seating plate and is about to be pulled off. The analysis terminated at this point due to a numerical instability associated with the failure mechanism, however all indications are that localised structural collapse is imminent.

The analysis did not progress into the cooling phase.

A4.2 Detailed Sequence of Events

The sequence of events for the 800°C fire with unfilled flutes is shown in Table 7. Identified connection failures are referenced using a beam numbering notation that is shown in Figure 113.

Table 7: Sequence of events for the 800°C fire with flutes unfilled. Red numbers indicate heating, blue numbers indicate cooling. Temperatures are taken as the top flange of Girder 79-44.

Event	Time (mins)	Observation	Temp (°C)
1	3	Both bolts on the seat plate connection to lower flange of Girder 79-44 at Column 79 break	100
2	8	Both bolts at the top clip plate to top flange of Girder 79-44 at Column 79 break	244
3	29	Both bolts on the seat plate connection to lower flange of Girder 79-44 at Column 44 break	548
-	30	Mid-span deflection of central beam in the north east corner bay: 440mm (17.3")	548
4	57	One bolt at the top plate to top flange of Girder 79-44 at Column 44 breaks	717
5	57	Analysis terminates due to numerical instabilities associated with the failure mechanism.	717

A4.3 Connection Failures

Figure 113 shows that no connection failures were observed during the analysis. Cases 1, 2 and 4 all progress into cooling and show connections to fail in tension as the beams they support contract.

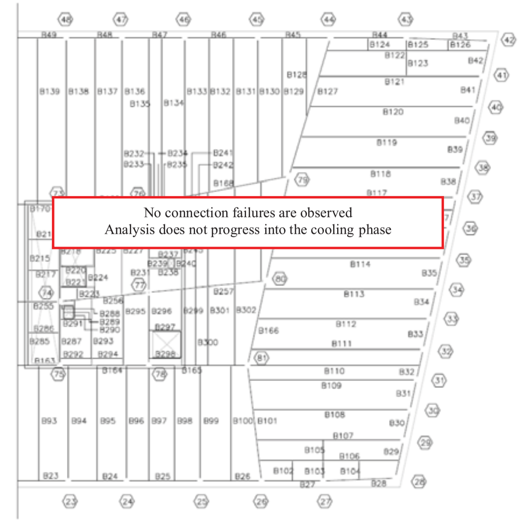

Figure 113: Locations and sequence of connection failures (sequence numbers correspond to Table 7)

JA-3223

A4.4 Column Lateral Movements

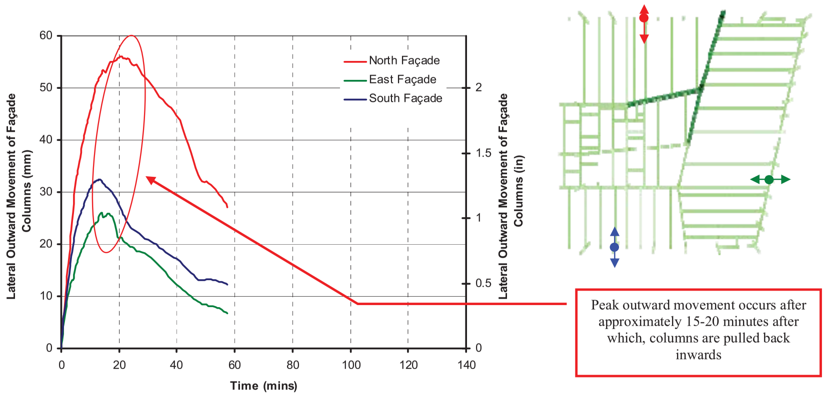

Figure 114: Lateral outward column movements at the façade of the building. Column locations see are shown to the right of the plot.

A4.5 Vertical Deflection Contours

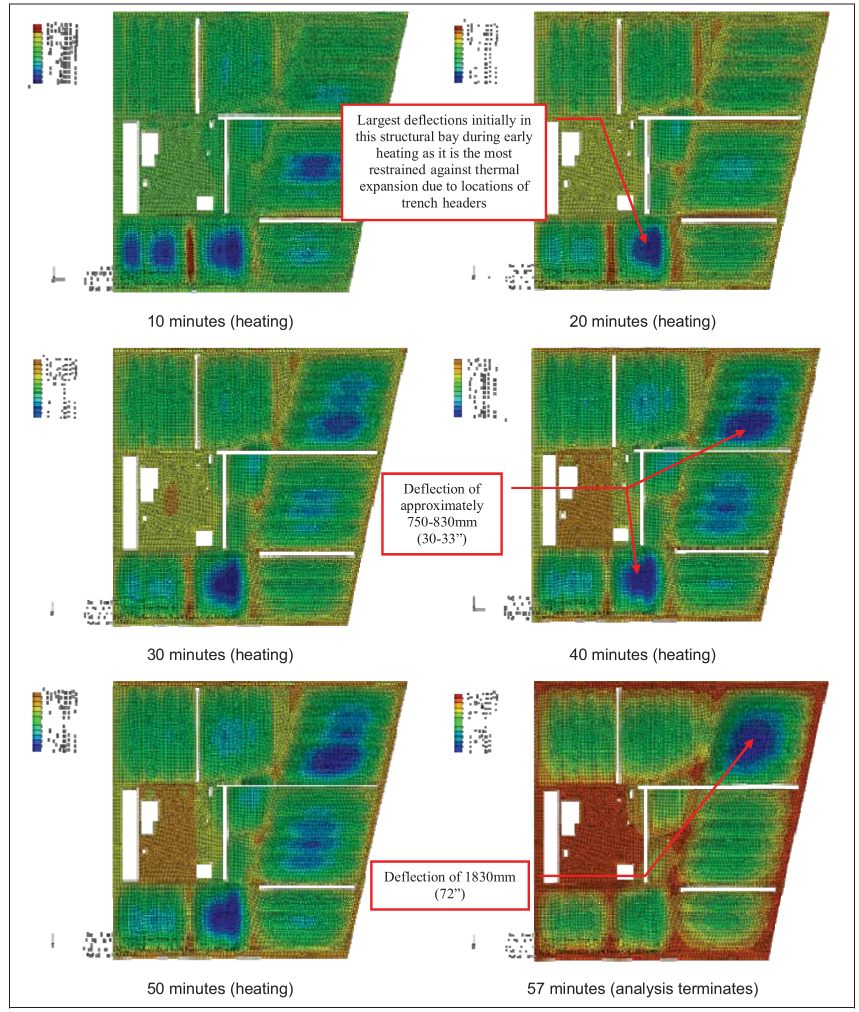

Figure 115: Vertical deflection contours on the slab for 10 minute intervals throughout the duration of the analysis. Key denotes the magnitude of vertical deflection (mm)

A4.6 Mid-span Vertical Deflections

Girder 79-44 (B127) shows runaway starting at approximately 47 minutes

B120 in the north-east bay shows runaway failure

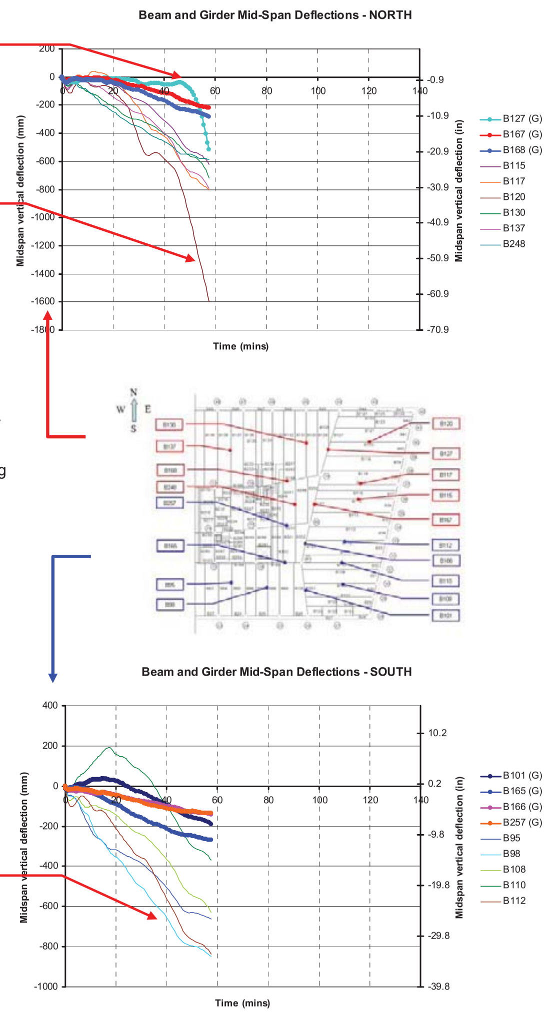

General Behaviour

B120 – a secondary beam in the north-east bay exhibits runaway failure

G79-44 exhibits runaway failure starting at 47 minutes.

All other girders do not show signs of failure

Largest deflections are observed in secondary beams

Greatest deflections observed in beams in the southern region of the structure coinciding with the largest deflections on the concrete slab

Figure 116: Vertical mid-span deflection of selected beams and girders (G) with evolution of the analysis. Key for beam and girder locations shown in the centre of the figure.

A4.7 Lateral Displacements at the End of the Girders Around Column 79

The plots on the right side of this page show the lateral movement of the top and bottom of the end of each girder framing into Column 79 as shown in the diagram image below.

Main Observations

- **Girder 79-44**

  The girder is pushed and pulled laterally by the secondary beams to the extent that in late heating it is being pulled off its seat at Column 79.

- **Girder 76-79**

  As the girder expands with heating its movements are accommodated by ductility in the knife angle plates. Angle plates remain intact and do not tear.

- **Girder 79-80**

  As the girder expands with heating its movements are accommodated by ductility in the knife angle plates. Angle plates remain intact and do not tear.

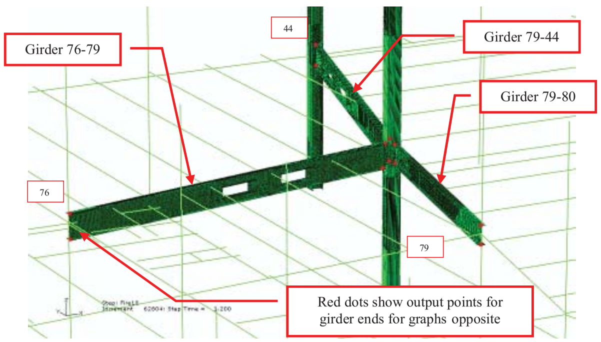

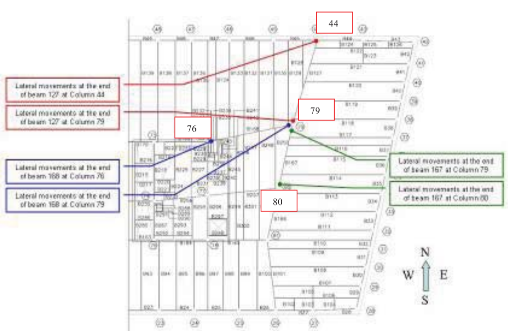

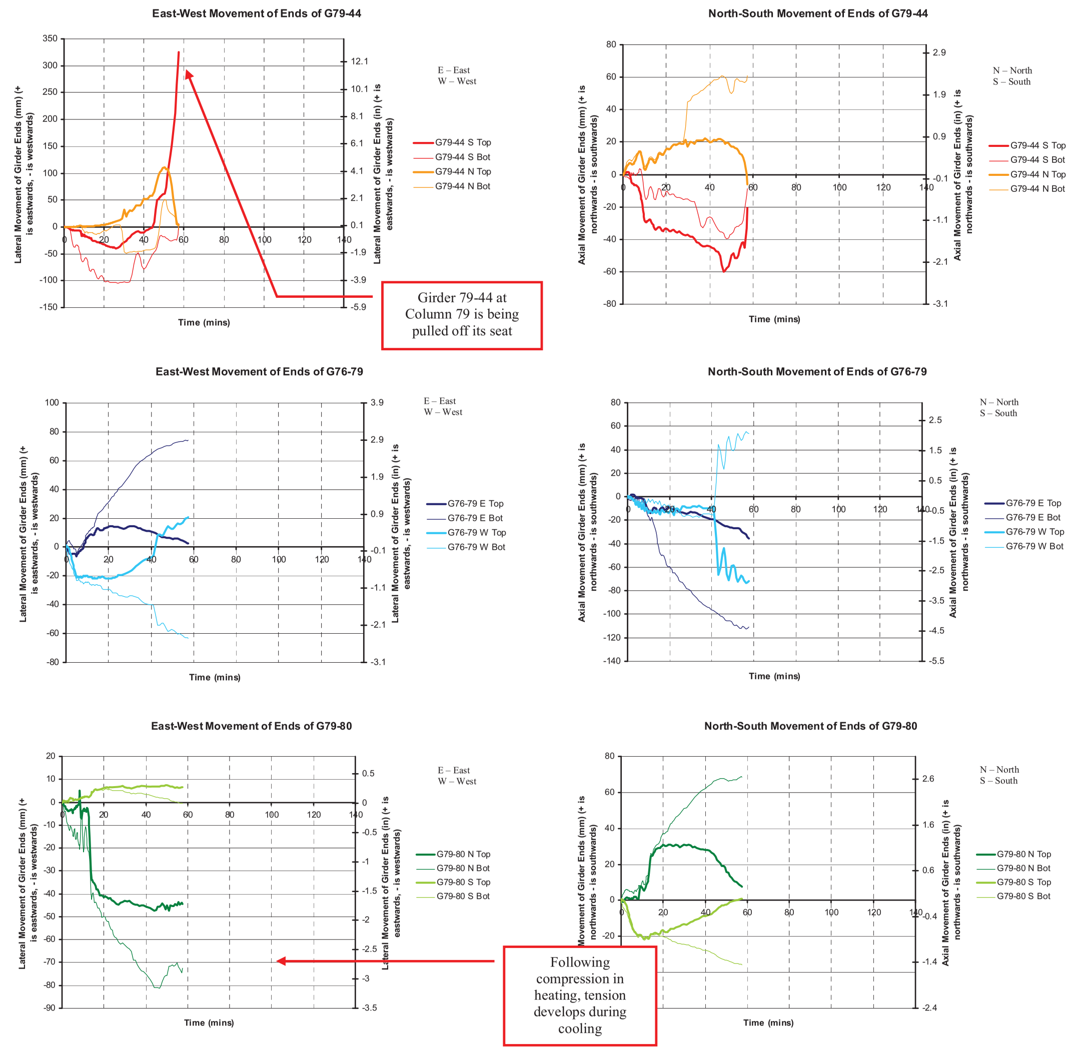

Figure 117: Lateral movements (top and bottom) at each end of the girders framing into Column 79. Images on the left show the locations of the output points on each girder.

A4.8 Lateral Movement at the Ends of the Beams in the North-East Bays

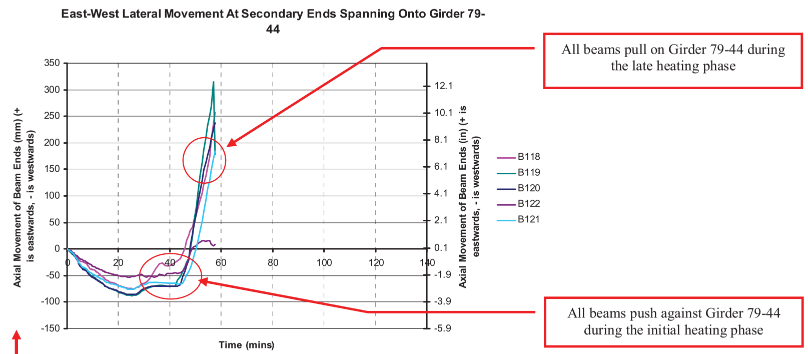

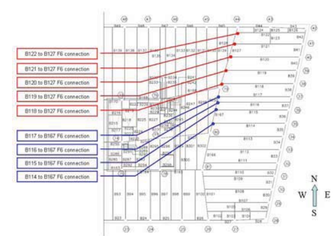

General Behaviour

Beams spanning onto Girder 79-44

Beams push on the girder during the initial phase they expand. As heating develops the beams sag at their mid-span and pull on the girder. Movement is to the West during early heating and to the East late heating.

Beams spanning onto Girder 79-80

Beams nearer to Column 79 exhibit largest push/pull movements due to the presence of a trench header in this area running over the girder.

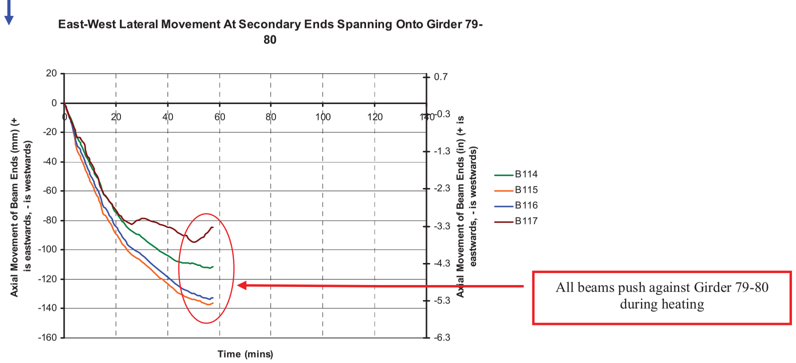

Figure 118: Lateral movements (east-west) of the western end of the beams framing into Girder 79-44 and Girder 79-80

A4.9 Shear Stud Failures

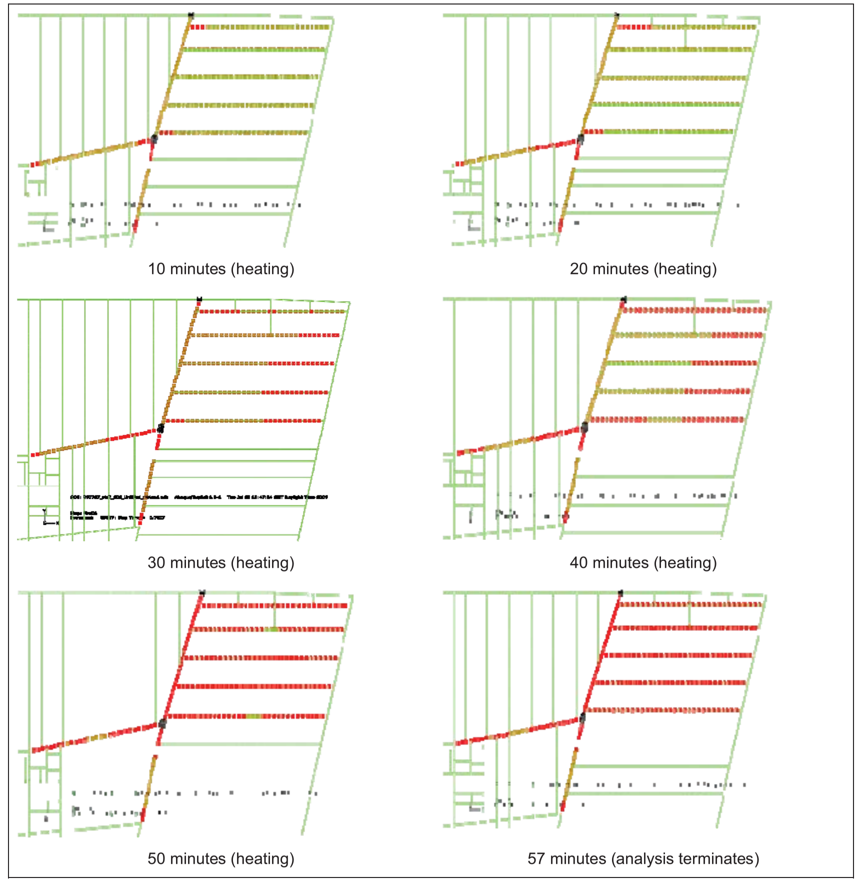

Figure 119: Shear stud failures within the north-east bay at 20 minute intervals throughout the duration of the analysis. Brown markers indicate unbroken shear studs while red markers indicate broken shear studs

During the early heating phase, shear stud breakages are mainly observed at either end of Girders 76-79 and 79-80 and also on the eastern half of beams in the north-east bay.

A large proportion of shear studs break at 40-50 minutes (late heating) to the extent that almost all shear studs have broken with the exception of those on Girder 79-80 south of the trench header.

JA-3227

A4.10 Knife Connection Bolt Deformations and North-East Secondary Beam Connector Forces

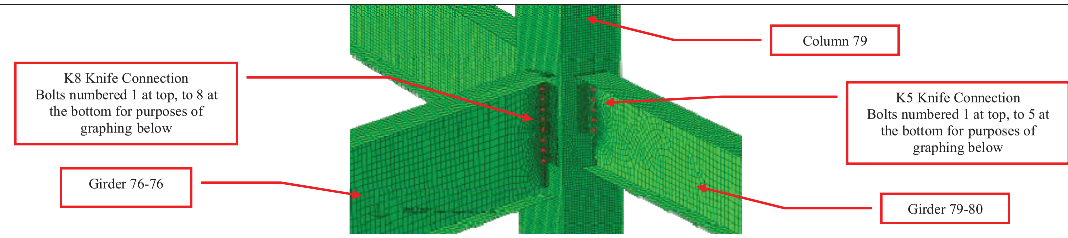

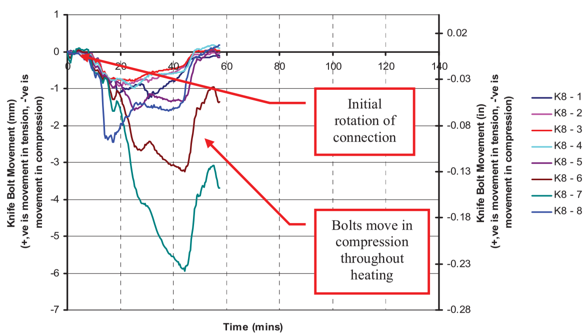

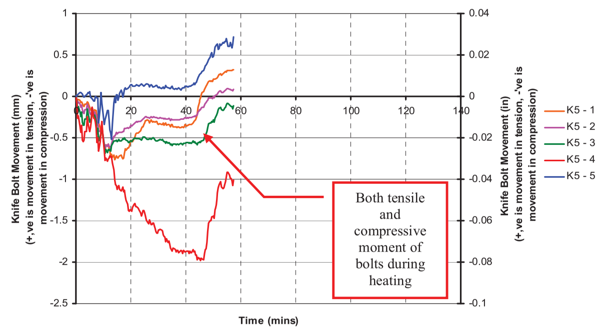

General behaviour of knife connections

During the early stages of the fire (up to 20 minutes), the knife connections rotate with the applied load as the girder expands and the coped bottom flanges move towards the column.

As the fire continues to heat the structure, the girders expand and push the bolts into compression and the bolts and plate start to deform.

The 'L' angles plates of the connection are displaced and bend laterally throughout the analysis. It is these actions and their associated induced forces that result in different patterns of bolt movements within the same connection.

This analysis terminated late in heating due to a numerical instability associated with the failure mechanism. Therefore, no cooling behaviour is observed in this Case.

K8 Knife Connection Bolts (Girder 76-79)

Maximum bolt deformation is in bottom bolt and occurs at peak heating of 6mm (0.24")

K5 Knife Connection Bolts (Girder 79-80)

Maximum bolt deformation is in top bolt during early heating of approximately 2mm (0.08")

The bolt deformation observed in the analysis is a representation of combined deformation of bolts, bolt holes and plates incorporated in the connection.

Note: simplified connectors have an associated movement prior to breakage that relates to bolt and plate ductility.

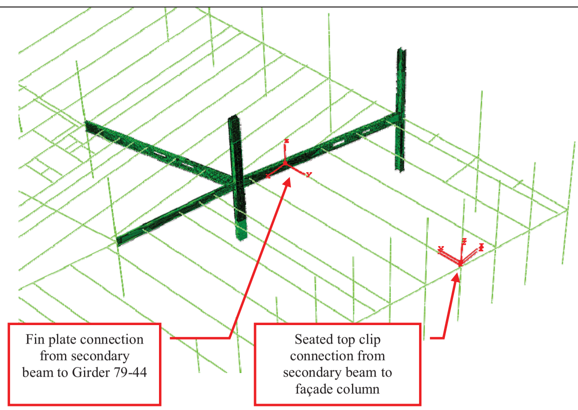

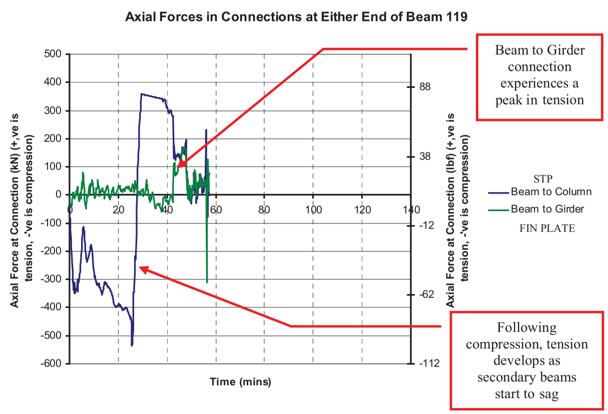

Push/Pull Forces At Either End of a Selected Secondary Beam in the North-East Bay

The fin plate connection of the secondary beam into the girder exhibits low axial force as the girder is relatively free to be pushed and pulled following early breakage of the bolts connecting it to the columns. It exhibits a small peak in tension as the girder is pulled across its seat plate and then pulled tight against the eastern side plate of Column 79. After a short period, the girder pulls away from Column 79 and it is able to continue being pulled to the east.

For the STP connection where the beam connects to the column, compressive forces are transferred to column during heating. As heating continues, the secondary beams in the north east bay sag at their mid-span and pulls on the column, developing tension forces.

Figure 120: Lateral movement of knife connection bolts for the K8 and K5 knife connections. Also shown are the axial forces in the connections at the end of one beam in the north-east corner.

A4.11 Seat Connection and K8 Knife Connection at Column 79 Deformations

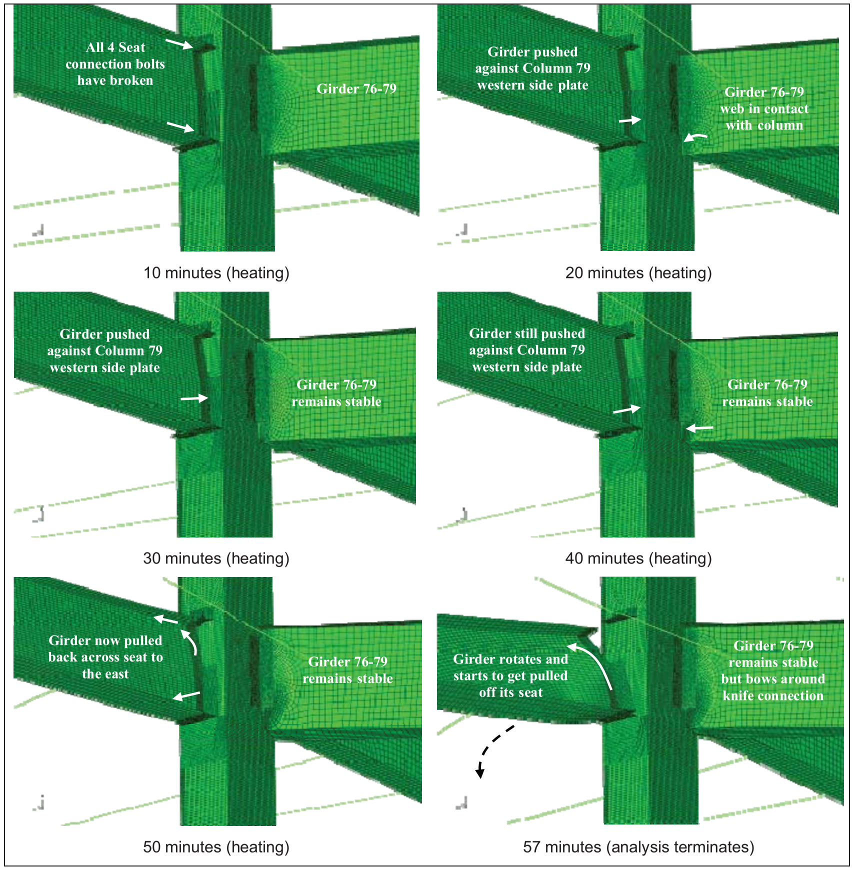

Figure 121: Deformed structure images of the seated connection at Column 79 and the K8 knife connection at 10 minute intervals throughout the fire

A4.12 Girder 79-44 Structural Deformations

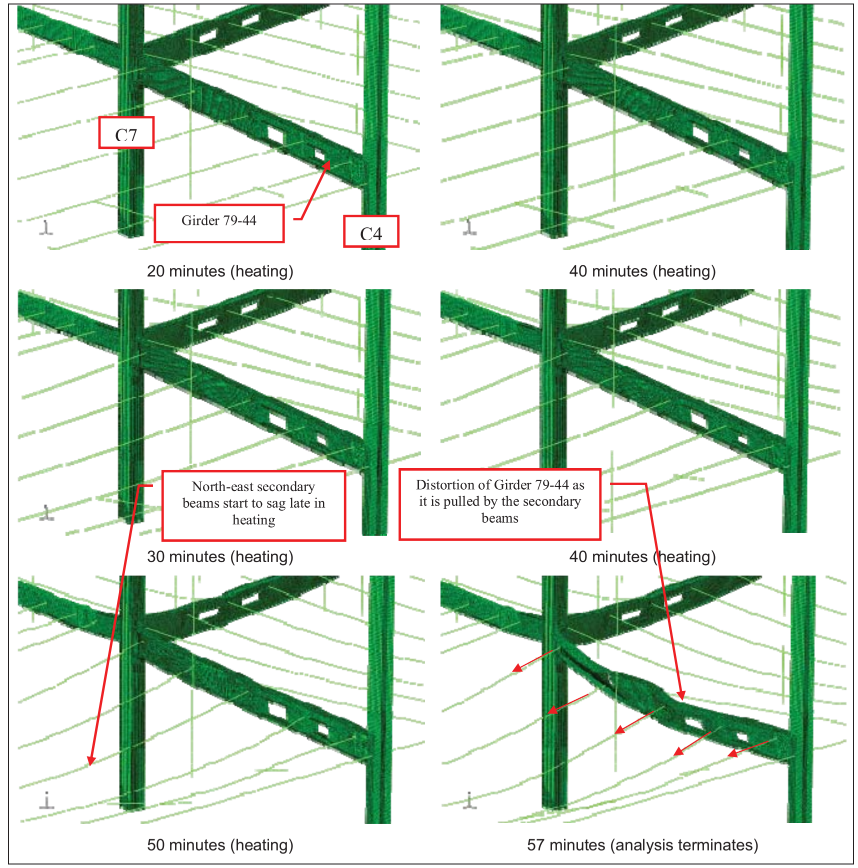

Figure 122: Deformed structure images of the Girder 79-44 in the north-east region of Floor 13 at 10 minute intervals throughout the analysis

Girder 79-44 is pulled across its seat plate late in heating by the secondary beams as they sag due to high temperature. The analysis terminated due to a numerical instability associated with the observed behaviour. The movement of the girder to the east at Column 79 forms the basis of a potential initiating collapse mechanism.

A5 CASE 4: 800°C Fire – Filled Flutes

A5.1 Overview

This section presents detailed output for the 800°C filled flutes assessment to complement the data presented as an overview in Section 8.

This analysis shows that no significant deformation or structural collapse is observed following exposure to the prescribed 1-hour of heating and 1-hour of cooling.

A limited number of connection failures of secondary beams framing into girders are observed during the cooling phase.

A5.2 Detailed Sequence of Events

The sequence of events for the 800°C fire with filled flutes is shown in Table 8. Identified connection failures are referenced using a beam numbering notation that is shown in Figure 123.

Table 8: Sequence of events for the 700°C fire with filled flutes. Red numbers indicate heating, blue numbers indicate cooling. Temperatures are taken as the top flange of Girder 79-44.

Event	Time (mins)	Observation	Temp (°C)
1	3	Both bolts on the seat plate connection to lower flange of Girder 79-44 at Column 79 break	72
2	10	Both bolts on the seat plate connection to lower flange of Girder 79-44 at Column 44 break	80
3	15	Both bolts at the top clip plate to top flange of Girder 79-44 at Column 79 break	170
-	30	Mid-span deflection of central beam in the north east corner bay: 315mm (12.4”)	366
4	35	Both bolts at the top plate to top flange of Girder 79-44 at Column 44 break	228
-	60	Mid-span deflection of central beam in the north east corner bay: 760mm (30”)	559
5	66	Connection B247 to B257 fails in tension	505
6	68	Connection B302 to B257 fails in tension	488
7	68	Connection B300 to B165 fails in tension	488
8	68	Connection B302 to B165 fails in tension	488
9	69	Connection B246 to B257 fails in tension	479
10	73	Connection B215 to B255 fails in tension	445
11	73	Connection B137 to B169 fails in tension	445
12	73	Connection B250 to B257 fails in tension	445
13	74	Connection B301 to B165 fails in tension	436
14	76	Connection B136 to B169 fails in tension	419
15	76	Connection B248 to B168 fails in tension	419
16	76	Connection B247 to B168 fails in tension	419
17	77	Connection B215 to B170fails in tension	410
18	80	Connection B120 to C40 fails in tension	385
19	80	Connection B250 to B168 fails in tension	385
20	80	Connection B121 to C41 fails in tension	385
21	84	Connection B300 to B257 fails in tension	360
-	90	Mid-span deflection of north east corner bay: 1270mm (50”)	323
22	91	Connection B301 to B257 fails in tension	317
23	119	Connection B246 to B168 fails in tension	182
24	120	Mid-span deflection of north east corner bay has now reached 1300mm (51.1”). Other, similar bays have returned to a deflection of 450 to 600mm (17.7 to 23.6”) Analysis completes. No structural collapse	178

A5.3 Connection Failures

Figure 123 shows the location and sequence of connection failures observed during the analysis. Refer to Table 8 for times of failures.

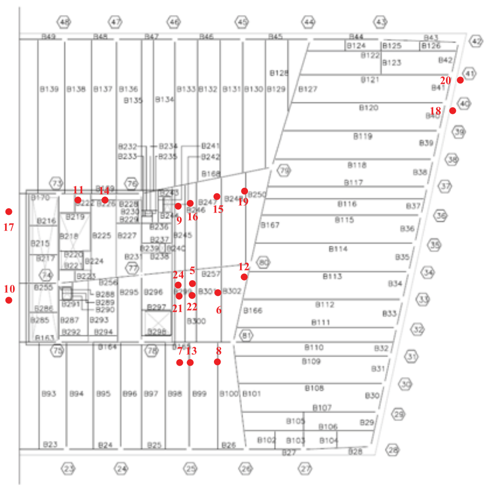

Figure 123: Locations and sequence of connection failures (sequence numbers correspond to Table 6)

A5.4 Column Lateral Movements

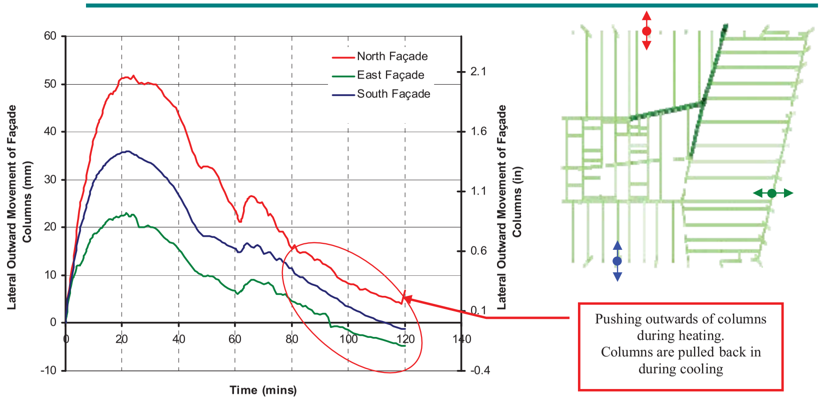

Figure 124: Lateral outward column movements at the façade of the building. Column locations see are shown to the right of the plot.

A5.5 Vertical Deflection Contours

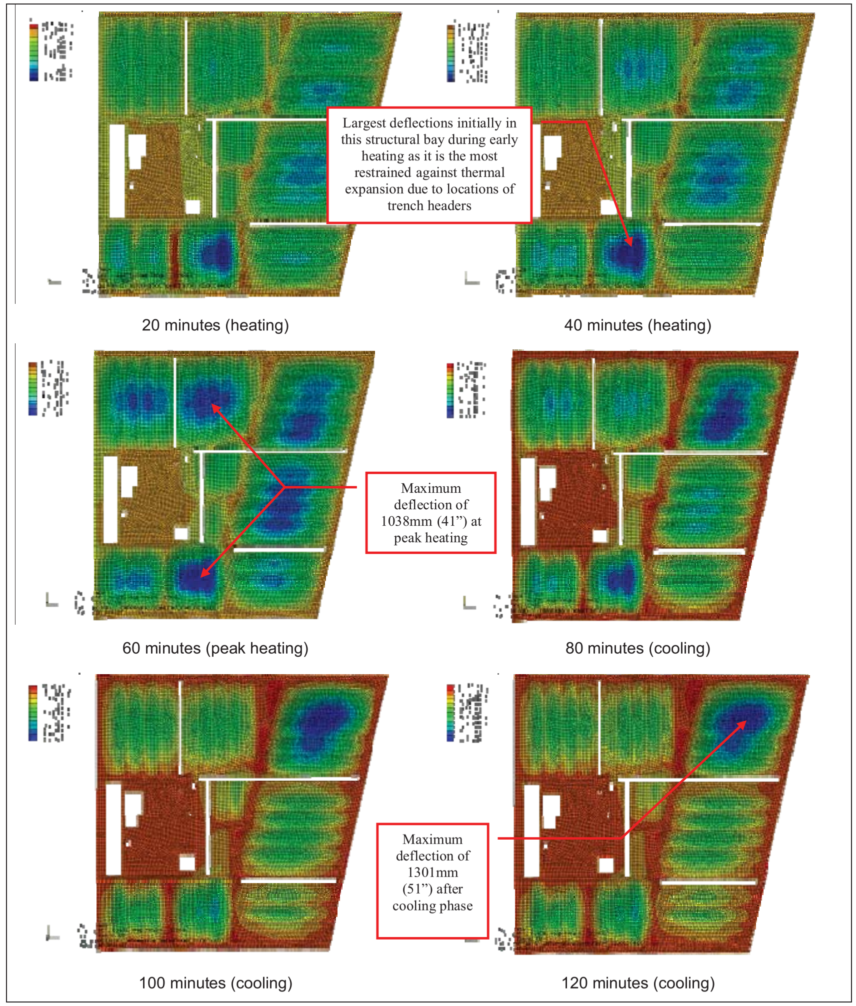

Figure 125: Vertical deflection contours on the slab for 20 minute intervals throughout the duration of the analysis. Key denotes the magnitude of vertical deflection (mm)

A5.6 Mid-span Vertical Deflections

B120 in the north-east bay shows runaway failure as its connection to the perimeter column fails in cooling

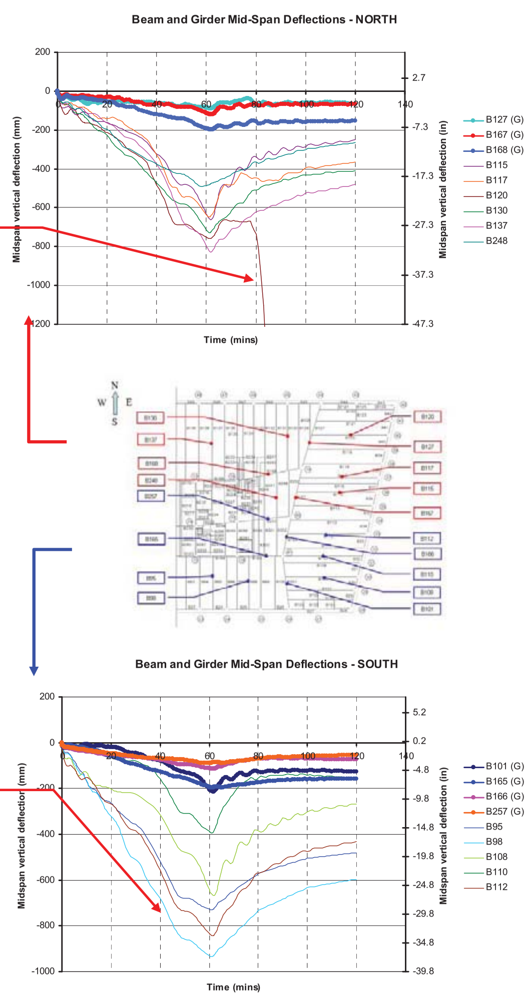

General Behaviour

All girders (in the north and south structural floor areas) exhibit low deflections.

Largest deflections are observed in secondary beams

Beams (not B120 and B121) and girders exhibit partial recovery of deflections. Some residual deflection occurs following cooling, i.e. they do not recover to their ambient position.

Greatest deflections observed in beams in the southern region of the structure coinciding with the largest deflections on the concrete slab

Figure 126: Vertical mid-span deflection of selected beams and girders (G) with evolution of the analysis. Key for beam and girder locations shown in the centre of the figure.

A5.7 Lateral Displacements at the End of the Girders Around Column 79

The plots on the right side of this page show the lateral movement of the top and bottom of the end of each girder framing into Column 79 as shown in the diagram image below.

Main Observations

- **Girder 79-44**
  The girder remains stable on its seats at Column 79 and Column 44 throughout the entire analysis despite the bolts breaking early in the fire. It is pushed and pulled laterally by the secondary beams but does fall off its seats.
- **Girder 76-79**
  As the girder expands and contracts with heating and cooling its movements are accommodated by ductility in the knife angle plates. Angle plates remain intact and do not tear.
- **Girder 79-80**
  As the girder expands and contracts with heating and cooling its movements are accommodated by ductility in the knife angle plates. Angle plates remain intact and do not tear.

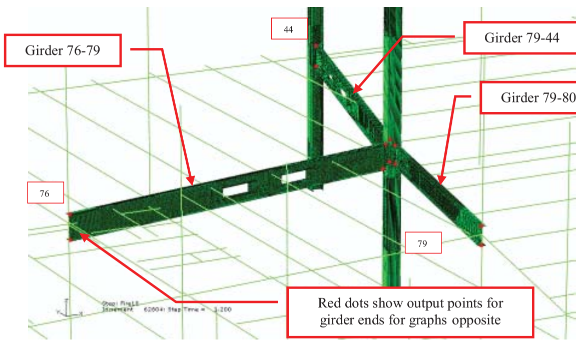

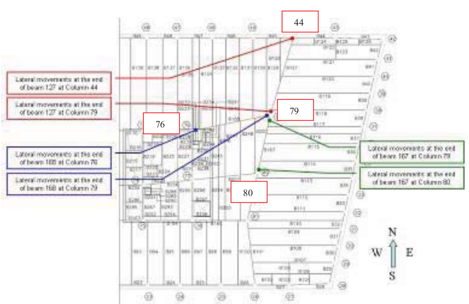

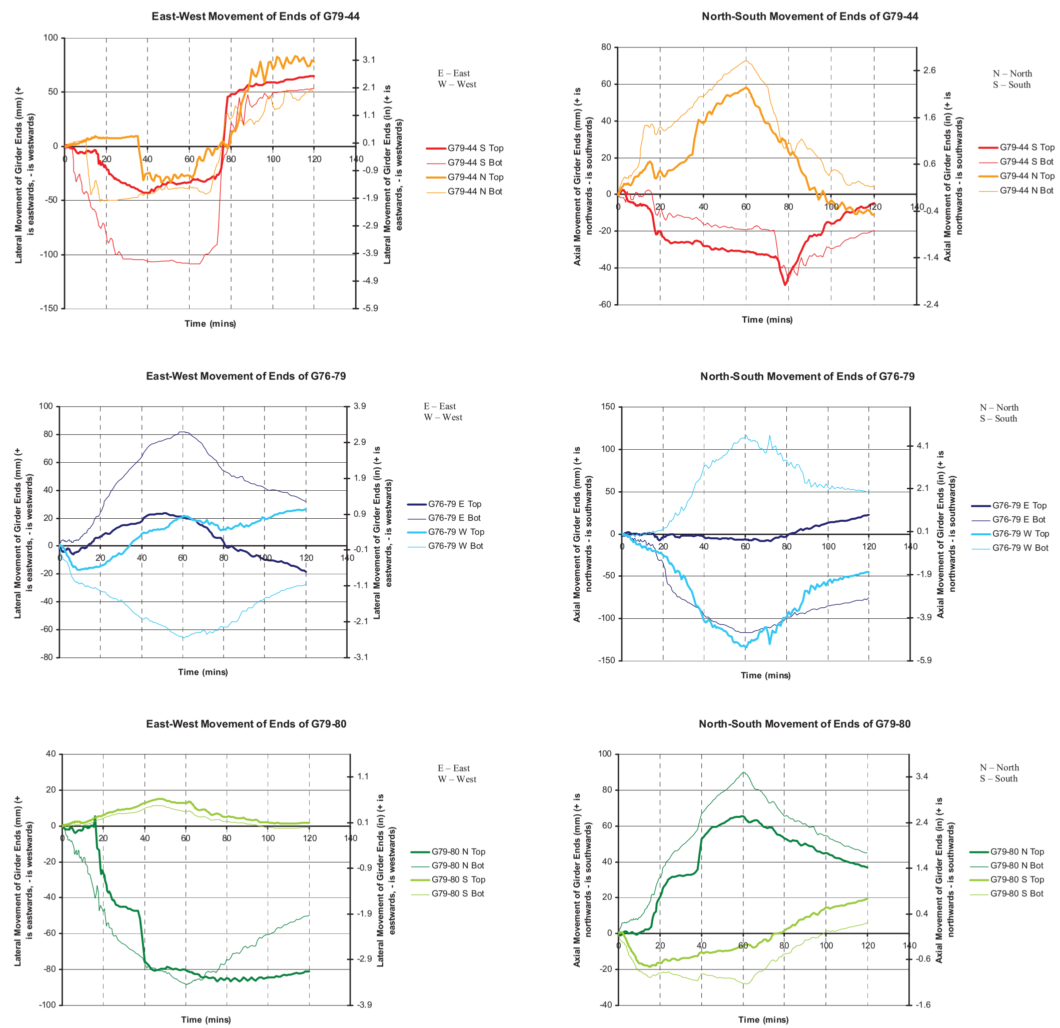

Figure 127: Lateral movements (top and bottom) at each end of the girders framing into Column 79. Images on the left show the locations of the output points on each girder

JA-3233

A5.8 Lateral Movement at the Ends of the Beams in the North-East Bays

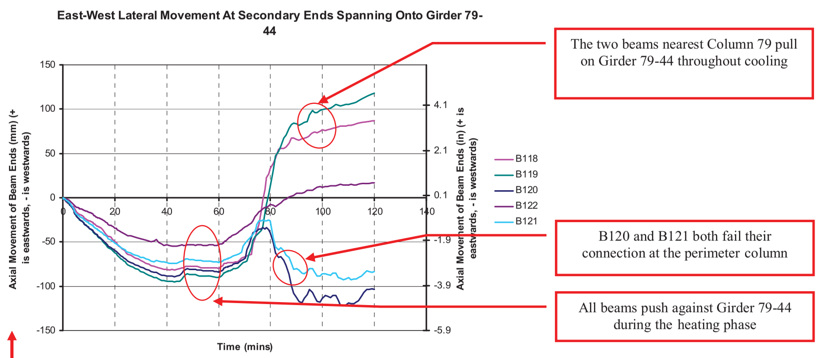

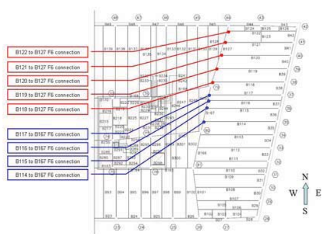

General Behaviour

Beams spanning onto Girder 79-44

Beams push on the girder throughout heating as they expand and pull on the girder during cooling as they contract. Movement generally to the West during heating and to the East during cooling.

Beams spanning onto Girder 79-80

Beams nearer to Column 79 exhibit largest push/pull movements due to the presence of a trench header in this area running over the girder.

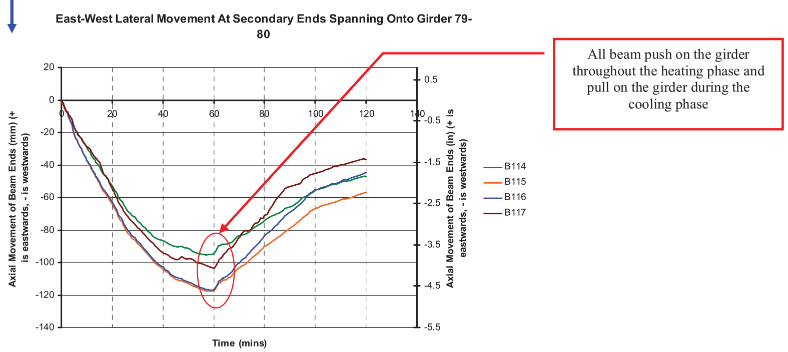

Figure 128: Lateral movements (east-west) of the western end of the beams framing into Girder 79-44 and Girder 79-80

A5.9 Shear Stud Failures

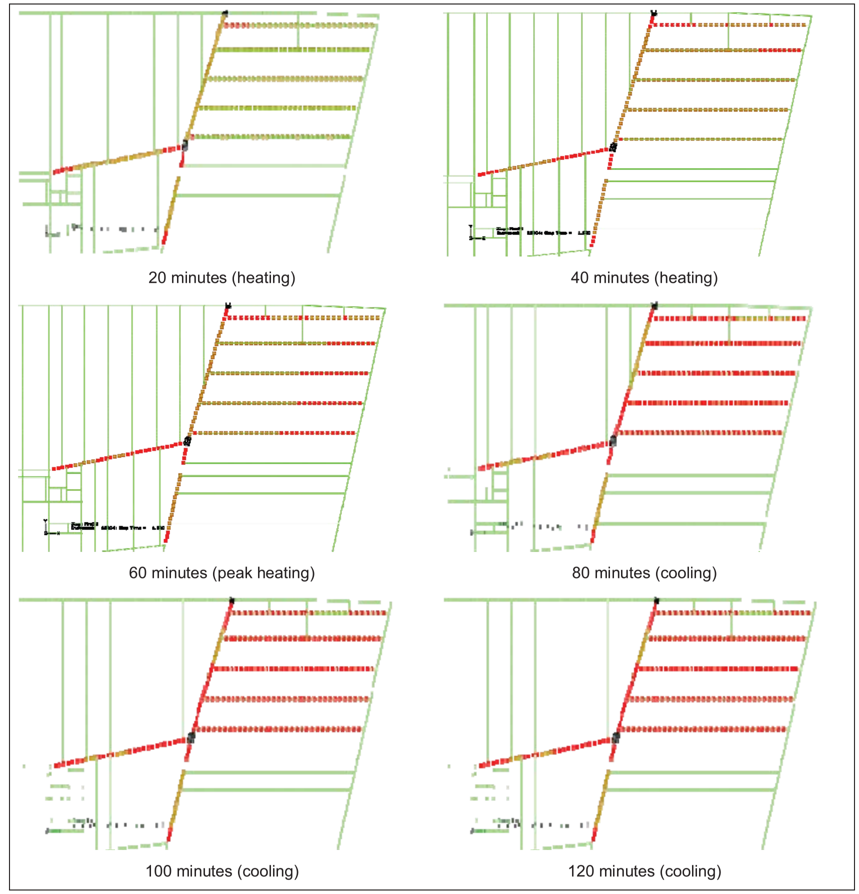

Figure 129: Shear stud failures within the north-east bay at 20 minute intervals throughout the duration of the analysis. Brown markers indicate unbroken shear studs while red markers indicate broken shear studs

During the heating phase of the fire, shear stud breakages are observed at either end of Girders 76-79 and 79-80 and also on the eastern third of beams in the north-east bay.

During the initial cooling phase, a significant number of shear studs break due to differential cooling between the concrete slab and the steel beams. These include almost all shear studs on the secondary beams and the majority on each of the three girders into Column 79.

JA-3234

A5.10 Knife Connection Bolt Deformations and North-East Secondary Beam Connector Forces

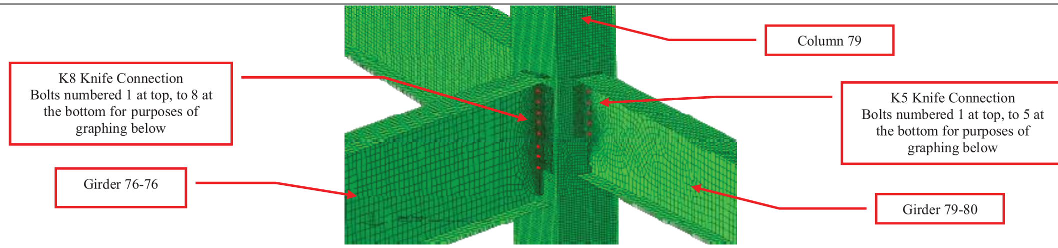

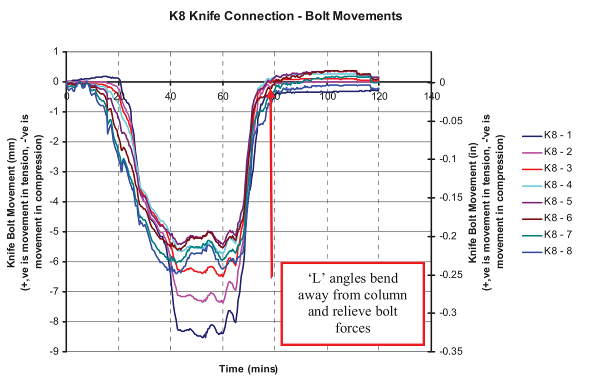

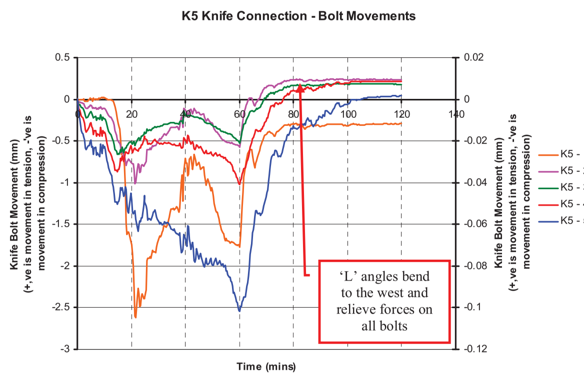

General behaviour of knife connections

During the early stages of the fire (up to 20 minutes), the knife connections rotate with the applied load as the girder expands and the coped bottom flanges move towards the column.

As the fire continues to heat the structure, the girders expand and push the bolts into compression and the bolts and plate start to deform.

As the structure starts to cool, the compression forces and bolt deformations are relieved.

As cooling continues, the girder contracts and starts to pull on the connection in tension.

As the tension forces develop, the 'L' angles forming the connection start to bend away from the column – only being connected to the column by their weld.

At this point, connection deformation is governed by the 'L' angle bending and no further change in bolt deformation is observed

K8 Knife Connection Bolts (Girder 76-79)

Maximum bolt deformation in all bolts occurs at peak heating of 5mm – 8.5mm (0.2"-0.33")

K5 Knife Connection Bolts (Girder 79-80)

Maximum bolt deformation in top bolt during heating of approximately 2.5mm (0.1")

The bolt deformation observed in the analysis is a representation of combined deformation of bolts, bolt holes and plates incorporated in the connection.

Note: simplified connectors have an associated movement prior to breakage that relates to bolt and plate ductility.

JA-3235

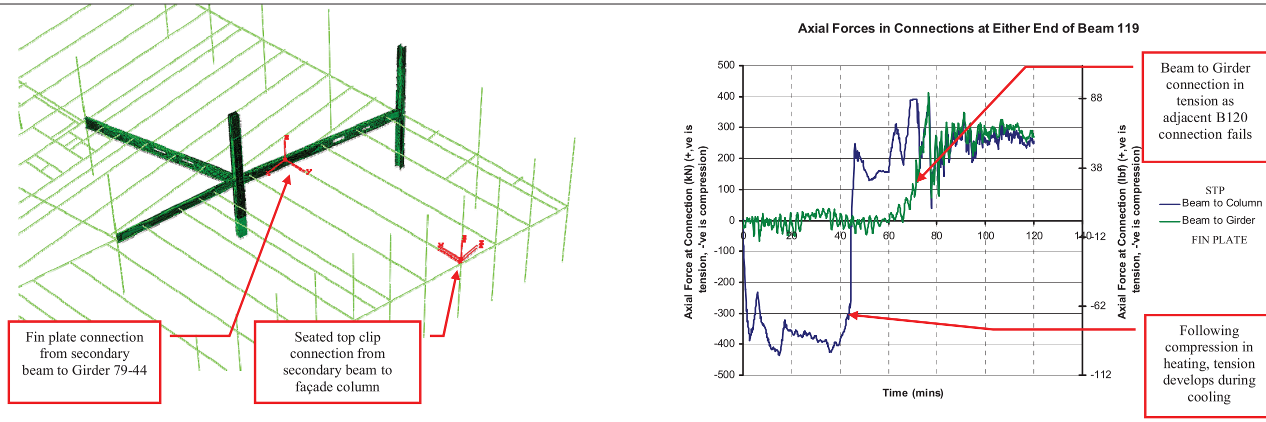

Push/Pull Forces At Either End of a Selected Secondary Beam in the North-East Bay

The fin plate connection of the secondary beam into the girder exhibits low axial force as the girder is relatively free to be pushed and pulled following early breakage of the bolts connecting it to the columns. It exhibits tension as it shares the load that was previously taken by the two adjacent beams that have failed at their connections.

For the STP connection where the beam connects to the column, compressive forces are transferred to column during heating. During cooling, the beam pulls on the column as tension forces develop.

Figure 130: Lateral movement of knife connection bolts for the K8 and K5 knife connections. Also shown are the axial forces in the connections at the end of one beam in the north-east corner.

JA-3236

A5.11 Seat Connection and K8 Knife Connection at Column 79 Deformations

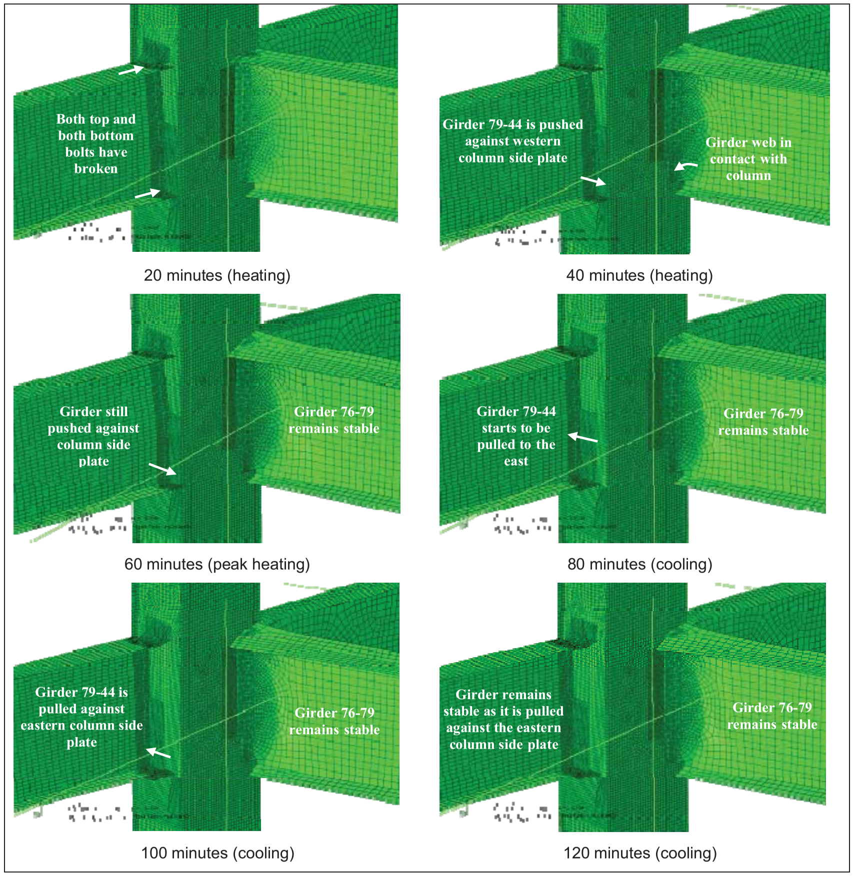

Figure 131: Deformed structure images of the seated connection at Column 79 and the K8 knife connection at 20 minute intervals throughout the fire

A5.12 Structural Deformations

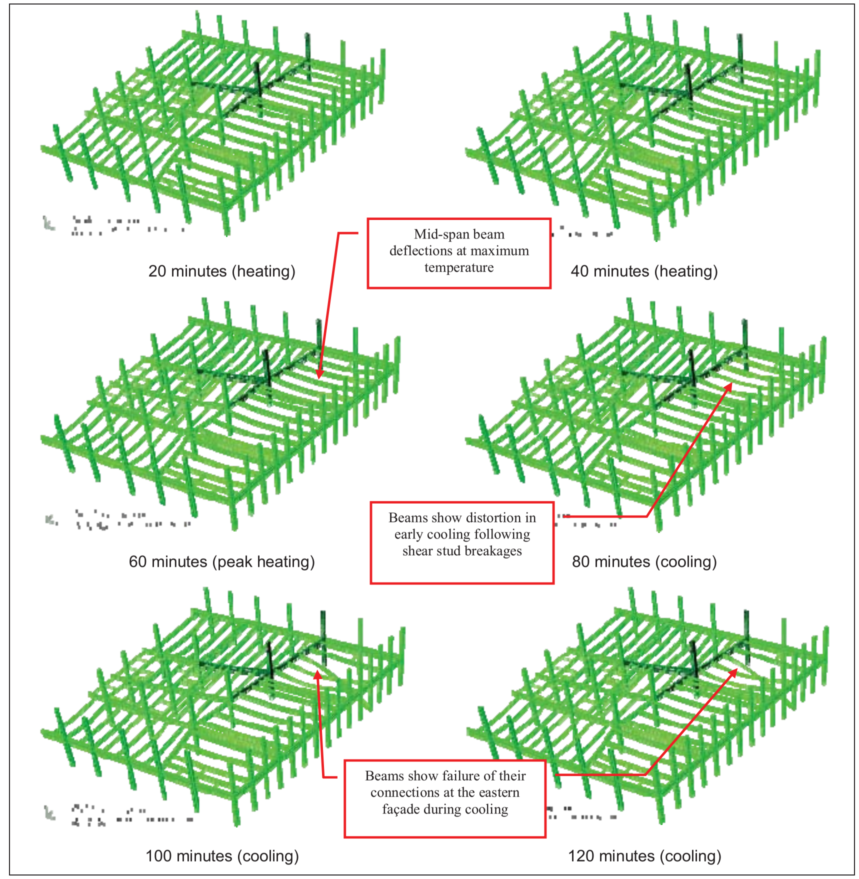

Figure 132: Deformed structure images of the structural frame of Floor 13 at 20 minute intervals throughout the analysis

Two secondary beams in the north-east bay fail at their connections to the eastern façade columns as the beams contract due to cooling and create large tension forces.

Girder 79-44 is pulled across its seat plate to the east during cooling by the secondary beams but remains stable on its seating plates at both Column 44 and Column 79.

No initiating collapse mechanism is observed.

Appendix B

ABAQUS Analysis: Basis for the numerical model

Contents

Executive Summary

This appendix outlines the modelling assumptions forming the basis of the four numerical models produced in the main Arup report, WTC-7 Structural Fire Analysis: Structural Fire Analysis Report (Runs 1-4) dated December 2009.

The numerical modelling to determine the collapse trigger mechanism for WTC7 was carried out using the ABAQUS finite element program.

A detailed set of assumptions was required in order to model the eastern side of Level 13 and its supporting columns during a fire on Level 12, to the level of detail required to determine the collapse trigger mechanism.

B1 Introduction

This appendix outlines the detailed assumptions forming the basis of the four numerical models presented in the main report.

B1.1 Report layout

The modelling assumptions fall into the following categories: -

- Overview of Modelling Strategy – Refer to Section B1.3
- Description of proposed finite element model – Refer to Section B2
- Numerical Analysis Software - Refer to Section B3
- Design Fires - Refer to Section B4
- Heat Transfer - Refer to Section B5
- Material Models - Refer to Section B6
- Specific Structural Aspects - Refer to Section B7
- Loads - Refer to Section B8

B1.2 Information used as basis of study

The structural layout used for the modelling aspect in the scope of work is taken from the Cantor Drawing Revision I and the Frankel steel erection and shop drawings (1985).

B1.3 Overview of Structural Fire Modelling Strategy

The structural fire numerical model that has been generated by Arup is a single storey sub-model for approximately half of the floor of level 13. The extent of the floor plate of the proposed sub-model is shown Figure 133.

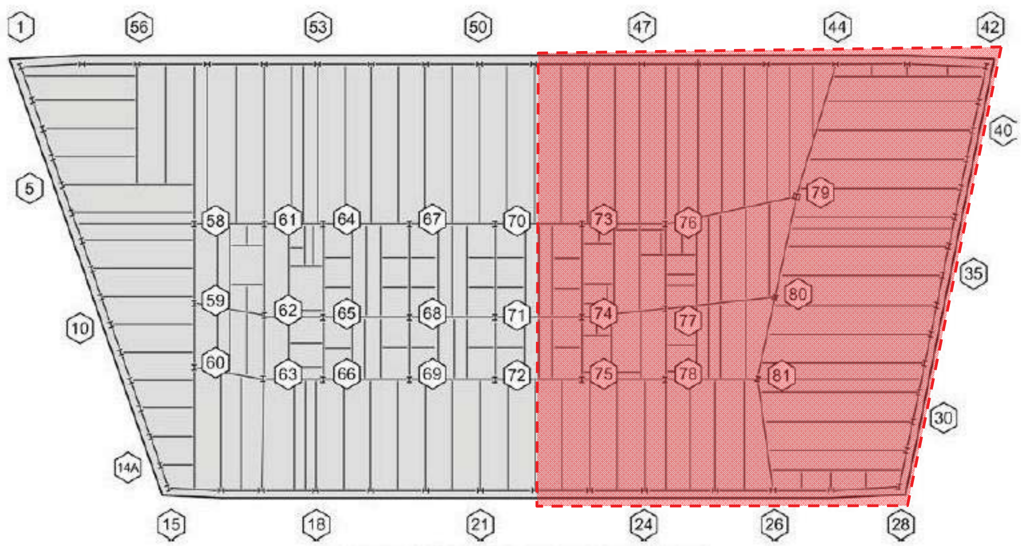

Figure 133: Extent of proposed detailed model (shaded in red) of level 13

B1.4 Intent of the sub-model

The area, layout, and modelling detailing in the sub-model is aimed to achieve the following:

5. The critical aspects of the structural behaviour in fire which were considered necessary for detailed analysis are:
    a. Movement of the main girder on the seated connection on Column 79 and whether or not it could be unseated as a result of the lateral movement of the girder caused by the expansion of the supported beams.
    b. The effects to the other two girders (spanning between Columns 79 and 80 and Columns 79 and 76) that were connected to Column 79 if the girder (between Column 79 and 44) was unseated.
    c. The influence of the shear studs that were welded onto the beams supported by the main girder, on the movement of the main girder, and to investigate whether or not failure of the shear studs could have caused the beams to push or pull the girder sideways resulting in the movement of the girder on the seated connection.
    d. The influence of the additional shear studs on the behaviour of the primary girders.
6. The detailed behaviour of the three girders that are supported off Columns 79 and 44 under fire conditions.
7. The detailed behaviour of the connections on Columns 79 and 44 which support the girders.

8. Investigate the behaviour of the floor running the entire width (North-south) of the floor plate on the eastern side of level 13, and to consider the effect of the girders spanning columns 76-79, 79-80, 80-81 and 81-26
9. To investigate other potential alternative column failure locations (for instance: columns 80, 81, 76, 26 and the beams/girders that are attached to these columns)
10. To investigate temperature bounds within which failure was and was not observed to occur to allow comparison with any available observed fire behaviour on September 11th 2001.

B1.5 Structural behaviour to be modelled

The complexity of the models is so complex that they incorporate the micro performance of building components such as bolts.

The model is set up to capture the following phenomena:

- Thermal expansion and contraction of the girders and beams due to heating,
- The lateral movement of the main girder (between columns 79 and 44) due to the thermal expansion and contraction of the supported secondary beams in the North –East corner of level 13 and to predict if the girder could slide off the seated connection.
- The behaviour and deformation of shear studs where modelled in detail.
- Deflection, rotations and local deformations of the primary girders spanning between columns 76-79, 79-80, 79-44.
- The influence of the web penetrations on the behaviour of the girders and beams (girders spanning from column 44 to 79 and column 76 to 79).
- Deformation of the bolts and steel plates of the seated connections on columns 79 and 44 and of the knife connections at column 79
- Influence of trench headers in the slab.
- Restraint created by columns 79 and 44 to prevent twisting of the ends of the girder 44-79 supported by these two columns (wedging effect)
- Torsional restraint created by top cleats and seating cleats of the connections of the primary girder supported by column 79 and 44
- Torsional restraint to the beams and girders due to contact between the top flange of the girders and the underside of the composite slab
- Rotational limits to certain connection types, in line with appropriate calculated values. These limits are designed to prevent unrealistic numerical errors.

B2 Description of ABAQUS finite element model

B2.1 Overview of finite element model

The sub-model is modelled in the ABAQUS finite element program using a combination of beam and shell finite elements for the beams, girders and columns, shown in Figure 134.

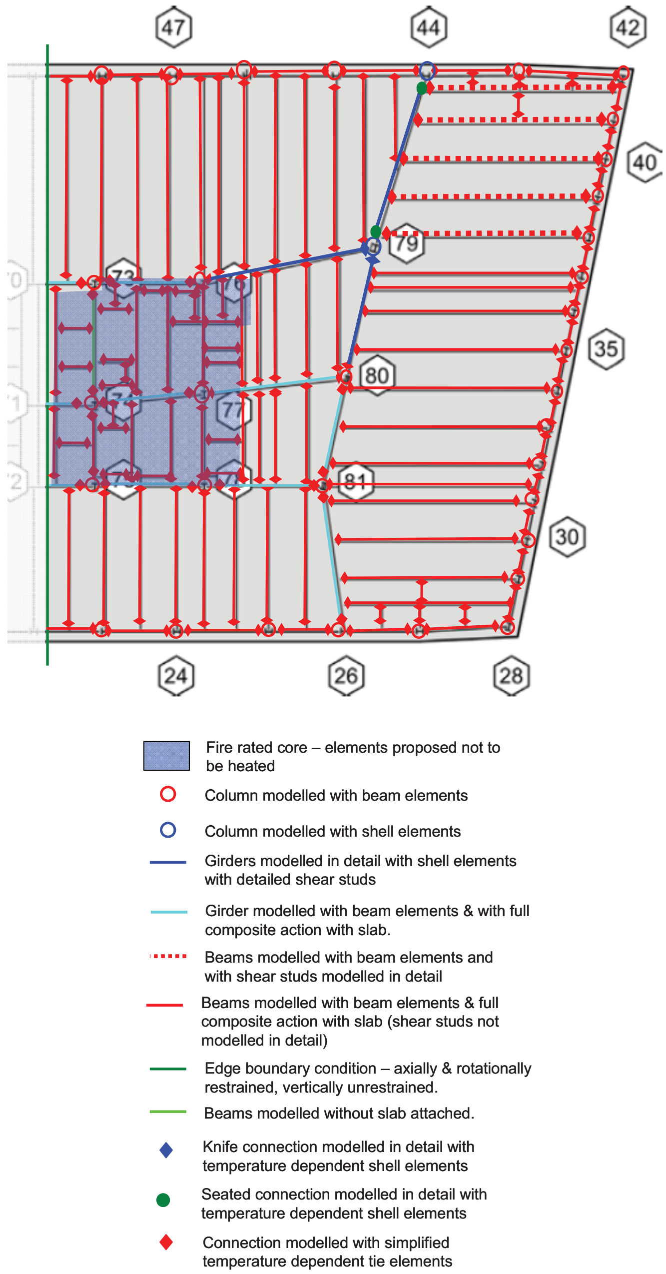

Figure 134: Description of structural fire model of the Eastern Side of Level 13

- This sub-model represents the three girders and two columns in detail using shell elements. This is because only the behaviour of these members are proposed to be studied in detail (marked in blue in Figure 134).
- Shell elements can be used to study the detailed behaviour of the girders and columns such as local buckling; this behaviour cannot be captured using beam elements. The other beams, girders and columns are modelled with beam elements.
- All the other beams, girders and columns are modelled using beam finite elements (i.e.: 2-noded linear elements).
- The blue shaded region shown in Figure 134 shows the extent of the fire rated core. All structural frame elements and the floor slab located within this shaded core region are not heated in the structural fire analysis. Elements located at the boundary of the fire rated core are heated.

B2.2 Beam / Girder Connections

B2.2.1 Simplified connections

- With the exception of the four connections modelled in detail (three at column 79 and one at column 44), connections are generally represented using temperature-dependent connecter elements with capacity limits (in shear, tie and/or moment) and with prescribed displacement limits.
- Connection capacities at ambient conditions are based on values calculated by Arup.
- The ambient connection strengths are extrapolated for high temperature response by the strength reduction factors based on Eurocode values.
- Detailed specific connection properties, incorporating ductility and breakage limits are incorporated as outlined in this appendix.

B2.2.2 Detailed Connections

- The connections that are modelled in detail are two knife connections and one seated connected at column 79, and one seated connection on column 44 (Refer to Figure 134).
- Details of the methodology of modelling the detailed connections are incorporated in this appendix.

B2.3 Slab

- The slab is modelled as a flat slab with an effective depth of 4” (102mm) to represent the 5.5” thick profiled deck that was present in the building (see Section B7.3.1).
- The 6/6 W1.4xW1.4 reinforcing steel mesh is modelled in ABAQUS assuming a smeared thin layer of steel in the slab, with the area of the steel sheet equal to the cross sectional area of the reinforcing steel.
- The orthotropic effects caused by the steel decking are represented through the use of an additional layer of steel reinforcement positioned at the underside of the concrete slab. The amount of reinforcement provided is related to the thickness of the metal deck. This additional layer of reinforcement spans in the strong direction of the metal decking only. It is proposed not to model the layer of reinforcement to span in the weak direction as it is considered that the bending strength and stiffness in the weak direction would have negligible effect and strength contribution to the composite slab in fire conditions.

- The slab is modelled using 4-noded shell finite elements. The exact size of shell elements for representing the slab varies and depends on the detailed layout of the floor structure.

B2.3.1 Trench Headers

The WTC7 Sub-model includes trench as indicated in Figure 135. The trench headers in WTC 7 provided ducts for services access throughout the floor plate of the building. The red marked lines in Figure 135 indicate the confirmed location and extent of the trench headers. Unless otherwise indicated the trench headers are included in the model, as can be seen in Figure 136.

The exact extent of each trench is not known in detail. Therefore each trench has been terminated a sufficient distance away from other significant parts of the geometry. This strategy is designed to prevent the creation of very small slab elements and therefore minimize potential model meshing issues in the slab around each trench.

The trench headers are represented in ABAQUS as holes in the slab at the location of the trenches. Each trench is approximately 3' wide, representing the gap between the edges of the beam flanges at the edge of the trench.

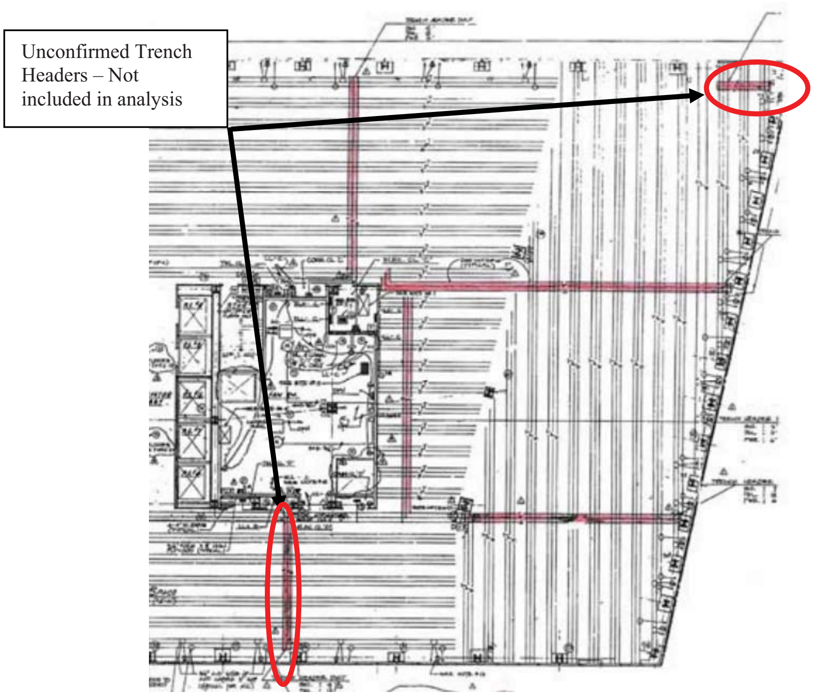

Figure 135: Location of Trench Headers in Sub-model

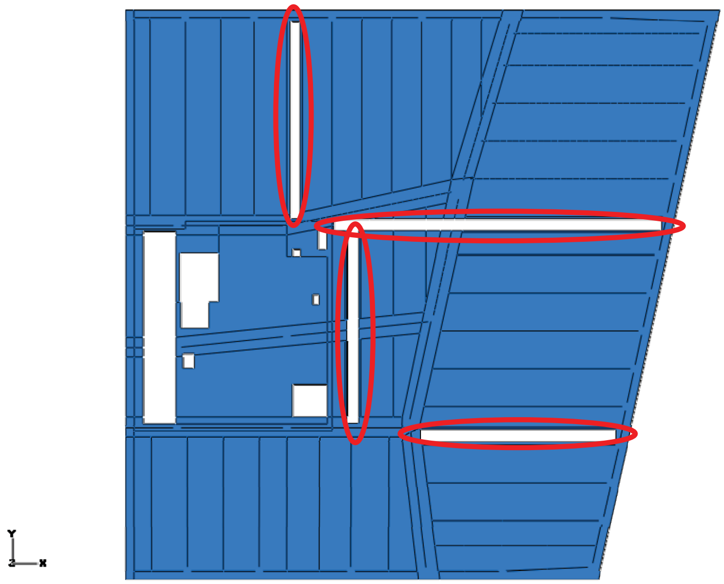

Figure 136: Trench headers locations in the ABAQUS sub-model (circled in red)

B2.4 Connection of Beams and Girders to the Slab

- There are five composite secondary beams on the east side of the girder that span between column 44 and 79 (See Figure 134) where the shear studs between the beams and the slab are modelled in detail. The shear studs are represented with tie elements, with prescribed temperature dependant force-slip relationships to simulate the shear studs (See Section B7.1.2 for more details of the detailed representation of the shear studs). A contact surface is also provided between these beams and the slab (Refer to Section B3.3).
- The girders modelled using shell elements between Column 79 and columns 44, 76 and 80 are also provided with shear studs represented using connector elements as above. If shear studs break, further interaction between the top surface of the top flange of the girder and the underside of the slab is provided using the general contact algorithm native to ABAQUS.
- All other composite beams and girders are rigidly tied to the slab to simulate full composite action between the slab and the beams.

B2.5 Vertical support boundary conditions

Figure 137 shows the boundary conditions included in the finite element model. The columns of the sub model extend 3 storeys, from halfway between floors 11 and 12 up to halfway between Floors 14 and 15.

To simulate the unheated structure above the floor of interest, the columns are restrained in lateral translation and axial rotation at Floor 14. This represents the restraint available from the floor slab and beams surrounding each column at the floor level. At the top of the columns, mid-way between Floors 14 and 15, rotational restraint is provided in the minor and major bending axes.

The columns above the floors of interest are free to move vertically. This combination of boundary conditions is intended to represent likely restraint available from the cool structure above Level 13, specifically the ability of columns to pivot about the floor.

To simulate the restraint of the cool structure below the floor of interest, all columns are restrained in horizontal and vertical translations and axial rotation at Level 12 floor level. This combination of boundary conditions is intended to incorporate a realistic assessment of the restraint available from the cool structure below Level 12, specifically the ability of columns are restrained against rotation around the major and minor bending axes of the columns.

The boundary conditions of the perimeter columns on the floors above and below the heated floor are restrained in rotation about their major bending axis (only) at Levels 12 and 14 to represent moment connections provided by the edge girders.

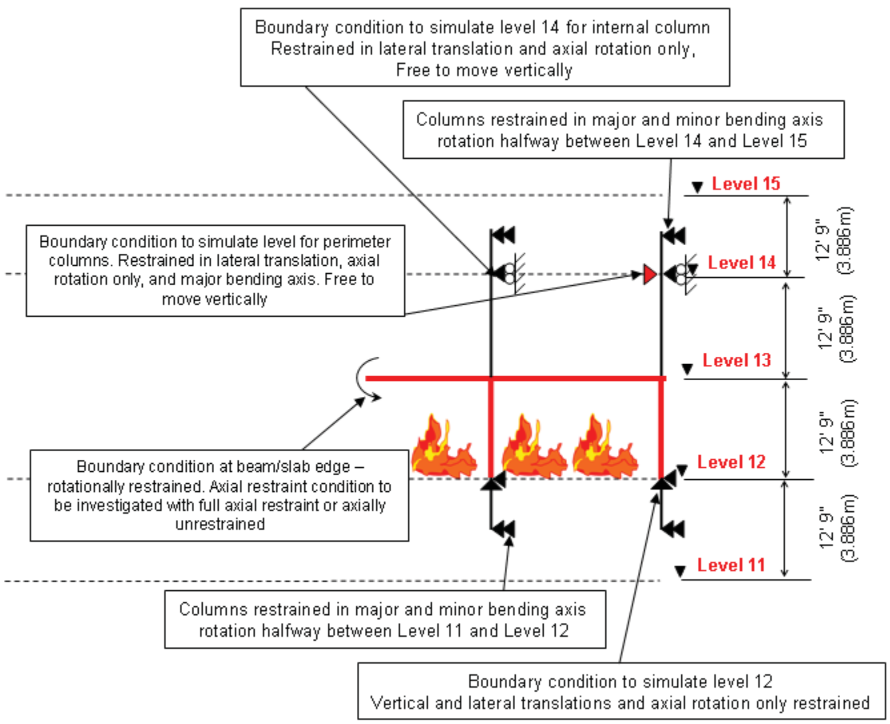

Figure 137: Description of Column Boundary Conditions in Sub-model

B3 Numerical Analysis Software

B3.1 Finite Element Analysis Code

ABAQUS is used for the finite element analysis of the structural fire models.

ABAQUS Version 6.9 is used.

A dynamic nonlinear stress/displacement analysis will be adopted using explicit integration in ABAQUS/Explicit.

B3.2 Finite Elements

B3.2.1 Shell elements

Certain beams, columns and some specific connections, where required (see Section B2.2.2), and all concrete slabs are modelled using shell finite elements. This allows detailed responses to be calculated numerically.

Conventional shell elements are used. These allow for structures to be modelled where in one dimension, the thickness, is significantly smaller than the other dimensions.

Details of the shell elements are as follows:

- Element type: 4-node, quadrilateral, stress/displacement shell element with reduced integration and a large-strain formulation (Designated as element type S4R in ABAQUS).
- Temperature specification across the thickness of the slab as described in Section B5.3.

B3.2.2 Beam elements

Beams and columns where required (see Section B2) are modelled using beam finite elements. Beam elements are an efficient modelling tool that require fewer computational resources than shell elements, yet provide an appropriate approximation of a structural member where very detailed responses are not a necessary output.

Details of the beam elements are as follows:

- Element type: Timoshenko beam elements are used. Beam element in 3D space, linear between 2 nodes with 1 integration point (Designated as element type B31 in ABAQUS). They allow for transverse shear deformation and can be used for both stocky and slender beams.
- The beam element can represent the common member cross-sectional profiles such as I, H, circular, rectangular or hollow sections.
- Different temperatures can be specified at 5 input points across the section of the beam.

B3.2.3 Connector elements

Where the connections in the structure (to connect between beam to beam or beam to columns) are modelled with simplified connector elements rather than shell elements (see Sections 77 and B7.2.1), the element is defined as:

- Element type: Connector element in 3D space between two nodes allowing for translational and rotational movement (Designated as element type CONN3D2 in ABAQUS).
- Temperature dependant force-deformation characteristics can be specified for shear, tie and bending for these elements.

B3.2.4 Mesh density

An appropriate mesh density has been chosen for all models to allow for non-linear effects and to allow appropriate connection between structural members.

B3.3 Contact Behaviour Between Finite Elements

- Contact elements are used in the models to simulate contact behaviour between finite elements.
- The general contact algorithm native to ABAQUS/Explicit is used.
- A frictionless contact interface is used. This includes a zero tension limit between surfaces. Where a girder flange is in contact with a connection seat it is assumed that any frictional resistance would be negligible compared to the potential displacement forces caused by the expansion of secondary beams.

B3.4 Time Scaling

To reduce the number of increments required by the analysis, the simulation time is changed from the time of the actual process. That is, the time period of the analysis is scaled.

This has the effect of reducing the computational cost by speeding up the simulation without affecting computational accuracy. The following time scaling definitions will be applied: -

- Non thermal loading – time/100
- Thermal loading – time/1000

The use of time scaling is applied in conjunction with mass scaling as defined in Section B3.5.

B3.5 Mass Scaling

Mass scaling is used throughout the analysis to scale the masses of a number of individual small elements that control the stable time increment. This allows the computational time and cost to be reduced. Mass scaling artificially increases the material densities within the finite element equation matrices of the model. It should be noted that while mass scaling will affect the inertia of the model it does not affect the gravity loading applied to the structure.

By scaling the masses of the smallest elements, the effect on the overall dynamic behaviour of the model will be negligible.

The following mass scaling definitions are used: -

- Semi-automatic mass scaling
- Applied throughout all steps
- Mass scaled to a target time increment of 0.00002
- Only scale element mass if the time increment is below the target time increment
- Potentially modify mass scaling at regular intervals through the analysis

The simulations have been monitored to ensure that any increased inertia force that may result from time scaling or mass scaling does not dominate the solution.

B4 Design Fires

The definition of the gas-phase temperature for the design fires was provided by Jose Torero in spreadsheet format on 5th March 2009 and is discussed in the report presented by Fred Mower.

B5 Heat Transfer

The definition of all steel and concrete temperatures was provided by Jose Torero in spreadsheet format.

The definition of temperature input into ABAQUS is described in the following sections for individual components of the structure that are being modelled.

B5.1 Beam and Girder Temperatures

Where beams and girders are modelled with beam elements or shell elements, different temperature-time curves can be applied at the top flange, bottom flange and the web, or alternatively a single temperature-time curve can be applied to the entire section based on the section factor of the beam.

Cross-sectional temperatures are taken as acting uniformly over the length of the beam or girder.

B5.2 Column Temperatures

Where columns are modelled with beam elements or shell elements, a uniform temperature is assumed to act over the cross-sectional area, and over the storey height of the column. Perimeter columns are heated on 3 sides. Internal heated columns are heated on 4 sides, except for column 73 which is located adjacent to the core and is only heated on 2 sides.

B5.3 Slab Temperatures

The 5.5" thick profiled composite concrete slab is modelled as an equivalent flat slab of depth 4" (102mm) (see Section B7.3.1).

The composite steel-concrete slab, modelled as shell elements is able to account for a temperature gradient over its depth.

Temperatures are applied at 5 points uniformly across the depth of the slab, as shown in Figure 138. The temperature distribution over the depth of the slab is assumed to act simultaneously over the slab area being heated.

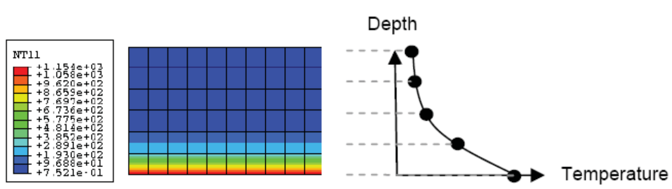

Figure 138: Temperature distribution through slab and allocation of 5 temperature points through the depth

Note: As the strength of the slab at elevated temperatures is largely attributed to the size and position of the reinforcement with respect to heating, the reinforcement in the proposed equivalent slab model is checked such that the thermal environment of the reinforcement will be similar to that of the reinforcement positioned in the actual trapezoidal profile. In this way, the temperature history of the reinforcement and effectively the performance of the slab at elevated temperatures will be more accurately represented. The 6/6 W1.4xW1.4 reinforcing mesh is located ¾" from the top surface of the slab (As per Drawing S24A from Cantor).

A comparison of the concrete temperatures based on temperature data by Jose Torero through the thinnest section of the profiled slab of 2.5" (63.5 mm) and the equivalent thickness slab of 4" (102mm), shows that the temperatures of the reinforcing steel in the thin section of the trapezoidal deck are under 300°C for the maximum heating condition. At temperatures under 300°C, the reinforcing mesh will not lose its strength (Refer to stress-strain curves shown in Figure 159). On this basis, it the reinforcing mesh in the equivalent flat slab is placed at the same position as that of the trapezoidal deck (i.e.: ¾" from the top surface).

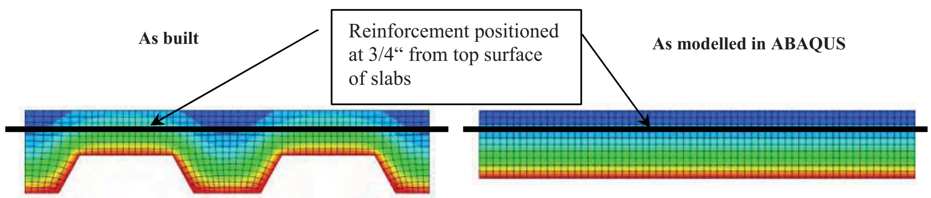

Figure 139: Positioning of reinforcement within an equivalent depth flat slab

B5.4 Connection Temperatures

B5.4.1 Simplified connections

Where connections are modelled using a simplified connection definition (see Section B1.3), the connection temperature are defined as being the average of the two structural members that it connects. Averaging the structural member temperatures gives a simplified, yet representative temperature definition for the entire connection.

B5.4.2 Detailed connections

Where connections are modelled explicitly in detail (see Section B1.3), the temperatures are specified directly to the plate components of the connections. A uniform temperature is applied to the plates of the detailed connections, based on Eurocode 3 **Error! Reference source not found.** Annex D, described below.

Knife Connections

- For the two knife connections modelled in detail (See Figure 140), the temperatures of the plates of the angles attached to the web of the girder are assumed to be the same as the temperature at the centreline of the connection which is represented as 0.88 x θ_{bf} (0.88 times the beam bottom flange temperature), as per Method 4 of Annex D of Eurocode 3 **Error! Reference source not found.**.
- The temperature of the angle plates attached to the face of the column is assumed to be the same as the temperature of the column, due to the degree of protection that would be present over the top of the angle.

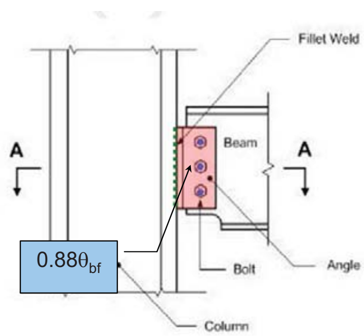

Figure 140: Temperature specification of the angles for the detailed knife connections.

Seated Connections

- For the two seated connections which are modelled in detail (Figure 141), the temperatures of the bottom plates of the connection are represented as 0.88 x θ_{bf} (0.88 times the beam bottom flange temperature), as per Method 4 of Annex D of Eurocode 3 **Error! Reference source not found.**.
- For the clip angles at the top of the girder the temperatures of the top clip angles are modelled as 0.5 x θ_{bf} (0.5 times the beam bottom flange temperature). Note that Eurocode 3 does not provide recommendations for connection elements which are located at the top of a beam and also embedded under a slab. A value of 0.5x θ_{bf} is used on the basis that the top clip is shielded from direct flame radiation and would be embedded within the slab and therefore is likely to be cooler compared with the fully exposed components of the connections..

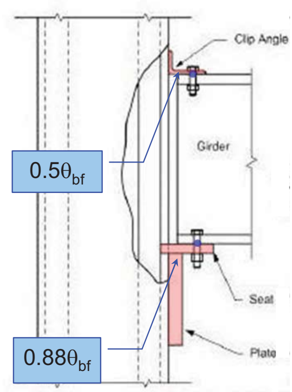

Figure 141: Temperature specification of the plates of the seated connections that will be modelled in detail.

The steel bolts of the detailed connections are defined as being the average of the two plate elements they connect.

B5.5 Shear Stud Temperatures

Where shear studs are modelled in detail in the north-eastern corner of the building (See Figure 134), they are modelled as simplified connections (see Section B7.1.2). Their temperatures are defined as being the average of the top flange beam temperatures and the temperature of the exposed surface of the slab to which they connect.

B5.6 Application of Temperatures to Structural Members

The fire step of the analysis in which the thermal loadings are applied are split into multiple sub-steps. For all structural components outlined above, temperatures are linearly ramped between these sub-steps.

The method of using sub-steps for the thermal loading is illustrated in Figure 142.

The time intervals of the steps are chosen such that peak temperatures of structural elements are included.

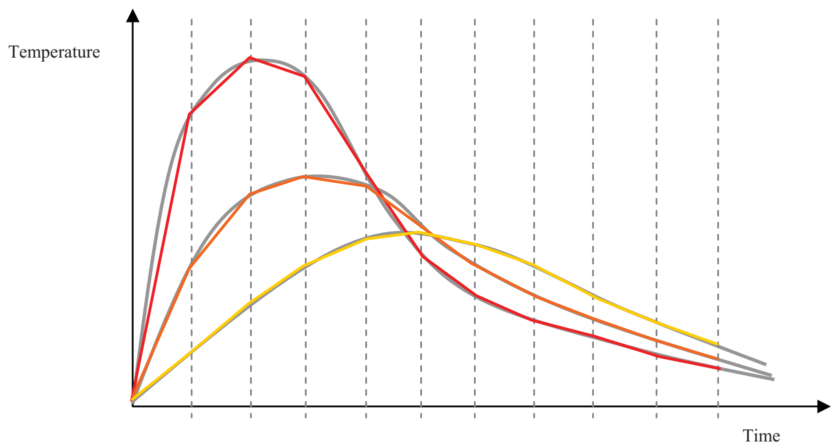

Figure 142: Illustration of approach to linearly ramp temperatures between sub-steps of the fire steps of the structural fire analyses

B6 Material Models

All material models allow for temperature dependant elastic and plastic behaviour and thermal expansion.

B6.1 Concrete

The compressive strength of all concrete is 4002 psi (27.6 MPa) at ambient temperature of 20°C .

B6.1.1 Stress-strain relationships

B6.1.1.1 Compression

BS EN 1992-1-2:2004 **Error! Reference source not found.** is used to define the compressive stress-strain relationships at varying temperatures.

The compressive stress-strain relationship is shown in Figure 143.

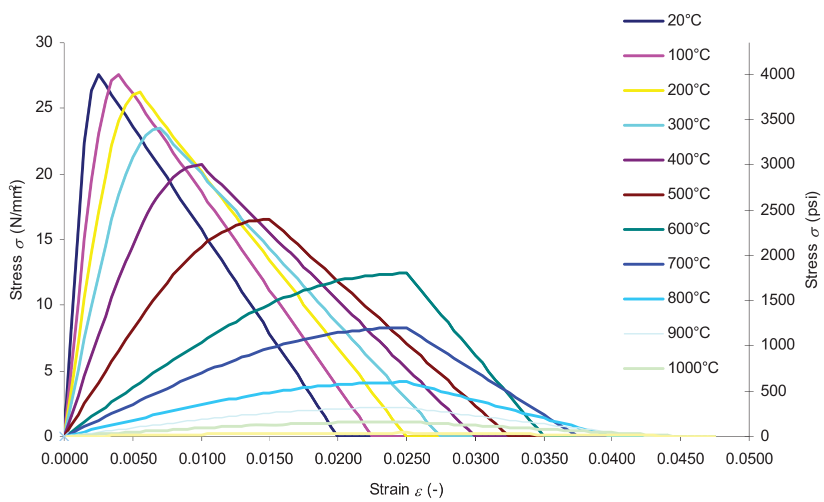

Figure 143: Compressive stress-strain relationship for concrete at high temperatures

B6.1.1.2 Tension

The tensile strength of concrete is poorly defined in BS EN 1992-1-2:2005 as it does not provide information on the corresponding strains or the ultimate strain of concrete in tension that should be used when modelling concrete stiffening.

Concrete tensile behaviour for the ABAQUS modelling is based on the method proposed by Rots *et al* (1984) **Error! Reference source not found.** which shows a bi-linear reduction in stress after cracking has occurred . This relationship is shown in Figure 144.

The work by Rots *et al*. **Error! Reference source not found.** also indicates that a simple linear reduction of stress with cracking strain does not allow computer models to accurately fit experimental data.

For the determination of the maximum tensile strength at elevated temperatures a linear degradation of the ambient tensile strength ($0.3321 f_t^{0.5}$ of the compressive strength) for temperatures ranging from 100°C to 600°C is assumed according to BS EN 1992-1-2:2004. The respective strain (ε_{cr}) is determined assuming the Young's Modulus for tension is equal to the Young's modulus in compression.

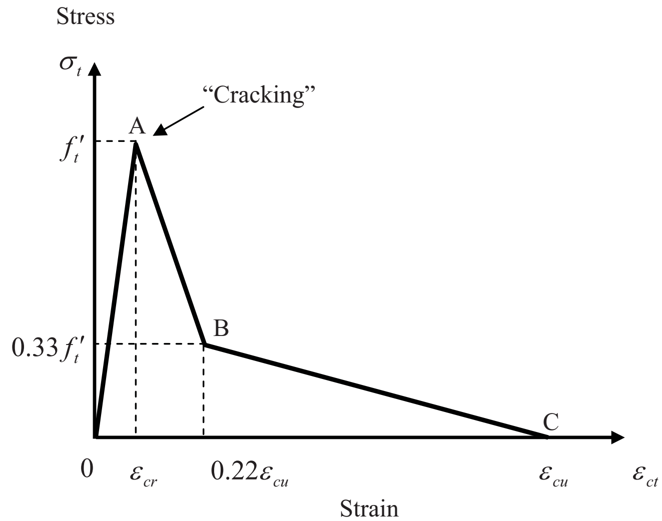

Figure 144: Tensile stress-strain relationship

One measure of how much tensile strain a unit area of concrete can withstand is the fracture energy. The CEB-FIP Model Code 1990 **Error! Reference source not found.** for concrete presents a method for calculating the fracture energy of concrete based on aggregate size and compressive strength. For concrete with a compressive strength of 4350 psi (30MPa) this gives a range of fracture energies from around 48 lbf.ft (65N/m) to around 70 lbf.ft (95N/m) with the lower end of the scale being appropriate for small aggregate sizes. Other research reported by Karihaloo *et al.* (2003) **Error! Reference source not found.** shows similar ranges.

To allow calculation of realistic ultimate tensile strains the following equation was used from Rots *et al*: -

$$\varepsilon_u = \frac{18}{5}\frac{G_f}{f_{ct}h}$$

where ε_u is the ultimate tensile strain, G_f is the fracture energy, f_{ct} is the tensile strength of concrete and h is the "crack bandwidth". This last term provides a characteristic length scale to the equation and in finite element models can be considered equivalent to the distance between integration points in an element.

Based on the CEB-FIP recommendations and the research reported in Karihaloo *et al.* (2003) a fracture energy of 60.5 lbf.ft (82N/m) was chosen as representative for the kind of concrete expected in WTC-7. As reduced integration elements are being used for the concrete slab in the models the distance between integration points is the same as the element size.

The proposed tensile stress-strain relationships for the ABAQUS modelling is shown in Figure 145.

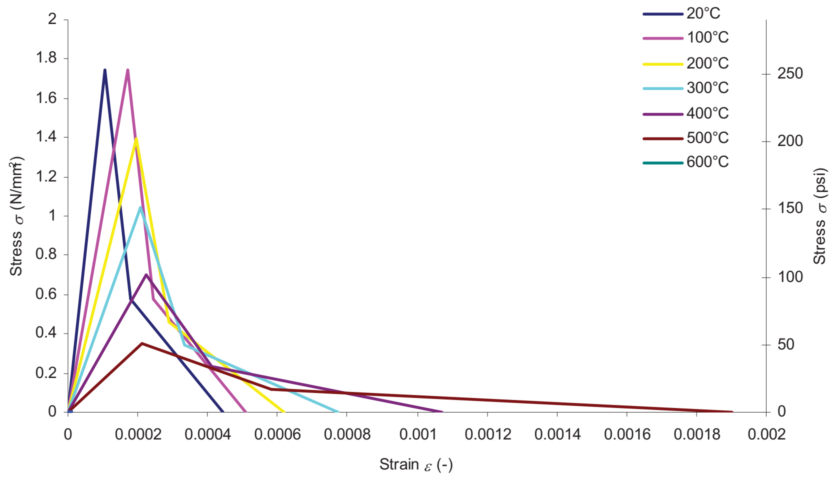

Figure 145: Tensile stress-strain relationship for concrete at elevated temperatures

B6.1.2 Biaxial Failure Envelope

An alternative biaxial concrete failure envelope, known as the ABAQUS Concrete Damaged Plasticity material model is used.

There are several material models available in ABAQUS to represent concrete. Two relevant models for this type of structural fire modelling are the Drucker Prager material model and the Concrete Damaged Plasticity model. The ABAQUS Concrete Damaged Plasticity material model is used due to the specific benefits as described below:

Drucker Prager

This method uses a group of equations to define a failure surface for the material. Originally used for soils it has been accepted as a reasonable match for other frictional solids such as concrete. This model allows various responses of such materials to be included, such as: pressure dependant yield, isotropic hardening/softening, dilation, creep and sensitivity to strain rate. In the ABAQUS program the user defines either the tensile OR the compressive stress-strain relationship for the material. The program then uses various parameters such as Frictional Coefficient and Dilation angle to extrapolate the full failure surface including the tensile or compressive part, depending on which was specified in the input parameters.

Arup has successfully used the Drucker Prager material model in projects before moving on to using the Concrete Damaged Plasticity material model in 2006.

However, previous experience indicates that the Drucker Prager material model is not as versatile for specifying detailed material behaviour, unique in terms of compression and in tension as the Concrete Damaged Plasticity material model. Based on the information given in the ABAQUS manual it is intended primarily for monotonic loading and only one behaviour (tensile OR compressive) may be defined, while the other is extrapolated. The Concrete Damaged Plasticity material model will benefit the analysis of WTC7 as it will allow for an increased level of accuracy of the concrete behaviour under tension in comparison to the Drucker Prager material model.

The Drucker Prager material model typically gives less satisfactory results when considering cyclic loading, i.e. when a cooling phase is considered.

Concrete Damaged Plasticity

This material model has been specifically designed for use with concrete. At its core the Damaged Plasticity material model incorporates a hyperbolic Drucker Prager yield condition and produces deviatoric and plane stress yield surfaces as indicated in Figure 146 and Figure 147.

Unlike the basic Drucker Prager model, the Damaged Plasticity material model allows the user to define both the compressive and the tensile inelastic behaviour of the material. Additionally the Damaged Plasticity model is designed for use in cyclic and dynamic loading, more closely matching the requirements for a structural fire analysis incorporating cooling phases.

The Concrete Damaged Plasticity model is used in the assessment of WTC7. Appropriate values are chosen for the inelastic behaviour based on the principles discussed in Section B6.1.1.

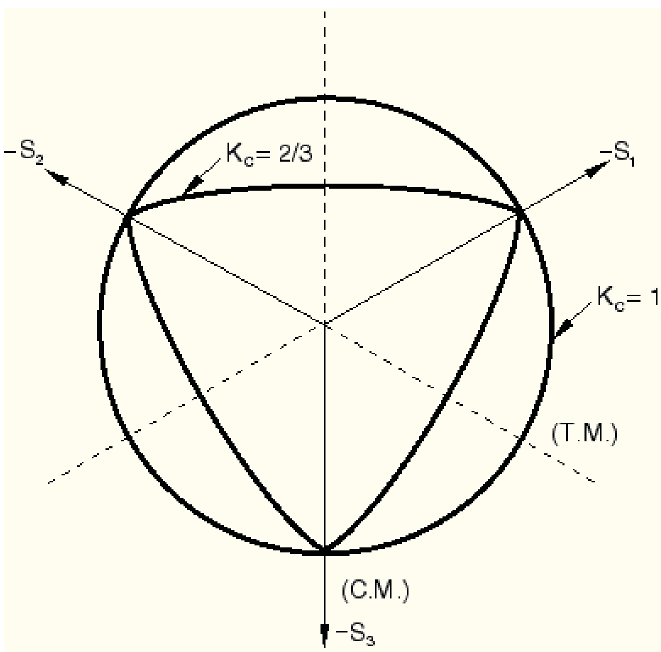

Figure 146: Damaged Plasticity model Yield Surface in Deviatoric Plane

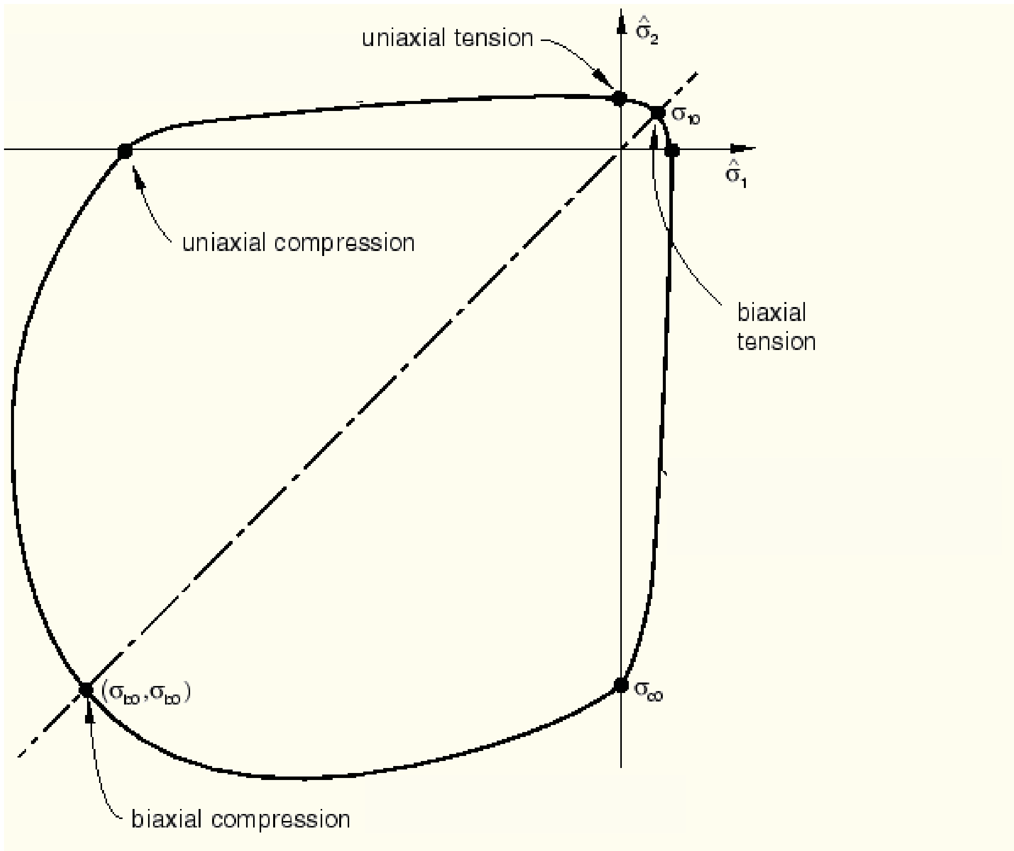

Figure 147: Damaged Plasticity Model Yield Surface in Plane Stress

B6.1.3 Density

No variation of concrete density with temperature is proposed for the ABAQUS structural fire modelling. The density of concrete is taken as 150 pcf (2400 kg/m^3) at ambient. A constant density in the concrete is proposed because the overall effect of using a varying concrete density is considered small on the structural fire behaviour, on the basis that:

- The effects of thermal curvature of the slab, strength reduction of the beams and slabs, and thermal restraint on the overall structural behaviour will overshadow any effects due to change in concrete density.
- The total change in density in the concrete is small. When the concrete slab is exposed to the highest temperature heating (i.e.: 800°C), the maximum temperature on the underside as evaluated by Jose Torero is 650^{o}C and the variation in density due to this temperature change is approximately 6%. This means that even if the entire section of the concrete is uniformly exposed to 650^{O}C, the concrete slab could lose up to 6% in weight. However, due to the steep non-linear thermal gradient across the depth of the concrete, only the bottom surface of the concrete would be exposed to very high temperatures (650^{o}C). The bottom surface would have a 6% change in density but the other areas of the concrete section would experience significantly less than 6% change in density.

B6.1.4 Poisson's Ratio

Poisson's Ratio is taken as 0.2 for all temperatures.

B6.1.5 Coefficient of Thermal Expansion

The variation of the concrete expansion coefficient with temperature is shown in Figure 148.

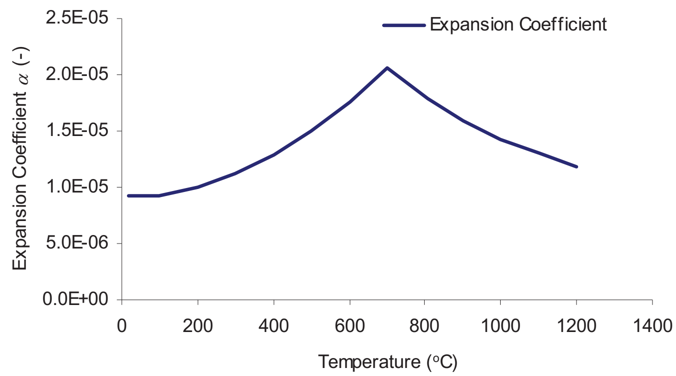

Figure 148: Concrete thermal expansion coefficient with temperature

B6.2 Steel beams, girders, columns and reinforcing plates

The following structural elements are assigned the associated Grades of steel: -

<u>A572 Grade 50 Structural Steel</u>

- All beams, girders and braces except W5x19 members, spandrel beams and wind girders
- Only columns labelled with a '#' on the column schedules in the structural drawings
- Column reinforcing plates for columns labelled with a '#' on the column schedules where the reinforcing plate thickness is greater than 2 in (50 mm) and less than 4 in (100 mm)
- Select plate girders as shown on the structural drawings

<u>Grade 36 Structural Steel (A36)</u>

- All columns and associated reinforcing cover plates except those labelled with a '#' on the column schedules in the structural drawings
- All column reinforcing plates with a thickness less than or equal to 2 in (50 mm)
- Select plate girders as shown on structural drawings

<u>A572 Grade 42 Structural Steel</u>

- Column reinforcing plates for columns labelled with a '#' on the column schedules where the reinforcing plate thickness is greater than 4 in (100mm)
- Select plate girders as shown on the structural drawings

B6.2.1 Stress-strain relationships

The stress strain relationships at varying temperatures are determined using BS EN 1993-1-2:2005 **Error! Reference source not found.**

The values of average yield strength and tensile strength are shown in

Table 9.

Table 9: Average yield and tensile strengths

	Grade 50 [1]	Grade 36 [1]	Grade 42 [1]
Average yield strength	59.9 ksi (413 MPa)	46.0 ksi (317 MPa)	50.5 ksi (348 MPa)
Average tensile strength	83.1 ksi (573 MPa)	73.3 ksi (505 MPa)	76.5 ksi (573 MPa)

[1] In accordance with the Average Material Test Report Data.

The stress-strain relationships for Grade 50, Grade 36 and Grade 42 steel are shown in Figure 149, Figure 150 and Figure 151 respectively.

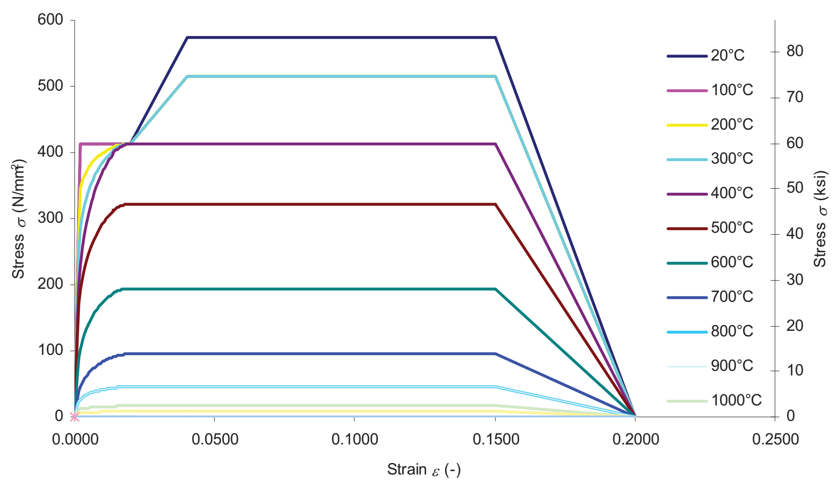

Figure 149: Stress-strain relationship for Grade 50 steel

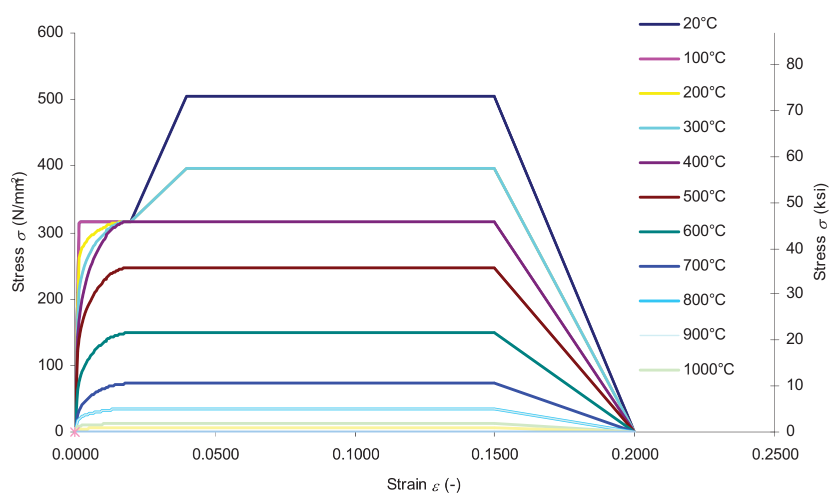

Figure 150: Stress-strain relationship for Grade 36 steel

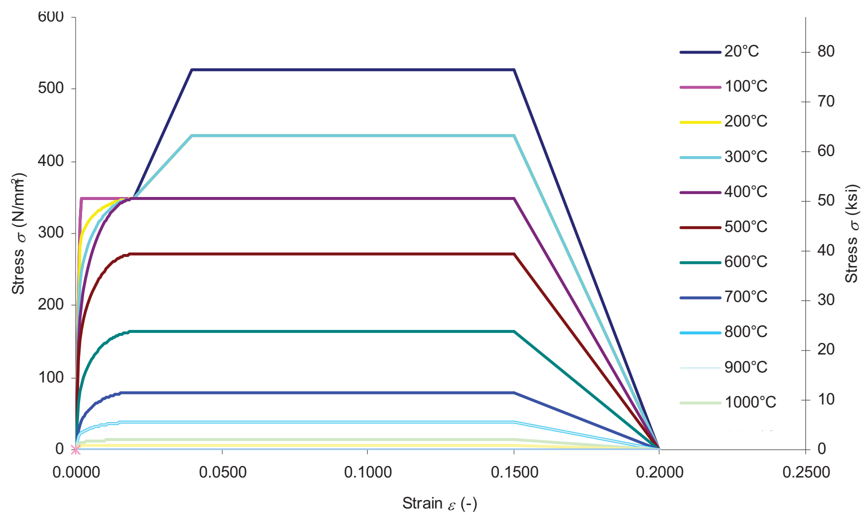

Figure 151: Stress-strain relationship for Grade 42 steel

B6.2.2 True stress-strain relationships

The stress-strain relationships defined in BS EN 1993-1-2:2005 **Error! Reference source not found.** are engineering stress-strain relationships.

The engineering stress-strain relationship does not give a true indication of the deformation characteristics of a metal because it is based entirely on the original dimensions of the specimen tested, and these dimensions can continuously change throughout the test. Ductile metal which is pulled in tension becomes unstable and necks down. Because the cross-sectional area of the specimen is decreased during the test, the load required to continue deformation is reduced. The stress based on the original area decreases, and this produces a fall-off in the stress-strain curve. The metal will actually continue to strain-harden up to the point of fracture, so the stress required to produce further deformation is increased. If the true stress, based on the cross-sectional area is used, it is found that stress-strain curve increases continuously up to fracture.

Conversion of engineering stress-strain relationships to true stress and strain (also called log strain) is required before inputting material properties within ABAQUS. For uni-axial stress-strain data, engineering stresses are converted to true stress–log strain by: -

Stress = $\sigma(1+\varepsilon)$

Log strain = $\ln(1+\varepsilon)$

Figure 152, Figure 153 and Figure 154 show the plastic region of the true stress-strain relationships for Grade 50, Grade 36 and Grade 42 steel respectively. It is these stress-strain relationships that are input into ABAQUS.

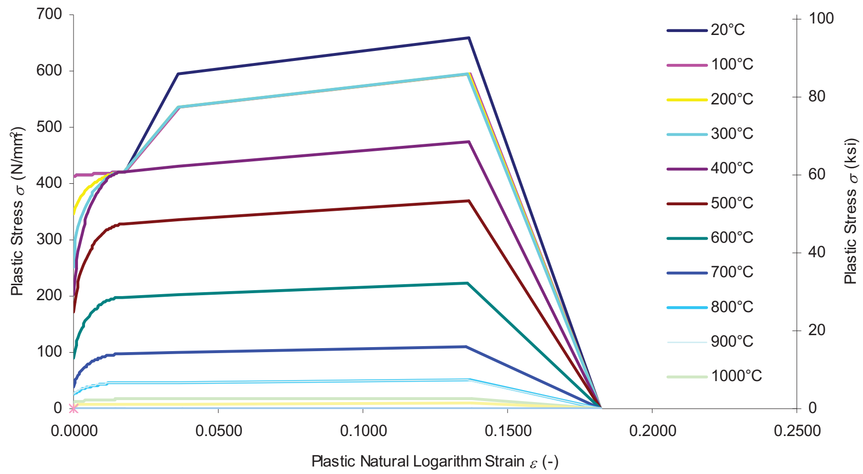

Figure 152: Plastic region of the true stress-strain relationship for Grade 50 steel

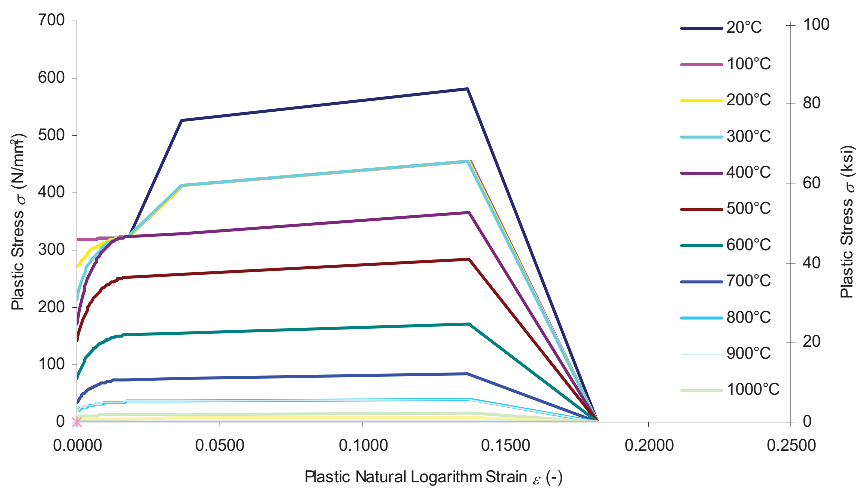

Figure 153: Plastic region of the true stress-strain relationship for Grade 36 steel

. 15/02/2010 12:45:00

JA-3266

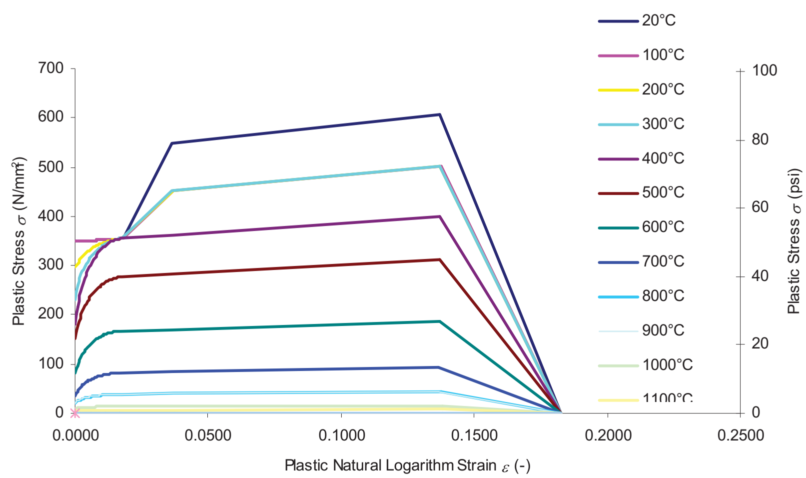

Figure 154: Plastic region of the true stress-strain relationship for Grade 42 steel

B6.2.3 Density

The density of steel is taken as a constant value of 490 pcf (7850 kg/m^3) at all temperatures.

B6.2.4 Poisson's Ratio

Poisson's Ratio is taken as 0.3 at all temperatures.

B6.2.5 Coefficient of Thermal Expansion

The coefficient of thermal expansion is shown in Figure 23.

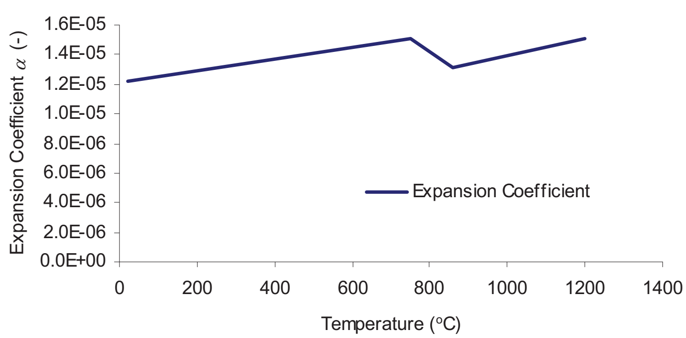

Figure 155: Coefficient of thermal expansion for steel

B6.3 Steel Connections

The connections around Column 79 and at Column 44 are included in the sub-model in a more detailed manner, to specifically investigate their performance in fire relating to a possible collapse trigger mechanism. These connections are modelled with individual plates as shell elements. In these areas (see Section B7.2) the plates use the material model for G40.21-44W type steel.

The stress-strain relationships at varying temperatures are determined using BS EN 1993-1-2:2005 **Error! Reference source not found.**.

The yield strength of G40.21-44W steel is taken as 49.6 ksi (342 MPa) and the tensile strength as 76.3 ksi (526 MPa). The stress-strain relationship is shown in Figure 156.

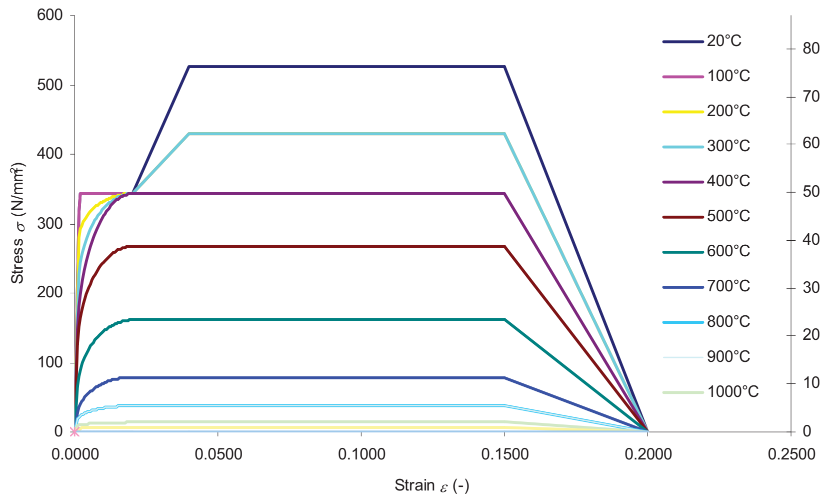

Figure 156: Stress-strain relationship for G40.21-44W steel

The engineering stress-strain relationship shown in Figure 156 is converted to true stress-strain relationships as defined in Section B6.2.2. These relationships, for the plastic region, are shown in Figure 157. This conversion is proposed as the various components of the connection will be explicitly included in the structural model. Therefore non-linear effects of necking will be incorporated.

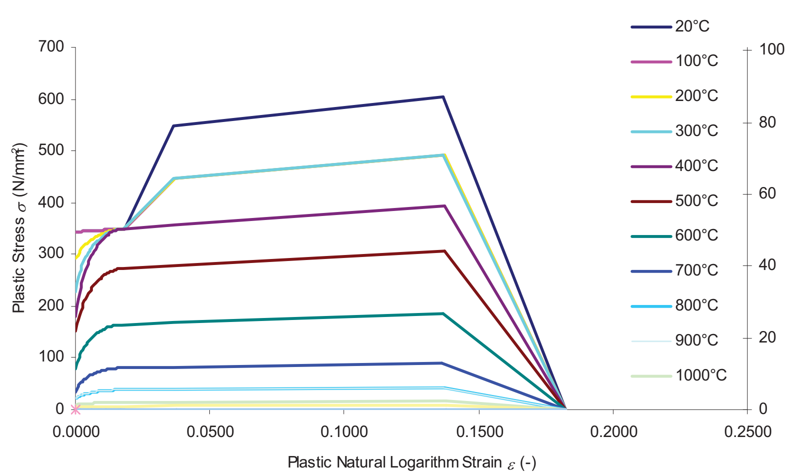

Figure 157: Plastic region of the true stress-strain relationship for G40.21-44W steel

Density, Poisson's Ratio and the coefficient of thermal expansion are taken as defined in Section B6.2.3, B6.2.4 and B6.2.5, respectively.

JA-3268

B6.4 Metal Deck

Where the metal deck is included in the model, the stress-strain relationships are based on BS EN 1993-1-2:2005 **Error! Reference source not found.** values. The Class N formulas have been used to calculate values at varying temperatures. As composite decking is typically a cold rolled product strain hardening has not been included, however temperature reduction factors have been used corresponding to hot rolled steel in tension.

The yield strength of the metal deck is taken as 33 ksi (228 MPa) and the tensile strength as 34.7 ksi (239 MPa) and the stress-strain relationship is shown in Figure 158.

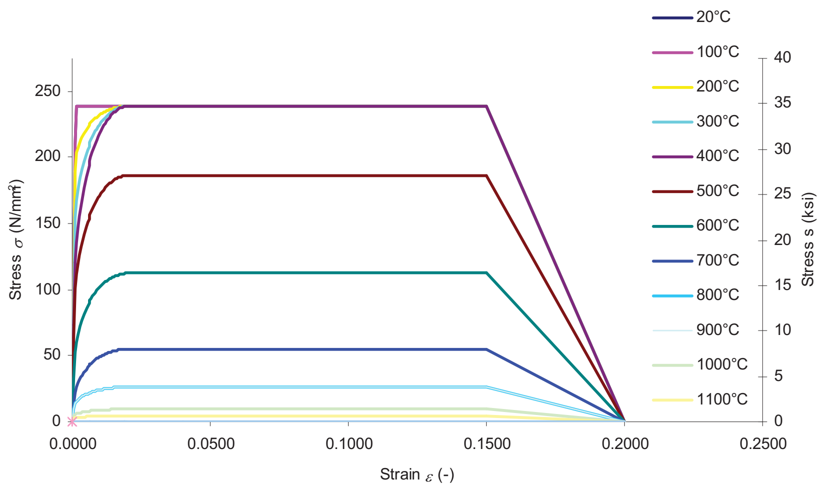

Figure 158: Stress-strain relationship of the metal deck

No conversion of the engineering stress-strain relationship to true stress-strain relationships is performed for the metal deck because ABAQUS does not determine the true area of the deck within a shell, but rather uses a smeared definition (see Section B7.3.1).

B6.4.1 Other temperature dependant steel properties

Density, Poisson's Ratio and the coefficient of thermal expansion are taken as defined in Section B6.2.3, B6.2.4 and B6.2.5 respectively.

B6.5 Plain Welded Wire Fabric Steel Reinforcement

The stress-strain relationships at varying temperatures for the plain welded wire fabric reinforcement (6/6 W1.4xW1.4) are determined using BS EN 1993-1-2:2005 **Error! Reference source not found.**.

The yield strength of the steel reinforcement is taken as 87.5 ksi (603 MPa) and the tensile strength as 100 ksi (689 MPa). The stress-strain relationship is shown in Figure 159.

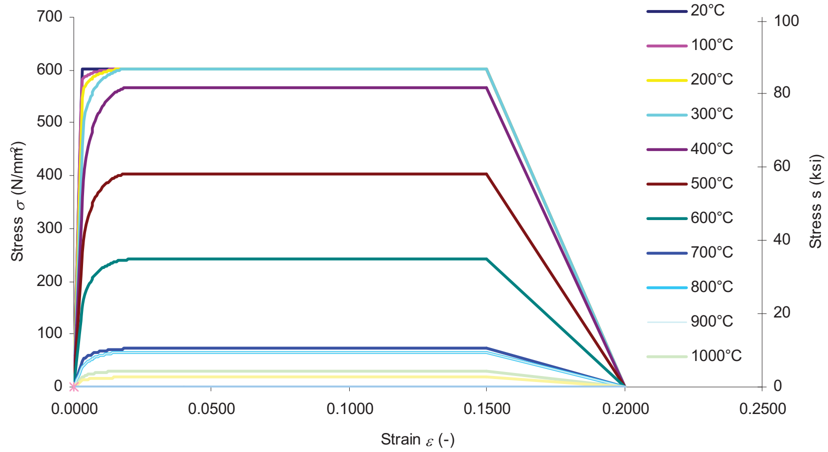

Figure 159: Stress-strain relationship of the plain welded wire fabric reinforcement

No conversion of the engineering stress-strain relationship to true stress-strain relationships is performed for the plain welded wire fabric reinforcement because ABAQUS does not determine the true area of the reinforcement bars within a shell element, but rather uses a smeared definition (see Section B7.3.2).

B6.5.1 Other temperature dependant steel properties

Density, Poisson's Ratio and the coefficient of thermal expansion are taken as defined in Section B6.2.3, B6.2.4 and B6.2.5 respectively.

B6.6 High Strength Steel Bolts

Where modelled in detail , the temperature dependant force capacities of the bolts are defined with associated strength reduction factors for bolts as defined in BS EN 1993-1-3: The strength reduction factors for the bolts are shown in Figure 160.

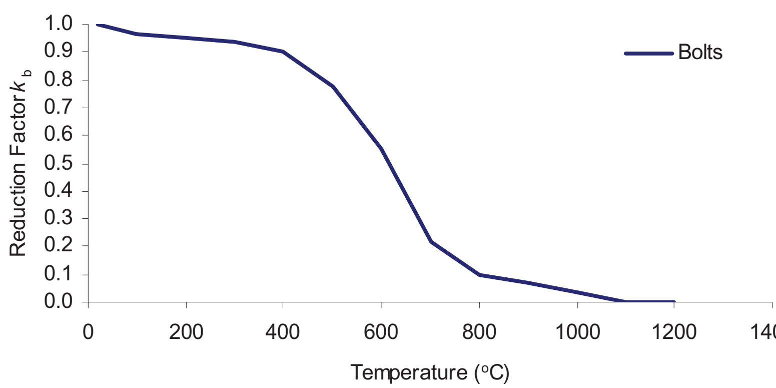

Figure 160: Strength reduction factors for bolts with temperature as per BS EN 1993-1-3:2005

B6.7 Shear Studs

The modelling of the shear studs in detail is described in Section B7.1.2. The ultimate strength of the shear studs is calculated based on the expected tensile strength of 97.5ksi (672MPa).

B6.8 Welds

Welds of connections between plates in the detailed model are modelled as rigid tie constraints without any temperature reduction of the weld strength (See Section B7.2.4). The strains of the plates around the welds have been monitored in the models.

B7 Specific Structural Aspects

B7.1 Composite and Non-Composite Action

B7.1.1 Tie Constraints

Where the slab is modelled with full composite action with the beam (See Figure 134), the composite action is incorporated between the slab and beams through the use of a TIE constraint. This links all translational and rotational degrees of freedom between the beam elements and the slab elements.

The use of TIE constraints means that temperature dependant properties and failure of shear studs are not modelled. This will maximise analysis efficiency and limit numerical issues in the model.

B7.1.2 Shear Studs

The shear studs for five of the composite beams (See Figure 134) on the north-eastern corner of the model are modelled explicitly. Additionally in accordance with the latest structural drawings explicit shear studs are provided between the slab and the three girders being modelled by shell elements (i.e. Girders 44-79, 76-79 and 79-80). The shear studs are 19mm diameter studs (based on Drawing S24A from Cantor) and are assumed to be uniformly spaced along the beams. The spacing is based on the number of connectors as indicated on Cantor Drawing S-8 Revision I dated October 1985.

1. Each shear stud is individually modelled as a 2-noded connector element which connects the beam and the slab. Shear force-slip capacities are specified to limit the horizontal shear forces that can be transferred between the beam and slab. The shear connectors are modelled so that the top and bottom connected nodes can move only in the horizontal plane relative to each other.

2. The shear stud behaviour is represented in the structural fire analysis as a series of force-displacement curves for movement in the horizontal plane, based on the model by Huang et al. **Error! Reference source not found.**. Huang's model specifies temperature dependant properties and shear stud breakage limits, based on elevated temperature tests by Kruppa et al.**Error! Reference source not found.** of 19mm shear studs. The model is shown in Figure 161.

3. For the structural fire modelling of the shear studs in ABAQUS, the shear studs are modelled to have a maximum slippage (horizontal movement) of 6mm, based on the maximum slippage proposed by Huang's model. When the shear studs reach a slippage limit of 6mm, the shear studs then break.

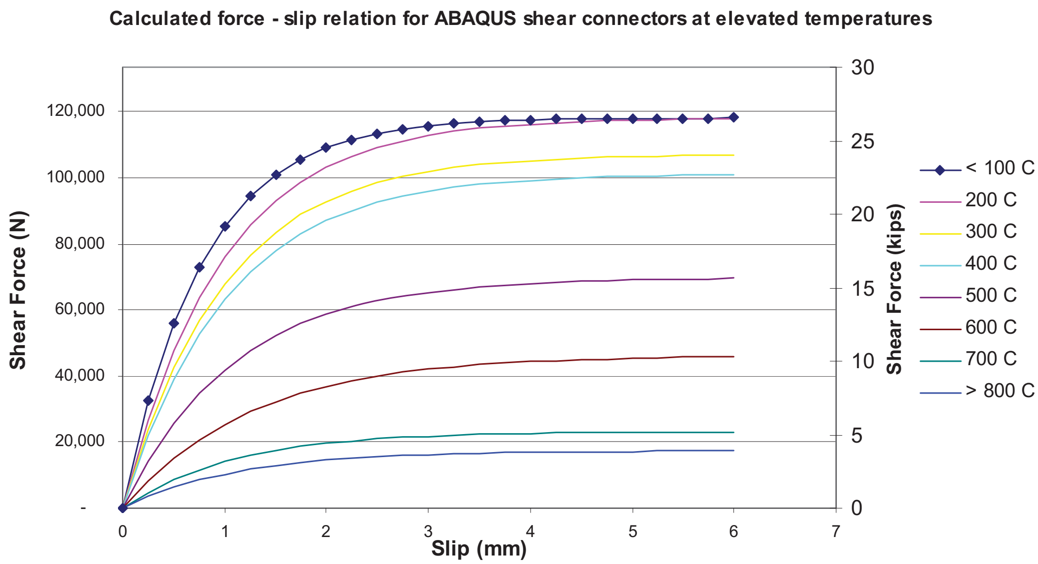

Figure 161: Force-slip relations for shear studs based on model proposed by Huang et al. Error! Reference source not found. **for 19mm shear studs.**

4. The shear stud capacities do not consider reduction in the capacities and limits as a result of two-directional loading in shear.

5. For the beams modelled with beam elements, the temperatures of the shear studs are calculated in ABAQUS as the average of the temperatures at the soffit of the slab and the top flange temperature of the beam.

6. For the girders modelled in detail with shell elements, the temperatures of the shear studs are calculated in ABAQUS as the average of the node at the soffit of the slab and the average of the top flange and the web temperatures.

B7.1.3 Contact Behaviour Between Beam/ Girder to Slab

The following two methods are used to represent the interaction between the slab and the beams or girders:

- The girders which are modelled in detail with shell elements have a contact algorithm between the top flange of the girder and the underside of the slab. The algorithm defines contact behaviour between the top of the girder and the underside of the slab when the girder touches the slab.

- Beams modelled with beam finite elements are provided with contact elements located at the top flange location. These contact elements are to simulate a realistic contact definition between the beam and the slab, which also provides some torsional restraint to the beam. An additional contact definition between the centroid of the beam element and the slab is also defined to prevent the beam from passing through the slab. This unrealistic mechanism has been observed in test models when the shear studs break and the beam twists.

B7.1.4 Beam-girder Interaction

For the detailed girders 44-79, 76-79 and 79-80 which support secondary beams on one side of each girder, Arup imposed a rotational limit to the ends of secondary beams to prevent unphysical "numerical" penetration of the girder web by the bottom flange of the secondary beam when the secondary beams rotate significantly, as indicated in Figure 162.

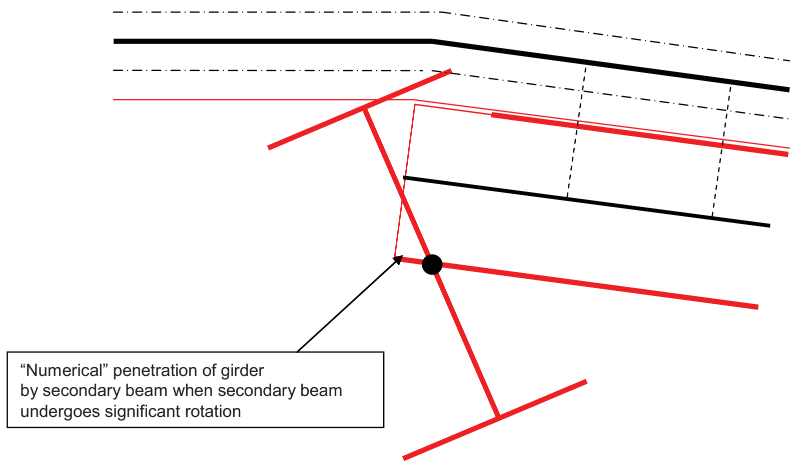

Figure 162: Unrealistic structural responses

A maximum rotational limit of 7° of the ends of the secondary beams has been implemented by Arup by linking the rotation of the two nodes involved in the connector element. This is to simulate a more realistic structural response so after 7° of relative rotation between the end of the secondary beam and the girder, the beam end cannot rotate any further due to either the top flange or the bottom flange of the secondary beam bearing against the web of the girder, preventing any further relative rotation. .

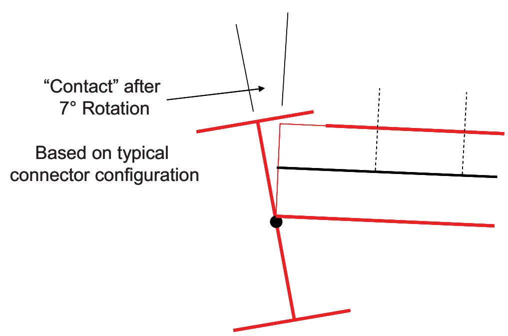

Figure 163: Application of girder rotation to prevent rotation of beams through depth of girder

The connector definition includes the following two phases in both directions of rotation:

- Rotation between from 0° to 7° under a low force
- A linearly increasing force up to a maximum of 8.9×10^6 kip-inch (1TNmm) at 8.5°

The 7° limit imposed by Arup was determined through a review of typical connector geometry from the connection drawings (Frankel 1985). The gradual linear increase in force up to 7° was defined in order to prevent potential numerical issues that might occur in the model. Due to the nature of computer models such numerical instability can potentially occur where sudden changes in force-displacement relationships are defined.

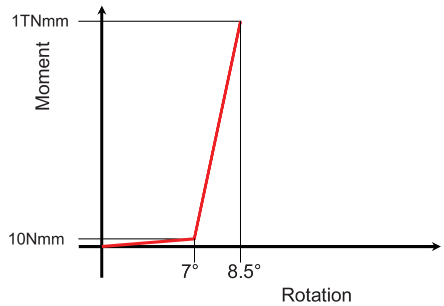

Figure 164: Moment- rotation limit applied at the end of the secondary beam connection

This rotational limit is modelled in ABAQUS to remain intact even if the connection between the beam and the girder fails in shear or axial directions. This is deemed appropriate as the secondary beam will still be held in place underneath the slab by the shear studs. This response has been observed from the Cardington tests (Figure 165), where the connections have clearly broken completely, but the secondary beams are still in place, providing torsional restraint to the girders. The secondary beams are supported by the shear studs attached to the slab as the beams are not heavy enough to break the shear stud though direct tension.

Figure 165: Secondary Beams held in place (Cardington Fire tests Error! Reference source not found.**)**

B7.2 Connections

B7.2.1 Simplified Connections

With the exception of the four connections modelled in detail (three at column 79 and one at column 44), all of the connections in the building are modelled using a 2-noded connector element native to ABAQUS with temperature-dependent capacity limits (in shear, tie and/or moment) and with prescribed displacement limits.

The capacity limits of the connections are calculated by Arup and presented in Section B9.2.

A representative diagram of proposed capacity-displacement characteristics to represent a simplified connector element is shown in Figure 166. This type of behaviour can be provided with temperature dependency and can be defined individually for different axes of motion.

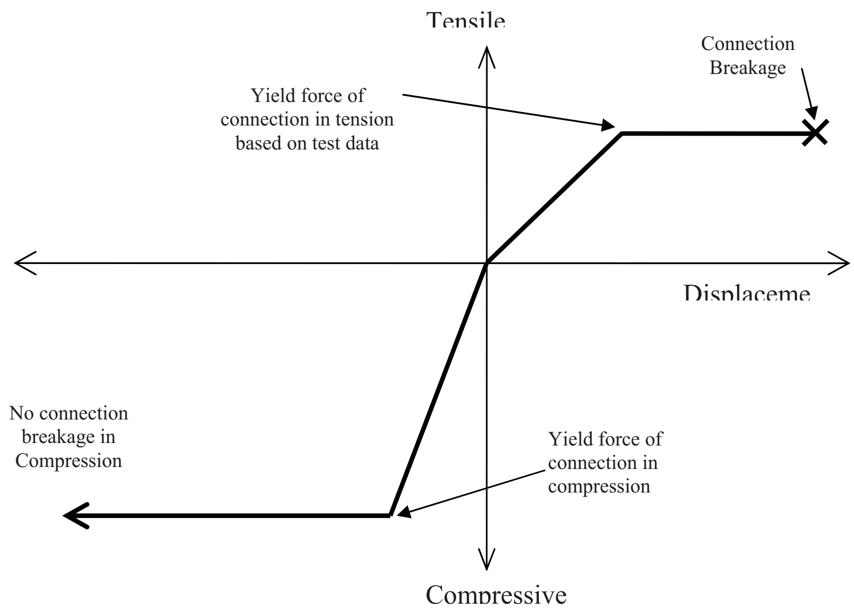

Figure 166: Representative simplified connection behaviour

To represent the reduction of the capacity of the simplified connections in shear, tension, compression and moment at elevated temperatures, the strength reduction factors of Eurocode 3 for bolts is applied to the ambient capacity values.

B7.2.2 Detailed seated connections

There are two seated connections modelled in detail. The plate components forming these connections are modelled using shell elements. A schematic of a seated connection is shown in Figure 167. This diagram indicates which components of the connection that are modelled, using shell elements and where simplified connection elements are used.

- The clip angle, the plate and the seat are all modelled using shell elements.
- Bolts between the top flange and the clip and between the seat and the bottom flange are defined using a simplified connector element (see Section B7.2.1) using an ABAQUS element type CONN3D2 (See Section B3.2.3). The bolts are represented with shear and tie capacities.
- Contact between all appropriate surfaces is defined (see Section B3.3).

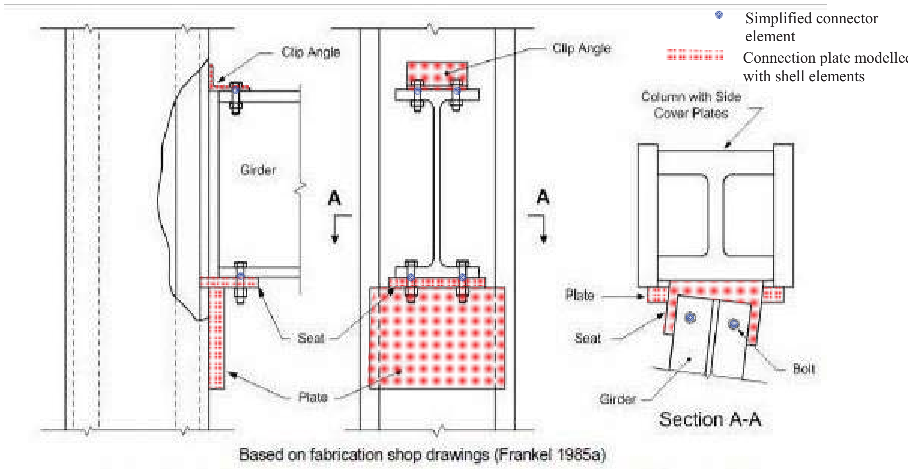

Figure 167: Schematic drawing of the seated connection at Column 79 identifying where shells and simplified connection elements will be used

B7.2.3 Knife connection

There are two knife connections modelled in detail. A schematic of a knife connection is shown in Figure 168. This diagram indicates which components of the connection are modelled using shells, where simplified bolt connection elements are used and where a fillet weld exists (note that the fillet weld will not be explicitly modelled to allow for deformation of the welds. See Section B7.2.4).

- The angles are both modelled as shell elements
- The angles are tied only where their edge meets the column (as shown in Figure 168)
- The bolts between the web and the flange are modelled as simplified connector elements (see Section B7.2.1)
- Contact between all appropriate surfaces is defined (see Section B3.3)

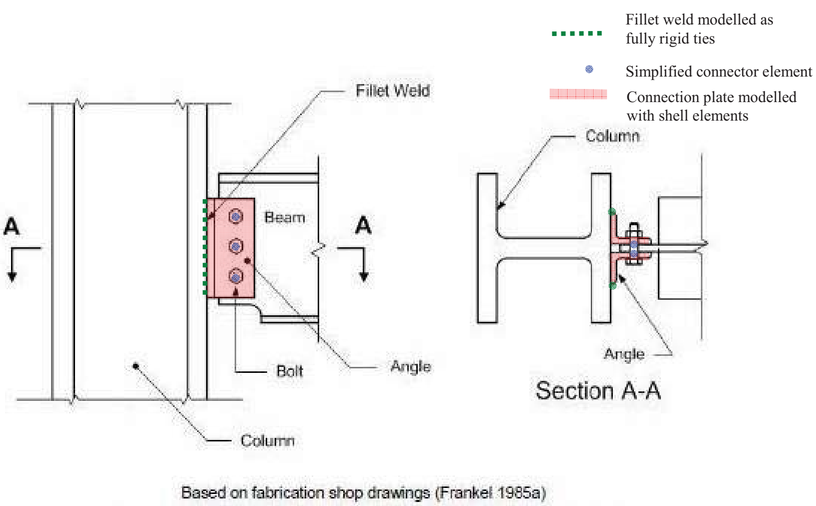

Figure 168: Schematic drawing of the knife connection at Column 79 identifying where shells and simplified connection elements will be used

B7.2.4 Welds

There are four connections (two seated and two knife) which are modelled in detail. The welds of these connections are modelled, unlike all the simple connections, as perfectly rigid links with no temperature dependency. Failure of the connection will therefore be captured in failure of plate materials and/or bolts only and deformation and tearing of the welds is not modelled.

The stresses of the steel plates are to be monitored to see if the stresses could potentially lead to a failure of the welds and the knife connection.

B7.2.5 Puddle Welds

It is understood that the composite deck in WTC7 was connected to beams using puddle welds. The puddle welds are provided in the real building to attach the metal deck to the beams prior to concrete being poured These welds are not modelled in the structural fire sub-model as the puddle welds are considered not to provide significant contribution to the composite action between the slabs and the beams in the fire case.

B7.3 Floor Structure

B7.3.1 Composite floor

The 5.5” thick floor slab in WTC7 was constructed using 3” deep trapezoidal profiled decking. For modelling purposes (heat transfer and structural response) this is modelled as a flat slab of equivalent thickness in all models. The equivalent thickness of 4” (102mm) is calculated using the method presented in Appendix D of BS EN 1994-1-2:2005 **Error! Reference source not found.** and is shown in Figure 170. The slab is modelled with shell finite elements.

The residual strength of the profiled deck is included in all models in the manner described in Section B7.3.3. Any spalling of the concrete above the steel deck is not considered.

Figure 169 shows the geometrical placement of the beams and slab elements with respect to each other for the as-built condition and as defined in ABAQUS. Also shown are the positions of the beam and slab elements that comprise the composite floor.

The beam node is positioned at the centroid of the beam cross section. The concrete shell element and its node are positioned at the mid-depth of the equivalent slab thickness. An offset between the beam and slab elements is provided that accounts for the original depth of the profiled concrete slab. This offset, which is the distance between the top of the beam and the underside of the slab, is calculated as: -

$$(3''+2.5'')-\left(\frac{4''}{2}\right)=3.5''\,(89\text{mm})$$

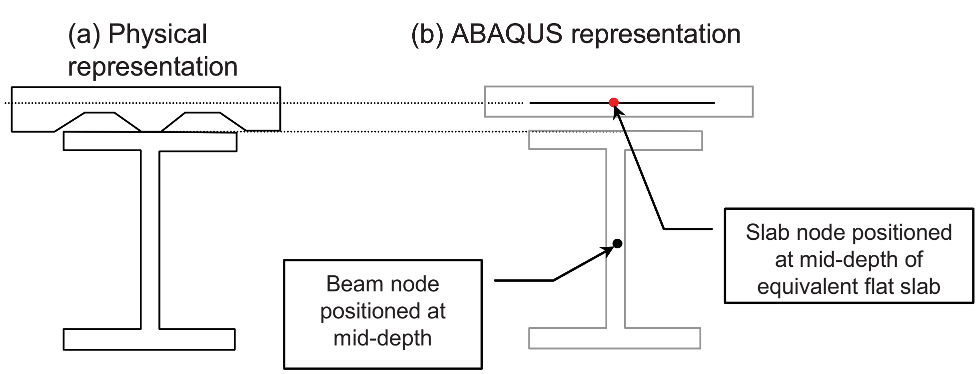

Figure 169: Slab and beam geometrical placement for (a) physical representation (b) as represented in ABAQUS using shell and beam structural elements

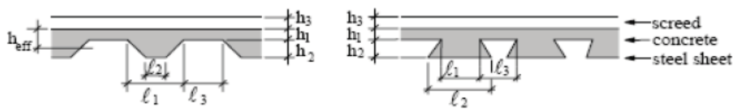

Figure 4.1: Symbols for trapezoidal sheeting **Figure 4.2: Symbols for re-entrant sheeting**

(1) The effective h_{eff} is given by the formula:

$$h_{eff} = h_1 + 0,5\, h_2 \left(\frac{\ell_1+\ell_2}{\ell_1+\ell_3}\right) \quad \text{for } h_2/h_1 \le 1,5 \text{ and } h_1 > 40 \text{ mm} \qquad \text{(D.15a)}$$

$$h_{eff} = h_1 \left[1 + 0,75 \left(\frac{\ell_1+\ell_2}{\ell_1+\ell_3}\right)\right] \quad \text{for } h_2/h_1 > 1,5 \text{ and } h_1 > 40 \text{ mm} \qquad \text{(D.15b)}$$

The cross sectional dimensions of the slab h_1, h_2, ℓ_1, ℓ_2 and ℓ_3 are given in Figures 4.1 and 4.2.

(2) If $\ell_3 > 2\,\ell_1$, the effective thickness may be taken equal to h_1.

Trapezoidal

l_1 =	184.0	mm	7.25"
l_2 =	120.7	mm	4.75"
l_3 =	120.7	mm	4.75"
h_1 =	63.5	mm	2.5"
h_2 =	76.2	mm	3"
h_3 =	0.0	mm	0"

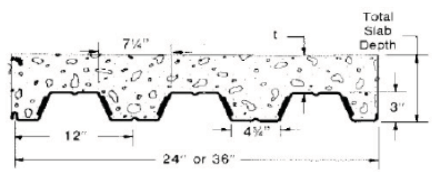

Floors 8 - 14	3" deep 20 gauge composite metal deck + 2.5" normal weight concrete
Floor 7	3" deep 18 gauge composite metal deck + 5" normal weight concrete
Floor 6	3" deep 20 gauge composite metal deck + 3" normal weight concrete
Floor 5	3" deep 18 gauge composite metal deck + 11" normal weight concrete

h_2/h_1 =	1.20
h_1 =	63.5 mm
$2l_1$ =	368 mm
(D.15a) h_{eff} =	102 mm
(D.15b) h_{eff} =	111 mm

h_{eff} = 102 mm 4"

Figure 170: Calculation of effective thickness of flat slab in accordance with BS EN 1994-1-2:2005

B7.3.2 Reinforcement

Slab reinforcement is modelled in the shell elements in ABAQUS as a smeared layer of steel. Reinforcement material properties are considered in accordance with Section B6.5 above.

Refer to Section B5.3 for a description of the location of the reinforcement within the depth of the equivalent depth concrete slab.

Reinforcement is included in the model as 6/6 W1.4xW1.4 welded wire fabric in accordance with drawing S-24A from Cantor.

B7.3.3 Metal deck

When considering composite steel framed structures under fire loading, the strength and stiffness contribution of the unprotected metal decking is normally not modelled in a numerical analysis as a conservative measure. This is because the metal deck is subjected

JA-3278

to extremely high temperatures over a short period of time and would have provided very little inherent strength and stiffness contribution to the overall slab.

However, in the case of WTC7, it is understood that the underside of the floor slab has been protected using spray applied cementitious material. Therefore, the metal deck may provide some additional strength and stiffness contribution to the behaviour the floor system.

Therefore, the metal deck is represented as a layer of steel reinforcement placed at the underside of the concrete slab, with the steel area equivalent to that of the cross sectional area of the steel decking. .

To account for the orthotropic nature of the steel decking (where the stiffness of the deck in one direction is greater than the other perpendicular direction), the model includes an additional layer of reinforcement to represent a flat sheet of steel in the strong direction. It is not proposed to model the shape of the troughs of the steel decking.

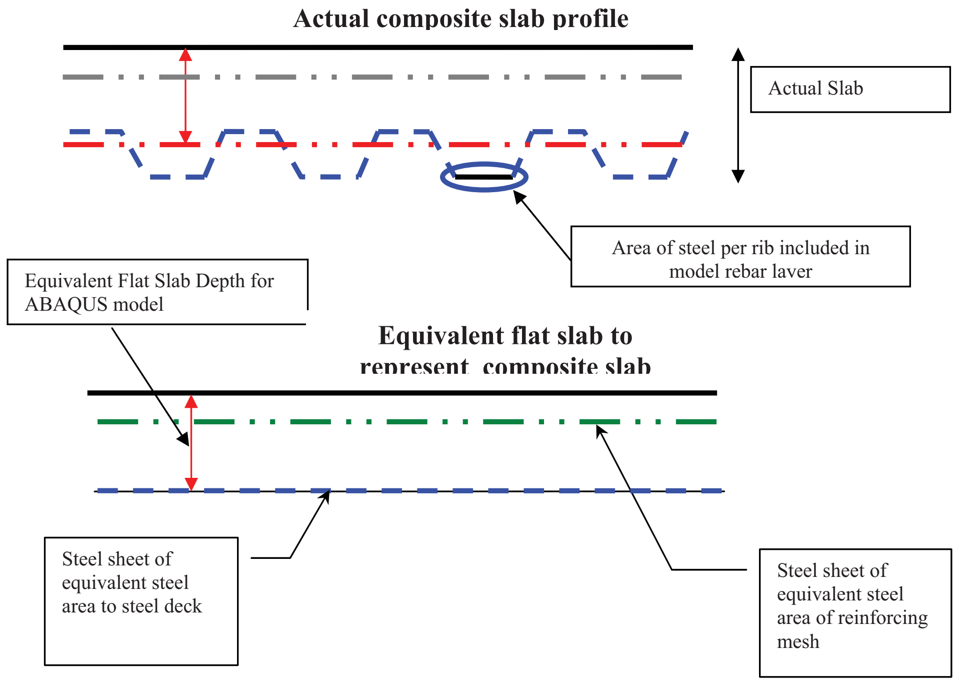

Figure 171: Method for including composite deck strength

B7.3.4 Trench Headers

The trench headers are represented in ABAQUS as holes in the slab at the location of the trenches. Each trench is approximately 3' wide, representing the gap between the edges of the beam flanges at the edge of the trench.

- In reality the trench would retain the metal deck, however this has been disregarded in the ABAQUS sub-model as it is considered that the small section of heated metal deck would not provide significant strength or stiffness to the slab, at elevated temperatures.
- The presence of the trench header is not considered to significantly affect heat transfer or member temperatures in the model zone. It is understood that where

trench headers are in place, additional fire protection material was provided to maintain floor to floor compartmentation. This additional protection, combined with the shielding effect of the composite deck, will prevent significant additional heat from passing into the floor slab. The trench headers do not in any way affect the heat being transferred into the steel beams.

B7.4 Web Openings in Beams and Girders

The effects of web openings are not included in the beams which will be modelled with beam finite elements.

Web openings are included in the detailed sub-model in the girders constructed with shell elements. These occur on the girder between Column 79 and Column 44 and on the girder between Column 79 and Column 76. The locations of openings and any associated stiffener plates are incorporated into the sub-model based on the drawings from Cantor.

B7.5 Column Splices

The column splices are not modelled in detail. Therefore, the columns are modelled as fully continuous across the splice. The column splices are treated as full moment connections.

B8 Loads

B8.1 Dead Load

Dead loads include the weight of steel and concrete of the structural elements. The weights are determined automatically by ABAQUS based on the material densities provided in Section B6.

B8.2 Superimposed Dead Loads

Superimposed dead loads include fill, finish, roof, ceiling, ductwork, partitions, flooring, beam encasement and fire proofing.

- Floor 13: superimposed dead load = 18.5 psf (0.88 kN/m^2).

B8.3 Curtain Wall Superimposed Dead Load

The curtain wall system consists of 1 in (25 mm) thick glass and granite.

- Curtain wall superimposed dead load (North and South facades) = 25 psf (1.2 kN/m^2)
- Curtain wall superimposed dead load (East and West facades) = 30 psf (1.44 kN/m^2)

The curtain wall superimposed dead load is transformed to an equivalent line load along the edge beams by accounting for the floor to floor height of the curtain wall.

B8.4 Live Loads

The Floor 13 design live load is 50 psf (2.39 kN/m^2), except in the Fan Room where is it is increased to 75psf (3.59kPa). The extent of the Fan Room is shown in Figure 172.

Figure 172: Extent of the fan room

Note that the design live load is factored to account for the load combination described in Section B8.8.

B8.5 Column Loads

Axial point loads due to the upper floors (Floors 14 and above) acting on the tops of the columns are required to simulate the upper portion of the building not explicitly modelled. Axial point loads are acting on the top of all columns at the location of Floor 14. Final axial loads received from GNA on the 20th April 09 are used as the inputs for the sub-model.

These loads are factored to account for the load combination described in Section B8.8.

Where shells are used to represent columns (see Section B1.3), the axial load is transformed into an equivalent line load acting on the flanges and web of the column.

B8.6 Thermal Loads

Ambient temperature is defined as 20°C.

Thermal loads applied to the steel and concrete in the structural fire analyses are determined from thermal analyses for various fire protection and ambient gas temperature scenarios.

The definition of the temperature-time curves for the structural elements is described in Section B5.

B8.7 Other Loads

No wind, snow or seismic loads are applied in the structural analyses

B8.8 Load Combinations

The following load combination was used: -

100% Dead Load + 100% Superimposed Dead Load + 25% Design Live Load

B9 Connection Modelling

B9.1 Connector definitions

Arup have collated information about the connection details (Frankel 1985 drawings) for the area of the 13th floor sub-model and identified the following connection details in this area:

- There are 268 connections in total
- Of the 268 connections, there are 9 basic connection types identified as follows:
  - Shear connections
    1. Fin plate
    2. Header
    3. Knife
    4. SWC (seated with web clip)
    5. STP (seated with plate on top flange)
    6. STC (seated with top clip)
    7. Single angle
  - Fully restrained (FR) moment connections
    8. North and South wall winder girder to column
    9. East wall winder girder moment splice

B9.2 General Approach to Connection Modelling

This section describes the general approach for the two connection models applied to the 13th floor structural fire sub-model.

	Detailed Connection Model	Simplified Connection Model
	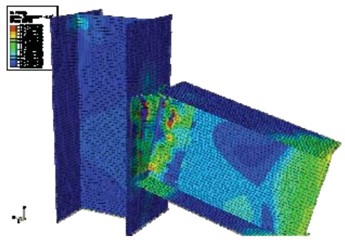	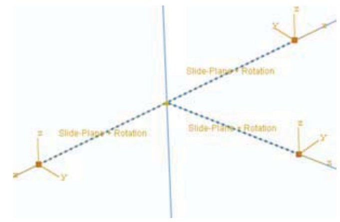
Location of the connections	Four (4) connections have been identified as requiring detailed study. These are as follows: • All beam-column connections around Column 79 (2 knife connections and 1 Seated Top Clip (STC) connection), and • One beam-column connection (Seated Top Plate - STP) on Column 44	All other connections (264) in the sub-model are represented with the simplified connection model
Description of the connection model	Each component of the connection is modelled in detail. This is achieved in the 3D model using the following element types: **Shell elements** – to represent the connecting elements, plates, clips, seats, etc. **User defined tie elements** – to represent the bolts. **Rigid tie elements –** to represent the welds.	For the simplified connections, each component of the connection is not modelled explicitly. Instead, the connection behaviour is defined by user-defined force-deformation curves for each of the different actions on the connections that are expected in a fire situation (i.e. shear, tension, compression and/or moment). As such, this is achieved in the 3D model using a two-noded connector element to represent the connection as a single lumped component.
Ambient capacities	This is captured explicitly by the ABAQUS Model	For each of the connection types in the building, their capacities have been calculated based on standard "ambient" design practise in the U.S using the latest LRFD manual (AISC 13th Edition). Additional checks for tension, but not for compression, are also included. In addition to determining the ultimate strength of the connections in ambient, these capacity

		calculations also identify the governing failure mode for each connection type and under each action (e.g. shear, tension, etc) at ambient conditions. Common failure modes include weld failure, bolt failure (shear), plate rupture, block shear failure, prying action, etc. These failure modes are used to identify the deformation limits in ambient and fire conditions. Arup proposed not to specify a capacity limit in compression on the basis of the observations of latest fire research (Cardington tests, Sheffield tests) and the general performance of whole steel frame systems in fire, which have shown that compression failures of connections have generally not been observed. Note: Material strength reduction factors are not be applied in assessing the ambient inherent capacities of the connections. This has been agreed with Colin Bailey in a meeting dated 8 April 2009, as this is common practice for determining failure capacities in ambient and fire conditions.
Temperature Dependent Material Properties	The bolt elements are modelled using the material properties of the bolts of Eurocode 3 **Error! Reference source not found.** and the plates of the connections are modelled using the structural steel properties of Eurocode 3 **Error! Reference source not found.**.	To represent the reduction of the capacity in shear, tension, compression and moment at elevated temperatures, the strength reduction factors of Eurocode 3 for bolts are applied to the ambient capacity values. This has been discussed and agreed between Arup and Colin Bailey in a phone conversation on 31st March 09 and meeting on 8th April 09. The Eurocode 3 reduction factors for bolts are proposed to be used because they have a higher rate of strength reduction with temperature compared with the structural steel plates and welds.
Connection deformation and failure	Deformation of each part of the connection is captured in detail. However, as the bolts are modelled with user defined connector	Failure and deformation of the connection is based on the ambient governing failure mode for each action (shear, tension and moment,

	elements, deformation and breakage limits of the bolts are still estimated. See following section for deformation and breakage limits (Section B9.3.1). The welds are are modelled using rigid links. Refer to Section B9.3.5. The approach was discussed and agreed with Colin Bailey in a meeting dated 8 April 2009.	where applicable). It is assumed that the ambient failure mode also applies for the fire condition. See following section for proposed deformation and breakage limits (Section B9.4.2).

B9.3 Detailed Connection Modelling

As described in the modelling assumptions, the detailed connections are modelled with:

- ***Shell elements*** – to model the plates, clips, seats, cover plates, etc.
- ***User-defined connector elements*** – to model the bolts
- ***Rigid links*** – to model the welds

Each of these element types are defined by separate deformation and breakage limits, which are presented in more detail below.

B9.3.1 Deformation Limit for Shell elements

For the detailed connections, the plates, clips, seats, and other connecting elements are modelled with shell elements. The deformation and breakage limits are captured explicitly in the ABAQUS analysis based on the stress-strain curves for the steel material model per Eurocode 3 **Error! Reference source not found.** (See Figure 173). That is, the deformation limit and breakage limit have been defined at 15% of the engineering strains (Note that this equates to a slightly lower strain value when converted to the true strains, as shown in Figure 173).

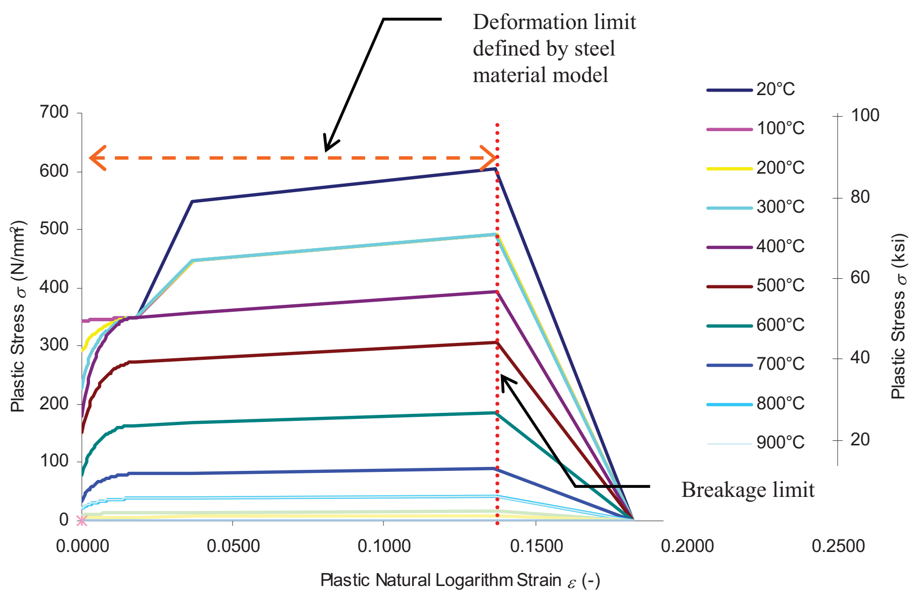

Figure 173 - Deformation and Breakage Limits for Shell Elements in Detailed connection model

Note: In the ABAQUS model, a damage initiation feature is applied to the steel shell elements which physically allow the connection to rupture or break once the strain reaches the peak strain.

B9.3.2 Deformation Limit for Bolts

The bolts in the detailed connections are modelled with tie elements with user-defined force-deformation relationships to describe the bolts' shear behaviour in ambient and in fire conditions. Note that the tension, compression and moment characteristics are not defined as the bolts in the detailed connections are assumed to be dominated by shear.

B9.3.3 Bolts acting in single shear

The bolts at the seated connections (modelled in detail) at the end of the girder between Column 79 and Column 44 act in single shear. Figure 174 and Figure 175 illustrates the shear deformation and breakage limits for the bolts in ambient and fire conditions. The shear deformation limit at ambient conditions is 0.2 inch and is based on typical tests of A325 bolts as described in Kulak et al, 1987 **Error! Reference source not found.**.

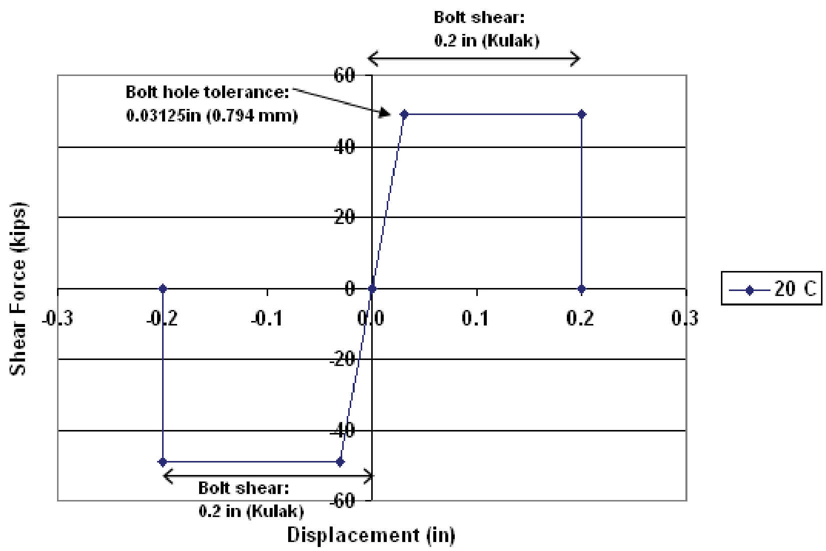

Figure 174 - A325 bolt shear force deformation curve (ambient)

For fire conditions, the deformation limit for the bolts acting in single shear is equal to that defined for ambient conditions (0.2 inch) as shown in Figure 174, as limited test data is available to justify an increased ductility limit in fire conditions (British Steel, 1992 **Error! Reference source not found.**). That is, no increase in ductility of the bolt is considered at elevated temperatures.

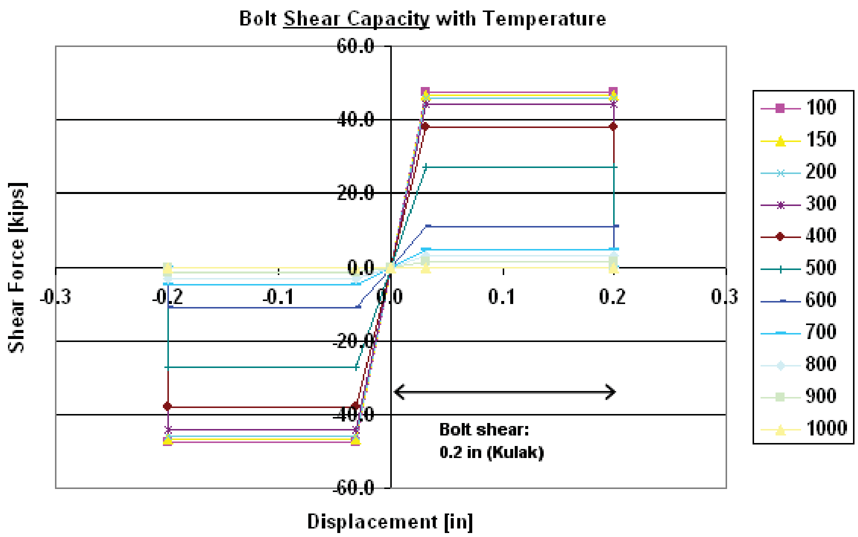

Figure 175 - A325 bolt shear force deformation curves (fire)

B9.3.4 Bolts acting in double shear

The bolts of the two knife connections (modelled in detail) at Column 79 act in double shear. These are modelled in the same way as bolts in single shear but have an increased breakage limit at elevated temperatures of 0.9 inch.

B9.3.5 Deformation Limit for Welds

The welds in the detailed connections are modelled using rigid links without any temperature reduction for the welds. This assumes that the welds are not the governing failure mode in ambient or fire conditions.

Although the behaviour of the welds are not modelled explicitly, their response will be monitored through other indicators in the model such as the localised stresses and strains in the surrounding steel elements.

B9.4 Simplified Connection Modelling

Other than the 4 connections that are modelled in detailed around Column 79 and Column 44, the other remaining connections in the 13th floor structural fire sub-model are described using the simplified connection model.

B9.4.1 General description

- The simplified connection model consists of a set of user-defined force-deformation curves for each connection type in ambient and fire conditions for shear, axial, and moment force (where applicable).
- Each connection type has individual characteristics to define the force-deformation of the connection under each action (shear, axial and/or moment) with force-deformation curves at ambient and 12 temperature points that range from 100°C to 1200°C.
- These ultimate strengths define the initial capacities for each connection and reduce in fire based on the material strength reduction factors for bolts, as per Eurocode 3 **Error! Reference source not found.**.

B9.4.2 Breakage and Failure of Connector

Connector breakage is defined for all the simplified connections except for the welded girders on the following basis. Connectors break when:

- The connection force reaches its limiting capacity (ultimate strength at a specific temperature) where there is no deformation limit specified, or
- Where there is maximum deformation limit specified, the connection breaks when the connection deforms and reaches the maximum specified deformation limit.

In the ABAQUS model, the connector element is removed from the model to simulate breakage of the connection in the building.

Deformations in the connections are modelled to allow for the expected ductility of the connection as a whole (e.g. bolt slip, bolt hole elongation, sliding of the seat, clearance gaps, deformation of the plate from bearing etc.) prior to failure for each action.

As such, different deformation and/or breakage limits are assigned for each connection type depending on the governing failure mode as identified in the ambient capacity calculations and on the applied action.

Error! Reference source not found. summarises the proposed force deformation curves at ambient conditions for each of the 9 generic connection types identified in the building, using the user-defined connector elements with force-deformation curves for shear, tie and moment forces (where applicable). This table only applies to the behaviour of the connection at ambient conditions.

B9.4.3 Simplified knife connection behaviour on detailed shell girders

For both girders between Columns 79-77 and Columns 79-80 that are modelled in detail using shell elements, one end knife connection is modelled in detail using shell elements (at Column 79), while the other end knife connection is modelled using a simplified connector element.

In the situation above where the knife connection is modelled using a simplified connector element, Arup propose that it is defined with a ductility limit in compression to allow a similar behaviour to that observed at the corresponding girder's detailed connection. This in effect produces a more balanced connection behaviour at either end of the girder and is deemed realistic for the connection's, and therefore, the structure's performance. At all other simplified knife connections, the definition of no ductility in compression was deemed acceptable as when these are used at either end of a beam or girder, both simplified connectors are acting in balance with each other.

The degree of ductility in compression is taken as the gap between the end of the girder web and the face of the column. For the K8 connection on girder 79-76 at Column 76, this is 1" (25.4mm). For the K5 connection on girder 79-80 at Column 80, this is ¾" (19mm).

Table 10 - Proposed Deformation and Breakage Limits for Simplified Connections

Connection Type		Deformation limit before breakage [1]			
		Vertical Shear	Compression	Tension	Moment
Fin		***Plate Yielding*** *Distance from top bolt to top of plate*	*No breakage limit*[3]	***Bolt shear failure*** *½ (diameter of bolt + diameter of hole)*	***n/a*** – not a moment resisting connection

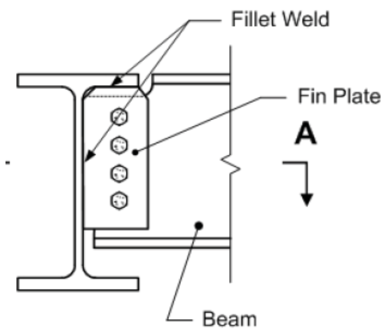

Basis for ductility limits (See Note 1):

Bolt shear failure

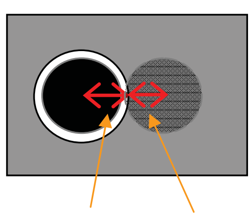

½ d_h

Plate yielding

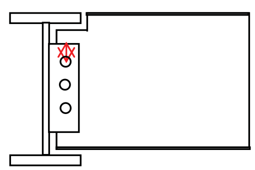

Distance from top bolt to top of plate

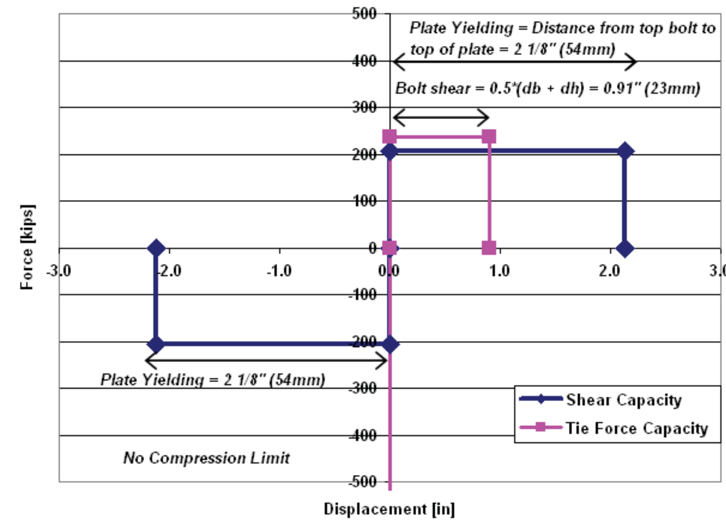

Connection Type		Deformation limit before breakage [1]			
		Vertical Shear	Compression	Tension	Moment
Header	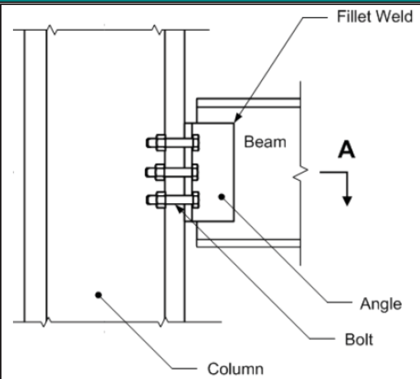 **<u>Basis for ductility limits (See Note 1):</u>** ***Prying action*** 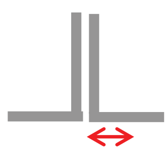 ½ Angle Leg	***Weld failure*** *No deformation – connection breaks when peak force is reached*	*No breakage limit[3]*	***Prying action failure*** Deformation equal to ½ the length of angle leg (L)	n/a – not a moment resisting connection
		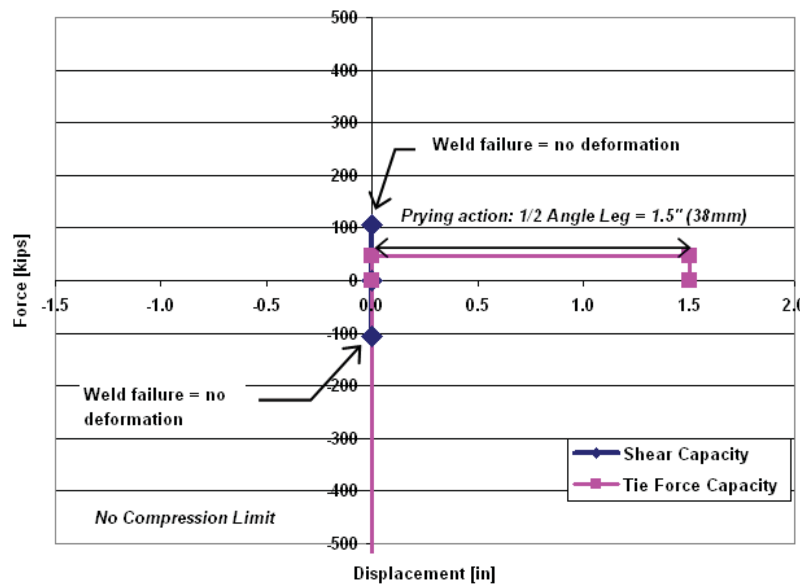			

Connection Type		Deformation limit before breakage[1]			
		Vertical Shear	Compression	Tension	Moment
Knife	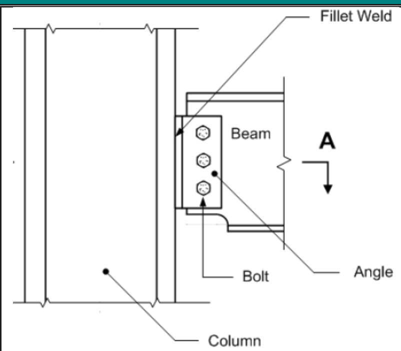	***Weld failure*** *No deformation – connection breaks when peak force is reached*	*No breakage limit*[3]	***Prying action failure*** Deformation equal to ½ the length of angle leg (L)	n/a – not a moment resisting connection
	Basis for ductility limits (See Note 1): ***Prying action*** 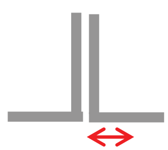	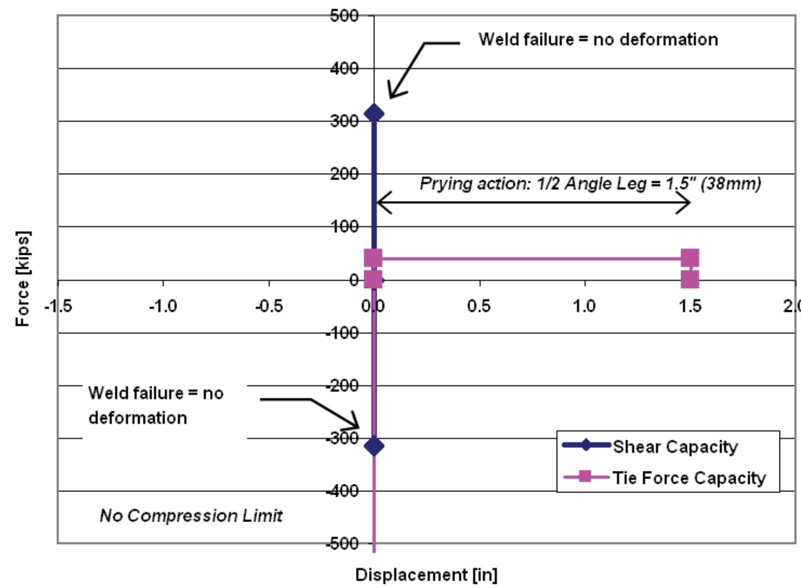			

JA-3292

Connection Type		Deformation limit before breakage[1]			
		Vertical Shear	Compression	Tension	Moment
SWC	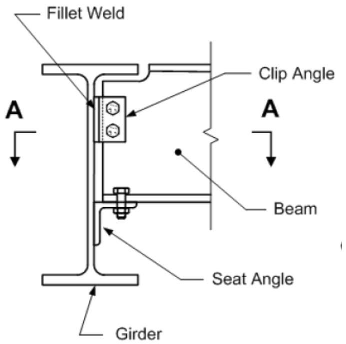	***Weld failure*** *No deformation – connection breaks when peak force is reached*	*No breakage limit[3]*	***Bolt hole bearing*** *Length of seat – Distance from beam end to column*	n/a – not a moment resisting connection

Basis for ductility limits (See Note 1):

Prying action

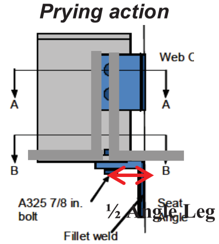

Bolt hole bearing

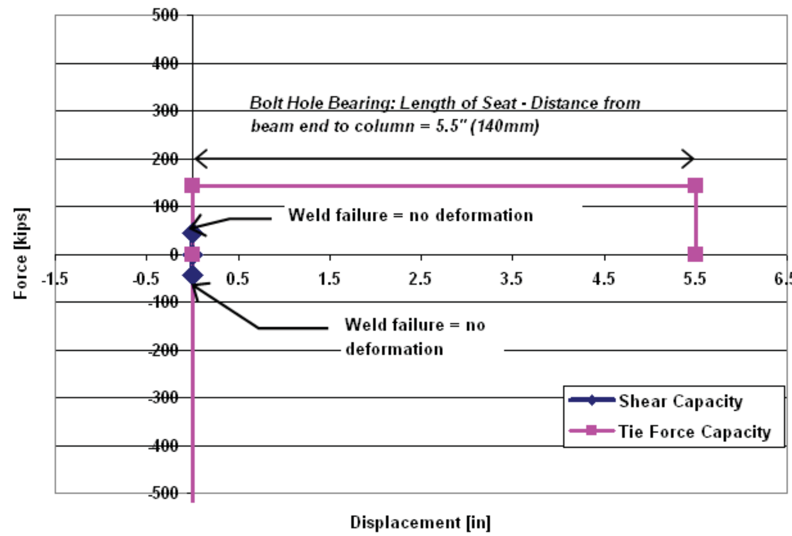

<table>
<tr><th colspan="2" rowspan="2">Connection Type</th><th colspan="4">Deformation limit before breakage [1]</th></tr>
<tr><th>Vertical Shear</th><th>Compression</th><th>Tension</th><th>Moment</th></tr>
<tr><td rowspan="2">STC, STP</td><td rowspan="2">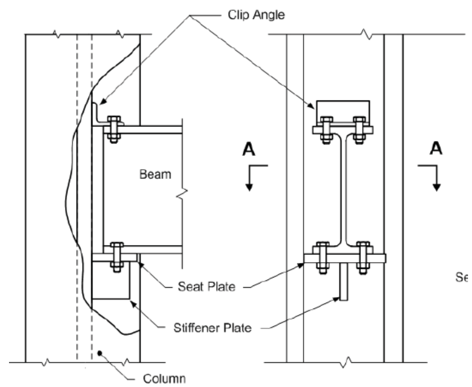
Basis for ductility limits (See Note 1):
Bolt shear failure
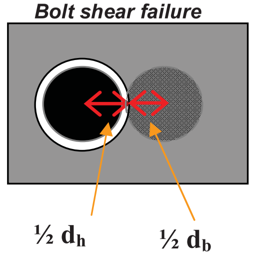</td><td>Weld failure
no deformation</td><td>No breakage limit[3]</td><td>Bolt shear failure
½ (diameter bolt + diameter hole)</td><td>n/a – not a moment resisting connection</td></tr>
<tr><td colspan="4">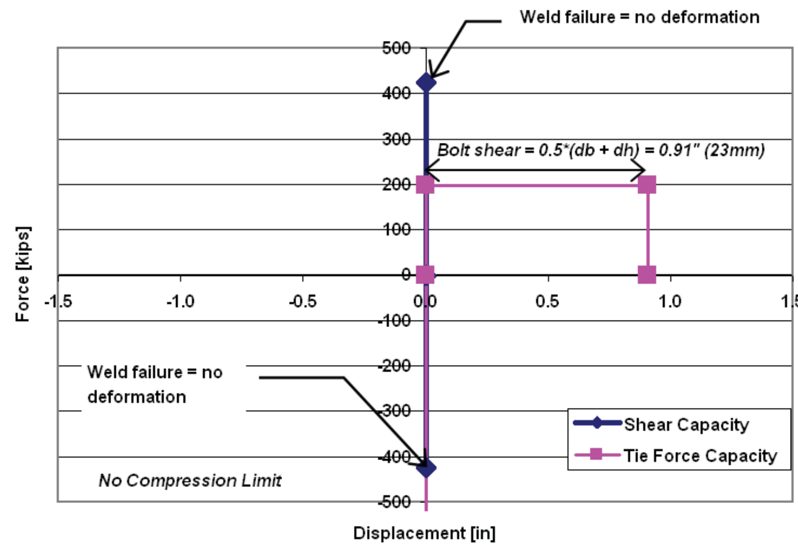</td></tr>
</table>

JA-3294

<table>
<tr><th colspan="2" rowspan="2">Connection Type</th><th colspan="4">Deformation limit before breakage [1]</th></tr>
<tr><th>Vertical Shear</th><th>Compression</th><th>Tension</th><th>Moment</th></tr>
<tr><td rowspan="2">Single Angle</td><td rowspan="2">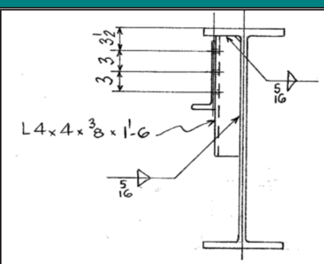

<u>Basis for ductility limits (See Note 1):</u>
Web bearing
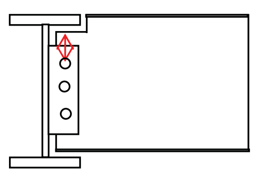
Distance from top bolt to top of beam</td><td>Web bearing
Distance from top bolt to top of beam</td><td>No breakage limit[3]</td><td>Web rupture
no deformation</td><td>n/a – not a moment resisting connection</td></tr>
<tr><td colspan="4">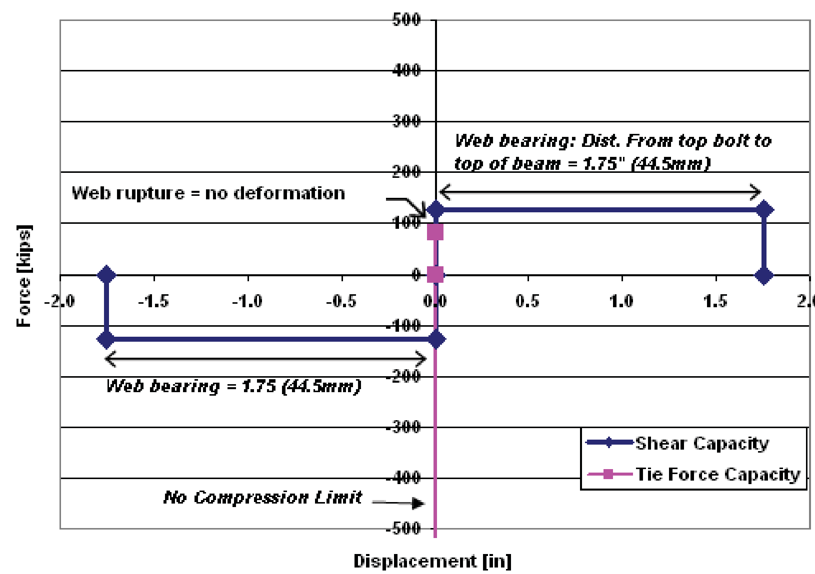
</td></tr>
</table>

JA-3295

Connection Type		Deformation limit before breakage[1]			
		Vertical Shear	Compression	Tension	Moment
WG	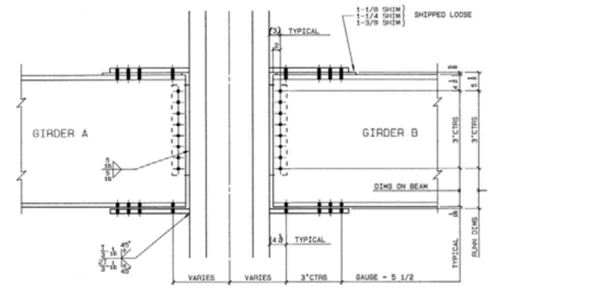	*No breakage limits are defined for the wind girder connections.*			
Welded WG[2]	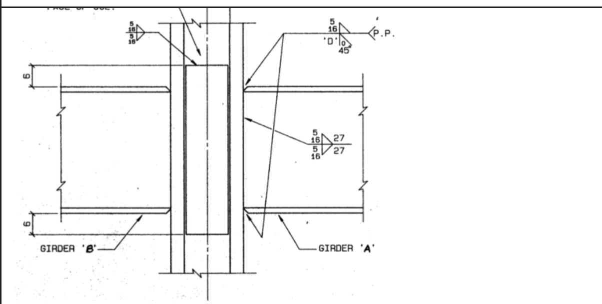	*No breakage limits are defined for the east wall wind girder connections.*			

Notes to accompany the above connection tables

Notes: [1] The specified deformations are intended to capture the expected ductility of the connection as a whole (e.g. bolt slip, bolt hole elongation, sliding of the seat, clearance gaps, deformation of the plate from bearing etc.) prior to failure for each action

[2] The welded wind girders (Welded WG) along the east wall are prefabricated column trees and therefore assumed to be fully fixed connections.

[3] The connections are assumed to have sufficient ductility in compression to allow the beam to expand against the supporting element during heating. This assumes that once the beam bears against column/supporting element, all forces are assumed to pass directly, without it being limited by a connection compression limit.

[4] Simplified connections are assumed to predominantly act in a vertical shear-plane. That is, no out-of-plane lateral movement can occur at the connection.

[5] To overcome certain numerical instabilities, full or limited torsional rigidity was applied to simplified connector elements where they (a) framed into a girder modelled with shell elements, and (b) framed into the eastern façade and formed the connection of a secondary beam that was modelled with breakable shear studs.

B10 References

[2] BS EN 1992-1-2:2005. Eurocode 2: Design of concrete structures – Part 1.-2: General rules – Structural fire design.

[3] BS EN 1993-1-2:2005. Eurocode 3: Design of steel structures – Part 1-2: General rules – Structural fire design.

[4] BS EN 1994-1-2:2005. Eurocode 4: Design of steel structures – Part 1-2: General rules – Structural fire design.

[5] Comite Euro-International Du Beton. CEB-FIP Model Code 1990. Thomas Telford Services Ltd. 1993. (First draft published 1991)

[6] Rots, J.G., et al. The need for fracture mechanics options in finite element models of concrete structures. Proceedings of the International Conference on Computer Aided Analysis and Design of Concrete Structures Part 1, F. Damjanic., ed,. Pineridge Press. pp19-32

[7] Karihaloo, B.L., Abdalla, H.M., and Imjai, T. (2003). " A Simple Method for Determining the True Specific Fracture Energy of Concrete." Mag. Concrete Res., 55(5), 471-481.

[8] Kruppa et at, Fire resistance of composite beams to Eurocode 4 Part 1.2, J. Constructional Steel Research 1995; 33: 51-69

[9] Huang et al, The Influence of shear connectors on the behaviour of composite steel framed buildings in fire, Journal of Constructional Steel Research, 1999.

[10] SCI Publication P288. Fire Safe Design: A new approach to multi-storey steel-framed buildings." Second Edition. The Steel Construction Institute. 2006.

[11] Connection capacities by CBM engineering (Received March 18, 2009)

[12] BS EN 1993-1-2:2005. Eurocode 3: Design of steel structures – Part 1-2: General rules – Structural fire design. 2005

[13] British Steel - *The Behaviour of High Strength Grade 8.8 Bolts in Fire*, Swinden Laboratories, Moorgate, Rotherham, United Kingdom, 1992.

[14] Kulak G et al, Guide to Design Criteria for Bolted and Riveted Joints, Second Edition, 2001.

Franklin M. Sachs (FS6036)
GREENBAUM, ROWE, SMITH & DAVIS LLP
Metro Corporate Campus One
P.O. Box 5600
Woodbridge, New Jersey 07095
Telephone: (732) 549-5600

UNITED STATES DISTRICT COURT
SOUTHERN DISTRICT OF NEW YORK

IN RE: SEPTEMBER 11 PROPERTY DAMAGE AND BUSINESS LOSS LITIGATION	:	21 MC 101 (AKH)
AEGIS INSURANCE SERVICES, INC., et al., Plaintiffs, -against- 7 WORLD TRADE CENTER COMPANY, L.P., et al., Defendants.	:	04 CV 7272 (AKH) **SUPPLEMENTAL AND AMENDED SECOND DECLARATION OF FREDERICK W. MOWRER**

I, Frederick W. Mowrer, declare:

1. I am an Associate Professor Emeritus in the Department of Fire Protection Engineering at the University of Maryland, where I served full-time on the faculty from 1987 to 2008. I currently serve as a Visiting Professor and Acting Director of Fire Protection Engineering Programs at California Polytechnic State University in San Luis Obispo, California. I have also served continuously as a self-employed consultant in the fields of fire protection engineering and fire science since 1980. Prior to 1980, I served as an engineering representative for the Insurance Services Office and as a fire protection engineer and building code consultant for Rolf Jensen and Associates, Inc. My curriculum vitae is attached hereto as Exhibit A.

2. I hold three academic degrees: 1) A Bachelor of Science in Fire Protection and Safety Engineering from the Illinois Institute of Technology; 2) A Master of Science in Engineering from the University of California, Berkeley; and 3) A Ph.D. in Fire Protection Engineering and Combustion Science from the University of California, Berkeley.

3. I am a Registered Professional Fire Protection Engineer in the State of California (#FP1094). I have authored several dozen scientific papers, technical reports and handbook chapters. I am a Fellow of the Society of Fire Protection Engineers and I served on the Board of Directors of the Society of Fire Protection Engineers from 1995 through 2003, including a term as President in 2002. I am a member of the National Fire Protection Association.

4. In 2002, I was retained by counsel for plaintiffs in this litigation to serve as consulting fire protection engineer. I make this affidavit based upon the work that I have done in studying the factors that contributed to the total collapse of 7 World Trade Center (WTC7).

5. Since that time, I have reviewed thousands of documents, drawings, and photographs, and actively participated in and reviewed the computer fire modeling performed on behalf of the Plaintiffs in this case.

6. The opinions that follow are based on that review and activity, and are made to a reasonable degree of scientific probability. These opinions and the data and materials relied upon in forming these opinions are more fully set forth in my report dated February 15, 2010, attached hereto as Exhibit D and made a part hereof.

7. Very tall buildings, such as the WTC7 building, are generally required to be of Type I construction, one of several construction types recognized by the Building Code of the City of New York, as well as by the model building codes that have existed in the United States for much of the past century. As noted in Report BMS92[1] in 1942, Type I construction is "that type of construction in which the structural elements are of incombustible materials with fire-resistance ratings sufficient to withstand the fire severity resulting from complete combustion of the contents and finish involved in the intended occupancy …"[2]. The WTC7 building was not able to withstand the fire severity resulting from complete combustion of its contents without collapsing, thereby violating this principle. Unlike the WTC1 and WTC2 buildings, the WTC7 building was not subject to the additional fuel loads and structural damage associated with the aircraft impacts.

---

[1] Subcommittee on Fire-Resistance Classifications of the Central Housing Committee on Research, Design, and Construction, "Fire-Resistance Classifications of Building Materials," *Report BMS92*, Building Materials and Structures, National Bureau of Standards, United States Department of Commerce, October 7, 1942.

[2] Ibid., p. 6.

8. This concept that fire resistance should exceed fire severity in fire resistive buildings is reiterated in an article that appeared in the *Quarterly* of the National Fire Protection Association in 1950.[3] Quoting from the NFPA *Handbook of Fire Protection*, this article notes that "As ordinarily used the term 'fire-resistive building' refers to a building with structural members constructed of noncombustible materials of such quality and so protected that they will resist the maximum severity of fire expected within the structure without collapse." This article goes on to say that "if a fire-resistive structure *does* possess the proper degree of fire-resistance, it *will* resist a fire without collapse ..." (Emphasis not added.) Since the WTC7 building did collapse, it clearly did not possess the proper degree of fire-resistance to resist the maximum severity of fire expected within the structure.

9. There is a reasonable expectation that firefighters will not engage in, or be effective in, offensive firefighting in high-rise buildings. This is one of the reasons why high-rise buildings are required to be of Type I construction. Indeed, firefighters could not reasonably be expected to enter high-rise buildings to fight fires if their structural stability was questionable. There have been a number of serious fires in high-rise building where firefighters have been unable to suppress the fire on multiple floors of the building. Two of these fires include the First Interstate Bank fire in Los Angeles in 1988 and the One Meridian Plaza fire in Philadelphia in 1991. In both of these fires, as well as in fires in other high-rise buildings, complete combustion of the contents occurred on the fire-affected floors, but did not result in total collapse of the buildings. A recent review of building collapse incidents[4] did not identify any steel-frame high-rise buildings, other than WTC7, that have completely collapsed primarily as a result of fire.

10. Because a high-rise building of Type I construction should be able to withstand complete combustion of its fuel load without collapsing and with no intervention by manual firefighting or automatic sprinkler protection, the lack of manual firefighting and the inoperative automatic sprinkler protection in the WTC7 building on September 11, 2001, should not have caused the collapse of the building.

11. The design of automatic sprinkler systems in the United States anticipates only a single fire source. As noted in the NFPA Fire Protection Handbook, "A number of assumptions have been employed in the writing of NFPA 13 to achieve an acceptable level of life safety and property protection while maintaining costs. For instance, the standard anticipates a single fire source, that is, no multiple ignitions in the building

---

[3] "Fires in 'Fireproof' Buildings," *Quarterly of the National Fire Protection Association*, Vol. 44, No. 1, July 1950.

[4] Beitel, J. and Iwankiw, N., "Analysis of Needs and Existing Capabilities for Full-Scale Fire Resistance Testing," *NIST GCR 02-843-1 (Revision),* National Institute of Standards and Technology, October 2008.

while the sprinkler system is operating. …"[5] Modern automatic sprinkler systems are hydraulically calculated to deliver the designed quantity of water to the area of a single fire source. When multiple fires occur, water is diverted to these additional fires, thereby decreasing the amount of water flowing to each of the multiple fire sources and increasing the probability that the sprinkler system will not control the fires.

12. Office contents fires generally burn for approximately 20 to 30 minutes in any one location until the fuel is consumed and then move on to the next area. That is why they are sometimes referred to in the Fire Protection industry as traveling fires. In tall buildings provided with a proper and appropriate level of fire resistance, ordinary office contents fires normally run out of fuel before sufficient structural damage can weaken steel to such an extent that it would fail.

13. The photographic and video evidence of the fires in WTC7 on September 11, 2001, from the collapse of WTC1 until approximately 3:30 PM, shows that the fires in WTC7 during that period appear to have been traveling fires limited to a few office floors. The office floors in WTC7 started at the seventh floor. The photographic and video evidence of the fires on the office floors of WTC7 indicate that these fires were consistent with ordinary office contents fires; they were not extraordinary fires.

14. After 3:30 PM, photographic evidence shows fires and smoke consistent with a petroleum-based diesel fuel fire emanating from the vicinity of the fifth/sixth floor louvers on the east side of WTC7. One such photograph is attached hereto as Exhibit B. Four of the nine generators comprising the Salomon Brothers' Standby Generator System were located in the northeast corner of the fifth floor.

15. The Standby Generator System installed by Solomon Brothers on the fifth floor of WTC7 constituted an electric power generating plant under Sections 27-250 and Reference Standard RS 3-3 of the NYC Building Code. As such, the area surrounding the generators and associated fuel piping required a higher fire resistance rating than the rest of the building. Sections 27-239 and 27-240 of NYC Building Code required that spaces having a higher fire index than the rest of the building be separated from adjoining spaces both vertically and horizontally by fire divisions having at least the fire resistance rating specified in Table 5-2 of NYC Building Code.

16. WTC7 was generally classified as a Group E occupancy. As an electric power generating plant, the Salomon Brothers' Standby Generator System was classified as Group D-1 occupancy under RS 3-3, thus mandating 3-hour fire resistive separation construction. Absence of such 3-hour fire resistive separation of the generator spaces on the fifth floor of WTC7 made it non-compliant with the NYC Building Code.

---

[5] Huggins, R., "Automatic Sprinkler Systems," Section 16, Chapter 3, Fire Protection Handbook, 20th edition, National Fire Protection Association, 2008.

17. An additional violation of the NYC Building Code was based upon misapplication of UL Design No. D739 to achieve the 2-hour fire resistance rating required of floor assemblies in buildings of Type 1B construction. The level of fireproofing applied at WTC7 would have been adequate to achieve a 2-hour fire resistance rating only if the floor assembly were classified as "restrained".

18. The Design Information Section in the 1983 edition of the UL Fire Resistance Directory provided the following definition for restraint in buildings: "Floor and roof assemblies and individual beams in buildings shall be considered restrained when the surrounding or supporting structure is capable of resisting substantial thermal expansion throughout the range of anticipated elevated temperatures. Constructions not complying with this definition are assumed to be free to rotate and expand and shall therefore be considered as unrestrained."

19. Given that WTC7 constituted an unrestrained assembly, the UL Design No. D739 only achieved a fire resistance rating of 1 hour, which would not have qualified it for use in a building of Type 1B construction.

20. The problem of inadequate fireproofing was compounded by the long floor spans in the north east corner of the WTC7.[6] ASTM E119 notes that "The test standard does not provide…Full information as to performance of assemblies constructed with components or lengths other than those tested."[7] In light of these admonitions within the ASTM E119 standard, it would have been prudent for the designer to evaluate the potential effects of the long span beams and girders on the expected fire performance of the floor assemblies in the WTC7 building, particularly with respect to the issue of thermal restraint. There is no evidence to indicate that this was done.

21. The WTC7 architect specified (Specification 9K.1.1.1) application of a sprayed- on cementitious coating over the "steel decking (fluted) and all floor support structural steel – occurring throughout the entire project – 2 hour rating." The WTC7 architect also specified (Specification 9K.4.1) that "The 'Design Information Section" including 'Floor-Ceiling Assemblies,' 'Roof-Ceiling Assemblies,' 'Beams,' 'Columns,' 'Wall and Partitions,' of the Underwriters' Laboratories 'Fire Resistance Index' dated January, 1975, and any later revisions and the 'Guide for Determining Conditions of Restraint.....' including Appendix 'C' from standard U.L. 263 shall form the basis of all required work and shall be referred to for guidance by the Sub-Contractor."

22. The Design Information Section in the 1983 and 1985 editions of the UL Fire Resistance Directory, which would have been the revisions applicable at the time of construction of WTC 7, included the following statement: "Cavities, if any, between

[6] The girder between columns 44 and 79 and the floor beams in the northeast corner of the building were more than 50 feet long.

[7] ASTM E119 is based on tests performed on an assembly having members 12-15feet long.

the upper beam flange and floor or roof units shall be filled with the fire protection material applied to the beam, unless stated otherwise on an individual design." This provision is still included in the current version of the UL Fire Resistance Directory.

23. The sprayed-on fireproofing material was not properly or adequately applied to the fluted steel decking and floor support structural steel beams and girders as required by the project specifications because the cavities between the upper beam flanges and the fluted steel deck were not filled with the fire protection material applied to the beam as required in the UL Fire Resistance Directory. Examples of the unfilled flute cavities are shown in the attached Morse Diesel photographs (Exhibit C). Based on my review of these and other Morse Diesel photographs, the fireproofing condition shown in these photographs appears to be representative of conditions throughout large areas of the WTC7 building if not the entire building. I have not seen any photographs showing flute cavities in the WTC7 building properly filled with the fire protection material as required.

24. Failure to construct the WTC 7 with the flute cavities above the beams and girders filled with the fire protection material applied to the beams, as required by the UL Fire Resistance Directory listing for the selected floor assembly and the project specification, reduced the fire resistance of the beams, girders and floor assemblies below the level that would have been achieved if these cavities had been properly filled in compliance with the requirements of the NYCBC.

25. The failure to properly fill the flute cavities with the fire protection material applied to the beams, as required, permitted the girders and beams to heat up more quickly than expected when exposed to an ordinary office contents fire. This more rapid heating would cause the girders, beams and floor assemblies to fail more quickly than expected when subjected to such a fire.

26. Computer modeling completed to date suggests that the failure to properly fill the cavities between the beams/girders and the fluted metal decking to ensure compliance with the Underwriters' Laboratories Fire Resistance Directory, as expressly referenced in the architect's specifications, was sufficient to cause a failure which would have led to the global collapse of WTC7.

I declare under penalty of perjury that the foregoing statements made by me are true. I am aware that if any of the foregoing statements made by me are willfully false, I may be subject to punishment.

Frederick W Mowrer

FREDERICK W. MOWRER

DATED: April 1, 2010

Curriculum Vita
FREDERICK W. MOWRER

Academic Degrees:

1987	**Ph.D.,** Fire Protection Engineering and Combustion Science University of California, Berkeley
1981	**M.S.,** Engineering University of California, Berkeley
1976	**B.S. (with High Honors),** Fire Protection and Safety Engineering Illinois Institute of Technology

Current Position: Fire Safety Consultant
4101 College Heights Drive
University Park, Maryland 20782

Previous Positions:

1987-2008	Assistant / Associate Professor Department of Fire Protection Engineering University of Maryland College Park, Maryland 20742-3031
1983	Lecturer, Department of Civil Engineering University of California, Berkeley Berkeley, California 94720
1982-1983	Associate Specialist, College of Engineering University of California, Berkeley Berkeley, California 94720
1980-1987	Fire Protection Engineer Pleasant Hill, California 94523
1978-1980	Fire Protection Engineer / Building Code Consultant Rolf Jensen and Associates, Inc. Washington, DC and San Francisco, California
1976-1978	Engineering Representative / Staff Supervisor Insurance Services Office - Southeastern Regional Office Atlanta, Georgia

Professional Registration: Registered Fire Protection Engineer (#1094)
State of California

Professional Service:

1978-Present Society of Fire Protection Engineers

1987-1989	Computer Committee
1988-1994	Research Committee
1989-1994	Education Registration Committee Subject Matter Expert - Fire Dynamics
1992-1994	Nominating Committee
1995-2003	Board of Directors
1995-2000	Vice President
1998-2000	Chair – Technical Steering Committee
2001	President-elect
2002	President
2003	Immediate Past President
2004-Present	Technical Steering Committee member 2006-Present: Chair

1978-Present National Fire Protection Association

1990-Present	Research Section 1992-1994 Chairman 1990-1992 Vice-Chairman
1992-1994	Task group on smoke management in large spaces
1999-Present	Technical Committee on Fire Tests
2005-Present	Chair, Research Advisory Committee Fire Protection Research Foundation

1988-2000
2008-Present International Association for Fire Safety Science

1988-1994	Auditor
1989-1994	International working group-model curriculum development
2008-Present	Committee member

2000-2002 International Standards Organization

2000-2002	Convenor – TC 92 / SC 4 / WG 9

Awards and Honors:

2009	Emeritus status, Department of Fire Protection Engineering, University of Maryland
2007	FM Global Best Paper Award, *5th International Seminar on Fire and Explosion Hazards*, Edinburgh, Scotland
2002	Harry C. Bigglestone Award for excellence in written communication of fire protection concepts in *Fire Technology*
2000	Best Technical Paper presented at the 8th International Conference on Nuclear Engineering ICONE-8
1999	Fellow, Society of Fire Protection Engineers
1991	Harry C. Bigglestone Award for excellence in written communication of fire protection concepts in *Fire Technology*
1988	Harry C. Bigglestone Award for excellence in written communication of fire protection concepts in *Fire Technology*
1976	Outstanding Senior Award - Society of Fire Protection Engineers - Chicago Chapter
1976	Clinton Stryker Award for outstanding service to the IIT community
1974	Tau Beta Pi National Engineering Honor Society
1974	Salamander Honorary Fire Protection Engineering Society

SELECTED PUBLICATIONS

1. F.L. Fisher, F.W. Mowrer and R.B. Williamson, "A Room Fire Screening Test Procedure," *Fire Technology*, Vol. 19, No. 4, pp. 238-250, November 1983.
2. R.B. Williamson, F.W. Mowrer and F.L. Fisher, "Observations of Large Scale Turbulence in Corner-Wall Experiments," *Combustion Science and Technology*, Vol. 41, pp. 83-99, 1984.
3. F.W. Mowrer and R.B. Williamson, "Estimating Room Temperatures from Fires along Walls and in Corners," *Fire Technology*, Vol. 23, No. 2, pp. 133-145, May 1987. (Recipient of 1988 Harry C. Bigglestone Award)
4. F.W. Mowrer and R.B. Williamson, "Room Fire Modeling within a Computer-aided Design Framework," *Fire Safety Science-Proceedings of the Second International Symposium*, Hemisphere Publishing Corporation, New York, 1989, pp. 453-462.
5. N.J. Brown, R.L. Dod, F.W. Mowrer, T. Novakov and R.B. Williamson, "Smoke Emission Factors from Medium Scale Fires, Part 1," *Aerosol Science and Technology*, Vol. 10 1989, pp. 2-19.
6. N.J. Brown, R.L. Dod, F.W. Mowrer, T. Novakov and R.B. Williamson, "Smoke Emission Factors from Medium Scale Fires, Part 2," *Aerosol Science and Technology*, Vol. 10 1989, pp. 20-37.
7. C.M. Fleischmann, R.L. Dod, N.J. Brown, T. Novakov, F.W. Mowrer and R.B. Williamson, "The Use of Medium Scale Experiments to Determine Smoke Characteristics," *Characterization and Toxicity of Smoke, ASTM STP1082*, H.K. Hasegawa, Ed., American Society for Testing and Materials, Philadelphia, 1990, pp. 147-164.
8. F.W. Mowrer and R.B. Williamson, "Methods to Characterize Heat Release Rate Data," *Fire Safety Journal*, Vol. 16, No. 5, 1990, pp. 367-387.
9. F.W. Mowrer, "Lag Times Associated with Fire Detection and Suppression," *Fire Technology*, Vol. 26, No. 3, August 1990, pp. 244-265. (Recipient of 1991 Harry C. Bigglestone Award)
10. R.B. Williamson, A. Revenaugh and F.W. Mowrer, "Ignition Sources in Room Fire Tests and Some Implications for Flame Spread Evaluation," *Fire Safety Science - Proceedings of the Third International Symposium*, Elsevier Science Publishers Ltd., 1991, pp. 657-666.
11. F.W. Mowrer and R.B. Williamson, "Flame Spread Evaluation for Thin Interior Finish Materials," *Fire Safety Science - Proceedings of the Third International Symposium*, Elsevier Science Publishers Ltd., 1991, pp. 689-698.
12. F.W. Mowrer, "Integration of Fire Models with the Design Process," *Fire Protection Handbook (17th Edition)*, A.E. Cote, Ed.-in-Chief, National Fire Protection Association, 1991, pp. 10-113 - 10-123.
13. F.W. Mowrer, "A Closed-Form Estimate of Fire-Induced Ventilation Through Single Rectangular Wall Openings," *Journal of Fire Protection Engineering*, Vol. 4, No. 3, 1992, pp. 105-114.
14. F.W. Mowrer, "Methods of Quantitative Fire Hazard Analysis," *EPRI TR-100443*, Electric Power Research Institute, Palo Alto, CA, May 1992, 72 p. (Reprinted and distributed by Society of Fire Protection Engineers)
15. J.A. Milke and F.W. Mowrer, "Computer-Aided Design for Smoke Management in Atria and Covered Malls," *ASHRAE Transactions*, Vol. 100, No. 2, 1994.
16. S.E. Magnusson, D.D. Drysdale, R.W. Fitzgerald, V. Motavelli, F.W. Mowrer, J.G. Quintiere and R.B. Williamson, "A Proposal for a Model Curriculum in Fire Safety Engineering," *Fire Safety Journal*, Vol. 25, 1995, pp. 1-88.
17. F.W. Mowrer, "Enclosure Smoke Filling Revisited," *Fire Safety Journal*, Vol. 33, 1999, pp. 93-114.
18. J.R. McGraw, Jr. and F.W. Mowrer, "Flammability and dehydration of painted gypsum wallboard subjected to fire heat fluxes," *6th International Symposium on Fire Safety Science*, Poitiers, France, 1999.
19. F.W. Mowrer and V.B. Brannigan, "Carbon Monoxide Production, Transport and Hazard in Building Fires," *Carbon Monoxide Toxicity* (D.G. Penney, MD, editor), CRC Press, 2000.

20. F. Joglar-Billoch, F.W. Mowrer and M. Modarres, "Description of a Two-Zone Fire Model for Hazard Screening," *Proceedings of ICONE 8 - 8th International Conference in Nuclear Engineering*, April 2-6, 2000, Baltimore, MD. (Recipient of Best Technical Paper award)
21. S.D. Wolin, N.L. Ryder, F. Leprince, J.A. Milke, F.W. Mowrer and J. Torero, "Measurements of Smoke Characteristics in HVAC Ducts," *Fire Technology*, Vol. 37, No. 4, October 2001, pp. 363-395. (Recipient of 2002 Harry C. Bigglestone Award)
22. F.W. Mowrer, "Enclosure Smoke Filling and Management with Mechanical Ventilation," *Fire Technology*, Volume 38, No. 1, January 2002, pp. 33-56.
23. H.E. Nelson and F.W. Mowrer, "Emergency Movement," Chapter 3-14, *SFPE Handbook of Fire Protection Engineering, 3rd Edition*, National Fire Protection Association, 2002, pp. 3-367 – 3-380.
24. J.A. Milke, J.L. Torero and F.W. Mowrer, "Use of Optical Density-Based Measurements as Metrics for Smoke Detectors," Paper AC-02-8-2, *ASHRAE Transactions: Symposia*, American Society of Heating, Refrigeration and Air-conditioning Engineers, 2002, pp. 699-711.
25. F.W. Mowrer, "Overview of Performance-Based Fire Protection Design," Section 3, Chapter 14, *Fire Protection Handbook*, 19th edition, National Fire Protection Association, 2003.
26. E. Avidor, F.J. Joglar-Billoch, F.W. Mowrer and M. Modarres, "Hazard Assessment of Fire in Electrical Cabinets," *Nuclear Technology*, Vol. 144, No. 3, December 2003, pp. 337-356.
27. F.W. Mowrer, "Fundamentals of the Fire Hazards of Materials," Chapter 1, *Handbook of Building Materials for Fire Protection*, McGraw-Hill, 2004, pp. 1.1 – 1.50.
28. F.W. Mowrer, "Flammability of Oil-based Painted Gypsum Wallboard Subjected to Fire Heat Fluxes," *Fire and Materials*, Vol. 28, 2004, pp. 355-385.
29. F.W. Mowrer, J.A. Milke and J.L. Torero, "A Comparison of Driving Forces for Smoke Movement in Buildings," *Journal of Fire Protection Engineering*, Vol. 14, No. 4, 2004, pp. 237-264.
30. F.W. Mowrer, "Analysis of Effective Thermal Properties of Thermally Thick Materials," *Fire Safety Journal*, Vol. 40, No. 5, 2005, pp. 395-410.
31. F. Joglar, F.W. Mowrer and M. Modarres, "A Probabilistic Model for Fire Detection with Applications," *Fire Technology*, Vol. 41, No. 3, July 2005, pp. 151-172.
32. F.W. Mowrer, "Thermal Response to Fire of Insulated Cylindrical Steel Elements," *Journal of Fire Protection Engineering*, Volume 17, No. 2, May 2007, pp. 129-143.
33. F.W. Mowrer and E.R. Rosenbaum, "Overview of Performance-Based Fire Protection Design," Section 3, Chapter 11, *Fire Protection Handbook*, 20th edition, National Fire Protection Association, 2008.
34. F.W. Mowrer, "Enclosure Smoke Filling and Fire-Generated Environmental Conditions," *SFPE Handbook of Fire Protection Engineering*, 4th edition, 2009.
35. F.W. Mowrer, "Driving Forces for Smoke Movement and Management," *Fire Technology*, 45, 147–162, 2009. DOI: 10.1007/s10694-008-0077-1
36. G. Rein, J.L. Torero, W. Jahn, J. Stern-Gottfried, N.L. Ryder, S. Desanghere, M. Lazaro, F. Mowrer, A. Coles, D. Joyeux, D. Alvear, J.A. Capote, A. Jowsey, C. Abecassis-Empis, P. Reszka, Round-Robin Study of a priori Modelling Predictions of The Dalmarnock Fire Test One, *Fire Safety Journal*, 44 (4) pp. 590-602, 2009. doi:10.1016/j.firesaf.2008.12.008

MISCELLANEOUS PUBLICATIONS

1. F.L. Fisher, F.W. Mowrer and R.B. Williamson, "ASTM E-119 Fire Endurance Tests of Flocon Inc.'s Gas Cylinder Storage Cabinets," *UCB Service to Industry Report No. 81-8*, University of California, Berkeley, September, 1981.
2. F.L. Fisher, F.W. Mowrer and R.B. Williamson "Large Scale Vertical Fire Spread Tests of STO Energy Conservation Inc.'s Exterior Wall Insulation System," *Service-to-Industry Report 82-1*, Fire Test Laboratory, University of California, Berkeley, March 1982.
3. F.L. Fisher, F.W. Mowrer and R.B. Williamson "Large Scale Vertical Fire Spread Tests of Insul/Crete Company Inc.'s Exterior Wall Insulation System," *Service-to-Industry Report 83-5*, Fire Test Laboratory, University of California, Berkeley, March 1983.
4. F.L. Fisher, F.W. Mowrer and R.B. Williamson "A Room Fire Screening Test Procedure," *WSS Paper 83-7*, Fall Meeting of the Western States Section, The Combustion Institute, Berkeley, 1983, 18 p.
5. F.L. Fisher, F.W. Mowrer and R.B. Williamson "Fire Safety of Electrical Cabinets," Final Report to U.S. Nuclear Regulatory Commission through Sandia National Laboratory, Lawrence Berkeley Laboratory, University of California, Berkeley, 1983, rev. 1984, 34 p.
6. P. Loubal, F.W. Mowrer and R.B. Williamson "Microcomputer Based Stochastic Fire Spread Analysis," *Report UCB FRG 84-2*, Presented at the National Bureau of Standards, October 17, 1984, University of California, Berkeley, 1984.
7. F.W. Mowrer, F.L. Fisher and R.B. Williamson "Full Scale Room Flame Spread Experiments Using a Line Burner Ignition Source," *UCB FRG Report 84-1*, Final Report to National Bureau of Standards, Center for Fire Research, University of California, Berkeley, Fire Research Group, 1984.
8. R.L. Dod, L.A. Gundel, F.W. Mowrer, R.B. Williamson and T. Novakov "Size Fractionation of Black and Organic Particulate Carbon from Fires: Final Report," *Lawrence Berkeley Laboratory Report LBL-20654, UC-11*, Lawrence Berkeley Laboratory, University of California, Berkeley, 1985, 24 p.
9. F.W. Mowrer and R.B. Williamson, "A Method to Characterize Heat Release Rate Data from Large-Scale Experiments," presented at 1987 Combined Meetings of the Eastern Section of The Combustion Institute and the Annual Conference on Fire Research of the National Bureau of Standards, November 2-5, 1987, 4 p.
10. R.L. Dod, N.J. Brown, F.W. Mowrer, R.B. Williamson and T. Novakov "Smoke Emission Factors from Medium Scale Fires: Part 2," *Report 24893*, Lawrence Berkeley Laboratory, University of California, Berkeley, 1988, 21 p.
11. F.W. Mowrer, "Software Review: FOAMSTAT Fire Emergency and Preplanning Software," *Fire Technology*, Vol. 24, No. 1, February 1988, pp. 87-90.
12. F.W. Mowrer, "Integration of Fire Models into the Design Process," *IFPEI-V*, International Fire Protection Engineering Institute, Carleton University, Ottawa, Ontario, Canada, May 1989, 26 p.
13. F.W. Mowrer, "Book Review: SFPE Handbook of Fire Protection Engineering," *Fire Technology*, Vol. 25, No. 2, May 1989, pp. 184-187.
14. F.W. Mowrer, J.A. Milke and R.M. Clarke "Heavy Truck Fuel System Fire Safety Study," *DOT HS 807 484*, National Highway Traffic Safety Administration, U.S. Department of Transportation, August, 1989, 129 p.
15. F.W. Mowrer, "A Comparison of Shoreside and Maritime Fire Protection Requirements," Department of Fire Protection Engineering, University of Maryland, College Park, MD, September, 1989, 105 p.
16. N. Lerner, R. Huey, M. Morrison and F.W. Mowrer, "Residential Smoke Alarms and Fire Safety for Older Adults," Prepared for The National Institute on Aging, National Institutes of Health, Grant No. 1R43AG08151-01, Comsis Corporation, Silver Spring, MD, June 1990, 89 p.
17. F.W. Mowrer, "Methods of Quantitative Fire Hazard Analysis," *TR-100443*, Electric Power Research Institute, Palo Alto, CA, May 1992, 72 p.

18. S.A. Denny and F.W. Mowrer, "Development of a Hypermedia Knowledge Base of Aircraft Fire Safety Regulations," *International Conference for the Promotion of Advanced Fire Resistant Aircraft Interior Materials*, Federal Aviation Administration, Atlantic City, February 1993, 11 p.
19. F.W. Mowrer, "Software Review: 'THE' Sprinkler Program," *Fire Technology*, Vol. 29, No. 1, February 1993, 9 p.
20. F.W. Mowrer and M.N. Ashman, "Flammability of Surgical Drapes," *Report No. FP93-01*, Department of Fire Protection Engineering, University of Maryland, College Park, MD, April, 1993, 26 p.
21. J.A. Milke and F.W. Mowrer, "A Design Algorithm for Smoke Management Systems in Atria and Covered Malls," *Report No. FP93-04*, Department of Fire Protection Engineering, University of Maryland, College Park, MD, May 1993, 215 p.
22. J.G. Quintiere, J.L. Bryan, F.W. Mowrer and J.A. Milke "Dynamics of Building Fires II - Course Notebook," *Report No. FP93-05*, Department of Fire Protection Engineering, University of Maryland, College Park, MD, June, 1993.
23. F.W. Mowrer, "Spreadsheet Templates for Fire Dynamics Calculations," *Report No. FP93-06*, Department of Fire Protection Engineering, University of Maryland, College Park, MD, July, 1993.
24. J.G. Quintiere and F.W. Mowrer, "Fire Development Analysis - Mount Carmel Branch Davidian Compound - Waco, Texas - April 19, 1993," September 8, 1993.
25. F.W. Mowrer, "Development of the Fire Data Management System," *NIST GCR 94-639*, National Institute of Standards and Technology, Gaithersburg, MD, June 1994, 35 p.
26. F.W. Mowrer, "Combustible Building Elements and Their Attributes," *Proceedings of the Third International Fire and Materials Conference* (Washington DC), Interscience Communications Limited, October 1994, p. 207-216.
27. F.W. Mowrer and M.G. Pecht "Exploratory Research on Nonthermal Damage to Electronics from Fires and Fire-Suppression Agents," *Proceedings of the Annual Reliability and Maintainability Symposium*, Washington, DC, 1995, pp. 1-6.
28. R.M Chung, N.H. Jason, B. Mohraz, F.W. Mowrer and W.D. Walton "Post-Earthquake Fire and Lifelines Workshop; Long Beach, California January 30-31, 1995 Proceedings," *NIST Special Publication 889*, National Institute of Standards and Technology, Gaithersburg, MD, August 1995.
29. J.A. Milke and F.W. Mowrer, "Computer Aided Design for Smoke Management," *ASHRAE Journal*, August 1995, pp. 153-157.
30. F.W. Mowrer, "Fire Safety in the Operating Room," *NFPA 1996 Fall Meeting*, Nashville, TN, November, 1996.
31. F.W. Mowrer, "Window Breakage Induced by Exterior Fires," *Proceedings of the 2nd International Conference on Fire Research and Engineering*, Gaithersburg, MD, August 1997.
32. F.W. Mowrer, R.B. Williamson and F.L. Fisher "Analysis of the Early Fire Development at the MGM Grand Hotel," *Proceedings of the 2nd International Conference on Fire Research and Engineering*, Gaithersburg, MD, August 1997.
33. F.W. Mowrer, "Window Breakage Induced by Exterior Fires," *NIST-GCR 98-751*, National Institute of Standards and Technology, Gaithersburg, MD, 1998.
34. B. Gautier and F.W. Mowrer, "Comparison of Fire Model Features and Computations," *Post-SMIRT conference proceedings*, Lyons, France, August, 1997.
35. F.W. Mowrer and J. Friedman, "Experimental Investigation of Heat and Smoke Detector Response," Proceedings of the Fire Suppression and Detection Research Application Symposium, Orlando, FL, February 24-26, 1998, pp. 256-264.
36. B. Gautier and F.W. Mowrer, "Fire Model Feature Comparison - Part I: Technical Comparison of the Codes," Electric Power Research Institute, 1998.

37. B. Gautier and F.W. Mowrer, "Fire Model Feature Comparison - Part II: Comparison of model simulations with fire test data," Electric Power Research Institute, 1998.

38. D.W. Stroup and F.W. Mowrer, "Features, Limitations and Uncertainties in Enclosure Fire Hazard Analyses - Preliminary Review," *NISTIR 6152*, National Institute of Standards and Technology, March 1998.

39. J. Friedman and F.W. Mowrer, "An Experimental Investigation of Heat and Smoke Detector Response," presented at *National Fire Protection Research Foundation Symposium*, Orlando, Florida, February 1999.

40. F.W. Mowrer and B. Gautier "A Comparison between Four Zone Fire Models Used in Nuclear Safety Studies," *Interflam '99 – Proceedings of the Eighth International Conference*, Interscience Communications, London, 1999.

41. J.R. McGraw, Jr. and F.W. Mowrer, "Flammability of painted gypsum wallboard subjected to fire heat fluxes," *Interflam '99 – Proceedings of the Eighth International Conference*, Interscience Communications, London, 1999.

42. F. Joglar, F.W. Mowrer, M. Modarres and A. Azarm "Description of a Fire Hazard Screening Methodology," *PSA Conference Proceedings*, Washington, DC, 1999.

43. F. Joglar, F.W. Mowrer, M. Modarres and A. Azarm "Description of a Fire Hazard Screening Methodology," *Fire & Safety '99*, Fire Protection and Prevention in Nuclear Facilities, Frankfurt, Germany, Feb. 1999.

44. F. Joglar, F.W. Mowrer, M. Modarres and A. Azarm, "Probabilistic-Deterministic Fire Risk Analysis," *Fire & Safety '99*, Fire Protection and Prevention in Nuclear Facilities, Frankfurt, Germany, Feb. 1999.

45. F.W. Mowrer and P. Friday, "Ready to Respond" (Videotape), United States Fire Administration, 1999.

46. F.W. Mowrer, "Fire Safe Student Housing: A Guide for Campus Housing Administrators," United States Fire Administration, 1999.

47. M. Spearpoint, F.W. Mowrer and K. McGrattan "Simulation of a Single Compartment Flashover Fire Using Hand Calculations, Zone Models and a Field Model," *Proceedings of the Third International Conference on Fire Research and Engineering*, Society of Fire Protection Engineers, 1999.

48. J.L. Torero and F.W. Mowrer, "A New-Approach to Interpreting LIFT Ignition Test Data," *Proceedings of the Thirty-First International Conference on Fire Safety*, Product Safety Corporation, Columbus, OH, July 2000, 13 p.

49. E. Avidor, F. Joglar, F.W. Mowrer and M. Modarres, "Hazard Assessment of Fires in Electrical Cabinets," *CTRS Report B5-07, Volume B5, No. 7*, Center for Technology Risk Studies, University of Maryland, College Park, MD, August 2000, 57 p.

50. F.W. Mowrer, "The Effect of Blistering on the Ignition and Flammability of Painted Gypsum Wallboard," *Fire and Materials Conference Proceedings*, January 2001, 12 p.

51. F.W. Mowrer, "Flammability of Oil-Based Painted Gypsum Wallboard Subjected to Fire Heat Fluxes," *NIST GCR 01-805*, National Institute of Standards and Technology, Gaithersburg, MD, January 2001, 43 p.

52. P. Friday and F.W. Mowrer, "Comparison of FDS Model Predictions With FM/SNL Fire Test Data," *NIST GCR 01-810*, National Institute of Standards and Technology, Gaithersburg, MD, April 2001, 104 p.

53. S.D. Wolin, N.L. Ryder, F. Leprince, J.A. Milke, F.W. Mowrer and J.L. Torero, "Measurements of smoke characteristics in HVAC ducts," *Proceedings of the Fire Suppression and Detection Research Application Symposium*, Fire Protection Research Foundation, Quincy, MA, 2001.

54. V. Brannigan, F.W. Mowrer and D.A. Purser "A Probabilistic Approach to Tenability Criteria," *Proceedings of the 4th International Conference on Performance-based Codes and Fire Safety Design Methods*, Society of Fire Protection Engineers, Bethesda, MD, 2002, pp. 174-179.

55. J.A. Milke, F.W. Mowrer and J.L. Torero "Investigation of the Application of Duct Smoke Detectors in Heating, Ventilating and Air Conditioning Systems," Final report submitted to the Fire Detection Institute, April, 2002.

56. S. Chamberlain, M. Modarres and F.W. Mowrer, "An Overview of Risk Issues in Compressed Natural Gas Buses," Proceedings of the 6th International Conference on Probabilistic Safety Assessment and Management (PSAM6), Elsevier Science Ltd., 2002, 7 p.

57. E. Avidor, F. Joglar-Billoch, F.W. Mowrer and M. Modarres "Hazard Assessment of Fire Risk in Electrical Cabinets," *PSA '02*, Detroit, MI, November 2002.

58. S. Chamberlain, M. Modarres and F.W. Mowrer, "Compressed Natural Gas Bus Safety: A Qualitative and Quantitative Risk Assessment," Report CTRS-MC1-02, Center for Technological Risk Studies, University of Maryland, 2002.

59. F.W. Mowrer, "The Right Tool for the Job," *Fire Protection Engineering*, Issue No. 13, Winter 2002, pp. 39-44.

60. F.W. Mowrer, "Ignition characteristics of various fire indicators subjected to radiant heat fluxes," *Fire and Materials Conference Proceedings*, January 2003, 12 p.

61. F.W. Mowrer, "Fire Protection Engineering Tools," *Making the Nation Safe from Fire: A Path Forward in Research*, Committee for Identifying Innovative Research Needs to Foster Improved Fire Safety in the United States, National Research Council, The National Academies Press, July 2003.

62. F.W. Mowrer, "Analysis of Effective Thermal Properties of Thermally Thick Materials," *NIST GCR 03-855*, National Institute of Standards and Technology, July 2003, 25 p.

63. R. Iding and F.W. Mowrer, "Evaluation and retrofit of existing buildings for structural fire safety," Workshop on National R&D Roadmap for Fire Safety Design and Retrofit of Structures, Society of Fire Protection Engineers and National Institute of Standards and Technology, October 2-3, 2003, Baltimore, MD.

64. M. Johansson, F.W. Mowrer and J. deJoseph "An Analysis of Conditions Resulting from Fires during Tunnel Boring Operations," *Interflam '04 – Proceedings of the Tenth International Conference*, Interscience Communications, London, 2004, pp. 1505-1516.

65. F.W. Mowrer, "Performance Requirements," *Fire Protection of Structural Steel in High-Rise Buildings,* NIST GCR 04-872, National Institute of Standards and Technology, July 29, 2004, pp. 28-50.

66. V. Brannigan and F.W. Mowrer, "Management of Conflicting Interests in Performance-based Fire Safety Design," *Proceedings of the 5th International Conference on Performance-Based Codes and Fire Safety Design Methods*, Society of Fire Protection Engineers, October 2004, 11 p.

67. R.B. Williamson and F.W. Mowrer, "The Role of Interior Finish in Fire Development," *Fire Protection Engineering*, Issue No. 24, Fall 2004, pp. 26-39.

68. F.W. Mowrer, "Geometric Effects on the Fire Resistance of Structural Steel Elements," *Proceedings of the ASCE Structures Congress*, New York, NY, 2005.

69. S.T. O'Rourke, J. Hubert and F.W. Mowrer, "Analysis of Vapor Density Effects on Leakage Rates for Total Flooding Clean Extinguishing Agents," *SFPE Symposium on Fire Suppression*, San Diego, CA, October 2005, 12 p.

70. F.W. Mowrer, "Analysis of Vapor Density Effects on Hold Times for Total Flooding Clean Extinguishing Agents," *Halon Options Technical Working Conference*, Albuquerque, NM, May 2006, 12 p.

71. F.W. Mowrer, "Analysis of the Cook County Administration Building Fire," *International Congress on Fire Safety in Tall Buildings*, University of Cantabria, Santander, Spain, 18-20 October, 2006, pp. 203-219.

72. F.W. Mowrer, "Flammability characteristics of finished oak veneer plywood," *Fire and Materials Conference Proceedings*, January 2007, 11 p.

73. F.W. Mowrer, J.A. Milke and P. Gandhi, "Validation of a Smoke Detection Performance Prediction Methodology: Status Report," *Suppression and Detection Research and Applications: A Technical Working Conference (SUPDET 2007)*, Orlando, Florida, March 2007, 4 p.

74. G. Rein, C. Abecassis-Empis, A. Amundatain, H. Biteau, A. Cowlatd, A. Chan, W. Jahn, A.Jowsey, P. Reszka, T. Steinhaus, R. Carvel, S. Welch, J.L. Torero, J. Stern-Gottfried, B.Hume, A. Coles, M. Lazaro, D. Alvear, J. A. Capote, S. Desanghere, D. Joyeux, N.L. Ryder, C. Schemel and F. Mowrer, "Round-Robin Study of Fire Modelling – Blind Predictions using the Dalmarnock Fire Experiments," *5th International Seminar on Fire and Explosion Hazards*, Edinburgh, UK, April 23-27, 2007. (Recipient of FM Global Best Paper Award)

75. F.W. Mowrer, "Validation Studies of the FDS Smoke Detection Prediction Methodology," *Proceedings of the Advanced Research Workshop on Fire Computer Modeling*, University of Cantabria, Santander, Spain, 18-20 October, 2007, pp. 53-64.

76. F.W. Mowrer, "Driving Forces for Smoke Movement and Management," *Proceedings of the International Congress on Smoke Control in Buildings and Tunnels*, University of Cantabria, Santander, Spain, 16 October, 2008, 16 p.

77. M. Brookman, F.W. Mowrer, J.A. Milke and P. Gandhi, "Validation of a Smoke Detection Performance Prediction Methodology, Volume 1. Characterization of incipient fire sources," Fire Protection Research Foundation, 2008.

78. F.W. Mowrer, J.A. Milke and P. Gandhi, "Validation of a Smoke Detection Performance Prediction Methodology, Volume 2. Large-scale room fire tests," Fire Protection Research Foundation, 2008.

79. J.A. Milke, F.W. Mowrer and P. Gandhi, "Validation of a Smoke Detection Performance Prediction Methodology, Volume 3. Evaluation of smoke detector performance," Fire Protection Research Foundation, 2008.

80. F.W. Mowrer, J.A. Milke and P. Gandhi, "Validation of a Smoke Detection Performance Prediction Methodology, Volume 4. Evaluation of FDS smoke detection prediction methodology," Fire Protection Research Foundation, 2008.

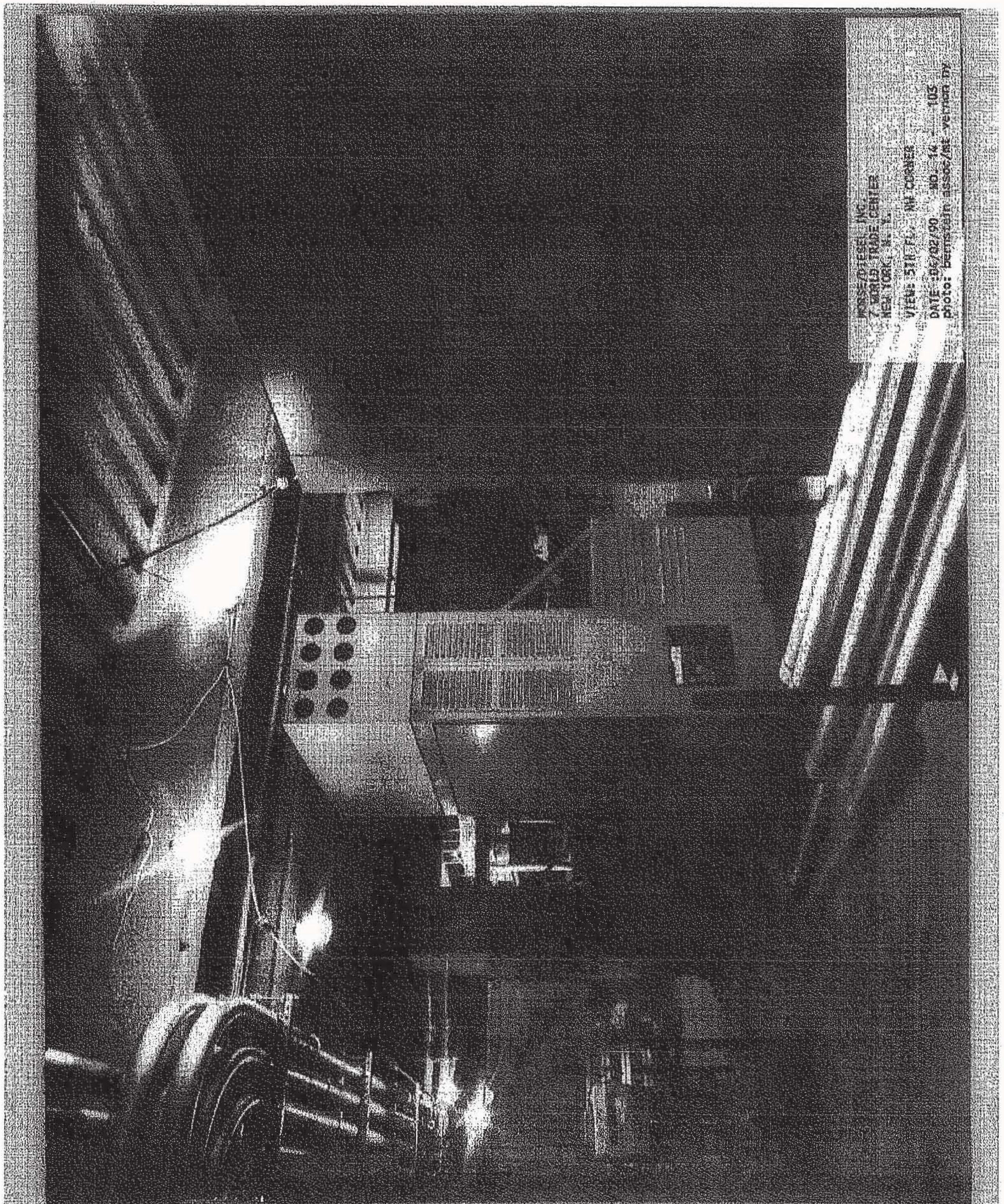

CITI-7WTC072570

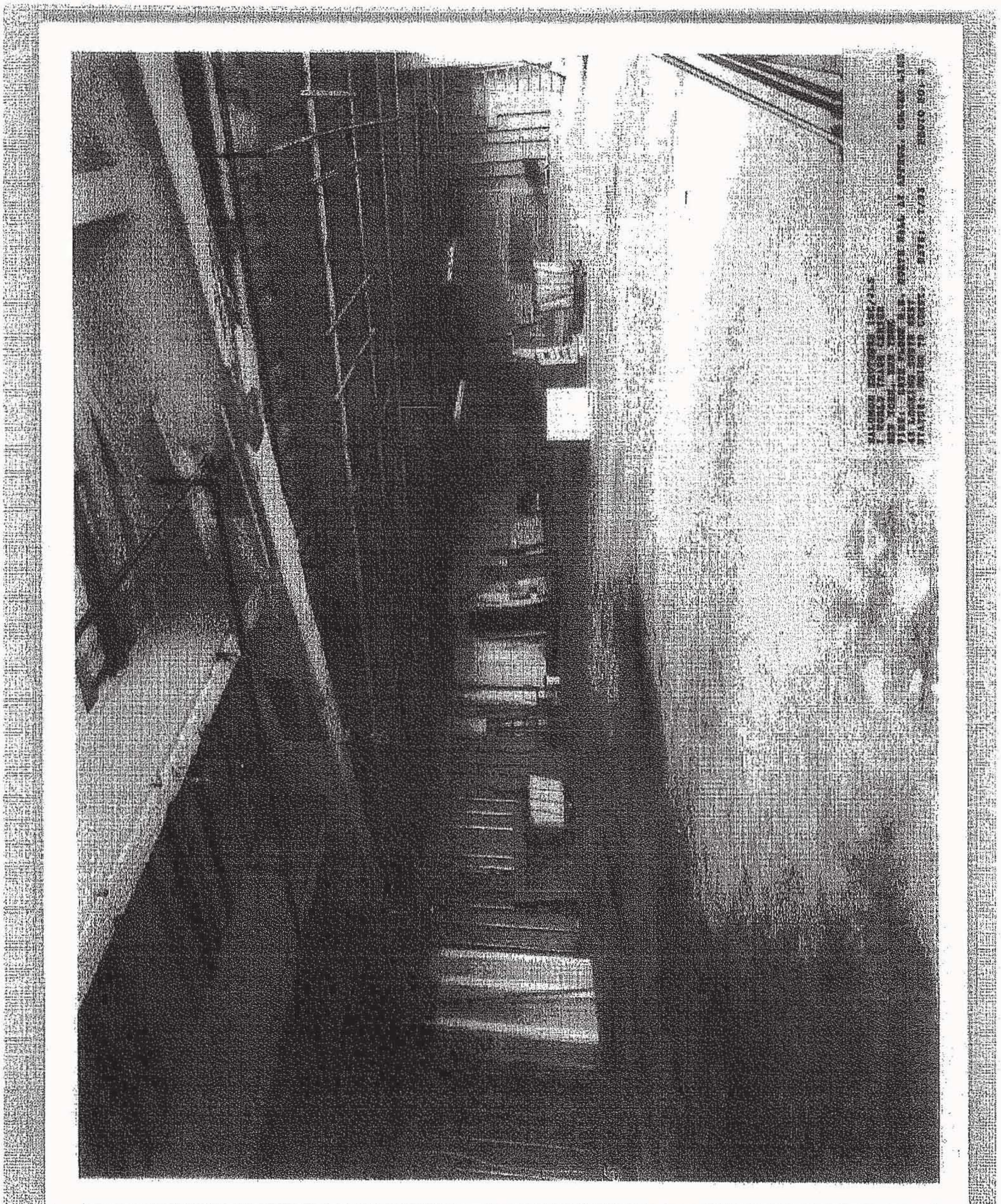

CITI-7WTC073704

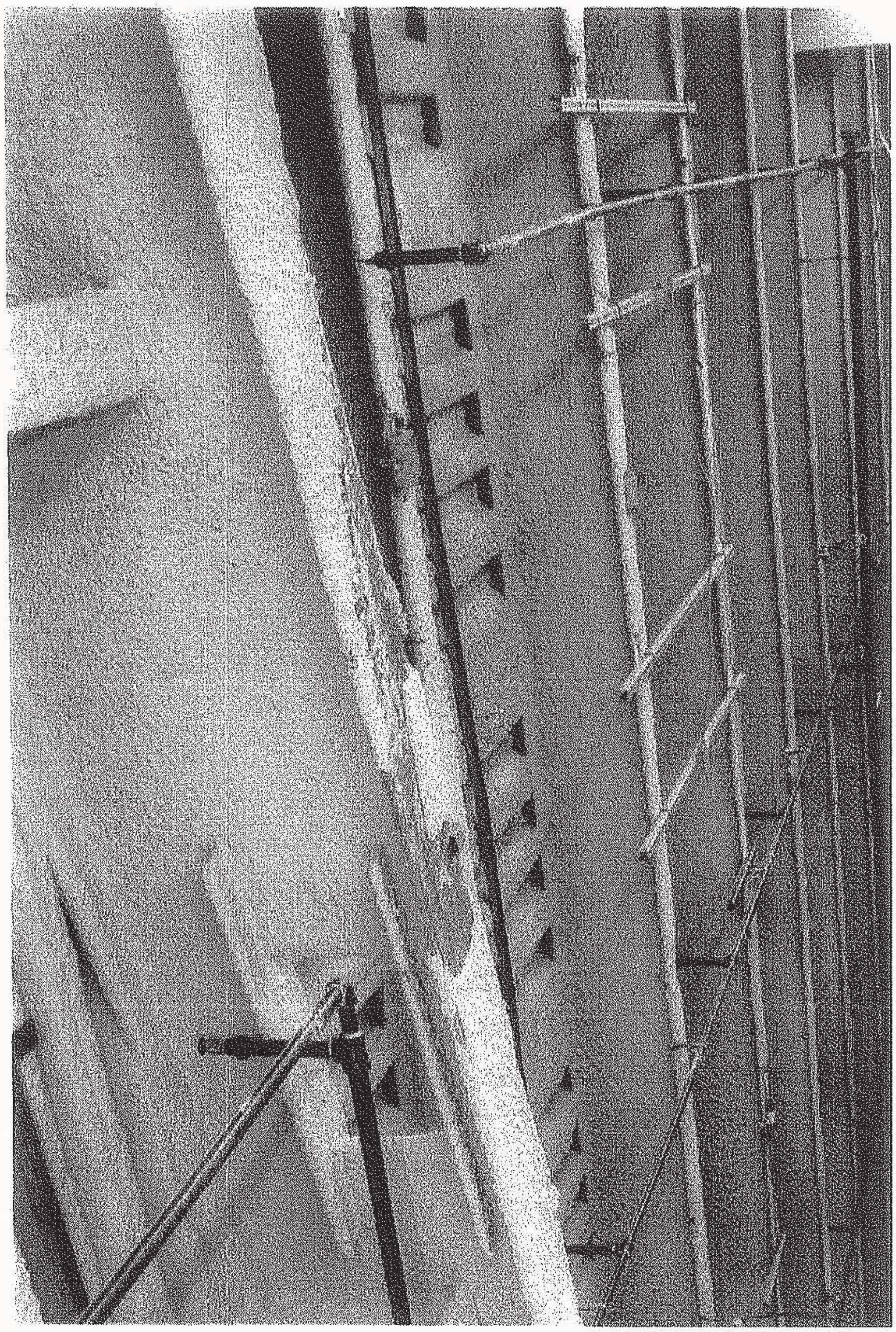

Due to its size, Exhibit D has not been e-filed. If you wish to receive a copy, please email Marilyn Francisquini at mfrancisquini@greenbaumlaw.com. A hardcopy of Exhibit D has been filed with the Court, and has been served upon the following counsel:

Katherine L. Pringle, Esq.
Friedman, Kaplan, Seiler & Adelman LLP
1633 Broadway, 46th Floor
New York, NY 10019

Christopher P. Moore, Esq.
Cleary, Gottlieb, Steen & Hamilton LLP
One Liberty Plaza
New York, NY 10006

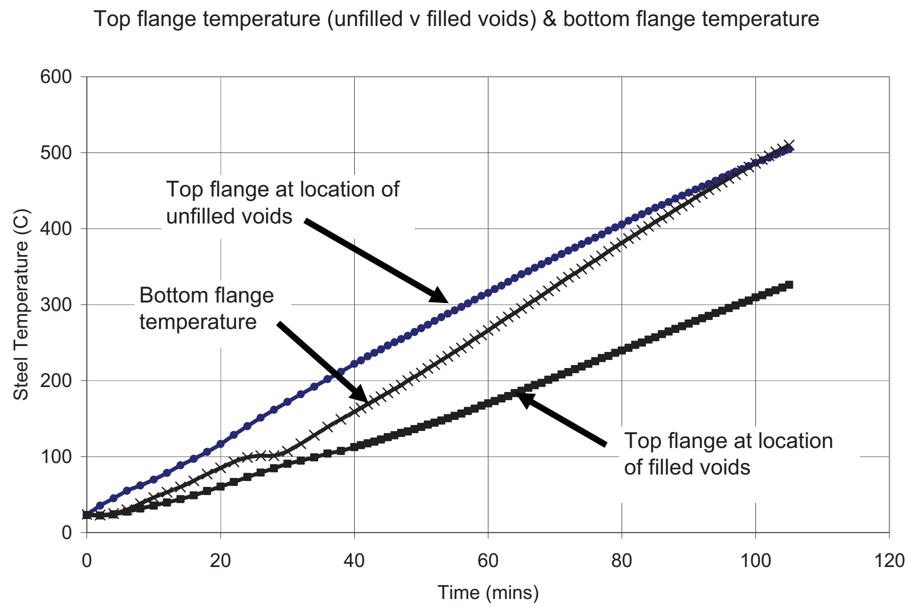

Figure C4 *Top flange temperatures at location of filled and unfilled voids for trapezoidal deck (PMF CF60) with normal weight concrete (Bottom flange temperatures also shown)*

Loaded tests

A test program comprising 4 tests(3,4) on loaded beams was carried out in the early 1990s. The 4 tests considered 3 types of protection; a dry board, cementitous spray and intumescent coating.

The first test comprised of a board protection with the voids filled. The other three tests with a board, spray and intumescent protection had the voids left unfilled. The protection was specified to keep the bottom flange below 600°C for 60 minutes. A summary of the tests is shown below.

Test 1: Dry board protection 18 mm thick. Voids filled with shaped pieces of the same board.
Test 2: Dry board protection 18 mm thick. Voids unfilled
Test 3: Cementitious spray 22mm thick (average) cover to edges to top flange 10mm. Voids unfilled.
Test 4: Intumescent coating 1.2mm thick (average) top flange not coated. Voids unfilled.

Test 1 is the control test. Ideally, there should have been a control test for all types of protection but cost restrictions prohibited these tests being carried out. For the purpose of this study Test 3 will be considered with some reference to Tests 1 and 2.

The temperatures were measured at a number of locations as shown in Figure C5.

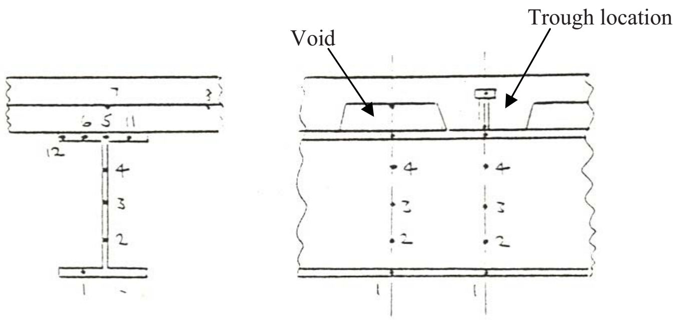

Figure C5: *Location of temperature measurements*

The temperatures recorded for Test 3 on the top flange (at the unfilled void location and trough location) and the bottom flange are shown in Figure C6. It can be seen that the top flange temperatures at the unfilled void location are greater than the temperatures at the trough location. In addition the top flange temperatures are greater than the bottom flange temperatures. If the voids were filled the top flange temperatures would be lower than the bottom flange temperatures. This was shown in Test 1, which had filled voids, with the temperatures shown in Figure C7.

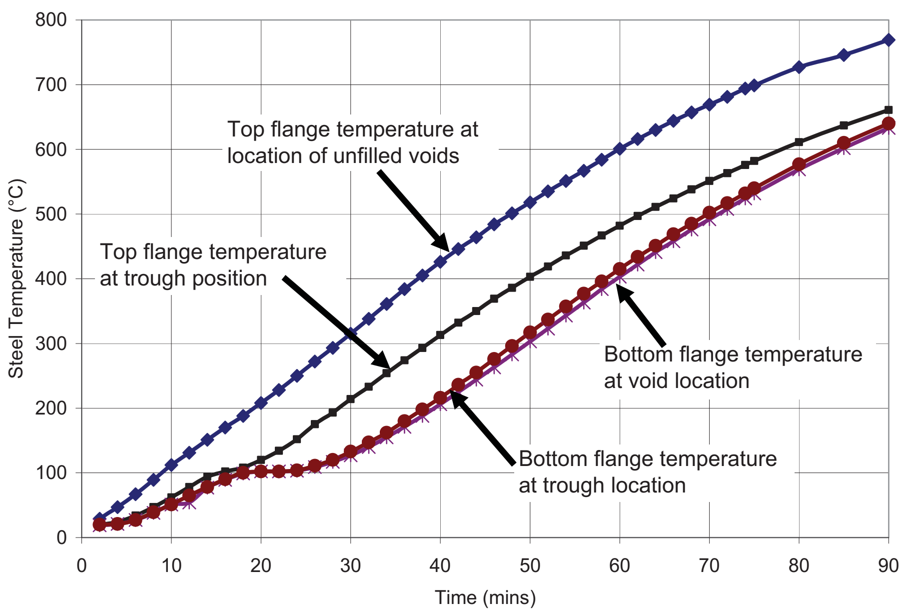

Figure C6: *Steel temperatures for Test 3; cementitious spray and voids unfilled.*

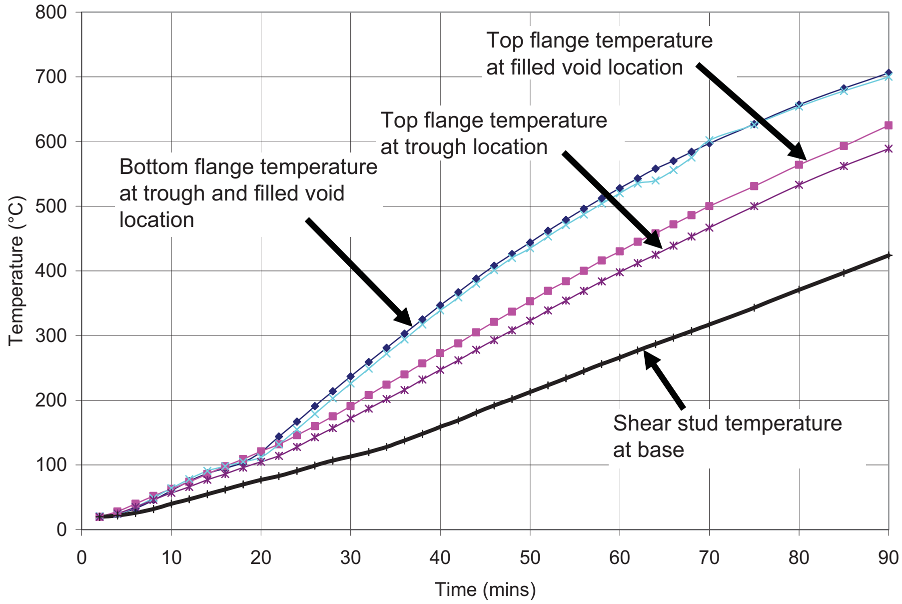

Figure C7 *Steel temperatures for Test 1; board protection voids filled.*

It is impossible to carry out a direct comparison between Tests 1 and 3 since different protection systems are used and the thickness of the SFRM in Test 3 was greater than that required.

One interesting comparison is between Test 1 and Test 2, which although had a board protection, shows the direct comparison between filled and unfilled voids. The difference in top flange temperature is shown in Figure C8.

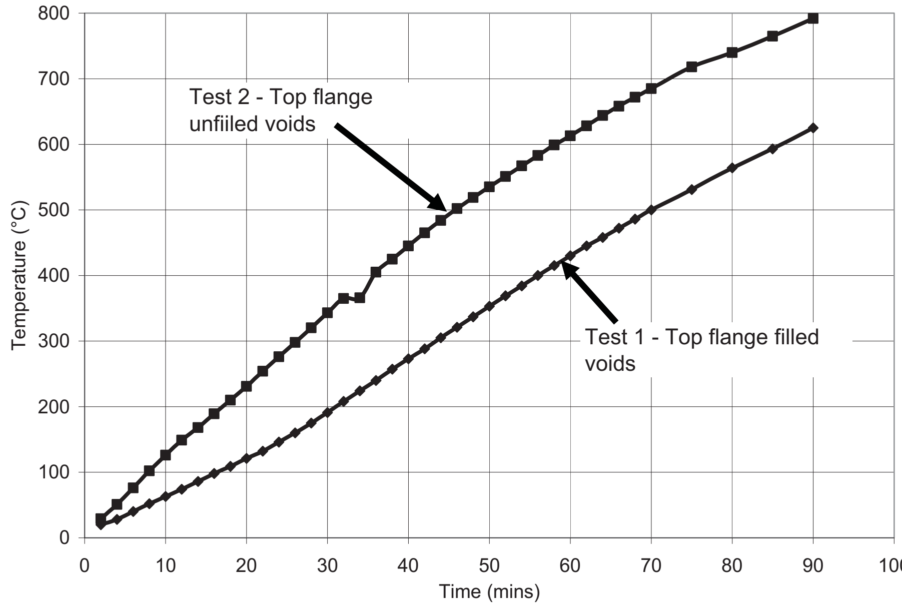

Figure C8 *Difference of top flange temperatures for Test 1 (filled voids) and Test 2 (unfilled voids)*

In the series of tests the temperature of the shear studs were measured. The temperature at the base of the shear stud in Test 3 is shown in Figure C9, where it can be seen that the stud temperature is only 84°C lower that the bottom flange temperature at 90 mins.

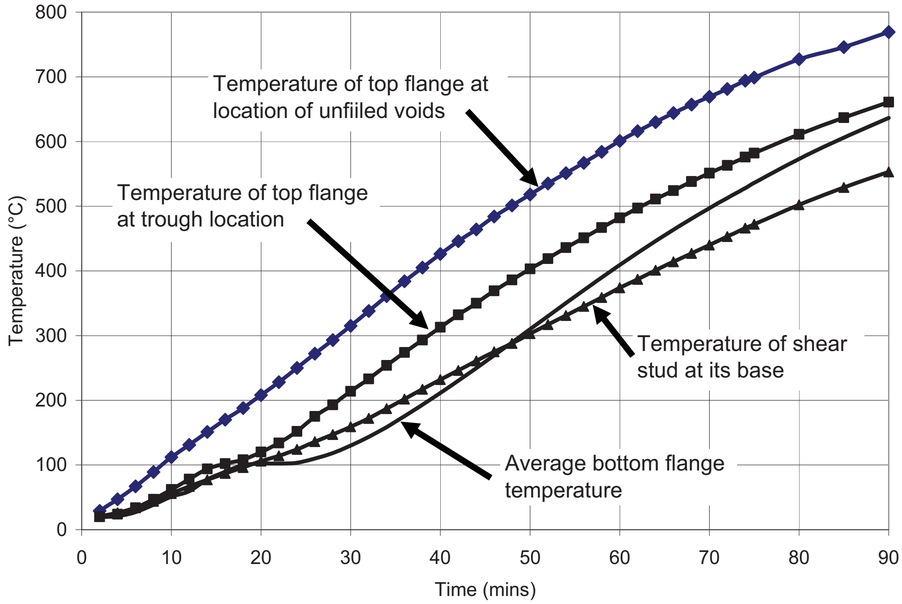

Figure C9 *Stud temperature and steel temperature for Test 3*

As a comparison for Test 1, the stud temperature is significantly lower than the bottom flange (279°C) at 90mins. A comparison between the bottom flange temperatures and shear stud temperatures for Tests 1 and 3 is shown in Figure C10. It is important when considering Figure C10 that comparisons are only made between stud and bottom flange temperatures and not between tests, since different fire protection systems are used.

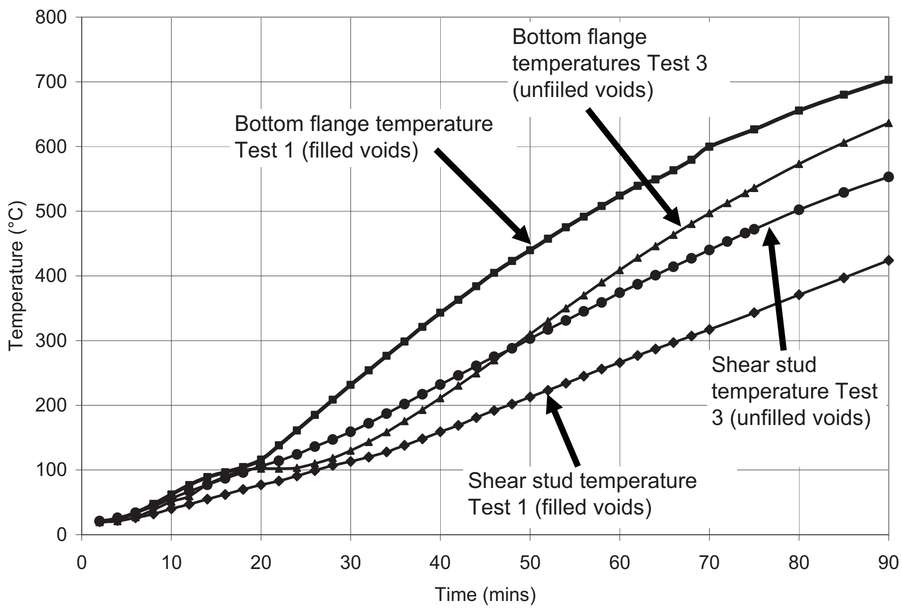

Figure C10 *Comparison between bottom flange temperatures and stud temperatures for Tests 1 and 2.*

The shear stud temperatures are significantly higher when the voids are unfilled leading to the possibility of shear stud failure. It should also be noted that the studs in the reported tests were placed in the centre of the trough whereas in practice they would be placed off-centre leading to even higher temperatures.

C4.0 Conclusion

1. If the voids are left unfilled the temperature of the top flange and upper part of the web at the void location is significantly higher compared to the case where the voids are filled. For unfilled voids the top flange is at a higher temperature compared to the bottom flange, whereas with filled voids the bottom flange is at a higher temperature.

2. With unfilled voids the temperature of the shear studs increases compared to the case where the voids are filled. This will reduce the strength of the studs and could lead to shear failure of the studs.

3. The UK has design rules, based on the test data presented in this report, which allows unfilled voids in composite beams up to 90 mins fire resistance. This involves <u>increasing</u> the thickness of the fire protection to compensate for the increased temperature of the top flange. For the WTC7 the fire resistance was 2 hours and according to the UK rules should have had filled voids. There was no evidence of the fire protection thickness being increased in WTC7 to compensate for unfilled voids. .

4. The Underwriters Laboratories (UL) document BXUV.D739 covered the specification of Monokote MK-5. This document together with the UL Fire Resistance Directory for 1983 states that the voids must be filled to achieve the required fire resistance.

C5.0 References

1) Fire Protection for Structural Steel in Buildings (3rd Edition) Revised 2004. Association for Specialist Fire Protection and The Steel Construction Institute. 2004.
2) Indicative Fire Test on Composite Concrete/Steel Deck Floor System. British Steel (RS/RSC/S10244/1/87/D) 1987
3) Joint Industry Sponsored Research: The Fire Resistance of Composite Beams with Unfilled Voids. The Steel Construction Institute. Document SCI/RT/135 July 1990.
4) Fire Resistance of Composite Beams. The Steel Construction Institute. Technical Report SCI Publication 109. 1991.

16.0 APPENDIX D

Arup Report

This Appendix presents the detailed finite element modeling carried out by Arup.

Gennet, Kallmann, Antin & Robinson, P.C

WTC -7 Structural Fire Analysis

Structural Fire Analysis Report (Runs 1-4)

January 2010

Job number 209534-00

Ove Arup & Partners Ltd
13 Fitzroy Street, London W1T 4BQ
Tel +44 (0)20 7636 1531 Fax +44 (0)20 7755 2001
www.arup.com

Contents

Appendices

Executive Summary

Introduction

Arup has been commissioned by Gennet, Kallmann, Antin & Robinson, P.C. (GKAR) to be part of an Expert Team investigating the technical reasons for the collapse of WTC 7. Specifically Arup's role is to determine the potential collapse initiating event for the global collapse, as observed on September 11th 2001, by carrying out a numerical analysis.

The aims of Arup's numerical analysis are to determine:

- The structural fire response of level 13 due to a fire on level 12
- The sequence of events, if any, that lead to collapse of that floor
- If the initiating mechanism observed in the numerical models can be related to the events of September 11th

The analysis is also to determine:

- The detailed response of critical structural components in the proximity of Column 79, since this location is deemed to contribute significantly to the observed mode of overall failure in the north-east corner of the building.
- The temperature bounds within which failure was and was not observed to occur to allow comparison with any available observed fire behaviour on September 11th

A detailed set of assumptions forming the basis of the numerical models have been created by Arup and agreed with the Expert Team

- These are intended to replicate numerically the as-built condition of the building on 11th September 2001 as per the drawings (Cantor Drawing Revision I and the Frankel steel erection and shop drawings, 1985), specifically the eastern half of the 13th floor
- Since March, over 150 models have been tested and analysed and approximately 1,000GB of data produced allowing the Expert Team to intensively review and understand the structural fire response of WTC 7
- Therefore, the complexity of the data modelled and the modelling techniques used, mean that any data produced can be considered as being substantially useful in interpreting the structural fire response of WTC 7.

This report is subdivided in the following main sections:

1. Executive summary which summarises the findings and conclusion of the analyses
2. The main body of the report which consists of 10 sections
    - Section 1 presents the introduction of the report.
    - Section 2 provides a brief description of the numerical model.
    - Section 3 describes the four cases that are presented in this report.
    - Section 4 describes the temperatures used in the structural fire analysis.
    - Sections 5 to 8 present the results from each of the four parametric runs.
    - Section 9 presents a comparison of the results of the four parametric runs.
    - The conclusions are presented in Section 10.
3. Appendices which contain the detailed output of the four parametric runs and the modelling assumptions forming the basis of all the numerical work.

Objectives of Structural Fire Analysis

The objective of the numerical analysis is to investigate:

- The detailed structural fire behaviour of the eastern side of level 13 due to a fire occurring on level 12 (the sub-model), and in particular:
    - The detailed responses of the three girders that are supported off column 79 – deemed to be the primary collapse initiating event as they corresponded to the area where collapse was observed to have initiated.
    - The detailed behaviour of the connections around columns 79 and 44 in fire.
    - The potential for alternative initiating collapse event locations in the east portion of the 13th floor (particularly around columns 80, 81, 76, 26 and the beams/girders that are attached to these columns).

As a result, the extent of the model and level of detail of the model reflects the intent of the analyses to investigate the above behaviours, as shown in Figure 1. Further description of the structural fire model is provided in Section 2.

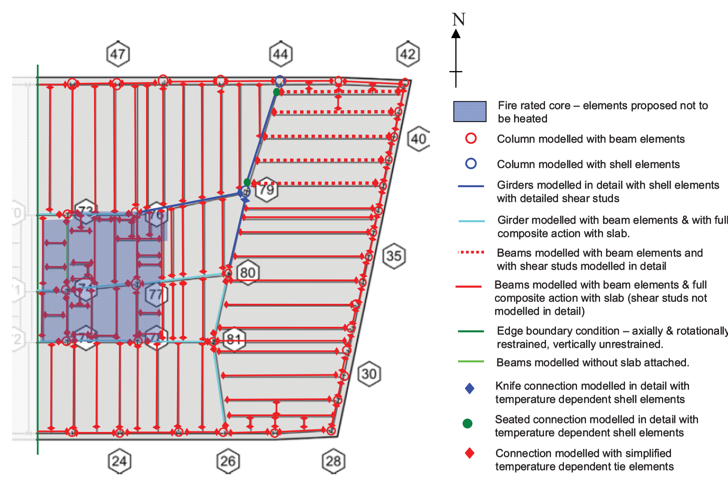

Figure 1: Schematic Description of the Extent of the Model of Level 13

Parametric Analyses

The description of the four parametric analyses that are presented in this report are summarised below. These four parametric analyses have been agreed as the most likely to demonstrate potential collapse initiating events and provide structural fire behaviours that are important to understand the resulting global collapse of WTC7.

They are as follows.

Case 1:

- ***Fire Exposure*** – Constant heating with 700°C gas phase temperatures for 1 hour occurring throughout the entire floor plate of the sub-model, followed by a 1 hour cooling period with the gas phase at 20°C (See Section 4.1 for further description of the fire).
- ***Flute Condition*** – Unfilled. This represents the condition of the as-built structure.

Case 2:

- ***Fire Exposure*** – As per case 1.
- ***Flute Condition*** – Filled with fire protection material. This represents the required fire protection state of the structure in accordance with the UL Fire Resistance Directory.

Case 3:

- ***Fire Exposure*** – Constant heating with 800°C gas phase temperatures for 1 hour, occurring throughout the entire floor plate of the sub-model, followed by a 1 hour cooling period with the gas phase at 20°C (See Section 4.1 for further description).
- ***Flute Condition*** – Unfilled

Case 4:

- ***Fire Exposure*** – As per case 3
- ***Flute Condition*** – Filled

Findings produced from the Results of the Numerical Analyses

Key Findings

A collapse initiating event is observed on the 13th floor. This mechanism is observed specifically when the peak temperature is 700°C and the flutes in the concrete deck are left unfilled. The mechanism occurred after the fire had decayed and the structure was cooling down.

An early failure is observed when the peak temperature is 800°C and flutes are left unfilled. Failure is not observed to occur in the other 2 parametric runs where the flutes in the concrete deck are filled.

The initiating collapse mechanism is when the primary girder spanning between columns 79 and 44 in the north-east is pulled off its seat at column 79.

Critical points to note:

- Collapse does not occur in fires less severe than 700°C heating for an hour
- The collapse mechanism only occurs when the flutes are unfilled
- When the flutes are filled, as was required by code, collapse at 800°C and 700°C fires is not observed

It is proposed that the structure supported by Column 79 is the primary instigator of collapse in fire because:

- Three large, long span girders span onto this column. The long span girders support the largest floor area and carry higher loads compared with shorter span girders. The long spans also mean that the girders would deflect downwards more due to thermal curvature. The thermal expansion of these three girders would exert high thermal thrust forces when heated, onto their end connections and also the column.
- The geometrical arrangement of the three girders on column 79 is unique compared to the rest of the floorplate. Girder 76-79 intersects column 79 at a higher angle from the perpendicular compared with other girders on this floor. This means that the end connections of this girder may not be able to transfer their thermal expansion thrust force to the columns. Instead the connections may undergo significant damage as they would have to resist the thermal expansion forces.
- Girder 79-44 supports secondary beams on only one side. The secondary beams (on one side of the girder) will freely be able to push and pull onto Girder 79-44 when they expand and contract without secondary beams on the other side of the girder to resist them. This damages the connections at the ends of Girder 79-44 and can cause it to be pulled off its seat.

The peak temperatures of the fire assumed in the numerical analyses are important as:

- They affect the temperatures and strength of the protected steel and the potential failure mechanisms that could occur in the structure.
- They affect the time when collapse occurs compared with observed physical events on September 11th 2001. A high peak fire temperature can cause a collapse initiating event during the heating phase of a fire; however, with a lower peak temperature, a collapse initiating event can be produced after the fire has decayed and when the structure is cooling down.

Specific Results from the four Parametric Studies

Flutes Unfilled Cases

- The Case 1 analysis (700 °C heating, flutes unfilled) showed a collapse initiating event at the end of the 2 hour analysis (60 minutes into the cooling period).
  - The collapse initiating event is in the form of girder 79-44 being pulled off its seat at column 79 by the secondary beams in the North-East corner, during the cooling period.
  - The average temperature of the secondary beams when this collapse mechanism is observed is 38°C and hence, the secondary beams would have regained their full strength and stiffness. Despite regaining their full strength and stiffness, the cooling causes the secondary beams in

the North-East corner to contract which forms additional tension forces in the beam and thereby pulls the supporting girder laterally off its seat.

- A significant number of shear studs on the five secondary beams break during the cooling phase, from 41% at the end of heating (60 minutes) to 86% at 10 minutes after the end of heating (70 minutes). At the end of the 2 hour analysis (60 minutes in cooling), nearly all (98%) of the shear studs on the five secondary beams attached have broken and approximately 75% of the shear studs on the girder 79-44 have broken.
- The breaking of the shear studs is important to girder 44-79 being pulled off because:
  - This allows the secondary beams to act as non-composite beams and to sag further (as a non-composite section has lower flexural stiffness), pulling the girder off its seat.
  - If the shear studs on girder 79-44 had not broken then it is unlikely it would have been pulled off the seated connection.

- When heated to a higher temperature of 800°C, Case 3 shows a similar structural response, i.e. the girder spanning between columns 79-44 is pulled off its seat at column 79 by the secondary beams which are supported by this girder (in the North-East corner of the building). However, in the 800°C fire, this occurs earlier, at the advanced stages of the heating phase, commencing 47 minutes into heating.

  At the point when the collapse initiating event commences (again the girder 79-44 is pulled off its seat):

  - The temperature of the top flange of the girder 79-44 is at 687°C. The strength and stiffness of the steel are 26% and 15%, respectively. All the shear studs on this girder have broken.
  - The residual strength and stiffness of the secondary beams are 16% and 11%, respectively. This low strength and stiffness of the secondary beams cause large sagging deflections in the beams. 96% of the shear studs on the five secondary beams attached to the girder have broken.
  - The breaking of the shear studs on the secondary beams and girder 79-44 has the effect of reducing the flexural rigidity of the weakened beams/girder. This induces larger deflections leading to the collapse of the secondary beams and then girder 79-44 being pulled off its seat.
- These two cases (Cases 1 and 3) show that the potential collapse initiating events are centred around column 79, which is the area consistent with the visually observed kink in the building frame on September 11th 2001.

Flutes Filled Cases

- The collapse mechanism (girder 79-44 being pulled off its seat associated with the connection to column 79) shown in the flutes unfilled condition are not observed. This is primarily due to the lower steel beam/girder temperatures in the flutes filled condition which in turn result in higher strengths and stiffnesses.
- If the flutes were filled, as was required by code, Cases 2 and 4 with the 700°C and 800°C heating, respectively, show that no potential collapse initiating events are observed.
- The structure is stable.
- The vertical deflections of the beams across the floor in the flutes filled condition are generally less compared with the flutes unfilled condition because of the difference in fire exposure between the flutes filled and unfilled cases.

Overall Global Structural Fire Behaviours observed from the analyses

Floor Structure

- The floor structure of the building during fire exposure, prior to any collapse initiating event occurring, shows that the largest vertical deflections occur in
  - the bays with long span secondary beams (e.g. North East and Eastern bays) and
  - where the floor panels are subjected to high axial restraint (e.g. Southern and South East bays).
- The deflections are attributed to:
  - The long spans, which mean more thermal expansion than in shorter beams
  - The axial restraint to beams/girders which means that only some thermal expansion is accommodated horizontally and therefore, members have to deflect downwards
  - The thermal gradients in the slab which cause the slab to deflect downwards, and
  - The decreasing stiffness of the heated beams/girders.
- Large vertical deflections are significant because they can reduce the stability of the structural arrangement which can increase the likelihood of collapse.
- The change in secondary beam spanning direction in the Eastern structural bays introduces an imbalance in the restraint provided to the primary girders. Expansion of the floor system leads to the girders supporting the Eastern bay secondary beams being moved in an east-west direction without significant restraint from adjacent structure.
- The inclusion of shear studs to the girders is significant because the girders in WTC 7 become composite sections, increasing their flexural rigidity compared to a non-composite girder of the same section size. The increased flexural stiffness in the composite girders is significant because:
  - They exhibit relatively small vertical deflections compared to that expected from a non-composite section of the same size.
  - Stiffer girders lead to lower deflections. This means that thermal expansion of the member results in high forces being transferred into the connections, rather than increased downward deflections.
  - The high compressive forces in the girders and their connections may increase the likelihood of failure of these members and therefore the likelihood of collapse.
- In the outer bays, (bays at the façade edge of the floor plate) thermal expansion of the floor results in outward movement of the perimeter beams and columns. Because the columns are highly protected and cold they are able to cope with this movement.
- In the internal bays, thermal expansion is restrained by the floor structure of the outer bays. This causes additional compression forces to form in the slab and the beams/girders. The compression forces result in deformation to the connections and also the beams/girder.
- During the cooling phase, the structural elements of the floor cool and contract. The contraction of the beams and slab mean that the vertical deflections of these elements start to reduce. However, the contraction of the beams also imposes additional tension forces on the connections of the beams and can cause failure of the connections if they cannot deform under this imposed load.

Column Behaviour

- Throughout the heating and cooling phases, the perimeter and internal columns showed small deformations and no buckling / collapse of the columns. This is attributed to the low temperatures of the columns because of their large size and the protection applied to the steel (maximum steel temperature of 122°C – for highest fire temperature). Therefore, the columns retain their full strength and stiffness.
- These cold columns, relative to the floor beams, provide a rigid restraint at the ends of the girders. The columns on the external edge of the building are pushed outwards by the expanding composite girders and secondary beams by about 40mm (1.6"). This is not considered to be significant in leading to a failure mechanism that could lead to collapse as the cool columns have significant reserve capacity to deal with the resulting eccentric loading.

Connections

- Breakages of connections were observed in secondary beams (beams which support the floor slab but are not connected directly to a column) that were modelled with simplified connections, in three of the four parametric runs. In all of these cases, the connections failed in tension during the cooling phase. The failures of these simplified connections did not cause instability in the structure in any of the four cases. It is considered reasonable that the global structure can survive the loss of some secondary beams due to the known effect of floor loads being carried through tensile membrane action in the slab.
- In all four cases, the simplified connections of the primary girders spanning between the columns remained intact and did not fail. This supports the theory that the connections modelled in detail are the most critical. Failure of the connections where primary girders span between columns only occurred in the seated connection modelled in detail at column 79.

Comparison with the Observed Events and Fire Locations on September 11th

At the time when WTC7 collapsed on September 11th2001, the fire on level 12 which was heating level 13, had already decayed in the north eastern corner of the building, which is the area where collapse of the building started. The timing of the potential collapse initiating event shown by the analysis of Case 1, which occurs late in the **cooling** phase, would be consistent with the events of September 11th if the collapse initiating event is located on the 13th floor.

The collapse initiating event shown in Case 3, which occurs late in the **heating** phase, could correspond to events of September 11th if the potential collapse initiating event was located on the 10th floor when at the time of collapse, there was a fire still burning on the 9th floor.

1 Introduction

Arup has been commissioned by Gennet, Kallmann, Antin & Robinson, P.C. (GKAR) as part of an Expert Team to investigate the structural fire response of Level 13 of WTC7 to determine what, if any, collapse initiating event in the North-East corner of WTC7 caused global collapse of the building on September 11th, 2001.

The numerical analysis is undertaken using a specialised finite element program, ABAQUS, which is specifically tailored to take account of the highly complex response of building structural elements under exposure to elevated temperatures.

This document presents the results of the structural responses observed in the numerical analysis of four final parametric runs that have been requested by the Expert Team.

1.1 Objective of Analysis

The objective of the analysis is to determine if there is a collapse initiating event which occurred on Level 13 of WTC7, due to fire, particularly in the area of Column 79.
The analysis is also intended to provide significant detail on behaviour leading to a collapse initiating event, in fire, in the area surrounding column 79.
It also investigates whether or not it was possible for a collapse initiating event to occur elsewhere on this floor, particularly around columns 80, 81, 76, 26 and the beams that are attached to these columns.
A few critical aspects of the structural behaviour in fire were considered necessary for a highly complex level of detailed analysis:

1. The detailed behaviour of the three girders that are supported by column 79 under fire conditions.
2. The detailed behaviour of the connections on columns 79 and 44 which support the girders.
3. Investigate the global behaviour of the floor running the entire width (North-south) of the floor plate on the eastern side of Level 13, and to consider the effect of the girders spanning columns 44-79, 76-79, 79-80, 80-81 and 81-26.
4. To investigate other potential alternative column failure locations (for instance: columns 80, 81, 76, 26 and the beams/girders that are attached to these columns).

1.2 Layout of Main Body of Report

The main body of this report is subdivided in to 8 sections:

- Section 1 presents the introduction of the report.
- Section 2 provides a brief description of the numerical model.
- Section 3 describes the 4 cases that are presented in this report.
- Section 4 describes the temperatures used in the structural fire analysis.
- Sections 5 to 8 present the results for each of the four parametric runs.
- Section 9 presents a comparison of the results of the four parametric runs.
- The conclusions are presented in Section 10.

2 Structural Fire Numerical Model of Level 13

Complete details of the build-up of the numerical model and all assumptions forming it are presented in Appendix B of this report.

The following is a short summary for the purposes of clarity prior to reading Appendix B.

2.1 Extent of Structural Model

The extent of the structural fire model proposed by Arup and as agreed with the Expert Team is shown in Figure 2. Full details of the assumptions made in the structural fire model are provided in Appendix B of this report.

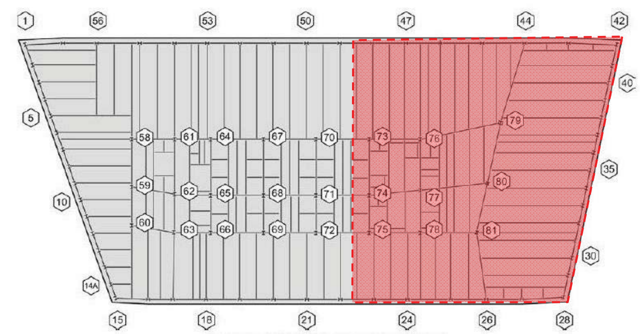

Figure 2: Extent of floor area of structural fire model of level 13 (shaded in red)

2.2 Description of ABAQUS Model

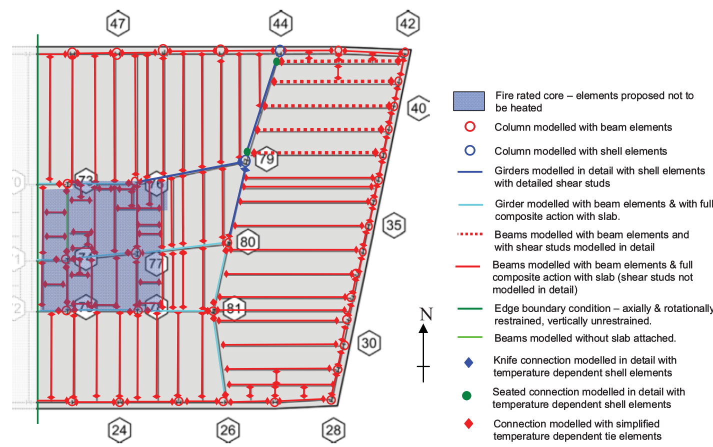

Figure 3: Description of the model of the Eastern Side of Level 13 (Numbers refer to the column numbers)

Figure 3 shows a schematic describing the key build-up of the structural fire model. The structural fire model consists of:

- 138 beams/girders – 3 girders are modelled in detail, between column 76-79, 79-44, 79- 80
- 35 columns – Columns 44 and 79 are modelled in detail
- 268 connections – 4 connections are modelled in detail, consisting of 2 knife connections at column 79, 1 seated connection at column 79 and 1 seated connection at column 44.
- This sub-model models three girders and two columns in detail using shell elements, (marked in blue in Figure 3). Shell elements are used to study the detailed behaviour of these girders and columns, such as local buckling.
- All the other beams, girders and columns are modelled using beam finite elements (i.e.: 2-noded linear elements).

The blue shaded region in Figure 3 shows the extent of the fire rated core. All structural frame elements and the floor slab located within this shaded core region are assumed to be not heated for the structural fire analysis. This is because the core is assumed to have remained intact and therefore no fire exposure to the core elements occurred.

The 3D model of the structural frame built in ABAQUS is shown in Figure 4.

The structural model includes the additional shear studs on the girders and secondary beams described in the memo "Construction Schedule/Shear Stud Addition" dated 25th June 2009 from GNA.

The model also includes the trench header ducts (gaps in the slab for services) running in the depth of the concrete slab as provided to Arup by GNA on 22nd June 09. The positions of the trench header ducts modelled in the ABAQUS model are shown in Figure 5.

Figure 6 shows the position of the key structural column, beam and girder locations that will form the basis of discussions in this report.

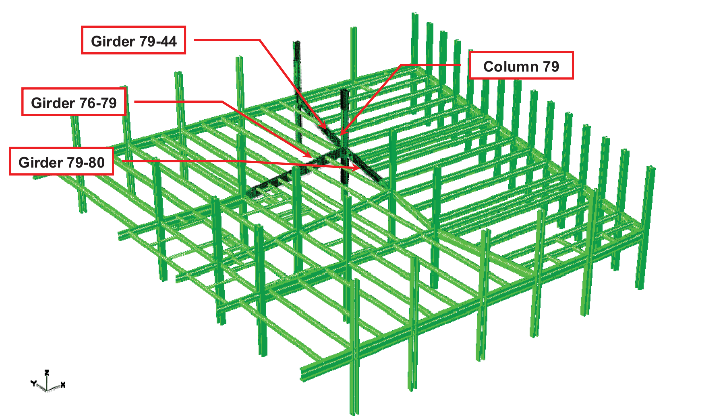

Figure 4: 3D image of structural fire model showing the beams of level 13 and columns spanning from the level below to the level above. (Slab surface not rendered to provide clarity of beam / girder locations)

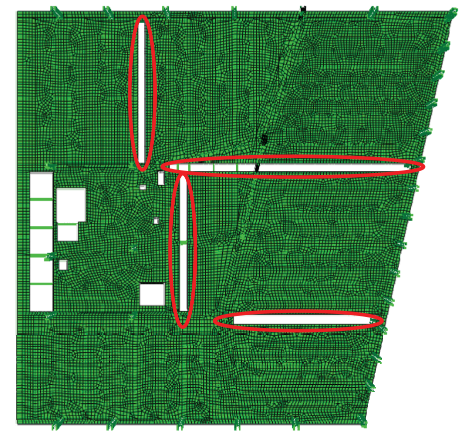

Figure 5: Plan view of ABAQUS model with slab surface rendered. Positions of trench header locations in are circled in red

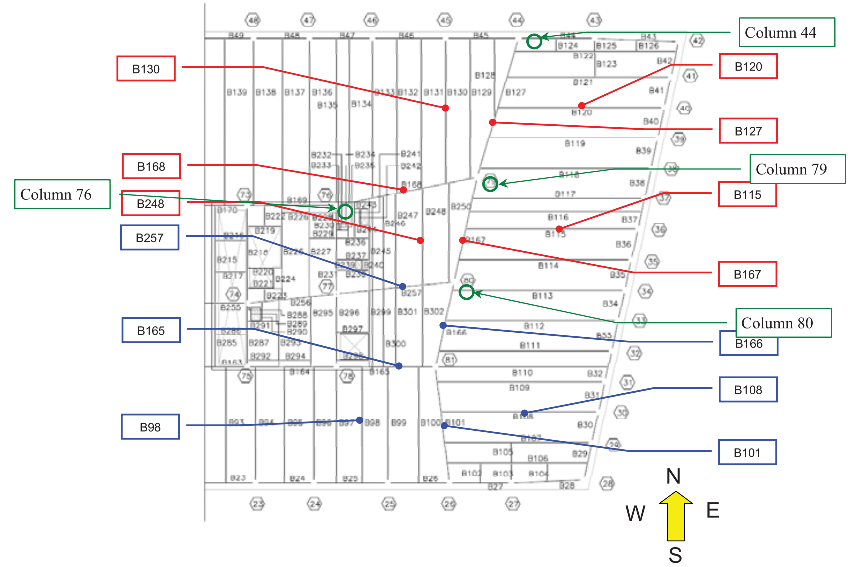

Figure 6: Plan view of ABAQUS model showing beam and column layout (Slab surface not rendered). Locations of key columns have been indicated.

JA-3172

2.3 Description of Detailed Connections

Figure 7 to Figure 12 show the configuration and layout of the girders and connections at columns 79 and 44 which have been modelled in detail using shell elements. Shells are used to represent the plates and can model the detailed behaviour of the plates of the girders and columns such as local buckling; this behaviour cannot be captured using beam elements.

Figure 9 to Figure 10 shows the details of the seated connections, particularly, locations of the connector elements which represent the bolts (represented by the small blue filled circles).

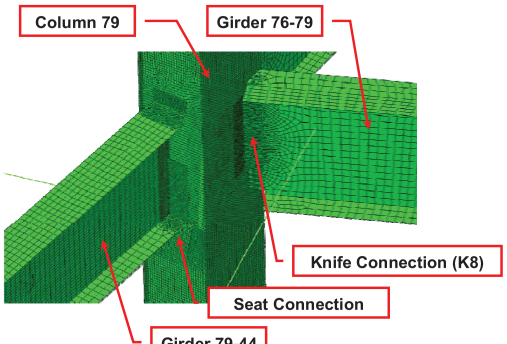

Figure 7: ABAQUS rendering of arrangement of detailed girders and connections at column 79 showing seated connection and the K8 knife connection.

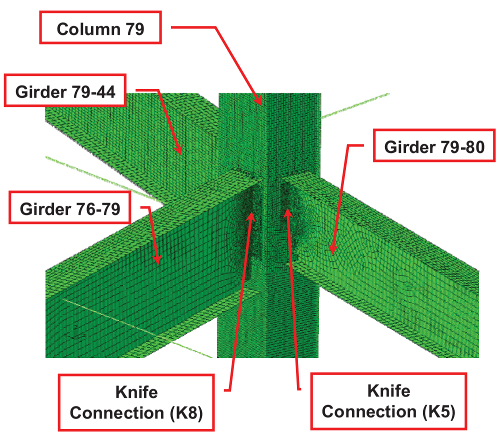

Figure 8: ABAQUS rendering of arrangement of detailed girders and connections at column 79 showing the K8 and K5 knife connections.

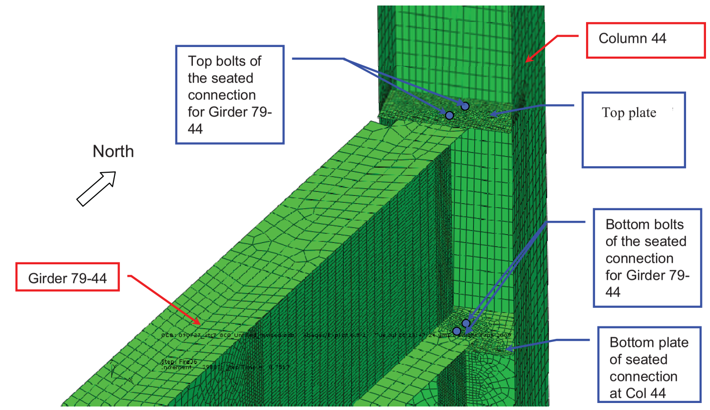

Figure 9: Isometric view of detailed girder and connection at column 44 (Connectors representing bolts are shown by the blue dots)

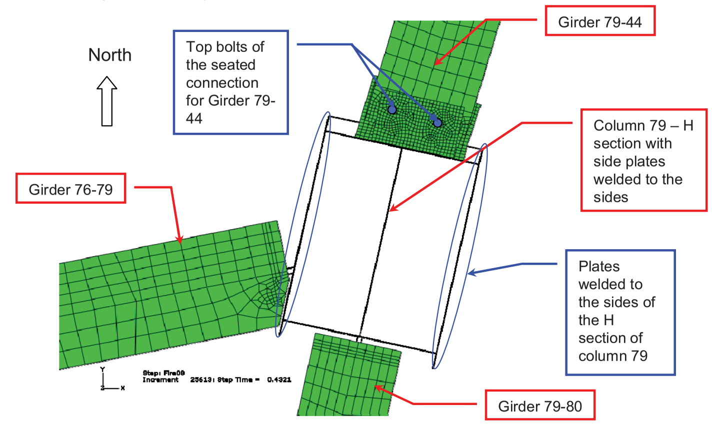

Figure 10: Plan view of girders intersecting at column 79 (Connectors representing bolts are shown by the blue dots)

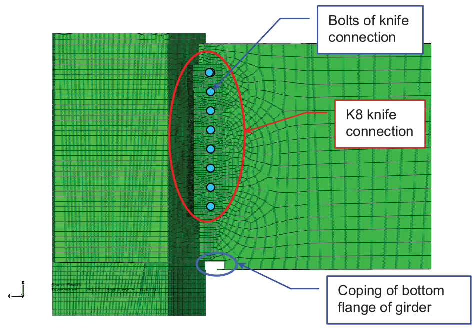

Figure 11: K8 Knife connection viewed from the north (Connectors representing bolts are shown by the blue dots)

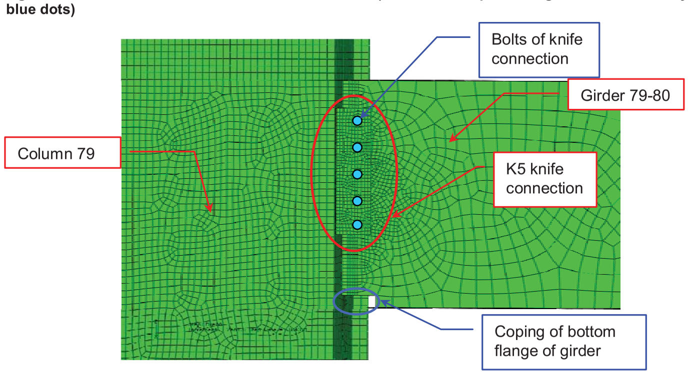

Figure 12: K5 Knife connection viewed from the west (Connectors representing bolts are shown by the blue dots)

3 Parametric Analysis: Definition of Case 1, 2, 3 and 4

The description of the four parametric runs that are presented in this report are summarised below. These four parametric runs have been agreed as the most likely to demonstrate a potential collapse initiating event and could provide structural fire responses important in understanding the resulting global collapse of WTC7.

These are as follows: -

Case 1:

- ***Fire Exposure*** – Constant heating with 700°C gas phase temperatures for 1 hour occurring throughout the entire floor plate of the sub-model, followed by a 1 hour cooling period with the gas phase at 20°C (See Section 4.1 for further description).
- ***Flute Condition*** – Unfilled. This represents the condition of the as-built structure. (Note that the flutes are the voids formed the steel decking and the steel beams).

Case 2:

- ***Fire Exposure*** – As per case 1.
- ***Flute Condition*** – Filled. This represents the required fire protection state of the structure in accordance with the UL Fire Resistance Directory.

Case 3:

- ***Fire Exposure*** – Constant heating with 800°C gas phase temperatures for 1 hour, occurring throughout the entire floor plate of the sub-model, followed by a 1 hour cooling period with the gas phase at 20°C (See Section 4.1 for further description).
- ***Flute Condition*** – Unfilled

Case 4:

- ***Fire Exposure*** – As per case 3
- ***Flute Condition*** – Filled

The numerical analyses reported here include the additional shear studs on the girders and secondary beams and trench headers in the slab.

4 Temperatures of Structural Elements

4.1 Design Fires

The duration of the structural fire analysis is up to 2 hours using the temperature-time relationships (fire curves) shown in Figure 13. These fire curves are discussed in more detail in the report submitted by Fred Mower.

- The first hour of the fire analysis is a constant gas temperature exposure over the entire floor of Level 12. The gas temperature is to be applied to simulate a fire on Level 12 which heats the underside of the floor slab of Level 13 and the columns of Level 12. For Cases 1 and 2, the gas temperature exposure is 700°C and for Cases 3 and 4, the gas temperature exposure is 800°C.
- The second hour of the analysis is a cooling period, where the structure is subjected to ambient temperatures (20°C).

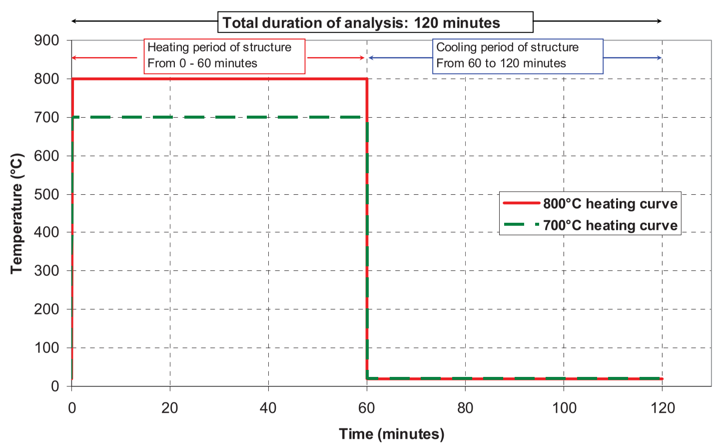

Figure 13: Temperature time curves for structural fire analyses

4.2 Temperatures of Structural Elements

Figure 14 shows a typical steel beam temperature over the 2-hour analysis duration, considering the bottom flange, web and top flange locations under exposure to the 800°C fire. The temperatures of the girder between columns 79-44 for both the flutes filled and unfilled condition are used as an example.

Figure 15 shows a typical column temperature, assumed uniform over its cross-section, for the same 800 °C fire exposure. The temperatures of column 79 under exposure to four sided exposure to the 800°C fire are shown as an example.

As the building structure consists of different steel section sizes, the temperature-time histories of each of the different structural steel members differ from each other depending on the size of the structural members and the number of sides of the section that are heated.

The temperature data for each of the different steel structural elements for different heating conditions were provided by Professor Jose Torero of the Expert Team and have been incorporated in the ABAQUS structural fire model. For more detail refer to expert report by Fred Mower.

Figure 16 shows the concrete slab temperatures at various depths through its equivalent thickness due to an 800°C fire heating the underside of the slab. This type of temperature-time history is applied uniformly throughout the heated areas of the floor slab (the core is not heated).

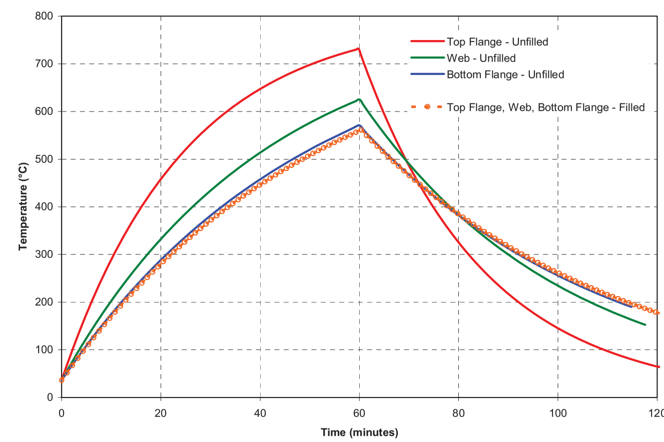

Figure 14: Typical girder temperatures used in the analysis (Girder 44-79, section type W33x130) under 800°C heating for the flutes filled and unfilled condition

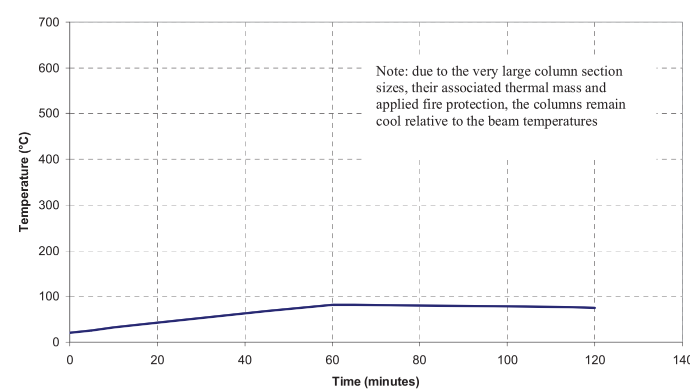

Figure 15: Typical column temperature used in the analysis (Temperatures shown for Column 79 under exposure to 800°C on four sides of the column)

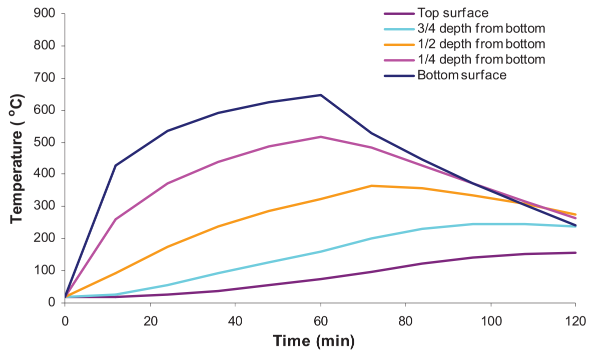

Figure 16: Temperatures across the equivalent depth (102mm, 4") of the concrete slab used for the analysis. Temperatures shown for the slab exposed to the 800°C fire from below

5 Case 1 (700°C Unfilled Flutes Model)

This section presents the response of the Case 1 sub-model of WTC7. It is split into the following sub-sections:

- Section 5.1 describes the general response of the model
- Section 5.2 presents details of the column response in the model
- Section 5.3 describes details of the composite floor and discusses the expected and observed responses.
- Section 5.4 reviews the response of connections in the model
- Section 5.5 presents a summary timeline of the key structural responses

5.1 Overview of Structural Response

The Case 1 model includes the following structural details:

- Heating phase of <u>700 °C</u> gas-phase for 1 hour, followed by 1 hour where gas phase is at 20°C
- <u>Flutes unfilled</u>, providing reduced protection to top flange of all beams

The response of this model is generally in accordance with known structural phenomena in fire:

Heating

- During the heating phase all structural members expand as they heat up, leading to relatively large mid-span deflections.
- Due to the relatively light, yet realistic floor load for the fire limit state condition applied to the model in accordance with the Master Assumptions List [1], the observed vertical deflections are low. In particular the primary girders deflect less than 200mm (8") at peak heating.
- As the girders are too stiff to deflect downwards under the realsitc live load, they expand longitudinally into the connections and columns. Note that if the loading were to be increased, the girders would still expand longitudinally in the early stages of the fire.
- When the girder between Column 44 and Column 79 is subjected to this horizontal expansion it quickly breaks its restraining bolts at column 79. This allows the girder to be moved around on the seat plate at Column 79. During the heating phase the girder end at Column 79 is pushed into contact with the western column side plate.
- K8 and K5 knife connections at Column 79 undergo some deformation caused by expansion of Girders 76-79 and 79-80. However at the point of peak heating the angle plates are not significantly damaged and none of the bolts have broken.
- During the heating phase a significant number of shear studs are broken, however it is considered that the secondary beams and girders retain enough connection to the slab in heating to act in a largely composite manner. It is to note that the spacing of the shear studs would indicate that full connection cannot be achieved and is therefore considered only as partial connection.
- As the model approaches maximum heating there are no signs of imminent structural failure.

Cooling

- During the early stages of the cooling phase a significant percentage of the remaining shear studs connecting the north-east bay secondary beams to the slab break. This leads to increased deflections in secondary beams in the north-east corner.
- Additionally a number of secondary beams begin to break their connections. The majority of these members are in the central bay and the breakage of the connections has no discernable effect on the global response of the structure in this analysis. This is because the concrete slab is able to redistribute the floor load directly to the primary girders.
- As the cooling phase continues the existing mid-span deflection of the secondary beams in the north-east corner, combined with the general contraction of the structure during cooling, leads to the South end of Girder 79-44 being pulled Eastward across its seating plate.

- Finally, at the end of 120 minutes of heating and cooling the end of the girder is sitting precariously at the side of the seat (Figure 17).

The structural response described above is presented in more detail in the following sections.

A more detailed timeline may be found in Section 5.5.

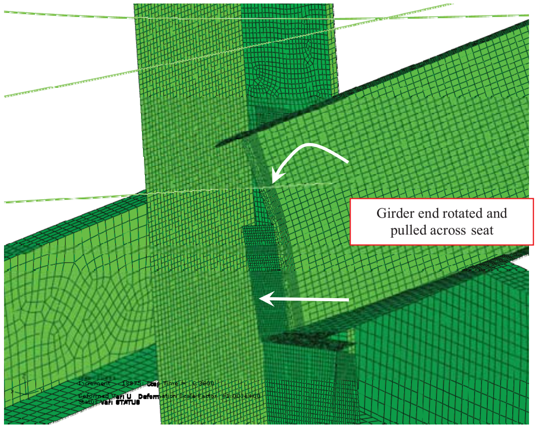

Figure 17: 700°C Unfilled Flutes Case 1 - Column 79 Seated Connection at End of Cooling

5.2 Details of Column Behaviour

No column buckling was observed in the model during the analysis. Figure 18 shows the undeformed shape of the columns.

All internal columns remained vertical throughout the analysis, with no significant lateral displacement observed while the perimeter columns showed some outward bowing.

Figure 19 shows the outward movements as a function of time of selected columns along the north, south and east façades.

The columns along the north façade and the south facade of the structure are observed to have greater outward movement (up to 50mm (2”) at the north façade at 20 minutes) compared to that of the eastern façade.

Figure 20 indicates the location of the columns being compared. The greater outward movement of the north and south façade columns is attributed to the thermal expansion of the north-south beams spanning onto these columns (Figure 21), which is resisted by the beams in the central bays and the cold core.

As there are no beams on the west side of the girders running between columns 44-26, there is no axial resistance to the thermal expansion of the secondary beams. Therefore, the thermal expansion of these secondary beams occurs in both the girders, and the eastern façade columns, thus resulting in comparatively smaller outward movement of the eastern façade (Figure 22). This means that the floor in these outer bays is relatively unrestrained, when compared to the bays with beams spanning north-south.

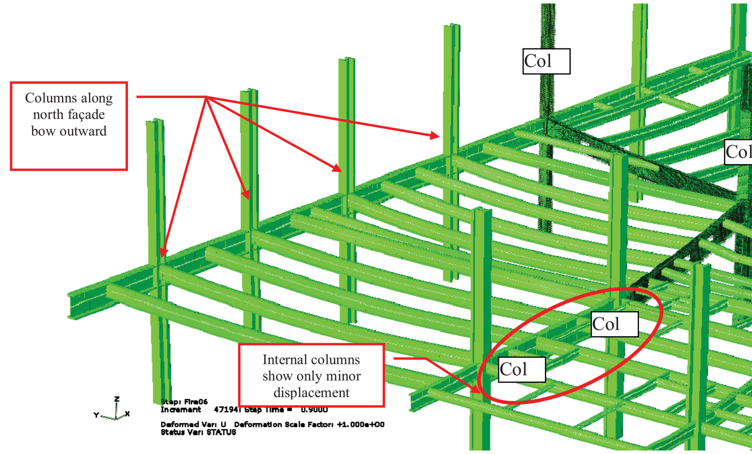

Figure 18: Deflected shape of structure along the north façade

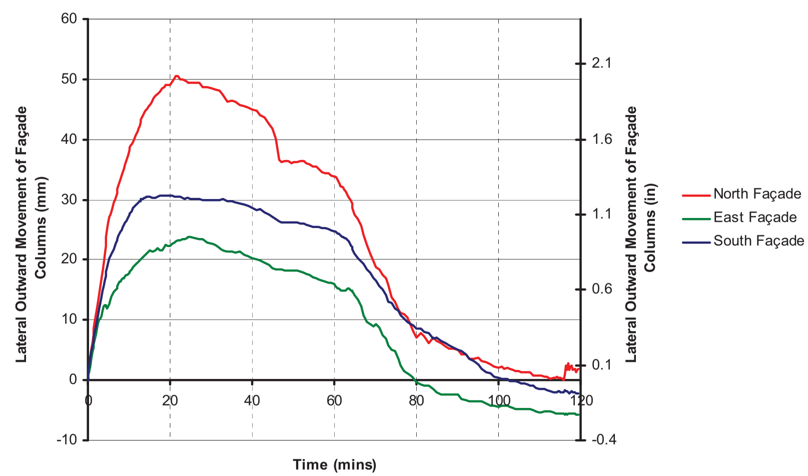

Figure 19: Outward movements of selected columns along the perimeter of the building. (Positive (+) movement indicates outward movement) Refer to the Figure below for the positions of the columns that were plotted.

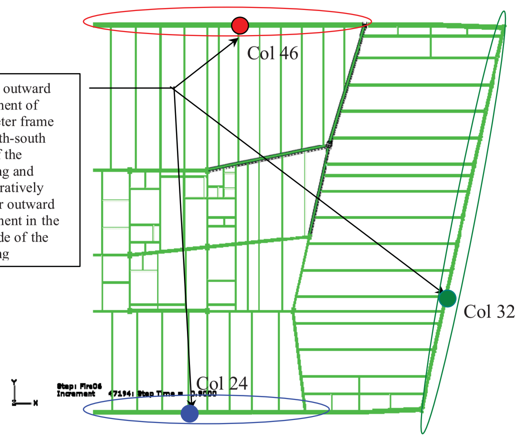

Figure 20: Structural Layout at Ambient highlighting column locations for Figure 19

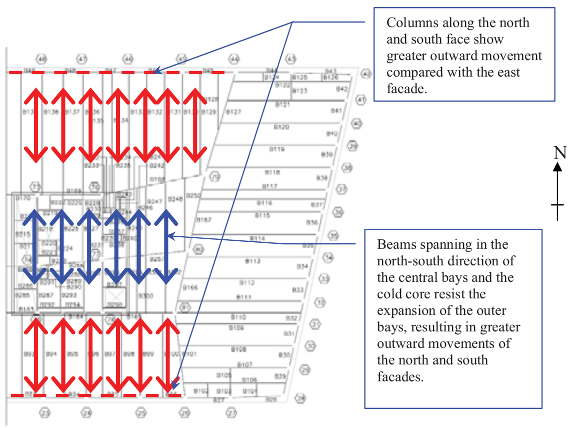

Figure 21: Mechanism which causes the greater observed movement of the north and south façades

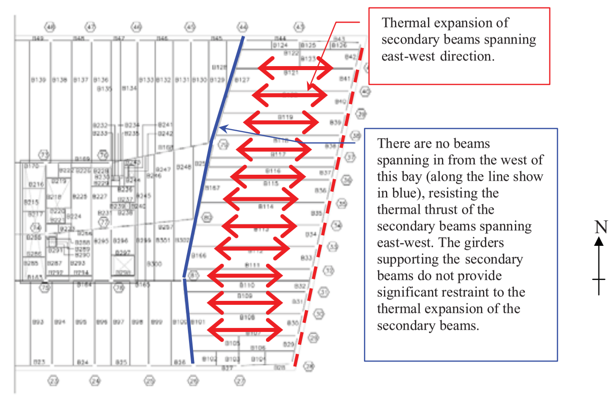

Figure 22: Mechanism which causes the smaller observed movement of the eastern façade

5.3 Details of Composite Floor Response

As with all structures that are heated, the sub-model of the WTC7 structure exhibited the combined effects of thermal expansion and thermal bowing. The effects of differential expansion between the various structural members lead to the range of responses observed in the model.

To ease understanding of the various responses observed in the model this section has been split into heating and cooling phases. Additionally a short discussion of the consequences of trench headers has been included.

Where appropriate, the results of the structural model have been compared to hand calculation methods to ensure that the model is providing reasonable results.

5.3.1 Heating phase

Throughout the heating phase the combined effects of restrained thermal expansion and thermal bowing act to increase floor deflections. This is the most visible response of a structure to fire, however a simple analysis of deflection does not give the full picture due to the ability of structures to redistribute loading. Please refer to Figure 23 for an example of deflections at peak heating

The primary girders were originally designed as non-composite members, but were then later, during construction, provided with shear studs. This means that they are significantly stronger and stiffer than either a non-composite structure, or a structure that was originally designed to be fully composite.

This leads to the following response:

- Mid-span deflections are small. This is particularly apparent in the primary girders.
- Low deflections encourage members to expand longitudinally, rather than deflecting vertically at their mid-span. This has a direct impact on the compression forces developed at the connections. This impact is discussed in more detail in Section 5.4.

JA-3178

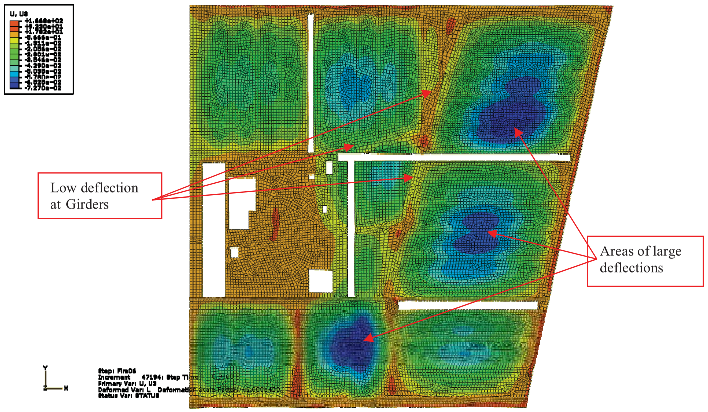

Figure 23: 700°C Unfilled Flutes Case 1 - Vertical Deflection Contours at Peak Heating

The response of a structure in fire will differ depending on whether composite action is available. If there is no composite action then the beam and the slab respond as separate entities. Therefore if the beam is not uniformly heated then the overall strength of the structure will be based on the portion of the beam that is heated most. In the case of unfilled flutes the hottest part of the beam is the top flange.

During the heating phase of the WTC7 analysis less then half the available shear studs in the north-east bay fail (Figure 24). This indicates that composite action is still largely available, assisting the strength and stiffness of the structure.

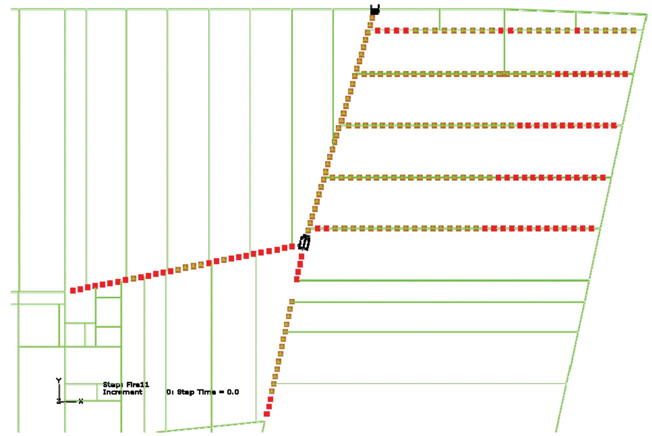

Figure 24: 700°C Unfilled Flutes Case 1 - Shear Stud Breakage (highlighted as red dots) at Peak Heating. Intact shear studs are shown in brown.

If composite action is available then the strength of the floor system is based on the beam and the slab working together. Concrete responds well under compression, however it is not good at resisting tension. Steel is equally good at resisting tension and compression; however it is a more expensive material. Composite floor systems are popular and effective precisely because they combine key benefits of concrete and steel to produce an efficient means of carrying floor loading.

As indicated in Figure 25 the slab effectively acts as a large top flange and resists compression forces, while the whole of the steel beam acts as a bottom flange and resists tension. Working together in this way allows each portion of the structure to act in ways they are well suited to and proportionally increases the overall strength of the structure compared to each part working in isolation.

Another important point to note is that heating of the top flange in a composite floor system will have less of an effect in flexure than if the beam was acting alone. This is because a beam acting alone relies on the top flange to resist compression, while in a composite floor system the compression forces are resisted by the concrete slab, with the top flange being largely unstressed.

Assuming a beam acting in isolation it is possible to do a simple calculation to work out the temperature at which failure of the beam will occur, based on the applied load. When this calculation is applied to the secondary beams in the north-east corner it is indicated that the beam failure will occur when the top flange reaches approximately **644°C (**Table 1**)**.

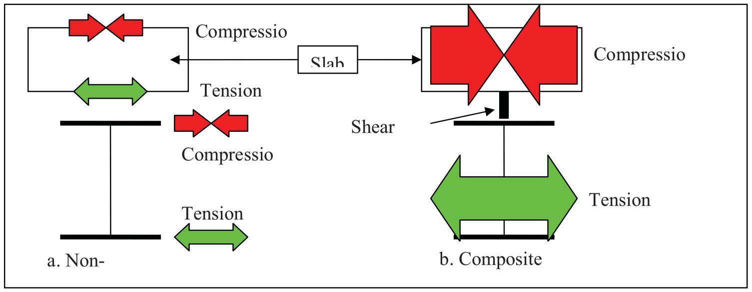

Figure 25: Non-composite Action vs. Composite Action

An example of heating in different parts of a beam is indicated in Figure 26. This figure shows the difference between a fully protected beam and a beam with unfilled flutes, as occurs in Case 1. Significant differences in temperature between the top and bottom flange are introduced due to the unprotected top surface of the top flange.

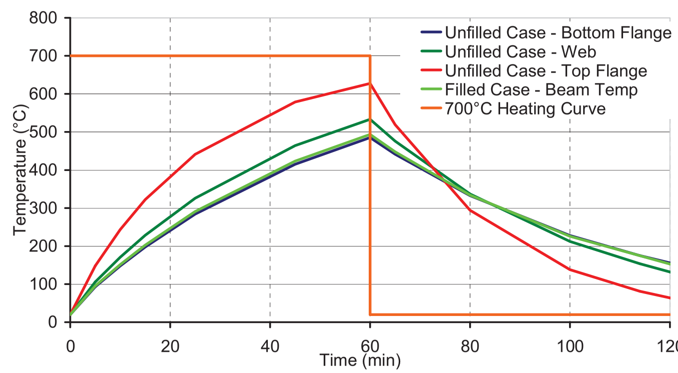

Figure 26: Comparison of temperatures of a typical beam/girder with flutes filled and unfilled condition.

In the 700°C fire case with unfilled flutes the top flange reaches approximately **675°C** indicating that if composite action has been fully lost then the north-east corner beams will fail during heating. This is not observed in the model, and therefore composite action must still exist to some degree, even if some shear studs have been broken.

In order for the beam to fail during heating (assuming positive composite connection) then more of the beam must be heated above a certain critical temperature. The next most heated part of the beam is the web. The web of a beam links the top and bottom flanges and allows them to act together in resisting loads.

The critical failure temperature for the web of the north-east bay secondary beams has been calculated at approximately **670°C** (Table 1). If the temperature attained by the web in the Case 1 analysis goes above this temperature then the stability of the floor system could be lost. The maximum temperature achieved by the web in the 700°C flutes unfilled analysis is approximately **625°C** based on the heat transfer data supplied by Jose Torero of the Expert Team.

Table 1: Secondary Beam Critical and Attained Temperatures

Beam section (W24x55)	Critical Temperature (calculated using AISC LRFD methods)	Maximum Temperature attained in analysis
Top Flange	644°C	675°C
Web	670°C	625°C

Therefore we would not expect the floor system to fail during heating as long as some composite action is available.

By the end of heating in the sub-model all the secondary beams in the north-east corner are largely upright, without signs of significant buckling. Hence it is considered that a failure of the floor system through loss of strength is unlikely and therefore the model is reporting reasonable results.

Due to the size and stiffness of the primary girders, relatively small vertical deflections are observed during the heating phase. It is considered that the thermal bowing of the floor system caused by differential heating between the slab and the girders can be resisted by the connections.

The vertical deflections lead to longitudinal expansion of the girders.

The key response linked to this mechanism is the longitudinal expansion of Girder 79-44. This member is supported on seated connections at both ends. The longitudinal expansion of this member rapidly breaks the bolts at the Column 79 end, allowing the on-going expansion of the floor to move the girder end about on the seating plate.

During the heating phase this leads to the end of the girder being wedged solidly into the corner formed by the flange and the western side plate of column 79.

The critical temperature for the top flange of G79-44 is presented in Table 2. As can be seen the critical temperature of the top flange is significantly in excess of the maximum temperature attained during the analysis. This indicates that even if composite action was fully lost, then the girder is unlikely to fail under the normal applied floor loading. It would still be possible, however, for the beam to fail in a mode other than bending failure, e.g. connection failure or lateral torsional failure.

Table 2: Girder 79-44 Critical and attained temperatures

Beam section (W33x130)	Critical Temperature (calculated using AISC LRFD methods)	Maximum Temperature attained in analysis
Top Flange	675°C	627°C

The key responses in the floor structure during the heating phase are:

- Primary girders deflect relatively little
- Large deflections of secondary beams caused by restrained thermal expansion and thermal bowing
- Early breakage of bolts at Column 79 seated connection
- End of G79-44 at Column 79 is pushed across its seating plate and into contact with the western column side plate
- Significant breakage of shear studs

- No observed failure mechanisms during the heating phase

5.3.2 Cooling phase

During the early stages of the cooling phase the vast majority of the remaining shear studs on the north-east secondary beams are broken due to differential cooling between the slab and the beams. This means the secondary beams are now dependent on the strength of their top flange for stability. However, before secondary beam failure can occur, rapid cooling of the top flange reduces its temperature below the critical failure temperature presented in Table 1.

As the secondary beams cool, they contract and try to return to their original position. In order for them to be able to do this they must lift the slab back up to its original position and this leads to increasing tension in the beam connections.

As indicated in Figure 27 the loss of composite connection between the slab and beams can lead to the secondary beams rotating around their long axis, reducing their bending strength.

Figure 27 also indicates that the large tensile forces developed as the secondary beams contract against the slab are sufficient to rupture their connections leading to local failure.

Over the course of the cooling phase, it is observed that there is little appreciable reduction in deflection in the north-east bay.

As the secondary beams cool they pull Girder 79-44 eastward across the seating plate at Column 79. Combined with the longitudinal contraction of the girder as it cools this brings the end of the girder to the edge of the seating plate by the end of cooling. Please see Section 5.4.1.1 for further details.

The key responses in the floor structure during the cooling phase are:

- Large displacements in north-east corner are not recovered during cooling
- Secondary beam connection failure reduces robustness of north-east corner floor
- Contraction of secondary beams act to pull Girder 79-44 eastward on seated connection

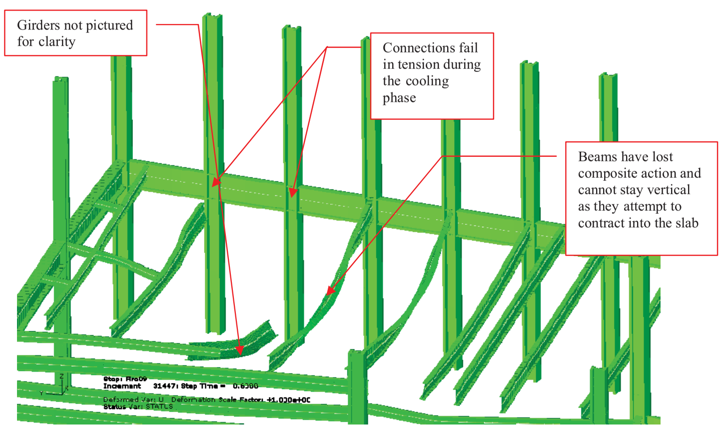

Figure 27: 700°C Unfilled Flutes Case 1 - Beam Orientation During Cooling Phase (90 minutes, Girders not pictured for clarity)

5.3.3 Consequences of Trench Headers

The locations of the trench headers are shown in Figure 5 as defined in a sketch received from GNA dated 22nd June 2009. It is understood that the purpose of the trenches is to allow access for services to be run within the structural depth of the floor. In practice the trench headers represent approximately 3' wide strips of floor that contain no concrete.

There are 2 primary effects of including these trench headers in the structural fire model:

- The trench headers act as large expansion joints. By allowing slab expansion to be accommodated in the trench headers, restraint to the floor as a whole is reduced. This will act to reduce restrained thermal expansion in the slab thereby reducing vertical deflections.
- The trench headers break the continuity of the slab. Reducing the membrane continuity of the slab has 2 primary consequences:
  - In heating, as noted above, deflections induced by restrained thermal expansion are reduced.
  - The robustness of the slab in tensile membrane action is reduced.

However the presence of the trench headers is not considered to significantly affect the final failure mode of the structure. It is considered that some local detailed responses may be affected (i.e. mid-bay slab deflections), however the final failure mechanism would remain the same. This assessment is based on two key data:

- The nature of the failure mechanisms exhibited to date, i.e. Girder 79-44 being pulled eastward by north-east bay.
- The order of magnitude of maximum deflections in the Southern bays, where there are no trench headers, is similar to maximum deflections observed elsewhere in the structure.

JA-3181

5.4 Details of Connection Behaviour

5.4.1 Detailed Connections

The movement of the 3 connections around Column 79 are shown in Figure 28, Figure 29 and Figure 30. These images are taken at ambient, peak heating and end of cooling.

5.4.1.1 Column 79 Seat

The most relevant connection response is that of the seated connection at Column 79 supporting Girder 79-44 as it is this connection that exhibits the most likely collapse initiation mechanism.

The following key responses are observed at this connection:

- Seating bolts break early in the fire due to longitudinal expansion of Girder 79-44. The longitudinal expansion of the girder is particularly important in this case because thermal expansion in the girder is not being transformed into vertical deflections.
- End of girder is then free to be moved about on the seating plate
- Toward the end of heating the girder end is jammed into the corner between the column flange and the extension of the column side plate beyond the flange (see Figure 29)
- During cooling the contraction of the secondary beams pulls the girder end back across the seating plate
- At the end of the analysis the girder end sits precariously at the edge of the seat

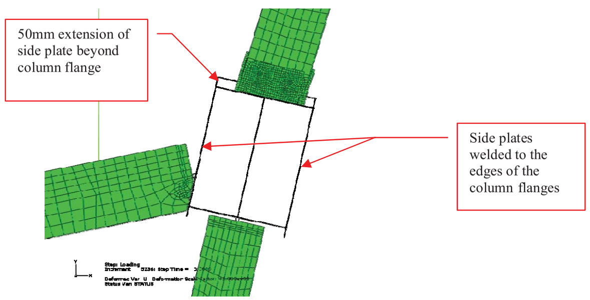

Figure 28: 700°C Unfilled Flutes Case 1 - Column 79 Seat Connection at Ambient

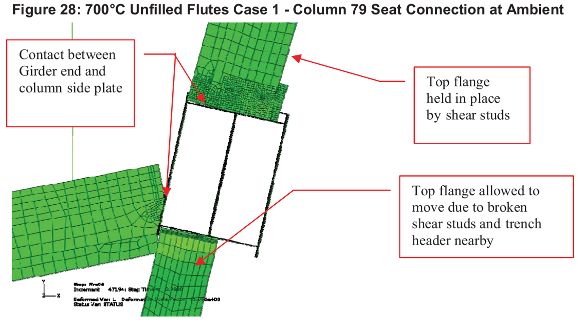

Figure 29: 700°C Unfilled Flutes Case 1 - Column 79 Seat Connection at Peak Heating

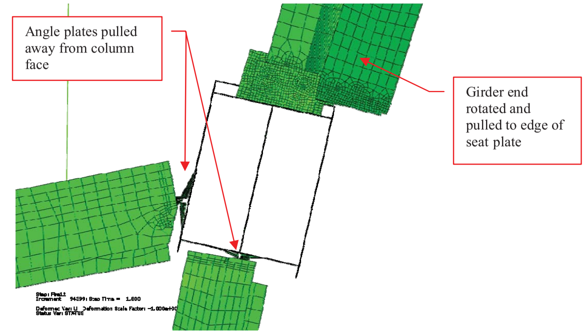

Figure 30: 700°C Unfilled Flutes Case 1 - Column 79 Seat Connection at End of Cooling

5.4.1.2 Column 79 Knife Connections

The other two connections at Column 79 (K8 and K5 knife connections) are also affected during the fire, although to a lesser extent than the seated connection, specifically

- During the heating phase of the fire, compression forces in the attached girders cause some plate bending as can be seen in Figure 31.
- No substantial damage is observed either in the plates or in the bolts of either knife connection. This is due to the ductility available in the knife connection assembly.
- Due to the large forces involved when structural members heat up, the force capacity of the connections is overcome relatively quickly. The forces are generated by thermally induced movement in the structure.
- If local deformations are allowed to occur then the force quickly drops. In order for the connection to fail completely the connection must undergo sufficient deformation such that the component parts (i.e. angle plates and bolts) fracture. In Case 1 local deformations are not sufficient to cause failure in either the plates or the connector elements representing the bolted assemblies.
- As the girders contract during the cooling phase the angle plates of the connection are pulled off the face of the column (Figure 32) thus relieving the forces shown in Figure 33.

JA-3182

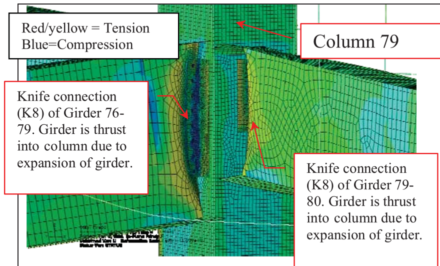

Figure 31: South west view of column 79 showing the knife connections, at 60 minutes (end of heating phase)

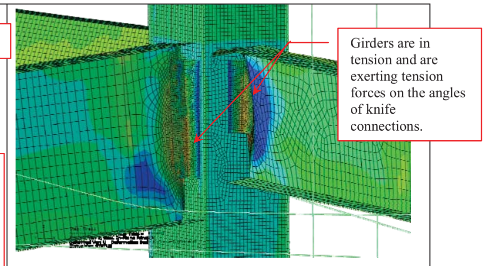

Figure 32: South west view of column 79 showing the knife connections, at 120 minutes (end of cooling)

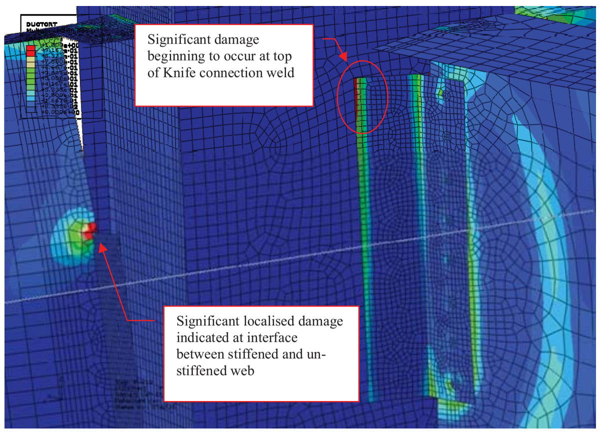

Figure 33: 700°C Unfilled Flutes Case 1 - Knife Connection Damage at End of Cooling (Red indicates heavy damage, dark blue indicates no damage)

5.4.2 Simplified Connections

As indicated in Figure 34 there are a small number of simplified connections that break during the analysis. All of these connections break during the cooling phase and are therefore linked to increasing tension forces generated as the secondary beams contract.

- In the majority of cases the breakage of the connection does not significantly affect the response of the structure as the floor loading is then redistributed into the primary girders via the concrete slab.
- The trench headers do not significantly affect this redistribution due to the composite connection between the beams and the slab.
- In the case of the 2 connections in the north-east corner, breakage of these connections allows the beams to fall away as they have also lost all shear studs. Connection failure occurred due to tension forces acting on the connections during the contraction of the beams during the cooling phase.
- Failure of these connections introduces a sudden redistribution of load between the failing beams and the beams directly adjacent to them.
- Local breakage of secondary beam connections does not cause global collapse. This is because the floor loading is redistributed into the floor slab which resists it through tensile membrane action. The slab is able to transfer this load directly into the surrounding primary girders and edge beams.

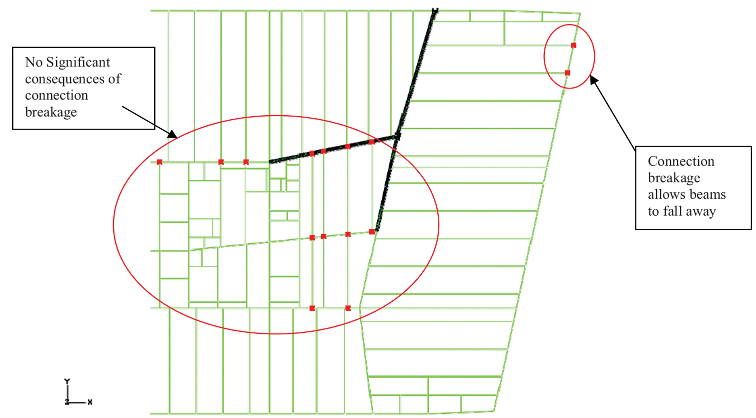

Figure 34: 700°C Unfilled Flutes Case 1 – Breakage of Simplified Connections at locations indicated by red dots

5.5 Timeline of Key Behaviour

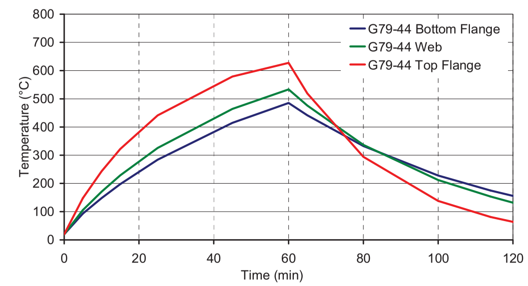

Figure 35: 700°C Unfilled Flutes Case 1 - G79-44 Temperatures

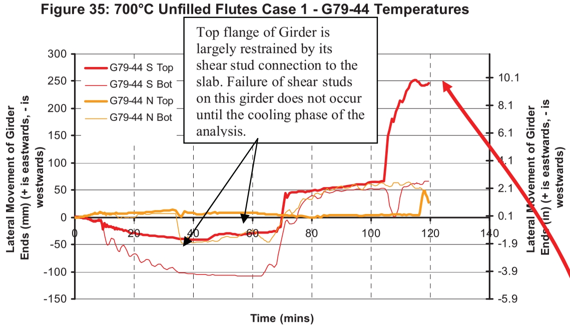

Figure 36: 700°C Unfilled Flutes Case 1 - G79-44 End Displacements (East-West)

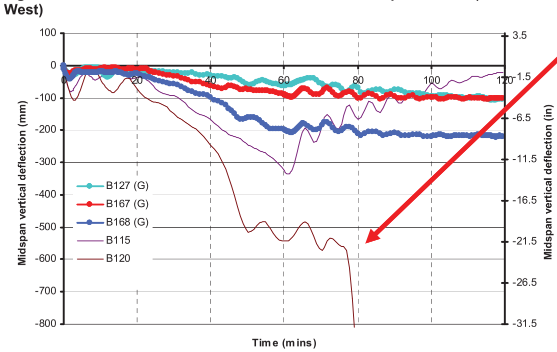

Figure 37: 700°C Unfilled Flutes Case 1 - Selected Beam and Girder Vertical Deflections

Event	Time Mins	Location and failure comments	Girder 79-44 Top Flange Temp °C
1	8.4 to 9.2	All 4 Bolts in seated connection at Column 79 break. This leaves the end of the girder free to slide on the seating plate.	212 to 230
2	30.0	Mid-span deflection of central beam in the north east corner bay has now reached 6" (150mm)	476
3	34 to 35	At column 44 all 4 bolts break. This allows the bottom flange to be pushed across the seat until it contacts the column flange. The top flange is largely restrained by the shear studs.	503 to 510
4	40	Bottom flange of G79-44 at Column 79 contacts the column side plate. After contact the girder stays wedged in the corner until cooling begins.	544
5	60	Mid-span deflection of central beam in the north east corner bay has now reached 21.8" (555mm).	627
6	65 to 75	Various simplified connector elements (SWC type connections) break in central bay. This breakage does not significantly affect response of structure in this area because floor loading is redistributed to the primary girders via the concrete slab.	519 to 369
7	76.3	Connection between Beam B120 and Column 40 breaks, allowing the beam to fall away. Floor loads are redistributed to the girder via the slab.	350
8	80	Connection between Beam B121 and Column 41 breaks, allowing the beam to fall away. Floor loads are redistributed to the girder via the slab.	294
9	90	Mid-span deflection of central beam in the north east corner bay has now reached 42.5" (1080mm) (Beams B120 and B121 have failed their connections and are falling away).	216
10	End	Mid-span deflection of secondary beams leads to the girder tending to rotate. This effect combines with the contraction of the secondary beams during the cooling phase to pull and rotate the end of the girder back across the seating plate.	81

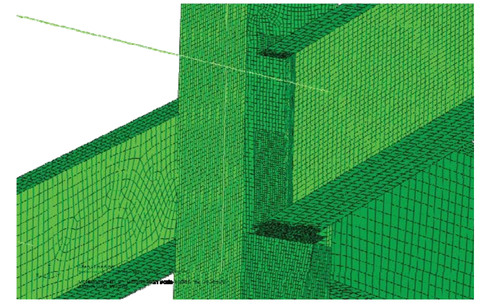

Figure 38: 700°C Unfilled Flutes Case 1 - Column 79 Seat Connection @ Ambient

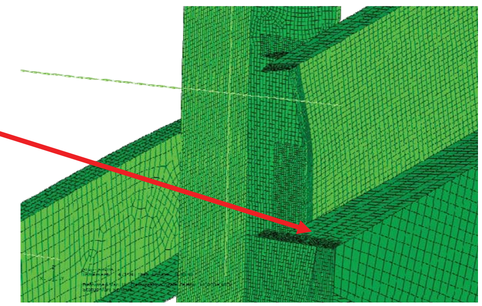

Figure 39: 700°C Unfilled Flutes Case 1 - Column 79 Seat Connection @ Peak Temperature

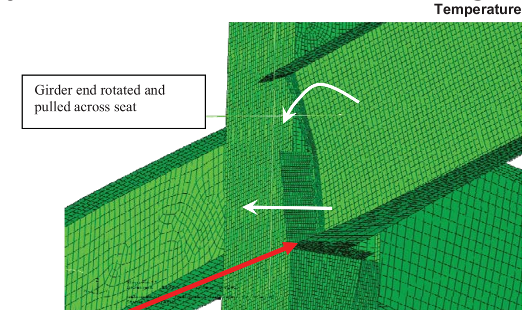

Figure 40: 700°C Unfilled Flutes Case 1 - Column 79 Seat Connection @ End Cooling

JA-3184

6 Case 2 (700°C Flutes Filled Model)

This section presents the response of the Case 2 sub-model of WTC7. It is split into the following sub-sections:

- Section 6.1 describes the general response of the model
- Section 6.2 presents details of the column response in the model
- Section 6.3 describes details of the composite floor and discusses the expected and observed responses
- Section 6.4 reviews the response of connections in the model
- Section 6.5 presents a summary timeline of the key structural responses

6.1 Overview of Structural Response

The Case 2 model includes the following structural details:

- Heating phase of 700 °C gas-phase for 1 hour, followed by 1 hour where gas phase is at 20°C
- Flutes filled with fire protection material, effectively protecting top flange of all beams

The response of this model is generally in accordance with known structural phenomena in fire:

Heating

- During the heating phase all structural members expand as they heat up, leading to relatively large mid-span deflections in the floor.
- As for Case 1 the girders are stiff and show relatively small deflections due to the provision of shear studs. Case 2 model maximum girder deflections at peak heating are approximately 150mm (6.0"), compared to 200mm (7.9") in Case 1. This is due to the lesser heating being applied.
- When the girder between Column 44 and Column 79 is subjected to longitudinal expansion it breaks the bottom two bolts at column 79 and at Column 44 during the early stages of heating (temperatures of girder top flange is 109°C) . This allows the girder to be moved around on the seat plate at Column 79 and 44.
- During the heating phase a significant number of shear studs are broken (but fewer than Case 1), however it is considered that the secondary beams and girders retain enough connection to the slab in heating to act in a largely composite manner.
- As the model approaches maximum heating there are no signs of imminent structural failure.

Cooling

- During the later stages of the cooling phase, a significant percentage of the remaining shear studs break, leading to increased deflections in secondary beams in the north-east bay. However it is considered that enough studs remained intact to provide some level of composite action throughout the analysis.
- A number of secondary beams begin to break their end connections. The majority of these members are in the central bay and the breakage of the connections has no obvious effect on the global response of the structure. The concrete slab is able to redistribute the floor load directly to the primary girders.
- As the cooling phase continues, the existing mid-span deflection of the secondary beams in the north-east corner, combined with the general contraction of the structure during cooling, leads to the South end of Girder 79-44 being pulled Eastward across its seating plate.
- At the end of 120 minutes of heating and cooling, the analysis shows that there is no structural collapse. The girder 79-44 at column 79 remains on its seat and is in solid contact with the inside face of the column side plate, unlike Case 1 where the girder end is left in a precarious position at the ends of the seating plate.

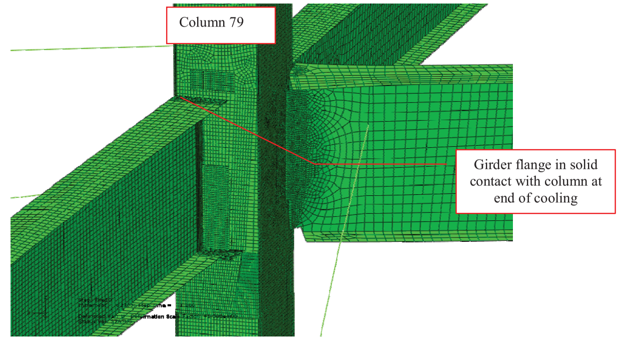

Figure 41: 700°C Filled Flutes Case 2 - Seated connection of girder 79-44 at the end of cooling

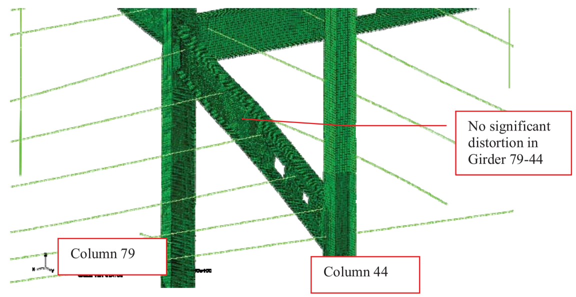

Figure 42: 700°C Filled Flutes Case 2 - Girder 79-44 at the end of cooling

6.2 Details of Column Behaviour

In Case 2, no column buckling was observed in the model during the period of the analysis up to the point when the analysis completed. This is similar to the 700°C flutes unfilled analysis (Case 1).

- All internal columns remained vertical throughout the analysis up to the point when the analysis stopped.
- No significant lateral displacement observed in internal columns while the perimeter columns showed some outward bowing.
- Figure 43 compares the lateral movements of selected columns along the north, south and east façades for Case 1 and Case 2, based on the locations of the columns shown in Figure 20. The movements of the columns show similar trends in both cases.
- During the heating phase, outward column movement in Case 1 is typically lower than in Case 2. This may be attributed to the larger downward movements of the floors in Case 1 that help dissipate longitudinal expansion of beams and girders and prevents movement of columns.
- During the cooling phase similar trends are apparent. The larger deflections in Case 1 lead to more inward movement as the floor structure contracts.

JA-3185

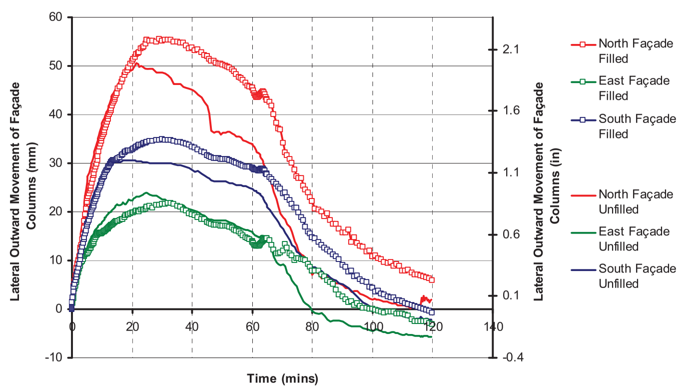

Figure 43: Comparison of outward movements of selected columns along the perimeter of the building for the flutes filled and unfilled condition under 700°C heating. (Positive (+) movement indicates outward movement) Refer to Figure 19 for the positions of the columns that were plotted.

6.3 Details of Composite Floor Response

When the flutes are filled and the structure is subjected to the 700°C heating curve, the overall behaviour of the composite floor system generally shows similar (but slightly smaller) vertical deflections compared with the flutes unfilled condition (Case 1). The variation between the cases is related to the differences in heating and therefore differences in restraint around the floor plate. No runaway failure of secondary beams or girders was observed. Also, there was no rotation of the girder end on column 79, such as that observed in the flutes unfilled condition.

By filling the flutes overall beam temperatures remain lower during the heating phase as shown in Figure 44 below. The lower temperatures allow the beams to retain greater strength and stiffness compared to Case 1 where the top flange and web temperatures become significantly higher due to the unfilled flutes.

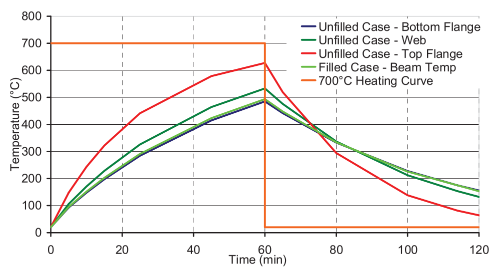

Figure 44: Comparison of temperatures of beams with flutes filled and unfilled condition (Case 2 to Case 1).

Figure 45 compares the mid-span vertical deflections of selected beams and girders between the flutes filled and unfilled condition.

- The peak mid-span deflections in the north eastern bay (represented by B120) in the flutes filled condition are generally similar compared with the flutes unfilled case.
  - In the flutes unfilled condition, the B120 secondary beam undergoes runaway failure at about 77 minutes due to failure of the connection connected to the eastern perimeter frame.
  - In the flutes filled condition, the connections at the end of the B120 secondary beam do not fail and hence shows much less vertical deflection in the later stages of cooling. The heating applied to the concrete slab is the same between the two models so the key differentiator is the difference in strength and stiffness introduced by the different heating cases in the beams.
- In Case 1 the connections in the NE corner failed in tension for secondary beams (B120 and B121). Failure of the connections is due to catenary action being activated in the beams and the connections fail when they cannot resist the tensile forces due to catenary action. These do not fail in the flutes filled case because significant number of shear studs do not break until later in the cooling phase. In Case 1 almost all shear studs have broken by 70 minutes into the analysis (10 minutes into cooling) when the secondary beams are still hot. In Case 2 the same degree of shear stud breakage does not occur until approximately 90 minutes into the analysis (30 minutes into cooling). This means that the secondary beams in the NE corner retain greater strength for longer through composite action.
- The girders B127 (spanning between column 79-44) and B168 (spanning between column 76-79) show relatively similar behaviour between the flutes filled and unfilled condition. This is indicative that the benefits of composite action help overcome the additional heating occurring in the top flange under Case 1. A bigger difference in responses would be expected if the girders were not compositely connected to the slab.
- The largest vertical deflection in the 700°C flutes filled condition occurs in Beam B98, located in the southern area of the floor plate. This is due to the slab continuity that exists along the whole of the south side of the building. The lateral expansion of the slab is being restrained by the symmetry boundary condition in the West and by the perimeter column system in the east. This restraint leads to increased vertical deflections. Due to the geometry of the structure and the lack of trench headers in the south of the building, the additional deflections caused by restrained thermal expansion are focussed into the middle bay in the south.
- Compared to the flutes unfilled condition, the overall deflection trend of this beam is similar for both cases, except:
  - The main difference occurs after 40 minutes of heating where the flutes filled condition shows larger deflections (approximately 100mm or 4") compared with the flutes unfilled condition. This can be attributed to the higher temperatures of the top flange of the beam (in the flutes unfilled case) relative to the bottom flange and the web. This forms a temperature gradient in the beam which causes the beam to attempt to bow upwards. Hence the overall downward deflection of the floor system is reduced due to the thermally induced action of the beam.
  - During the cooling period, the smaller vertical deflections in Case 1 can be attributed to the faster rate of cooling and greater contraction of the beam. Fire protection acts in both directions; lack of protection means that the structure heats up more quickly, however it also means that the structure cools down more quickly. As the upper surface of the top flange is not protected heat can be easily radiated away. This causes the vertical deflections to recover faster in Case 1 than in Case 2.

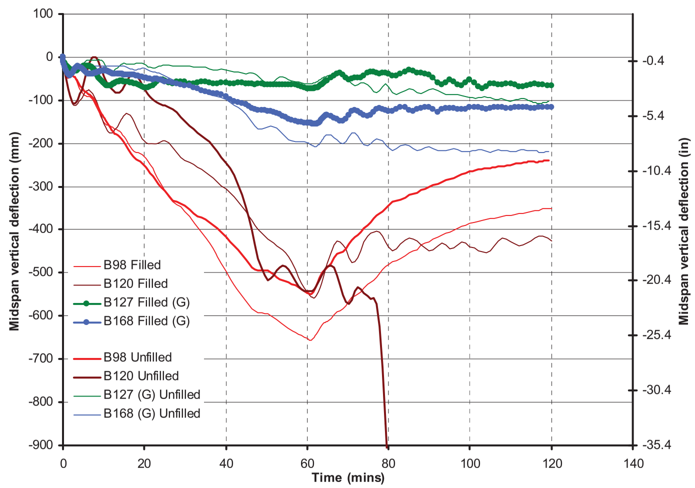

Figure 45: Comparison of mid-span vertical deflections of selected beams and girders for flutes filled and unfilled condition under 700°C heating (Case 1 and Case 2). B120 unfilled is a secondary beam in the NE bay that undergoes connection failure and falls away from the underside of the slab.

6.4 Details of Connection Behaviour

6.4.1 Detailed Connections

The K8 and K5 knife connections at Column 79 showed similar response to that shown in the flutes unfilled condition.

- During the heating phase, as the girders expanded, the connections are subjected to compression forces from the expanding girders and the angles experienced local bending. As the girders expanded and were thrust into the column, there was some local twisting of the girder ends as shown in Figure 46.
- During the cooling phase, as the girders started to cool and contract, the angles of the connections were subjected to tension forces from the girders and were pulled away from the surface of the column 79 (Figure 47).
- In both the heating and cooling phase, there was no breakage of the bolts or tearing of the plates.

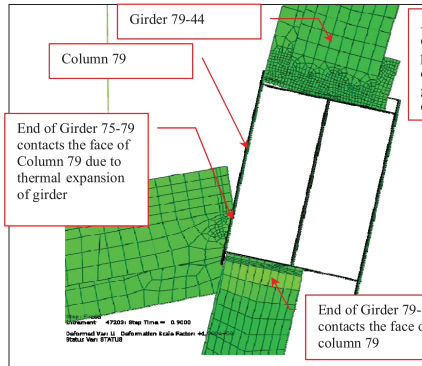

Figure 46: 700°C Filled Flutes Case 2 - Plan view of connections at column 79 at 60 minutes (End of heating)

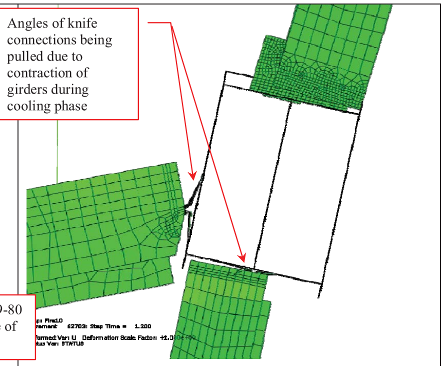

Figure 47: 700°C Filled Flutes Case 2 - Plan view of connections at column 79 at 120 minutes (60 minutes into cooling phase)

Girder 79-44 supported by the seated connections at columns 79 and 44 did show the same response as in the flutes unfilled case.

In Case 2, after 60 minutes of cooling, Girder 79-44 did not exhibit the kind of twisting deformation at column 79 (refer to Figure 49) that was observed in Case 1. This is due to the top flange of the girder remaining in solid contact with the column side plate throughout cooling. At the end of cooling in Case 2 there was no indication that the end of the girder was close to being displaced off its seat at Column 79.

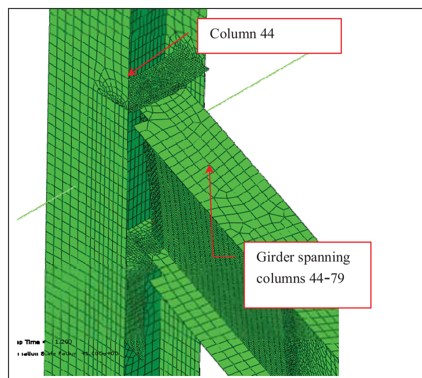

Figure 48: 700°C Filled Flutes Case 2 - Condition of detailed connection at column 44 supporting girder 44-79 at 120 minutes (end of cooling)

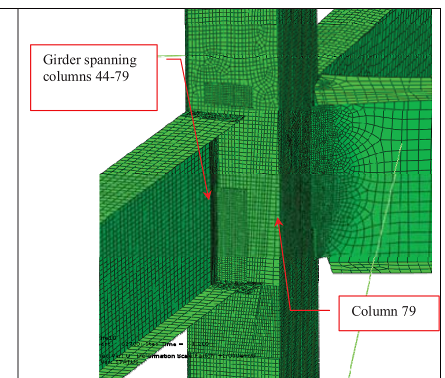

Figure 49: 700°C Filled Flutes Case 2 - Condition of detailed connection at column 79 supporting girder 44-79 at 120 minutes (end of cooling)

6.4.2 Simplified Connections

- Figure 50 shows that a number of numerically simplified connections break during the analysis. All of these connections break during the cooling phase in the numerical model.
- The connections break in tension due to the tension forces generated in the associated secondary beams as they contract during the cooling phase.
- The breakages of the connections do not significantly affect the response of the structure, nor cause significant deformation, as the floor loads are redistributed directly to the primary girders via the concrete slab. In Case 2 none of the secondary beams fall away after breaking their connections. This is because, despite the presence of trench headers, all affected beams are attached to the slab numerically by the rigid links which represent the shear studs. Please refer to the Modelling Assumptions report for more information. This type of response, i.e. secondary beams remaining attached to the slab after connection breakage, has been observed in the Cardington tests. It is therefore considered that this type of behaviour will not significantly affect global stability.

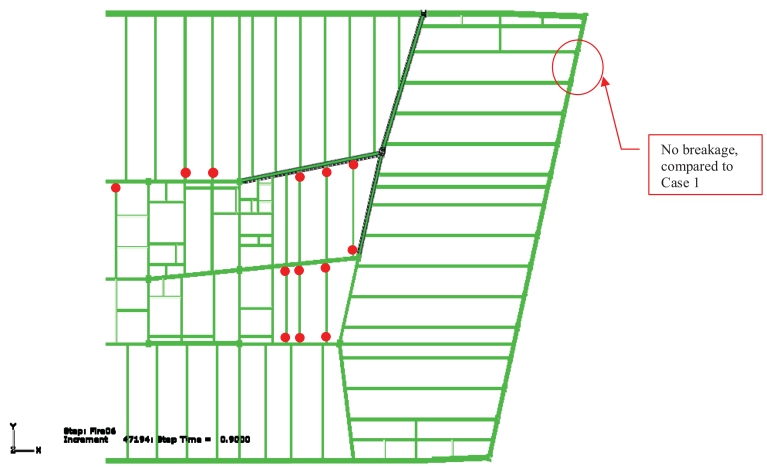

Figure 50: 700°C Filled Flutes Case 2 - Locations of simplified connections that break throughout the analysis, up to the end of cooling

6.5 Key Floor Structure Behaviour

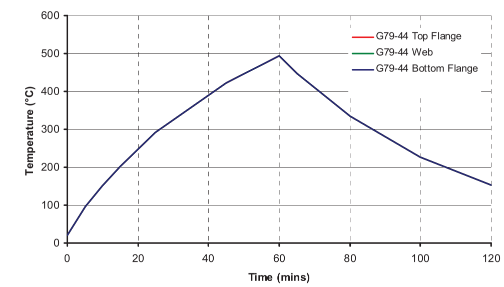

Figure 51: 700°C Filled Flutes Case 2 - G79-44 Temperatures

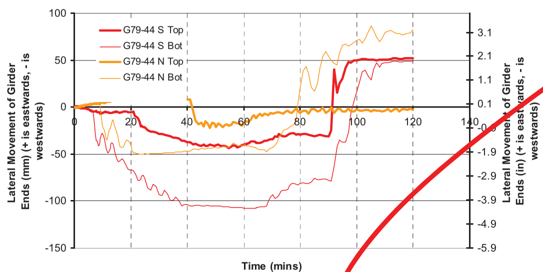

Figure 52: 700°C Filled Flutes Case 2 - G79-44 End Displacements (East-West)

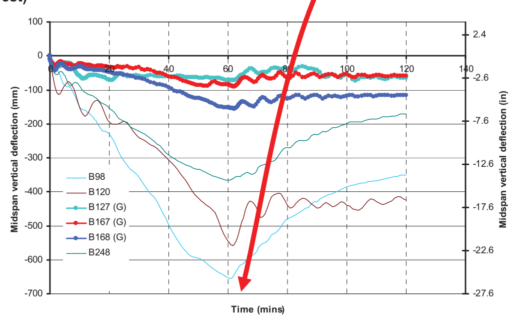

Figure 53: 700°C Filled Flutes Case 2 - Selected Beam and Girder Vertical Deflections

Event	Time Mins	Location and failure comments	Girder 79-44 Top Flange Temp °C
1	4.2 to 8.8	The bottom bolts of girder 79-44 break at both column 79 and column 44.	85 to 137
2	21 to 23	The top clip of girder 79-44 ruptures at column 79. This allows the girder to be able to move laterally and longitudinally at the seated connection at the column 79 end.	247
3	30	Largest mid-span deflections are observed in the south at beam 98, reaching 350mm (13.7")	324
4	41	The bolts of the top clip of girder 79-44 break at column 44 break. The girder is also free to move laterally and longitudinally at the seated connection at column 44.	397
5	60	Largest mid-span deflections in the floor plate are observed in the south at beam 98, reaching 650mm (25.5"). Mid-span deflections of the secondary beams in the north –east corner are 560mm (22").	494
6	85	Significant shear stud breakage begins at approximately 85 minutes (25 minutes into cooling phase). It is considered that this sudden rise in breakages is caused by differential contraction between the slab and secondary beams. Secondary beams are cooler when stud breakage occurs and therefore residual deflections in these beams are lower than in other cases.	311
7	90	Vertical deflections of floor slab and beams decrease because structure is cooling and starts to contract. Largest mid-span deflections in the floor plate are observed in the south at beam 98, i.e.: 424mm (16.7"). Mid-span deflections of the secondary beams in the north–east corner are 440mm (17.3").	279
8	120	Vertical mid-span deflections continue to decrease because structure is cooling. Largest mid-span deflections in the floor plate are observed in the north–east corner i.e. 425mm (16.7") at the end of cooling. Greater recovery of deflections is observed in Beam 98 in the south, i.e.: 352mm (13.9").	153

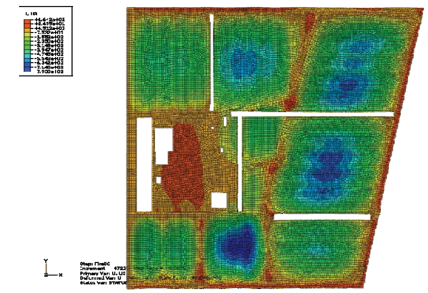

Figure 54: 700°C Filled Flutes Case 2 - Deflection contours at peak heating

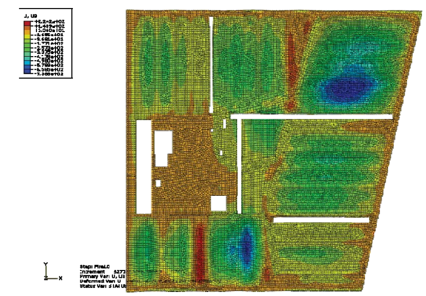

Figure 55: 700°C Filled Flutes Case 2 - Deflection contours at end of cooling (2 hours)

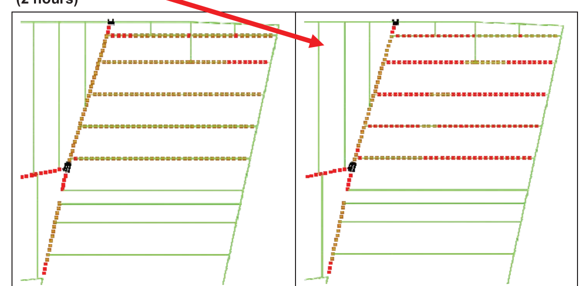

Shear Stud Breakage at 60 Minutes | Shear Stud Breakage at 90 Minutes

JA-3189

7 Case 3 (800°C Unfilled Flutes Model)

This section presents the response of the Case 3 sub-model of WTC7. It is split into the following sub-sections:

- Section 7.1 describes the general response of the model
- Section 7.2 presents details of the column response in the model
- Section 7.3 describes details of the composite floor and discusses the expected and observed responses.
- Section 7.4 reviews the response of connections in the model
- Section 7.5 presents a summary timeline of the key structural responses

7.1 Overview of Structural Response

The Case 3 model includes the following structural details:

- Heating phase of <u>800°C</u> gas-phase for 1 hour, followed by 1 hour where gas phase is at 20°C
- <u>Flutes unfilled</u> providing reduced protection to top flange of all beams

The response of this model is generally in accordance with well known structural phenomena in fire:

Heating

- During the heating phase all structural members expand as they heat up, leading to relatively large mid-span deflections.
- Due to the relatively light, yet realistic floor load applied to the slab within the model, vertical deflections are low. In particular the primary girders deflect very little (less than 250mm or 10"). This deflection is greater than the 200mm (8") observed in Case 1, due to the significantly higher temperatures attained in this case. Higher temperatures affect the strength and stiffness of the girders as well as producing more deflection through restrained thermal expansion.
- This leads to increased longitudinal expansion, compared to vertical deflections caused by thermal bowing.
- When the girder between Column 44 and Column 79 is subjected to this longitudinal expansion it quickly breaks its restraining bolts at column 79. This allows the girder to be moved around on the seat plate at Column 79.
- During the early and middle stages of the heating phase a significant number (approximately 40%) of shear studs are broken, however it is considered that the secondary beams and girders retain enough connection to the slab to act in a composite manner. This is because collapse of the north-east corner bay does not occur as soon as top flange temperatures exceed calculated critical temperatures.
- Breakage of shear studs on secondary beams in the north-east corner accelerates from approximately 42 minutes into the fire. This is believed to be caused by increasing deflection rates as beam strength is lost through thermal degradation of material properties.
- A combination of shear stud breakage and thermal degradation of secondary beam strength leads to rapidly increasing deflections in the north-east bay from approximately 44 minutes into the heating phase
- Runaway failure of the seated connection at column 79 is observed from approximately 47 minutes into the fire. Runaway is defined as a rapid and irrecoverable increase in deflection rate in a structural member. At this point the top flange temperatures of all beams and girders are in excess of 700°C and web temperatures are generally above 620°C. At 620°C steel has lost approximately 55% of its strength and 70% of its stiffness.
- Due to the ongoing failure of Girder 79-44 and its seated connection at Column 79 the analysis terminates at approximately 57 minutes into the heating phase of the fire and does not reach the cooling phase. The early termination was caused by numerical issues linked to the on-going failure mechanism.

The structural response described above is presented in more detail in the following sections, with the mode of failure shown in Figures 56 to 58..

A more detailed timeline may be found in Section 7.5.

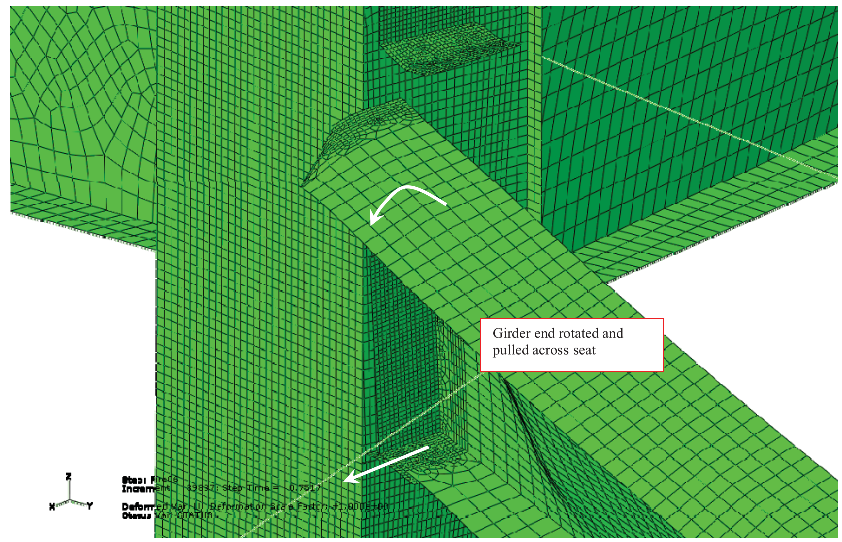

Figure 56: 800°C Unfilled Flutes Case 3 - Column 79 Seated Connection at Analysis Termination

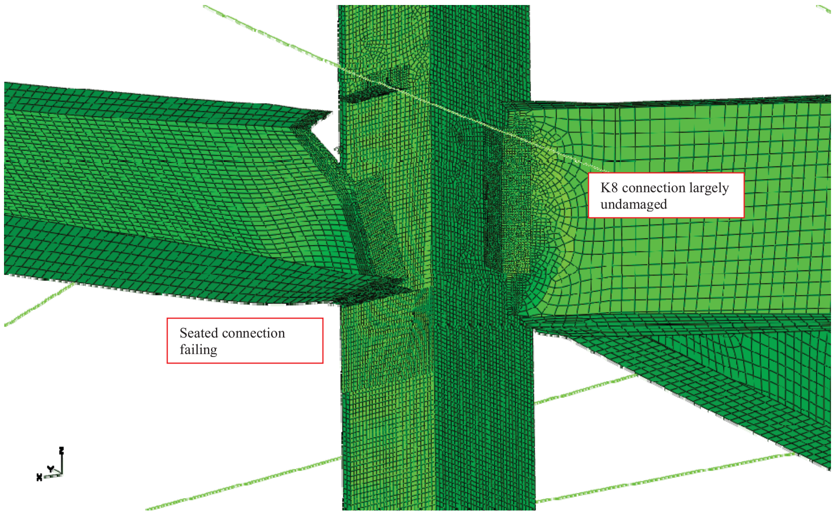

Figure 57: 800°C Unfilled Flutes Case 3 - Column 79 Seat and K8 Connections at Analysis Termination

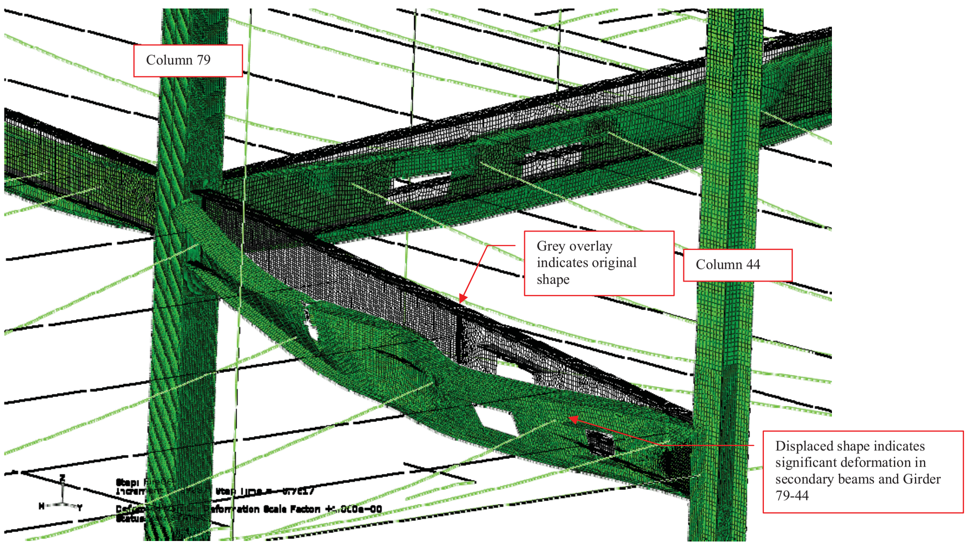

Figure 58: 800°C Unfilled Flutes Case 3 - Failure Mechanism of Girder 79-44 at Analysis Termination

7.2 Details of Column Behaviour

No column buckling was observed in the model during the analysis.

All internal columns remained vertical throughout the analysis, with no significant lateral displacement observed while the perimeter columns showed some outward bowing of the columns.

The response of the columns in Case 3 is similar in nature to the response of the Case 1 model and therefore is not discussed here in detail. Please refer to Section 5.2 for further discussion.

7.3 Details of Composite Floor Response

The response of the floor structure to Case 3 is largely similar to the response described for the Case 1 model in Section 5. This is because the rate of heating is similar in the early stages of each case. The results of the models begin to diverge after approximately 30-40 minutes due to the increasing difference in temperatures between Case 1 and Case 3.

The key differences are highlighted in the sections below.

7.3.1 Heating phase

The response of the floor during heating bears a close resemblance to the response of the Case 1 model (700°C, unfilled flutes). Key points of comparison are described below:

- Figure 59 presents the vertical deflection contours of the Case 3 floor slab when the top flange of Girder 79-44 is approximately 640°C. At this time the floor has undergone very similar heating to the Case 1 model (700°C, unfilled flutes) at peak temperature and as can be seen the general trends are similar (please refer to Figure 23 for comparison).
- Figure 60 shows the vertical deflection contours of the slab as the analysis terminates, after failure has been initiated and the runaway failure of the north-east corner is clear from the blue contours dominating the north-east bay.
- Figure 61 indicates the shear studs that have broken in the Case 3 model when Girder 79-44 top flange temperature is approximately 640°C (40 minutes into the heating phase) and again the pattern is extremely similar to that of the Case 1 model at peak heating (please refer to Figure 24 for comparison).

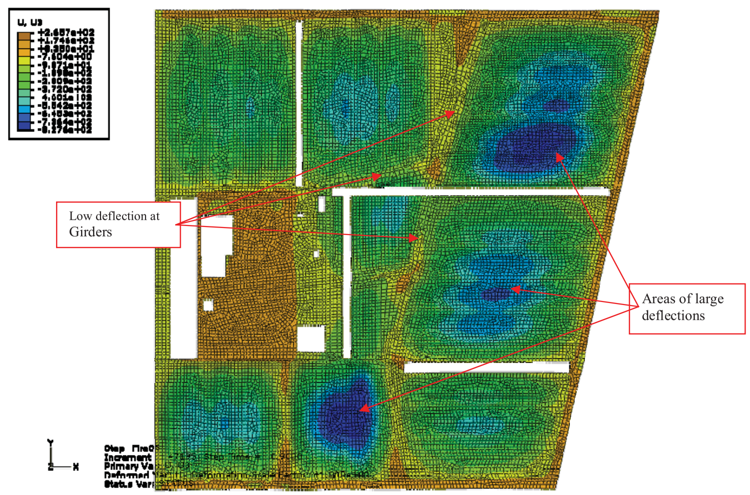

Figure 59: 800°C Unfilled Flutes Case 3 - Vertical Deflection Contours at 640°C Girder Top Flange Temperature (to be compared to Figure 23)

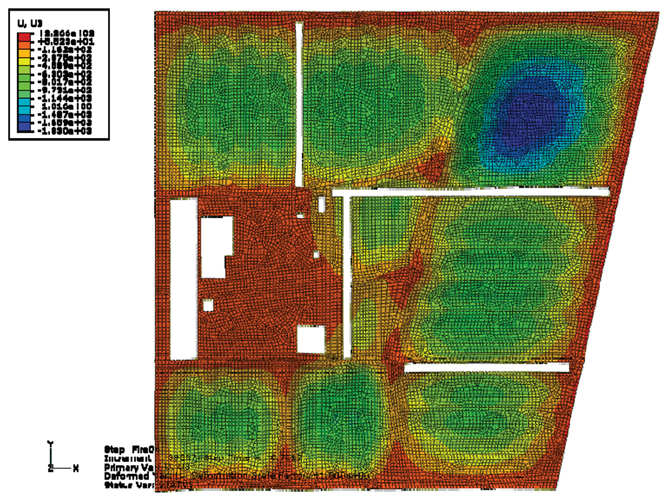

Figure 60: 800°C Unfilled Flutes Case 3 - Vertical Deflection Contours at Analysis Termination (57 minutes of heating at 800°C)

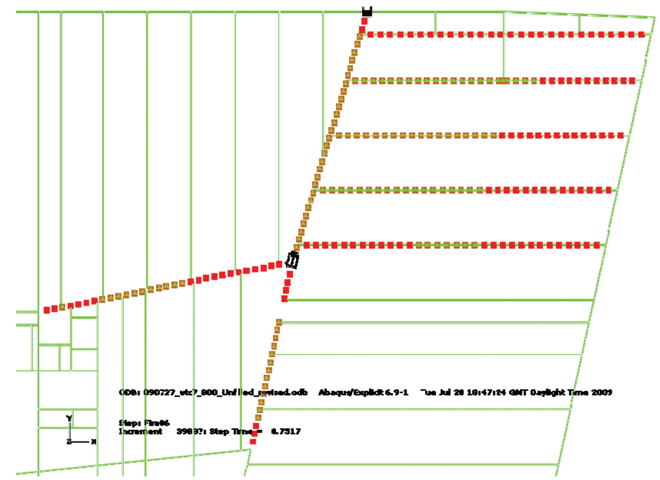

Figure 61: 800°C Unfilled Flutes Case 3 - Shear Stud Breakage 640°C Girder Top Flange Temperature (to be compared to Figure 24)

Table 3 presents the critical temperatures for the secondary beams in the north-east corner of the structure, compared to the temperature attained by those members at the point of failure, i.e. 47 minutes into the analysis.

This data supports the theory that a combination of loss of composite action and thermal degradation of material properties are responsible for the runaway failure of Case 3.

As in Case 1 the temperature in the relatively unprotected top flange exceeds the calculated critical temperature part-way through the heating phase. The significant difference between Case 1 and Case 3 is that in Case 3 the web also significantly exceeds the critical temperature during the heating phase of the analysis. In Case 1 the web did not reach its critical temperature.

At around 47 minutes the secondary beams in the north-east bay have lost their ability to support the floor above and begin to collapse. As the secondary beams sag further the floor system increases tensile loading to the East side of Girder 79-44. This girder is also being significantly affected by thermal degradation of strength and is unable to resist this new load case.

Through a combination of lateral and vertical loading Girder 79-44 is deformed to the point where it can no longer support the applied load and begins to fail laterally. The girder runs away in vertical and horizontal deflection, at which point the analysis terminates. It is considered that the girder can no longer support the applied load and that it will inevitably be pulled sideways off the seated connection at Column 79. This mechanism is demonstrated in Figure 58.

Table 3: Secondary Beam Critical and Temperatures Attained at 47 Minutes into Heating

Beam section (W24x55)	Calculated Critical Temperature (calculated using AISC LRFD methods)	Temperature attained in analysis @ initiation of girder runaway
Top Flange	644°C	758°C
Web	670°C	674°C

Mid-span deflections between Case 1 and Case 3 are presented against time in Figure 62 and against temperature in Figure 63. It is apparent that the difference of approximately 100°C in peak temperature of the top flange and web is enough to trigger a potential global failure mechanism in Case 3.

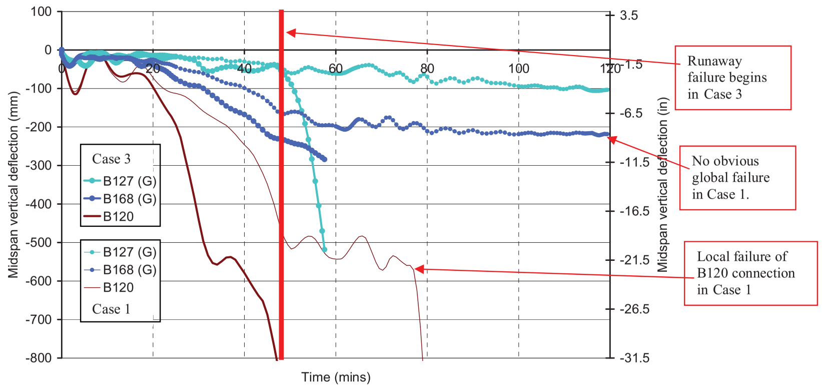

Figure 62: Comparison of Mid-span Deflection between Case 1 and Case 3 (Against Time)

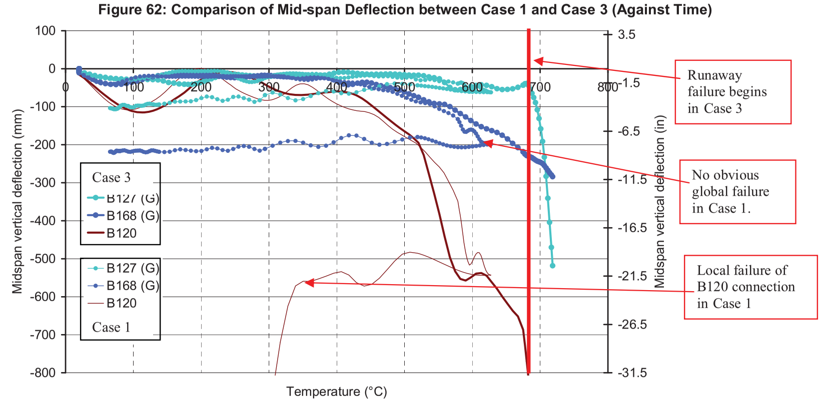

Figure 63: Comparison of Mid-span Deflection between Case 1 and Case 3 (Against Girder 79-44 Top Flange Temperature)

The key responses in the floor structure of Case 3 during the heating phase are:

- Large deflections in heating caused by restrained thermal expansion and thermal bowing
- Breakage of bolts at Column 79 seated connection is earlier than other cases due to more rapid temperature rise.
- Significant breakage of shear studs at an earlier stage than all other models
- Significant loss of strength in secondary beams, especially in north-east corner where composite action is also compromised.
- The temperatures in Case 3 appear to exceed critical temperatures for the secondary beams in the north-east corner, causing runaway failure of the north-east bay and subsequently to the failure of the girder between Columns 79 and 44.
- The cooling phase is not reached due to widespread structural failure leading to numerical issues in the analysis.

7.4 Details of Connection Behaviour

7.4.1 Detailed Connections

The movement of the 3 connections around Column 79 are imaged in Figure 64, Figure 65 and Figure 66. These images are taken at ambient, halfway through the heating phase and just before the end of heating (failure), respectively.

7.4.1.1 Column 79 Seat

The most relevant connection response is that of the seated connection at Column 79. It is this connection that has been highlighted as the most likely potential failure mechanism. The following key responses are observed at this connection:

- Seating bolts break early in the fire due to longitudinal expansion of Girder 79-44. Top clip bolts fail shortly afterward
- End of girder is then free to be moved about on the seating plate
- Toward the middle of the heating phase the girder end is jammed into the corner between the column flange and the extension of the column side plate beyond the flange
- At approximately 47 minutes into the heating phase runaway failure of the north-east corner begins, focussed around the Column 79 seated connection

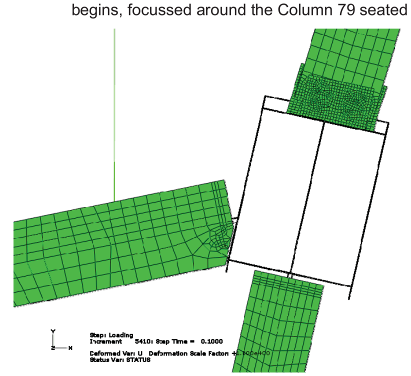

Figure 64: 800°C Unfilled Flutes Case 3 - Column 79 Seat Connection at Ambient

JA-3193

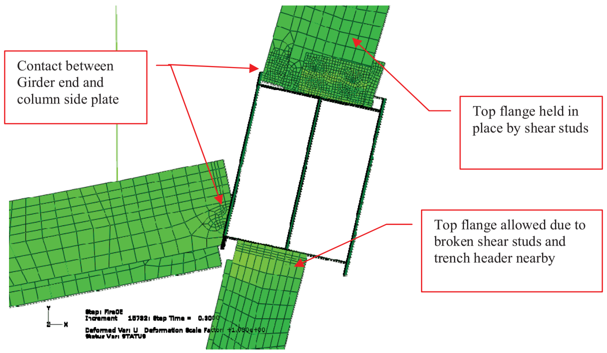

Figure 65: 800°C Unfilled Flutes Case 3 - Column 79 Seat Connection at 30 Mins

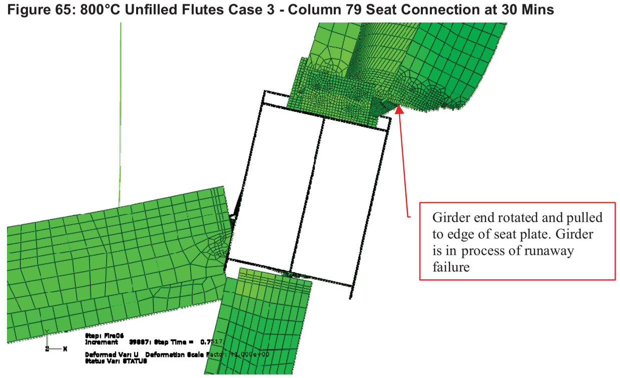

Figure 66: 800°C Unfilled Flutes Case 3 - Column 79 Seat Connection at Analysis Termination

7.4.1.2 Column 79 Knife Connections

The other 2 connections at Column 79 (K8 and K5 knife connections) also undergo some local deformation during the fire, although to a lesser extent than the seated connection.

- During the heating phase of the fire compression forces in the attached girders cause some plate bending, however no substantial damage is observed either in the plates or in the bolts of either knife connection.
- At the point the analysis terminates, the K8 and K5 connections exhibit little damage
- It appears that the top of the angle plates are being pulled outward slightly in both knife connections. This may be a sign that floor forces are being redistributed from the seated connection to the knife connections. Alternatively it may be caused by rotations in the connection after the bottom flange of the girders have contacted the column face

It is considered that neither of the knife connections at Column 79 exhibit definite signs of failure in Case 3.

7.4.2 Simplified Connections

None of the simplified connection elements are observed to break during the course of the analysis. In the other Cases breakage of the simplified connections was only observed during cooling. Case 3 does not enter the cooling phase due to the formation of a collapse initiating event. Therefore significant tension forces are not developed in the simplified connections to cause them to break

..

7.5 Timeline of Key Behaviour

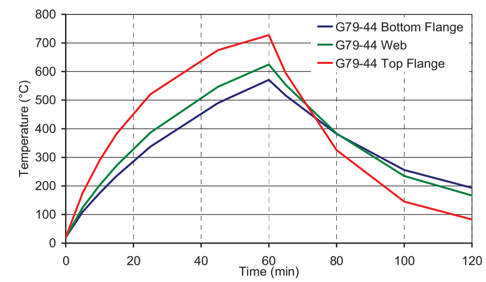

Figure 67: 800°C Unfilled Flutes Case 3 - G79-44 Temperatures

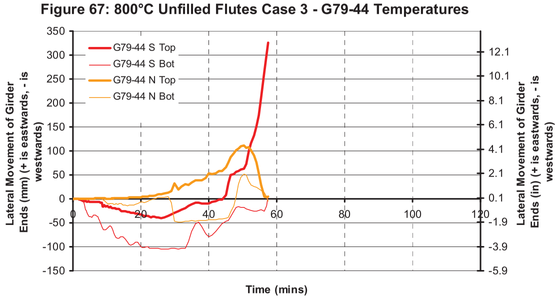

Figure 68: 800°C Unfilled Flutes Case 3 - G79-44 End Displacements (East-West)

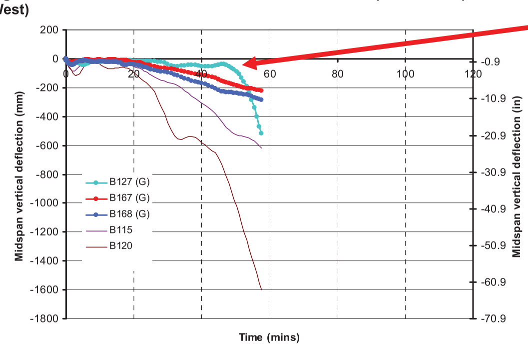

Figure 69: 800°C Unfilled Flutes Case 3 - Selected Beam and Girder Vertical Deflections

Event	Time Mins	Location and failure comments	Girder 79-44 Top Flange Temp °C
1	2.5	Bottom Bolts in seated connection at Column 79 break. This allows the end of the girder to slide on the seating plate. Restraint from the top clip is minimal.	100
2	8.0	Top bolts in seated connection at Column 79 break. Lateral restraint to the girder comes only from shear studs to slab.	244
3	20.0	Bottom flange of G79-44 at Column 79 contacts the column side plate.	451
4	28.5	At column 44 the bottom bolts break. The bottom flange on this connection is then pushed across the seat to contact the column flange	548
5	30.0	Mid-span deflection of central beam in the north east corner bay has now reached 440mm (17.3")	560
6	31	Bottom flange of G79-44 contacts column flange.	567
7	35	Bottom flange of G79-44 at Column 79 seat is pulled eastward. Eastward movement initiated due to sagging in north-east bay.	598
8	47	Runaway failure of north-east corner of structure begins. Centered around Girder 79-44 and its seated connection at Column 79.	682
9	57	Analysis terminates due to numerical issues caused by on-going failure of structure	717

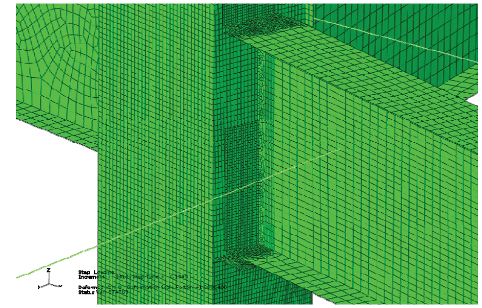

Figure 70: 800°C Unfilled Flutes Case 3 - Column 79 Seat Connection @ Ambient

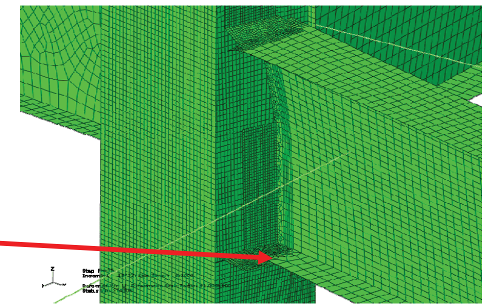

Figure 71: 800°C Unfilled Flutes Case 3 - Column 79 Seat Connection @ 30 Mins

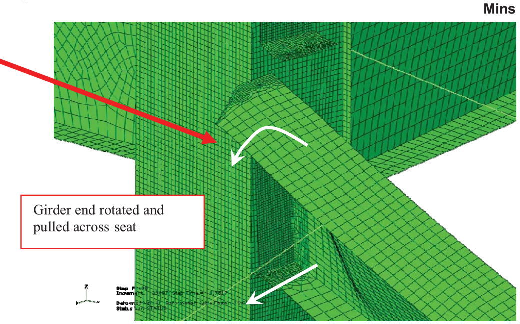

Figure 72: 800°C Unfilled Flutes Case 3 - Column 79 Seat Connection @ Analysis Termination

JA-3195

8 Case 4 (800°C Filled Flutes Model)

This section presents the response of the Case 4 sub-model of WTC7. It is split into the following sub-sections:

- Section 8.1 describes the general response of the model
- Section 8.2 presents details of the column response in the model
- Section 8.3 describes details of the composite floor and discusses the expected and observed responses.
- Section 8.4 reviews the response of connections in the model
- Section 8.5 presents a summary timeline of the key structural responses

8.1 Overview of Structural Response

The Case 4 model includes the following structural details:

- Heating phase of 800 °C gas-phase for 1 hour, followed by 1 hour where gas phase is at 20°C
- Flutes filled with fire protection material, effectively protecting top flange of all beams

The response of this model is generally in accordance with known structural phenomena in fire:

Heating

- During the heating phase all structural members expand as they heat up, leading to relatively large mid-span deflections.
- Due to the relatively light, yet realistic floor load applied to the model vertical deflections are low. In particular the primary girders deflect very little (less than 200mm or 8"). By comparison, Case 3 (800°C flutes unfilled) indicates a maximum vertical deflection of Girders of approximately 250mm (10") away from the region of failure. Filling of the flutes therefore shows a definite difference in structural response.
- This leads to greater longitudinal expansion, compared to vertical deflections caused by thermal bowing.
- When the girder between Column 44 and Column 79 is subjected to this lateral expansion it breaks it's the bottom two bolts on the seat at column 79 and on the seat at column 44 during the early stages of heating (temperatures of girder top flange is between 75°C and 170°C) . This allows the girder to be moved around on the seat plate at Column 79 and 44.
- During the heating phase a significant number of shear studs are broken, however it is considered that the secondary beams and girders retain enough connection to the slab in heating to act in a largely composite manner.
- Fewer than half of the shear studs on the secondary beams in the north-east bay are broken during the heating phase. It is therefore considered that a substantial amount of composite action is still retained. This compares well to Case 1, where the differences in heating regime and protection provide a heating case that is similar. This response is different to both Case 2 and Case 3 where significantly different heating regimes cause lesser or greater breakage, respectively.
- As the model approaches maximum heating there are no signs of imminent structural failure.

Cooling

- During the early stages of the cooling phase, the vast majority of the remaining shear studs break. It is considered that the sudden increase in stud breakage is related to the differential contraction between the steel structure and the concrete slab above. Concrete and steel heat and cool in different ways. This breakage leads to increased deflections in secondary beams.
- Additionally a number of secondary beams begin to break their connections. The majority of these members are in the central bay and the breakage of the connections has no obvious effect on the global response of the structure. The concrete slab is able to redistribute the floor load directly to the primary girders. The breakage pattern is focussed on a particular type of connection (SWC type) and it is understood that the tensile capacity of these connections is limited, compared to the rest of the structure.
- As the cooling phase continues the existing mid-span deflection of the secondary beams in the north-east corner, combined with the general contraction of the structure during cooling, leads to the South end of Girder 79-44 being pulled Eastward across its seating plate.
- At the end of 120 minutes of heating and cooling, the analysis shows there is no structural collapse. The girder 79-44 at column 79 does not appear to be pulled off its seat, unlike the case with the flutes unfilled.

The structural response described above is presented in more detail in the following sections.

A more detailed timeline may be found in Section 8.5.

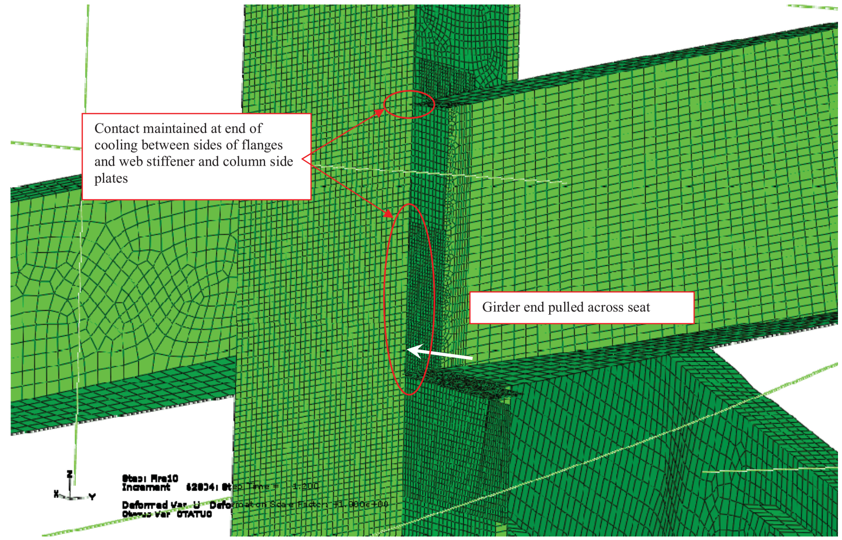

Figure 73: 800°C Filled Flutes Case 4 - Column 79 Seated Connection at End of Cooling

8.2 Details of Column Behaviour

No column buckling was observed in the model during the analysis.

All internal columns remained vertical throughout the analysis, with no significant lateral displacement observed while the perimeter columns showed some outward bowing of the columns.

The response of the columns in Case 4 is similar in nature to the response of all other cases and therefore is not discussed here in detail. Please refer to Section 5.2 for further discussion.

8.3 Details of Composite Floor Response

The response of the floor structure to Case 4 is largely similar to the response described for all other cases.

The key differences are highlighted in the sections below.

JA-3196

8.3.1 Heating phase

The response of the floor during heating can be compared to the response of the Case 3 model. Key points of comparison are described below:

- Figure 74 presents the vertical deflection contours of the Case 4 floor slab at peak heating. At this point the top flange of Girder 79-44 is approximately 560°C. The floor steel has undergone lesser heating compared to the Case 3 model at peak temperature; however, the general trends in terms of location of maximum deflections are similar.

Table 4 presents the critical temperatures for the secondary beams in the north-east corner of the structure, compared to the temperature attained by those members at peak heating.

The temperatures attained by the secondary beams are slightly in excess of the calculated critical temperatures, however no failure of the floor system is observed. This indicates that sufficient strength remains in the composite system to support the applied floor loading because of the composite connection available between the beams and the slab. The ability of the floor system to resist runaway failure will also be enhanced by the cooler temperatures, compared to Case 3, in the supporting girder between columns 79 and 44. It is considered that the cooler temperature in Girder 79-44 is the key reason that a heating phase initiating event is not observed.

Table 4: Secondary Beam Critical and Temperatures Attained at Peak Heating (Case 4 – 800°C flutes filled)

Beam section (W24x55)	Calculated Critical Temperature (calculated using AISC LRFD methods)	Temperature attained in analysis
Top Flange	644°C	677°C
Web	670°C	677°C

The key responses in the floor structure during the heating phase are:

- Large deflections of secondary beams caused by restrained thermal expansion and thermal bowing
- Early breakage of bolts at Column 79 seated connection
- Significant breakage of shear studs
- Significant loss of strength in secondary beams, especially in north-east corner where composite action is also compromised
- Runaway failure of north-east corner structure centred around failure of Column 79 seated connection

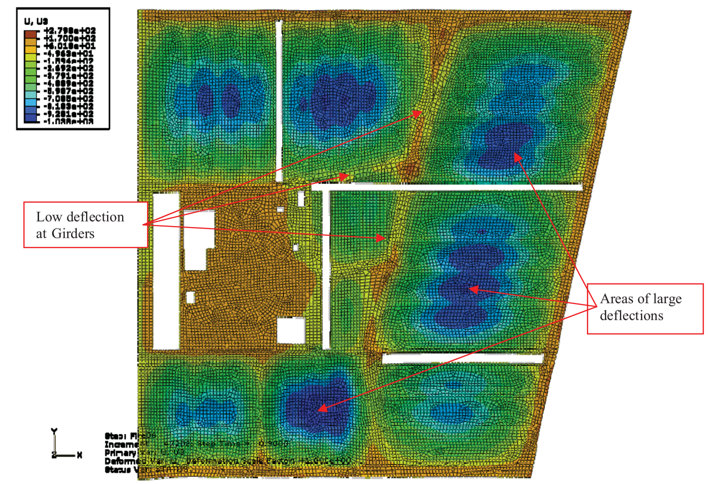

Figure 74: 800°C Filled Flutes Case 4 - Vertical Deflection Contours at Peak Heating

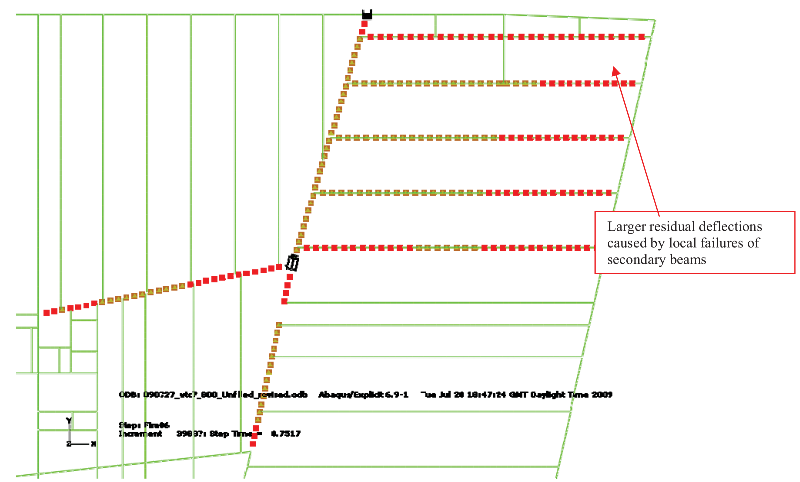

Figure 75: 800°C Filled Flutes Case 4 - Shear Stud Breakage at Peak Heating